Mechanistic Pharmacokinetic / Pharmacodynamic Modelling of Acute Inflammatory Challenge Models

Robert Willis

A thesis submitted for a Degree of Doctor of Philosophy

Strathclyde Institute of Pharmacy and Biomedical Sciences

University of Strathclyde and GlaxoSmithKline

2017

Declaration of Authenticity and Author's Rights

This thesis is the result of the author's original research. It has been composed by the author and has not been previously submitted for examination which has led to the award of a degree.

Signed: Date:

Table of Contents

Acknowledgments

I would like to thank my academic supervisors Professor Robin Plevin and Dr. Alison Thomson and my industrial supervisors Dr. Lia Liefaard, Dr. Phil Jeffrey and Dr. Alex MacDonald for their support and guidance throughout this collaborative DPhil programme. Their input and discussion was extremely valuable in enabling the completion of this thesis, particularly the support and patience Lia has shown me as I have begun to learn the concepts of population PK/PD modelling, and Alison and Robin for their valuable comments on the writing, content and structure that got me to the end thesis. I would like to acknowledge the following colleagues who assisted in the generation of the data and completion of the mouse model including Helena Clarke, Lynn Griffiths-King, Peter John-Baptiste, Sean Bater and Dave Parker (GSK, Laboratory Animal Sciences, Study delivery team) for their assistance during the in life phase of the study, Edward Hooper-Greenhill (GSK, Quantitative Pharmacology) for his patience guidance and assistance as I remembered how to use the LC-MSMS and learnt how to conduct ELISA assays, Dr Nicholas Galwey (GSK, Statistics) for his advice around the statistical analysis and Dr. Diana Quint (GSK, Respiratory TAU) for the background information and discussion around TLR7 biology and the GSK TLR7 agonist programme. I would also like to thank the following colleagues who assisted in the generation of the data and completion of the primate model; the GSK Laboratory Animal Sciences primate study delivery team for their completion of the in life phase of the study particularly Jennifer Deutsch and Sean Maguire who took my concept and study design and with their hard work, diligence and enthusiasm made it happen, Thom Lohr and Jonathan Larkin (GSK, II TAU) for their input into the study design and cytokine/chemokine analysis of the primate samples and Roberta Thomas (GSK, *in vitro in vivo* translation) for her analysis of the IFN gene signature from the primate samples. I would also like to thank my wife Louise and my two children Oliver and Annabelle for their support, understanding and encouragement throughout the 5 years I have been working on this project. They have kept me focused on the final goal and have played a large part in helping me cross the line. Finally I would like to thank Harry Kelly for his support advice and direction in all aspects of the PhD programme, my line management within QP, the II TAU, Martin Bayliss and the DMPK council and GSK for allowing me the opportunity and continued support throughout the project. Also all my colleagues who took the time to listen and offer advice whenever I asked “Can I ask you a quick question” as they inevitably were never quick.

Acronyms and Definitions

A_B	Amount in blood/central compartment
$A_B(0)$	Amount in blood/central compartment at time 0
A_D	Amount of dose
$A_D(0)$	Amount of dose at time 0
ACR	American College of Rheumatology
A_D	Amount in the dose compartment
AI_B	Amount of inhibitor in blood/central compartment
$AI_B(0)$	Amount of inhibitor in serum/central compartment at time 0
AI_S	Amount of inhibitor in serum/central compartment
$AI_S(0)$	Amount of inhibitor in serum/central compartment at time 0
AKT	Protein Kinase B
ANA	Antinuclear antibodies
APC	Antigen presenting cell
APRIL	A proliferation-inducing ligand
A_S	Amount in serum/central compartment
$A_S(0)$	Amount in serum/central compartment at time 0
A_T	Amount in the peripheral / tissue compartment
$A_T(0)$	Amount in peripheral / tissue compartment at time 0
AUC	Area under the curve
AUCD	Dose normalised AUC
AUC_{last}	AUC to time point of last measurable concentration
AUC_∞	AUC extrapolated to infinity
BAFF	B cell activating factor
BEW	Base equivalent weight
BHMA	9-Benzyl-8-hydroxy-2-(2methoxyethoxy) adenine
BILAG	British Isles Lupus Assessment Group
BLyS	B-lymphocyte stimulator
C_B	Concentration in blood/central compartment
$C_{biomarker}$	Concentration of biomarker in serum/central compartment
CCL2	Chemokine (C-C) motif ligand 2 also known as MCP1
CCL3	Chemokine (C-C) motif ligand 3 also known as M1P1α
CCL4	Chemokine (C-C) motif ligand 4 also known as M1P1β
CCL5	Chemokine (C-C) motif ligand 5 also known as eotaxin
C_{eff}	Concentration in the effect compartment
CI	Concentration of Inhibitor
CI_B	Concentration of inhibitor in blood/central compartment
CI_{eff}	Concentration of inhibitor in the effect compartment

C_{IFN}	Concentration of IFN
C_{IFN0}	Baseline concentration of IFN
CI_S	Concentration of inhibitor in serum/central compartment
CL_b	Blood clearance
CLinhibitor	Clearance of inhibitor
C_{last}	Last measurable concentration
CD	Cluster of differentiation i.e $CD8^+$ T cells
CL/F	Blood clearance expressed as a function of bioavailability
C_{max}	Concentration maximum
C_{min}	Concentration minimum
CMT	Compartment
COV	Covariance
CpG	5'-C-phosphate-G-3'
CpG-ODN	CpG-Oligodeoxynucleotides
CRP	C reactive protein
C_T	Concentration in the peripheral /tissue compartment
CV	Coefficient of variation
CWRES	Conditional weighted residuals
CXCL10	C-X-C motif chemokine 10 also known as IP10
CXCR3	C-C chemokine receptor type 3
CXCR4	C-C chemokine receptor type 4
CXCR7	C-C chemokine receptor type 7
D	Dose
DAMPS	Damage associated molecular patterns
DC	Dendritic cell
DI	Dose of inhibitor
DMSO	dimethyl sulfoxide
DNA	Deoxyribonucleic acid
D_{PO}	Oral dose
dsDNA	Double stranded DNA
D_{SC}	Subcutaneous dose
DV	Dependent Variable (observed data)
EC_{50}	The drug concentration which produces 50% of the maximum stimulation
ECLAM	The European consensus lupus activity measurement
EGF	Epidermal growth factor
ELISA	Enzyme-linked immunosorbent assay
EMA	European Medicines Agency
E_{max}	The maximum stimulatory effect attributed to the drug
EMCV	Encephalomyocarditis virus

ESR	Erthyrocyte sedimentation rate
F	Bioavailability
FDA	U.S. Food and Drug Agency
FOCE	First-order conditional estimation
Fu_b	Fraction unbound in blood
GCSF	Granulocyte colony stimulating factor
GMCSF	Granulocyte macrophage colony stimulating factor
GSK	GlaxoSmithKline
HCQ	Hydroxychloroquine
HCV	Hepatitis C Virus
HLQ	Higher limit of quantification
HMG-CoA	3-hydroxy-3-methylglutaryl-coenzyme A
HRP	Horseradish peroxidase
IBD	Inflammatory bowel disease
IC	Immune Complex
IC_{50}	The drug concentration which produces 50% of the maximum inhibition
ICL	Clearance of the inhibitor
ID	Identification
ID_{po}	Oral dose of inhibitor
IF	Bioavailability of the inhibitor
IFIT	Interferon induced protein with tetratricopeptide repeats
IFN	Interferon
IFNAR	Type I IFN receptor
Ig	Immunoglobulin
II TAU	Immuno-Inflammation Therapy Area Unit
IIV	Inter-individal variability
IK_a	Absorption rate constant of the inhibitor
IκBα	Inhibitor of Kappa B
IKK	IκB Kinase
IL	Interleukin
IL1Ra	IL1 receptor antagonist
IL15α	IL15 receptor α
I_{max}	The maximum inhibitory effect attributed to the drug
IK_{10}	Elimination rate constant of the inhibitor
IOV	Inter-occasion variability
IPRED	Individual Predicted
IP10	Interferon-gamma induced protein 10
ip	Intraperitoneal
IRAK	Interleukin-1receptor associated kinase

IRF	Interferon response factor
IRM	Immune system response modifier
ISG	IFN stimulated gene
ISGF	IFN stimulated gene factor
ISRE	Interferon stimulated response elements
iv	Intravenous
JAK	Janus kinase
K_{01}	Absorption rate constant also written as K_a
K_{10}	Elimination rate constant also written as K_{el}
K_{12}	Rate constant determining the movement of drug from the central to peripheral compartment
K_{21}	Rate constant determining the movement of drug from the peripheral to central compartment
K_a	Absorption rate constant
K_{el}	Elimination rate constant
K_{eo}	Rate constant determining the rate of drug movement into the effect compartment
K_{eo}Inhibitor	Rate constant determining the rate of inhibitor movement into the effect compartment
K_{in}	Zero order turnover rate for production of response
Kleptose™HPB	hydroxypropyl-beta-cyclodextrin
K_{mod}	First order rate constant for the turnover of M
K_{out}	First order rate constant for the loss of the response
LBF	Liver blood flow
LC	Liquid Chromatography
LLQ	Lower limit of quantification
LPS	Lipopolysaccharide
Ly6E	Lymphocyte antigen 6E
M	Endogenous modulator
M_0	Baseline response of M
M_{50}	Value of M that double K_{out}
mAb	Monoclonal antibody
MCP1	Monocyte chemotactic protein1
mDC	Myeloid DC
MyD88	myeloid differentiation primary response gene 88
MHC	Major histocompatability complex
MIP	Macrophage inflammatory protein
MIU	Million international units
MRM	Multiple reaction monitoring
MS/MS	Tandem mass spectrometry

MVOF	Minimim value of the objective function
mTOR	Mechanistic target of rapamycin
MW	Molecular Weight
Mx	Myxovirus resistance
NCA	Non compartmental analysis
NFκB	Nuclear factor kappa –light-chain-enhancer of activated B cells
NK cell	Natural Killer Cell
OAS	2'-5' oligoadenylate synthetase
ORNs	Oligoribonucleotides
OPN	Osteopontin
p38 MAPK	p38 mitogen-activated protein kinases
PAMP	Pathogen associated molecular patterns
PBMC	Peripheral Blood Mononuclear Cells
PBPK	Physiologically based pharmacokinetic modelling
PBS	Phosphate buffered saline
PCR	Polymerase chain reaction
PD	Pharmacodynamic
PDA	Photodiode Array
pDC	Plasmacytoid Dendritic Cell
PEG	Polyethylene glycol
PI3K	Phosphatidylinosiyol-4,5-biphosphate 3-kinase
PK	Pharmacokinetic
PK/PD	Pharmacokinetic / Pharmacodynamic
PKR	dsDNA dependent protein kinase R
PLSCR1	Phospholipid scramblase 1
PMR	Polymorphonuclear leukocytes
POM	Proof of mechanism
PRED	Population Predicted
PRR	Pattern recognition receptor
Q	Clearance from the peripheral/tissue compartment
QC	Quality control
QSP	Quantitative systems pharmacology
QP	Quantitative Pharmacology
RA	Rheumatoid Arthritis
RANTES	Regulated on activation, normal T cells expressed and secreted
REML	Restricted maximum likelihood
ROS	Reactive oxygen species
RNA	Ribonucleic acid
ssRNA	Single stranded RNA

RNP	Ribonuclear protein
RPM	Revolutions per minute
RSE	Relative Standard Error
sc	Subcutaneous
sIL2R	Soluble IL2 receptor
SLAM	Systemic Lupus Activity Measurement
SELENA-SLEDAI	Safety of Estrogen in Lupus National Assessment – SLEDAI
SLE	Systemic Lupus Erythematosus
SLEDAI	Systemic Lupus Erythamtosus Disease Activity Index
SOCS	Suppressors of cytokine signalling
STAT	Signal transduction and transcription
SYK	Spleen tyrosine kinase
$t_{1/2}$	Terminal half-life
T_0	Time zero
Th1	T helper cell 1
Th2	T helper cell 2
Th17	T helper cell 17
T_{lag}	Lag Time
T_{last}	Time of last measurable concentration
TLR	Toll like receptor
T_{max}	Time to maximum concentration or effect
TMB	Tetramethyl benzidine
TMDD	Target Mediated Drug Disposition
TNF	Tumour Necrosis Factor
TRADD	TNF receptor-1 associated death domain protein
TRAF	TNF receptor associated factor
TRAIL	TNF related apoptosis inducing ligand
Treg	Regulatory T cell
TYK	Tyrosine kinase
UPLC	Ultra performance liquid chromatography
UV	Ultra violet
V	Volume of distribution / volume of the central compartment
VI	Volume of the central compartment for the inhibitor
VEGF	Vascualr endothelial growth factor
V/F	Volume of distribution expressed as a function of bioavailability
V_{ss}	Volume of distribution at steady-state
V_T	Volume of the peripheral/tissue compartment
WHO	World Health Organisation

Abstract

Introduction

Systemic Lupus Erythematosus (SLE), is a chronic autoimmune disease that can affect multiple organ systems. Survival rates have improved in recent years but SLE is still currently "managed" rather than "cured" and traditional treatments can cause irreversible damage, sometimes leading to death. Consequently, there is a need for new therapeutic agents that target specific components of the disease pathogenesis. This has proved challenging since the exact aetiology of SLE is undefined, although most of the cells of the immune system have been implicated in the disease process.

The cytokine interferon (IFN) α has a key role in the early induction of the disease and ongoing pathogenesis. Immune complexes of autoantigens and autoantibodies have been found in the sera of SLE patients and induce the production of IFNα by plasmacytoid dendritic cells (pDCs) through toll like receptors. IFNα binds to a specific receptor which results in the regulation of genes associated with the viral response (the IFN gene signature). This signature has been correlated with disease activity in SLE patients reinforcing a role of IFNα in SLE. IFNα can also stimulate and inhibit a wide range of cytokines. In SLE, a vicious circle is established with an ongoing production of IFNα from pDCs that maintains the autoimmune process.

Lupus mouse models that mimic a human SLE like disease have previously been used to investigate new treatments for SLE, but have only delivered drugs that treat the symptoms rather than modifying the disease. An alternative approach is to use mechanism based models to investigate the role of a particular pathway or disease mechanism. PK/PD modelling of the data arising from challenge models can provide confidence that the efficacy observed in preclinical studies can be translated to the clinical setting and may improve the overall efficiency and success of drug discovery programmes. The IFNα pathway looks a promising target for new treatments for SLE and the induction of IFNα and related biomarkers appear to be translatable between preclinical and clinical species. Therefore this looks an appropriate pathway to investigate using mechanistic preclinical PK/PD challenge models where the selected challenge agent would induces elements of the IFNα pathway under investigation.

Aims

The aim of this project was to take a disease focused approach to select and investigate two preclinical mechanistic acute *in vivo* PK/PD models. These models were selected based on the hypothesis that the IFNα pathway has a key role in the pathogenesis of SLE.

Methods

This project investigated two preclinical mechanistic *in vivo* PK/PD challenge models with challenge agents that stimulate different components of IFNα pathway. One was a high throughput rodent model designed to enable screening of a number of compounds while the other was a primate model that was considered translatable to human.

Mouse model

A mouse model was investigated that used the small molecule TLR7 agonist resiquimod to induce IFNα production from pDCs. First, the pharmacokinetics of resiquimod were determined after iv infusion of 0.25 mg/kg. The relationship between IFNα response and dose was then determined over the range 0.04 to 4.8 mg/kg. Finally, a fixed dose of 0.4 mg/kg was used to determine the reproducibility of the IFNα response between study days. Concentrations of resiquimod and IFNα were determined by LC-MSMS and ELISA analysis respectively.

The data were initially analysed by non-compartmental analysis to determine the pharmacokinetics of resiquimod. Statistical and power analysis were then applied to determine the reproducibility of the model between study days and to understand the potential utility of the model in the drug discovery. Finally, a population PK/PD analysis of the dose response relationship was conducted using a range of models that included an endogenous modulator function to describe the inhibition of excessive IFNα production.

Primate model

A primate model was investigated that used recombinant human IFNα2b (INTRON A) to investigate the induction of a range of biomarkers downstream of the IFN receptor. Cynonologus monkeys received a subcutaneous administration of vehicle and IFNα2b at both 3 MIU/kg and 10 MIU/kg. The pharmacokinetics of IFNα2b were determined and the induction of 29 cytokines/chemokines, neopterin and body temperature was investigated.

Concentrations of IFNα2b and other cytokines/chemokines were determined by Milliplex® magnetic bead panel, concentrations of neopterin were determined by ELISA analysis and body temperature was determined using a rectal thermometer.

The data were initially analysed by non-compartmental analysis to determine the pharmacokinetics of IFNα2b. A population PK/PD analysis of the IFNα2b induction of 6 biomarkers was then conducted using an indirect response model with stimulation of input.

Results

Mouse model

Following iv infusion, resiquimod had a blood clearance of 69 mL/min/kg, a volume of distribution at steady state of 2.4 L/kg and a terminal half-life of 0.5 h. There was low inter-animal variability in pharmacokinetic parameters and similar results were obtained for iv infusion and iv bolus administration. Linearity in pharmacokinetics was demonstrated over a 120 fold dose range.

Following iv administration of resiquimod, IFNα concentrations were observed from 0.75 h post dose, C_{max} occurred at 1-2 h and the last measurable concentration was observed at approximately 3 h. A bell shaped dose response curve was observed with the maximum response observed at 0.09 mg/kg. A dose of 0.4 mg/kg achieved reproducible response results across four study days and was recommended as the challenge dose for future studies. Power analysis demonstrated that the model could be used to investigate multiple compounds at a single dose and the dose response of a single compound.

Population PK/PD modelling was conducted in a sequential manner. The pharmacokinetics of resiquimod were described with a 1 compartment iv bolus model with IIV on clearance. The final PK/PD model comprised an indirect response model with stimulation of input, an effect compartment and endogenous modulator function with fixed parameter estimates for $K_{eo,}$ the Hill co-efficient, and M_{50} and IIV on K_{eo}, EC_{50} and E_{max}. The final model did not adequately predict the IFNα time profile in individual mice and highlights that increased data may be required to provide robust estimates of the induction and elimination phase of the IFNα response. The final model did characterise the dose response relationship but predicted a reduction in response at higher doses of resiquimod when IIV was included on E_{max} rather than the modulator function.

Primate model

Following sc administration, IFNα2b had an apparent blood clearance of 2.9 mL/min/kg, a apparent volume of distribution of 3.1 L/kg and a terminal half-life of 13 h. There was low inter-animal variability in the systemic exposure (CV of 25-40%) and clearance (CV of 22-37%), however the volume and half-life demonstrated greater variability (CV of >100%) Linearity in pharmacokinetics was demonstrated over a 3 fold dose range. The pharmacokinetics were broadly comparable to those previously reported in the literature. Following IFNα2b treatment induction of neopterin and the cytokines/chemokines IL15, IL1Ra, MCP1, IL6 and eotaxin was observed. There was a sub proportional increase in the concentrations of biomarkers with the increase of IFNα2b dose from 3 MIU/kg to 10 MIU/kg. An induction of body temperature was not observed.

Population PK/PD modelling was conducted in a sequential manner. The pharmacokinetics of IFNα2b were described with a 2 compartment model with first order absorption and IIV on clearance and IOV on volume. A covariate analysis indicated there was no relationship with either clearance or volume with body weight. The final PK/PD model for all 6 biomarkers comprised an indirect response model with stimulation of input and IIV on baseline. In addition IIV on E_{max} was included for neopterin, IL15, IL6 and MCP1, on K_{out} for IL15 and EC_{50} for IL1Ra and eotaxin. High values for IIV were determined for IL6 and IL1Ra and the parameters for MCP1 and IL6 demonstrated poor precision. The model did not give a robust prediction of EC_{50} for any biomarker or E_{max} for IL6, MCP1 and eotaxin due to the investigated doses giving a comparable response.

Conclusions

Mouse Model

The pharmacokinetics of resiquimod were successfully determined in the mouse for the first time following both iv infusion and iv bolus administration of resiquimod. The investigation of the dose response relationship delivered comparable data to that previously reported in the literature whereby the greatest response was observed at low doses of resiquimod and further increase in dose results in an apparent reduction in the IFNα response to a plateau. A reproducible IFNα response can be achieved between mice receiving the same resiquimod treatment across multiple study days and suggests that model that may be used in drug discovery to investigate therapeutics that have an action

on the IFNα pathway. Population PK/PD modelling with the incorporation of an endogenous modulator has highlighted the gaps in the data set and improved the understanding of the model that can be used to guide future PK/PD modelling efforts.

Monkey Model

The pharmacokinetics of IFNα2b demonstrated that at the doses investigated in this study the receptor mediated clearance had become saturated and the clearance was driven by renal elimination and catabolism. The induction of serum neopterin concentrations and cytokines/chemokines IL15, IL6, MCP1, eotaxin and IL1Ra, which have all been implicated in the pathogenesis of SLE, was observed in the challenged primates. A less than proportional increase in biomarker concentrations was observed with the increase in dose indicating that the concentrations of IFNα2b associated with these doses may be near the top of the concentration response curve. A population PK/PD model that describes the induction of the 6 biomarkers was developed. However, the model was limited by the small number of doses investigated. Due to the translatability of the biology between primate and humans this project has delivered a PK/PD model with disease relevant endpoints that can be used to screen compounds and potentially predict efficacious clinical doses.

This project has successfully designed and validated two preclinical *in vivo* mechanistic PK/PD challenge models based on the hypothesis that the cytokine IFNα is central to the pathogenesis in SLE and that the mechanisms behind the induced response are translatable between species. This project has demonstrated that both models have potential in drug discovery to be used as tools to select the most appropriate compounds for progression to the clinic and to predict efficacious doses.

Chapter 1: Introduction

Developing and validating a Pharmacokinetic/Pharmacodynamic (PK/PD) model for acute inflammation can support drug development in both the early discovery and later development stages. In early discovery, a model may be used to identify potential drug targets, and for compound screening and selection. As compounds progress to candidate selection, a model may be used to predict efficacious clinical doses. The models can provide confidence in the target, the mechanism of disease and the likely impact of the compound on the disease progression, as well as providing integral information into the design of early clinical trials.

Figure 1.1 describes a potential approach to drug discovery and development where the focus is on the disease itself. Once the target disease has been selected, a clinical question can be formed which enables research into the mechanisms and pathways implicated in the disease. Based on these mechanisms a suitable model system, which may be an *in vitro* or *in vivo* system, is selected. At this stage, assays can be used to demonstrate that a compound affects the underlying mechanism, which in turn may allow a better understanding of the drug exposure required for efficacy at either a cellular or systems level. These model systems may be used to select and establish confidence in the therapeutic target, to screen for potential compounds and to select the most suitable compound for progression to the clinic. It is likely that a potential therapy will then be investigated in a validated *in vivo* preclinical PK/PD model that may confirm the efficacy of the compound, predict and select the doses to be administered in the clinic and help in designing the clinical trial. Central to the selection and development of a PK/PD model is an understanding of the mechanisms and pathways behind the model, which ideally should be relevant to the human disease situation through incorporating mechanisms of the target disease and translatable biomarkers. With increased knowledge of the PK/PD model will come increased confidence in the preclinical assessment of the efficacy of novel medicines, and later in the translation of the *in vivo* preclinical observations to generate a predicted clinical dose. As described in Figure 1.1, this is a cyclical approach and it may be that following administration of the therapeutic agent in the clinic, it may become apparent that the therapy may be suitable for other disease indications.

Figure 1.1 A disease focused approach to drug discovery and development. Adapted from Perera (2009)

This project will adapt the disease focused approach presented in Figure 1.1 to investigate a number of acute *in vivo* PK/PD models that have been selected based on the target disease entity Systemic Lupus Erythematosus (SLE). This is a complex, clinically diverse chronic autoimmune disease that is managed rather than cured by current therapies. As a result there is a demand for new therapeutic agents that target specific mechanisms of the disease or certain patient populations. Research into this disease highlights the many cell types and pathways implicated in this complex disease; however the excessive production of Interferon alpha (IFNα) and its subsequent downstream actions have been suggested by some researchers as central to the disease.

Across the pharmaceutical industry, there is an increased requirement to use simulation approaches to prioritize compounds prior to *in vivo* experimentation (Jones et al, 2012). An efficient PK/PD model that increases the understanding of the target mechanisms may support this by enabling a reduction in the number of *in vivo* animal studies performed in the discovery stage of drug development. An example of the successful development, calibration and validation of an *in silico* model for acute inflammation has been reported in the literature (Vodovotz et al, 2006). The authors developed a mathematical model using a set of ordinary differential equations and an iterative and repeating process of model creation (Figure 1.2), to describe multiple components of the inflammatory response observed during lipopolysaccharide (LPS) induced mouse endotoxaemia. The authors of the LPS mouse endotoxaemia model attempted to link the simulation of acute inflammation

across several species, including humans, which was to allow for the extrapolation from studies in animals to simulated human clinical trials of therapeutic agents (Vodovotz et al, 2006). It is the expectation that a similar approach to that presented in the literature may be adopted for this project whereby initial research leads to a study design and collection of experimental data which is subsequently described using an *in silico* model incorporating differential equations. Simulations and predictions of the response using the model will allow a better understanding of the target mechanism, challenge agent and the PK/PD relationship and will guide the optimisation of the in life phase of the model i.e. sampling regime, dose of challenge agent etc to deliver a valuable tool to the drug discovery process.

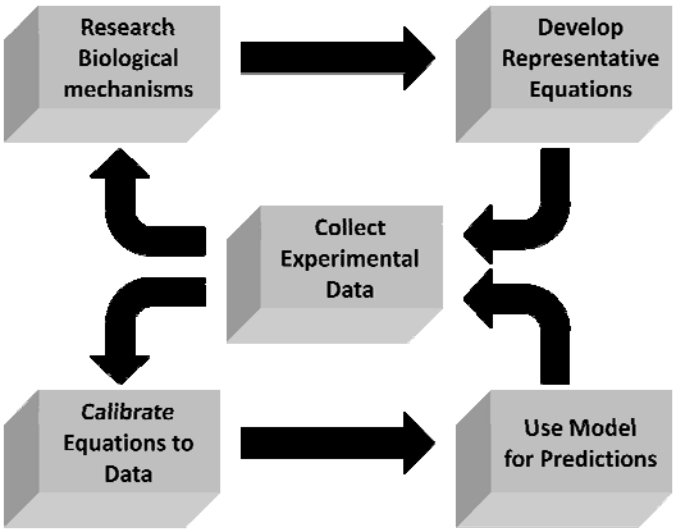

Figure 1.2 Iterative approach to modelling inflammation. The approach taken by Vodovotz et al (2006) involved an iterative and repeating process of model creation based on existing literature, validation in relevant experimental paradigms, and hypothesis generation. Recreated with permission Vodovotz et al (2006)

The project will initially investigate an *in vivo* mouse PK/PD model in which systemic concentrations of IFNα are induced by the administration of a challenge agent. It is anticipated that this model will represent the first model system presented in Figure 1.1 and will enable the investigation of inhibition of systemic concentrations of IFNα by compounds of interest. This model is viewed as a high throughput model that may be used

to select and rank the most appropriate compounds for progression for further development. This model should provide early confidence in the target mechanism and confidence in the translation of efficacy to the clinic.

The holy-grail for drug discovery programmes is to deliver a model that can translate preclinical efficacy to a confident prediction of clinical efficacy, and it is viewed that this is the objective for the second model system presented in Figure 1.1. In parallel to delivery of a mouse PK/PD model this project will investigate an *in vivo* primate PK/PD model whereby IFNα is administered as the challenge agent and the inhibition of the downstream effects by compounds of interest may be investigated. The response to an IFNα challenge, measured as the induction of clinically relevant biomarkers, has been reported to be translatable between primates and human (Mager and Jusko, 2002; Mager et al, 2003) which provides the expectancy this may deliver a truly translatable model.

As well as investigating and validating the *in vivo* models a primary objective of this project is to model the response in each species using computational software to derive a set of equations and parameters that describe the pharmacokinetics of the challenge agent and the associated time course and magnitude of the response or effect (pharmacodynamics). Establishing definitive parameter estimates that describe the induction of the response is a key requirement in developing an *in silco* model similar to that developed to describe the inflammatory response observed during (LPS) induced mouse endotoxaemia (Vodovotz et al 2006). An *in silico* model will be invaluable to the drug discovery process as it will enable the simulation and prediction of the response in preclinical species and potentially human. This may be used amongst many other things to predict the action of compounds of interest, predict the clinically efficacious dose and in the optimisation of PK/PD studies dependent on the required outcome.

Chapter 2: Background

2.1. Systemic Lupus Erythematosus

The immune system comprises both innate and acquired immune responses, which together control a host's inflammatory response to damage incurred to its cells, organs and tissues by a variety of pathogens, chemicals or physical insults. The immune system functions to prevent or control serious illnesses, caused by infections, tumours and allergic responses. If the inflammatory response becomes dysregulated, inflammation can lead to disease pathology. In some cases, activation of the innate immune system results in the promotion of self-directed immune responses (Marshak-Rothstein, 2006) which are categorised as autoimmune diseases and can lead to chronic inflammation, tissue destruction and/or dysfunction. Autoimmune diseases are multifactorial and both intrinsic factors and environmental factors may contribute to the induction, development and progression of the disease. They form an important health problem, affecting at least 5% of the population and despite progress in the research of autoimmune processes, the aetiologies and pathological mechanisms involved in the development of autoimmune disease are incompletely understood (WHO, 2006).

One of the most complex and clinically diverse autoimmune diseases is Systemic Lupus Erythematosus (SLE), which is a chronic disease that can affect skin, joints, kidneys, lungs, nervous vasculature, serous membranes and other organs (Marshak-Rothstein, 2006; Smith et al, 2009; FDA, 2010; Pathak and Mohan, 2011). SLE has a prevalence of 40-50 cases per 100,000 persons in the general population with onset typically occurring between the ages of 15-45 years, it shows a clear female preponderance and is more prevalent in African Americans and Asians (WHO, 2006; EMA, 2013). Survival rates have improved in recent years with a 10 year survival rate now at approximately 92-98% although SLE patients still have two to five fold increased risk of death compared to the general population with infections accounting for between 20-40% of all deaths (Goldblatt and Isenberg, 2005; Bertsias, Salmon and Boumpas 2010). SLE is a lifelong disease of variable severity. Persistent active flares (defined as a clinically significant measurable increase in disease activity) interspersed among periods of remission can lead to both disease and treatment-related damage (Bertsias, Salmon and Boumpas 2010). Symptoms can range from fatigue and musco-skeletal complaints to life threatening renal and cerebral disease (Goldblatt and Isenberg, 2005). In about 15-20% of cases, disease onset occurs during childhood and tends to be more severe with faster and more severe damage accrual (EMA, 2013). SLE is highly

heterogeneous which has led researchers to suggest that it should be considered a syndrome rather than a single disease (Via, 2010).

2.2. Pathways of disease

As with most autoimmune diseases, the exact aetiology of SLE has yet to be defined, although most if not all of the cells of the immune system have been implicated in the disease process (Schmidt and Ouyang, 2004; Rönnblom, 2010). Figure 2.1 adapted from Rönnblom (2010) presents a schematic of the pathways involved in etiology of SLE and clearly highlights the number of different cell types involved in the disease pathogenesis. Due to the cyclic nature of the disease with many positive feedback loops it is possible to draw the pathway with a particular cell type or cytokine at the centre depending on the focus. However there is a large body of evidence that demonstrates a key role for the cytokine Interferon (IFN) α in the early induction of the disease and ongoing pathogenesis and as such it warrants its place as a central mediator in the pathways of SLE. Research has attributed insufficient clearance of apoptotic material and the release of auto-antigens to be involved in the development and progression of the disease (Fransen et al, 2010). The auto-antigens stimulate the plasmacytoid dendritic cells (pDCs) to release IFNα which goes on to have a multitude of effects on numerous cell types including the activation of T and B cells. The activation of the B cells results in the production of auto-antibodies which have the capacity to form immune complexes with the autoantigens. These immune complexes are potent activators for the pDCs and so a viscous circle is established with the continuous exposure of the immune system to IFNα that maintains the auto-immune process (Rönnblom, 2010).

A large number of potential genetic and environmental factors have been proposed to contribute to the onset of disease. It is likely that the induction and progression of the disease is due to multiple factors and different combinations of these factors are responsible in each patient (Rottman and Willis, 2010). Key components relating to the role of IFNα in the pathogenesis of SLE will be reviewed in more detail below.

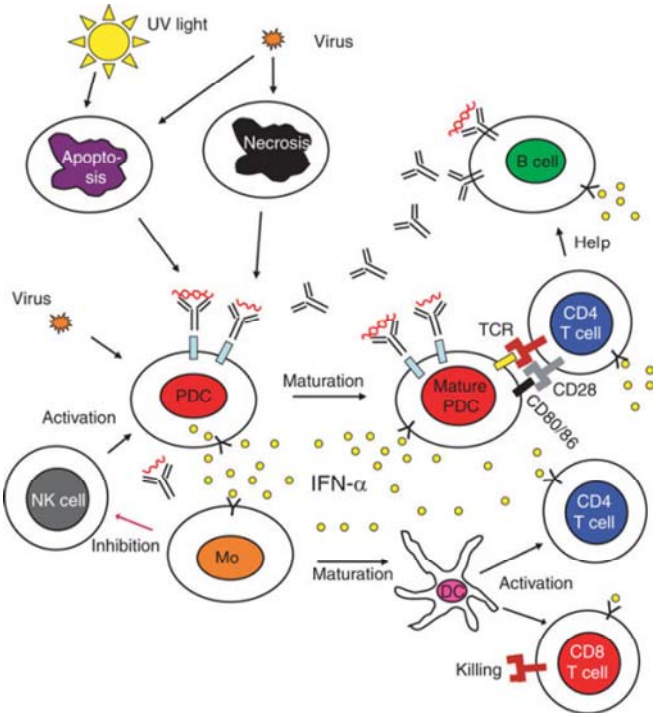

Figure 2.1 **Role of the type I interferon system in the etiopathogenesis of lupus. A viral infection induces IFNα production in pDCs and the release of autoantigens from dying cells. Produced IFNα promotes maturation of monocytes to denritic cells, activation of T cells and stimulation of B cells. Antibodies against nucleic acid containing autoantigens are produced, these autoantibodies together with the autoantigens form immune complexes (IC) which are inducers of IFNα from pDCs. In addition these ICs can directly stimulate B cells to increased autoantibody production. UV-light induced apoptosis will increase the release of autoantigens and the formation of more ICs. NK cells promote the IFNα production while the down regulation of NK cells by activated monocytes is deficient in SLE. All these events with establish a vicious circle with an ongoing production of IFNα from pDCs that maintains the autoimmue process. Adapted from Rönnblom (2010).**

2.2.1. Triggers of disease

There is evidence to suggest that genetic factors play an important role in the predisposition to the disease (Mok and Lau, 2003; Marshak-Rothstein, 2006; Guggino et al, 2012). Studies investigating the genes that may contribute to SLE have been conducted by

whole-genome scans from families in which multiple members have SLE (Rahman and Isenberg, 2008). Such studies have identified over 50 SLE associated gene loci which affect pathways implicated earlier in SLE etiopathology, such as immune complex processing, Toll-like receptor (TLR) signalling and type I IFN production/response all of which are topics that will be discussed later in this chapter (Eloranta and Rönnblom, 2016). The various genetic factors are outside of the scope of this project but have been reviewed in depth by Illei et al (2004) and Eloranta and Rönnblom (2016).

Despite this, most cases of SLE are sporadic without easily identifiable genetic predisposing factors. This suggests that multiple genetic and environmental factors, together with abnormalities of both the innate and the adaptive immune system may be involved (Mok and Lau, 2003; Guggino et al, 2012). These factors may contribute to both the induction as well as the progression of the disease over time, for example flares in disease activity in SLE are frequently associated with or follow a viral infection (Baccala et al, 2007; Bertsias, Salmon and Boumpas 2010). A number of environmental factors have been attributed to the development of lupus including infectious agents, smoking, exogenous hormones, dietary factors and ultraviolet (UV) radiation amongst others (Barbhaiya and Costenbaber, 2014). The American College of Rheumatology (ACR) diagnostic criteria for SLE includes photosensitivity, which occurs in 40-50% of patients and current therapies for treatment of SLE include education around avoiding UV exposure. Despite this the involvement of UV radiation in SLE is complicated, for example, UVA exposure has been found to decrease clinical disease activity in SLE but in other studies has been shown to induce cutaneous lupus skin lesions. The role for UVB which is responsible for sunburn and skin damage may be clearer cut as UVB has been shown to induce DNA damage which leads to antigen-specific immunotolerance and is thought to be a mechanism involved in SLE. Although the exact role of UV radiation in SLE is still to be defined, it does appear to exacerbate pre-existing SLE, and does highlight the impact that environmental factors may play in SLE (Barbhaiya and Costenbader, 2014).

SLE has a noted female preponderance with a 9:1 female to male ratio (Petri, 2008) thus there is a potential for a role of hormones in the disease pathogenesis. Observational and interventional clinical studies have suggested that estrogens may have a deleterious effect in SLE, and the risk of developing of SLE is higher in women taking oral contraceptive pills or on hormone replacement therapy (Chan and Mok, 2013). In addition, there is evidence to

suggest that androgens exhibit the opposite effect to estrogens and are protective in SLE. However, the role of sex hormones is not clear and does not provide a simple explanation for the female bias. For example, SLE can occur in situations where estrogens levels are generally low such as in children, in women after the menopause and in men (Petri, 2008).

2.2.2. Apoptosis

The self-antigens that are involved in the induction and development of SLE are released by apoptosis. Apoptosis is programmed cell death and plays important roles in maintaining tissue homeostasis as well as regulating the maturation of T and B cells and modulating the immune response (Prasad and Prabhakar, 2003). The apparently static peripheral population of mature lymphocytes is the result of a fine balance between newly matured lymphocytes released from the central lymphoid organs and the constant depletion of lymphocytes due to death by neglect and activation induced cell death. During apoptosis the cells shrink, form apoptotic blebs on the surface membranes and the chromatin structure and composition changes and condenses.

Evidence that apoptotic material may be one of the triggers for SLE comes from studies in non-autoimmune mouse strains where investigators demonstrated that administration of apoptotic bodies resulted in the development of auto-antibodies similar to those seen in SLE (Pathak and Mohan, 2011). Studies have demonstrated an increase in apoptosis coupled with a corresponding reduction in both the number (phagocytic cells) and function (phagocytosis) of the population of cells that clear the apoptotic material, resulting in an accumulation of apoptotic debris in the circulation (Rottman and Willis, 2010; Pathak and Mohan, 2011). An alternative study demonstrated a positive correlation between lymphocyte apoptosis, macrophage function and disease activity in SLE patients again highlighting an important role for apoptosis in the pathogenesis of SLE (Jin et al, 2005).

One suggestion for the increased apoptosis is due to sensitivity to environmental triggers such as UVB, however, researchers have demonstrated both increased susceptibility and no increased susceptibility of lymphocytes in SLE patients to UVB compared to healthy donors. The Fas receptor mediates apoptosis in human lymphocytes and has been implicated to have a role in both spontaneous and UVB induced cell death. Two mouse models that spontaneously express lupus like syndrome have abnormal function in the Fas receptor (lpr) and Fas ligand (gld). Basal levels of Fas are generally elevated on cells freshly isolated from

SLE patients although this does not necessarily reflect increased Fas function in mediating cell death (Caricchio and Cohen, 1999).

This review so far has focused on the role of apoptosis in the appearance of self-antigens observed in SLE patients; however apoptosis also plays another potential role in SLE. That is the inefficient removal of self-reactive lymphocyte clones, leading to a breakdown in central and peripheral tolerance. Lymphocytes are subjected to several checks at various stages during their maturation and subsequent release into the periphery. The cells undergo positive and negative selection with the goal of the deletion of the lymphocytes that strongly react with self-antigens by apoptosis. A defect in this negative selection can lead to an accumulation of self-reactive T and B cell clones (Prasad and Prabhakar, 2003).

2.2.3. Antigens

A substance that provokes a specific immune response is called an antigen and in practice any material foreign to the body and of sufficient size can act as an antigen (WHO, 2006). When a pathogen enters the body the cells of the innate immune system act as a first line of defence. Firstly they are involved in the recognition of the pathogen and/or associated antigens, and subsequently initiate the required response to eliminate it. The vast majority of infections are dealt with locally by cells of the innate immune system, such as natural killer (NK) cells and macrophages. On other occasions, when infections outrun the innate immune system, the cells of the system can call upon the adaptive immune response with its T and B lymphocytes to increase the power and specificity of the immune response. The adaptive response is targeted to a particular pathogen and as a result is more powerful but more restricted in its effects (WHO, 2006; Medzhitov, 2008). Apoptotic cells provide a source of self antigens or auto-antigens in SLE which are generally nucleic acid containing macromolecules (Jin et al, 2010). Self-derived nucleic acids do not activate the innate immune system under normal conditions as they are degraded by serum nucleases before being recognized by the relevant receptors to induce an immune response (Kawai and Akira, 2010). During apoptosis the nucleic acids that form the auto-antigens are clustered in blebs on the surface of apoptotic cells (Munoz et al, 2008; Jin et al, 2010) and ordinarily, phagocytes quickly remove apoptotic cells and blebs long before they could have released their modified contents (Munoz et al, 2008). However, the failure of the phagocytic cells, such as in SLE, to remove the apoptotic cells allows the auto-antigen release from these cells, revealing previously cryptic epitopes or neoepitopes that can activate the immune

system (Jin et al, 2005; Jin et al, 2010). Studies using the sera from SLE patients have demonstrated that isolated DNA fragments from the sera were the same size as inter-nucleosomal digested DNA from apoptotic cells (Jin et al, 2010). There is no structural difference between microbial and mammalian DNA and RNA suggesting it is very difficult to distinguish between pathogen and self nuclear material. However pathogen and mammalian DNA can be distinguished by the level of methylation with mammalian DNA generally expressing more methylated groups. The body has implemented defence mechanisms to maintain tolerance to self-antigens. One example of which is the localisation of receptors that recognize DNA and RNA products in intra-cellular compartments in an effort to prevent undesirable activation by endogenous RNA and DNA (Barrat et al, 2005).

It has been demonstrated that self-antigens, such as double stranded (ds)DNA from apoptotic cells, and not living cells are able to activate antigen presenting cells (APCs) and are potent autoantigens for both B and T cells (Rottman and Willis, 2010). They bind to immunoglobulin on the surface of B lymphocytes thereby stimulating the cells to proliferate. The higher the affinity of the surface immunoglobulin for the antigen the more strongly the cells are stimulated and the more they proliferate. In the presence of the stimulating antigen, B cells that display and secrete immunoglobulin with high affinity for that antigen are preferentially selected. The B cells require stimulation by activated T cells as well as by the antigen. As such, each T cell carries a surface receptor molecule with the ability to interact best with one particular antigen when it is presented to the T cell receptor in a complex with a major histocompatibility complex on the surface of the antigen presenting cell. This process ultimately drives antibody class switching from Imuunoglobulin(Ig)M to IgG and the secretion of antibodies that bind more strongly to the driving antigen (Rahman and Isenberg, 2008). The auto-antigen specific B and T cells that interact are generally absent in healthy people. That being said, a significant percentage of the cells generated in the lymphoid tissue invariably have T and B receptors directed against self antigen. Under normal circumstances, those T and B cells with high affinity for self antigen are eliminated, reprogrammed, or inactivated in the primary or secondary lymph organs. However, these processes do not delete T and B cells with lower affinity for self antigen with 25% and 40% of circulating T cells having the ability to recognize self antigen and the potential to induce immunity (Rottman and Willis, 2010).

2.2.4. Autoantibodies

SLE is characterised by the production of auto-antibodies against nuclear components and these auto-antibodies form classic biomarkers involved in the diagnosis of the disease. Auto-antibodies are so called as they bind a normal constituent such as dsDNA from the patient's cells and tissues (Rahman and Isenberg, 2008). More than 200 auto-antibodies have been described in SLE (Eloranta and Rönnblom, 2016) and 9 of the most common auto-antibodies are presented in more detail in a review by Rahman and Isenberg (2008). They range in prevalence from 10-90% within the patient and have a range of clinical effects. The most commonly found auto-antibodies are directed against single stranded (ss) and dsDNA, Ro/La antigens and ribonuclear protein (RNP) and can be present years before the clinical onset of SLE.

Anti-dsDNA antibodies are highly specific for lupus and are present in 70% of patients but only in 0.5% of healthy people or patients with other autoimmune disease, highlighting why these have been used as a key biomarker in SLE for many years. Among patients who have both elevated dsDNA antibodies and clinically quiescent disease, 80% have disease that becomes clinically active within 5 years after the detection of these antibodies (Rahman and Isenberg, 2008) suggesting that these antibodies can be used to some degree as biomarkers to predict future flares in the disease.

2.2.5. Immune complexes

Serum samples from SLE patients were found to contain immune complexes (ICs) which are capable of inducing a rare type of antigen presenting cell known as the plasmacytoid dendritic cell (pDC) to produce large amounts of the cytokine interferon (IFN)α (Meyer, 2009; Ohl and Tenbrook, 2011). In healthy individuals pDCs are unable to ingest apoptotic and necrotic material including DNA, so it is unable to reach the endosomal compartment in the pDCs required for the production of IFNα. However, if self DNA and RNA forms an IC with an autoantibody, pDCs are able to ingest the material. In addition the complex enables both DNA and RNA to escape extra and intra cellular degradation and reach the endosomal compartment where is has been demonstrated in pDC to induce IFNα production (Barrat et al, 2005; Meyer, 2009; Fransen et al, 2010). Work with human peripheral blood mononuclear cells (PBMC) have demonstrated that both the nucleic acids and the anti-dsDNA and anti-RNP antibodies are required for optimal induction of IFNα by ICs, as both

treatment with nucleosomes to denature the nucleic acids and the absence of the anti-dsDNA and anti-RNP antibodies inhibited the induction of IFNα (Barrat et al, 2005). The ICs enter the pDC via endocytosis through FcγRIIa (Lee, et al, 2008; Eloranta and Ronnblom, 2016). This is a crucial step as studies have demonstrated that ICs were unable to stimulate pDCs that have previously been treated with FcγRIIa blocking antibodies (Marshak-Rothstein, 2006).

The process described above is presented in Figure 2.2 as a two stage model of IFNα induction in autoimmune disease. Early apoptotic material is internalised by dendritic cells (DC) that activate B cells, and produce the first auto-antibodies. These bind the antigens to form immune complexes containing nucleoproteins released during late phase apoptosis. These immune complexes are internalised via FcγR expressed on the surface of pDCs and other DCs and increase the IFNα/β production as well as increased B cell stimulation. In addition, the immune complexes bind directly to B cell antigen receptors and are internalised for the activation of receptors within the B cells activating autoreactive B cells. These two processes result in further generation of auto-antibodies, which results in a self perpetuating vicious cycle in which immune complexes maintain a continual supply of IFNα/β (Meyer et al, 2009; Kawai and Akira, 2010).

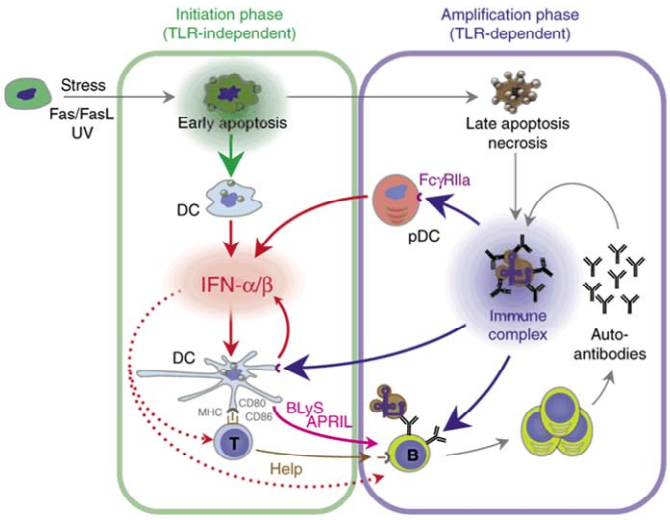

Figure 2.2 **Proposed two phase IFNα/β induction in systemic autoimmunity. The initiation phase is TLR independent and mediated by apoptotic cell material taken up by a specialized subset of lymphoid DCs, leading to IFNα/β production. Under the effect of IFNα/β, lymphoid and myeloid DCs upregulate MHC and co-stimulatory molecules and differentiate into efficient self-antigen presenting cells, leading to activation of quiescent autoreactive T helper cells. As a result of T-cell help, and the effects of BlyS, April and IFNα/β, autoreactive B cells proliferate and differentiate into plasma cells. Subsequent to the formation of nucleic acid containing immune complexes, the amplification phase is induced, which encompasses TLR-dependent IFNα/β induction in pDCs and DCs and enhanced B-cell proliferation and autoantibody production. Reprinted by permission from Macmillan Publisers Ltd: Nature Medicine 13: 543-551, © 2007.**

2.2.6. Plasmacytoid Dendritic cells

The dendritic cells (DC) are professional antigen presenting cells (APC), which circulate in peripheral tissues capturing pathogens or dying cells by phagocytosis upon which the DCs migrate to lymph nodes and present the antigens to T cells. This stimulates the T cells which then proliferate and differentiate into Th1 (cell immunity), Th2 (humoral immunity) or T regulatory (Treg) (suppressive) resulting in the induction of immunity or tolerance (Jin et al, 2008; Jin et al, 2010). It should be noted that the primary function of the DCs is not to

destroy the pathogens themselves but to prime the naive T cells (Ito et al, 2002) thus activating the adaptive immune response.

Two types of DC exist in human blood the plasmacytoid DC (pDC) and the myeloid DC (mDC). The two cells express different levels of surface markers which distinguish them from each other also indicating that they may play different roles within the immune system. For example, pDCs in healthy subjects express high levels of the major histocompatability complex (MHC) I but low levels of the co-stimulatory molecule cluster of differentiation (CD)86, both of which are required to stimulate T cells. In contrast, mDCs express high levels of both MHC I and CD86 suggesting that these cells are more effective than pDCs in stimulating T cells (Jin et al, 2008). In addition pDCs, have weak phagocytic activity and reduced capacity to produce Interleukin (IL)12 compared to mDCs (Asselin-Paturel, 2003).

In addition, mDCs have a distinctive start shaped morphology whereas pDCs look like plasma cells with a spherical morphology, extensive endoplasmic reticulum and the absence of dendrites (Reizis et al, 2011). During adult life pDCs are produced constantly from bone marrow, following which they circulate in the blood and also migrate to T cell rich areas such as the lymph nodes, spleen and thymus and tend to accumulate at sites of infection (McKenna, Beignon and Bhardwaj, 2005; Liu et al, 2005). They constitute less than 1% of human peripheral blood mononuclear cells, yet they produce the majority of type I IFNs, in the human body in response to detection of viral particles (Kim et al, 2015). Liu et al (2005) demonstrated that pDCs produced 100 to 1000 times more type I IFN than other cell types (approximately 3-10 pg/cell) in response to viral infection and it has also been reported that IFNs account for 60% of the genes expressed by the pDC (Fitzegerald-Bocarsly, Dai and Singh, 2008). pDCs are able to produce type I IFNs very rapidly due to the high expression levels of interferon regulatory factor (IRF) 7, which is a key component of the signal transduction complex required for the induction of IFN levels. Other cell types although capable of producing IFNα do not express IRF7 constitutively and require its up regulation therefore cannot deliver the large and rapid production of IFNα that pDCs are able to (Reizis et al, 2011). Due to the poor phagocytic activity of pDCs, the uptake of nucleic acids, including ICs, requires the expression of the FcγRIIa on the surface of the PDCs allowing efficient uptake into the endosomal compartments (Barrat and Coffman, 2008).

As well as being the main producers of type I IFNs, it has been well documented that human pDCs produce moderate levels of tumour necrosis factor (TNF)α and IL6 (Liu et al, 2005) and are capable of producing IL12, RANTES, IL10, interferon-gamma induced protein (IP) 10 and macrohage inflammatory protein (MIP)1α and MIP1β (Fuchsberger, Hochrein and O'Keeffe, 2005). The evidence for production of IL12, a key cytokine responsible for the induction of IFNγ and consequently the induction of Th1 cells, is controversial. It is widely accepted that human pDCs do not produce IL12, which is one of the main differences between human and mouse pDCs. The levels of IL12 that have on occasions been observed in human pDCs, have been attributed to inefficient cell sorting resulting in the presence of other cell types such as mDCs (Liu et al, 2005) which are considered the major source of IL12. pDCs also produce chemokines in the response to virus stimulation including CCL2, CCL3, CCL4, CCL5, CXCL10 (IP10) and IL8 in order to recruit both activated T cells, B cells, macrophages and NK cells, amongst others (Fitzgerald-Bocarsly, Dai and Singh, 2008). Two chemokine receptors are altered in expression upon activation of pDC by TLR7 agonists; CXCR4 which is decreased in expression and CCR7 which is increased in expression. The increased expression of CCR7 on dendritic cells is critical for the migration to the lymph node and together with the decrease in the expression of CXCR4 more specifically predisposes activated pDC to migrate to lymph nodes (Birmachu et al, 2007).

Prior to activation and maturation pDCs are inefficient at priming naive $CD4^+$ T cells compared to mDCs. However, once primed by mDCs, $CD4^+$ T cells can be skewed towards a Th1 response by pDCs. pDCs can promote the activation and expansion of memory $CD4^+$ T cell populations, thereby facilitating secondary or adaptive immune response, and in addition pDCs can contribute to the priming of antigen specific $CD8^+$ T cells and promote their survival (McKenna, Beignon and Bhardwaj, 2005; Reizis et al, 2011).

Following activation by either viral antigens or immune complexes, pDCs mature and change function from predominantly antigen capturing cells towards antigen presenting cells. The maturation is driven at least in part by the cytokine TNFα produced by the pDC, which drives the differentiation of the pDC into a mature antigen presenting cell (Fitzgerald-Bocarsly, Dai and Singh, 2008). During the process of maturation, pDCs lose their plasmacytoid morphology and their ability to produce large amounts of type I IFNs, and differentiate into cells with dendritic morphology (Reizis et al, 2011). In addition, during maturation the pDC develop an increased ability to load antigens on the MHC class I

(Guiducci, Coffman and Barrat, 2008), as well as increased expression of the MHC class II and co-stimulatory molecules CD80 and CD86 and thus acquire enhanced T cell stimulatory capacity (Liu et al, 2005; Reizis et al, 2011). Despite this increase, even after maturation pDCs remain less efficient at priming antigen specific naive T cells compared to mDCs. During the activation and maturation the pDCs secrete pro-inflammatory cytokines and chemokines. The signature of the cytokines secreted during this process and the co-stimulatory molecules expressed determine the type of T cell polarization e.g. Th1, Th2, Th17 or Treg (Fransen et al, 2010). They can also either directly or indirectly activate many other cell types such as monocytes, mDCs, B cells NK cells and T cells (McKenna, Beignon and Bhardwaj, 2005).

Jin et al (2010) examined the function of pDCs from healthy and SLE subjects in the absence and presence of apoptotic cells. They demonstrated that pDCs from healthy subjects in the presence of apoptotic cells did not induce autologous T cell proliferation, but did induce low levels of allogenous T cell proliferation and Treg development. From this they conclude that pDCs may play a tolerance role in immunity in health. In contrast, the pDCs from SLE patients induced allogenous T cell proliferation both with and without the presence of apoptotic cells and did not induce Treg development suggesting that this may contribute to a breakdown of immune tolerance and the development of autoimmunity. In addition the cytokine profile in stimulated pDCs from SLE patients suggested a Th1/Th2 imbalance toward Th2 dominance due to the presence of IL10 which induced a Th2 response, and decreased levels of IL18, which is involved in the induction of a Th1 response.

There is conflicting evidence around the numbers of pDCs in SLE patients. Studies have demonstrated increased numbers of circulating pDCs, and that disease activity was greater the higher the number of circulating pDCs in the blood (Jin et al, 2008). However others have reported that the frequency of circulating pDCs in the blood is markedly reduced in SLE patients (50-100 fold) which has been attributed to the migration of cells to lymphoid tissues and sites of inflammation as an increased number of pDCs can readily be detected in the skin, lymph nodes and in renal tissue from lupus patients (Barrat and Coffman, 2008; Rönnblom, 2010). This apparent reduction in the number of pDCs should be interpreted with caution as one of the primary therapies administered in SLE are corticosteroids which reduce the number of pDCs.

There is evidence to suggest a lack of negative feedback signals to the pDCs in SLE. In healthy humans B cells and NK cells strongly promote the function of pDCs after IC stimulation while monocytes decrease the function of pDCs via the inhibition of NK cells. In SLE the regulation of pDC function by monocytes is deficient due to a reduced production of reactive oxygen species (ROS) by monocytes. In addition, there is a deficiency of the complement protein C1q in SLE patients, which suppresses the activation of pDCs by IC (Rönnblom and Eloranta, 2013). Activation of pDCs increases their survival. *In vitro* studies have demonstrated that pDC survival was 60-70% and 30-40% after 24 and 48 h respectively, however, pDCs treated with IFNα they were 80-90% viable after 24 and 48 h respectively (Gibson et al, 2002).

In summary, pDC play a role in both the innate immunity through the production of type I IFN which activates the cells of innate immune system such as the NK cells and adaptive immunity through their ability to mature into potent antigen presenting cells (Guiducci, Coffman and Barrat, 2008).

2.2.7. Toll-Like Receptors (TLRs)

In considering immune conditions one important element is the recognition of foreign pathogens so that an appropriate immune response can be initiated. Pattern recognition receptors (PRR) on cells of the innate immune system recognize pathogen-associated molecule patterns (PAMPs) and/or danger-associated molecular patterns (DAMPs) from damaged tissue (Fuchsberger, Hochrein and O'Keeffe, 2005; O'Neill, Golenbock and Bowie, 2013).

The most widely expressed pattern recognition receptors in the innate immune system are a family of receptors known as the Toll Like receptors (TLRs) (Barrat and Coffman, 2008). They are the best characterised of the PRRs and are evolutionarily conserved across a diverse range of species (Horscroft, Pryde and Bright, 2012). To date, 13 mammalian TLRs have been identified, localised on cell surfaces, the endoplasmic reticulum or endosomal compartments (Baccala et al, 2007). They have a wide range of ligands including microbial (viral and bacterial) and endogenous ligands (Khoo, Forster and Mansell, 2011). The pDCs express a number of different PRR including the Toll like receptors (TLR) TLR7 and TLR9, the only other cell type to express both the TLR7 and TLR9 in humans are B cells. TLR7, TLR8 and TLR9 belong to a sub family based on their genomic structure, sequence, similarities

and homology (Forsbach et al, 2012). They are nucleic acid receptors that recognize pathogenic material particularly viral nucleic acids and well as self nucleic acids. Specifically the natural ligand for TLR9 is dsDNA containing un-methylated 5'-C-phospahte-G-3' (CpG) groups, while for TLR7 and TLR8 the natural ligand is ssRNA, including material complexed with auto-antibodies to form ICs. Studies using pDCs obtained from TLR7 knockout mice have confirmed that the stimulation of pDCs by ICs is dependent on this receptor (Marshak-Rothstein, 2006). TLRs 7 and 9 are located intra-cellularly on the endosome, which may be a safety mechanism to stop aberrant stimulation of the cell and maintain tolerance to self-antigens. In addition, a number of synthetic compounds that resemble nucleic acids have also been demonstrated to transduce their viral activities via the TLR receptors (Baccala et al, 2007; Meyer, 2009).

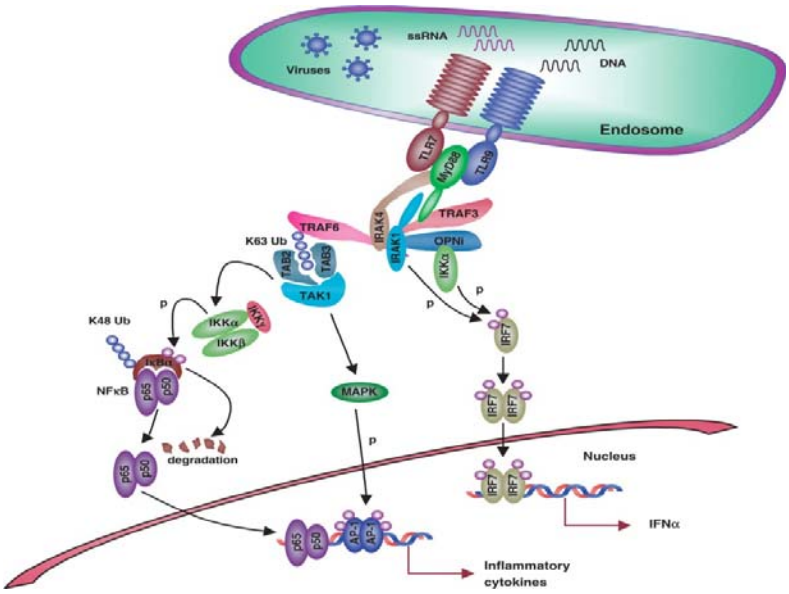

Figure 2.3 **TLR7 and TLR9 signalling pathway in pDCs. TLR7 and TLR9 recruit MyD88 to induce Type I IFN and inflammatory responses through the activation of IRF7 and NFκB respectively. In pDC, MyD88 for a signalling complex with IRAK1, IRAK4, IKKα, TRAF3, TRAF6, OPNi and IRF7. In response to ligand stimulation, IRF7 is phosphorylated by IRAK1 and IKKα, and translocates to the nuclei to regulate expression of type I IFN genes, espeacially IFNα. TRAF3, IRAK1, IKKα and OPNi are indispensable for IRF7 activation and dispensable for NFκB activation, however, IRAK4 and TRAF6 are indispensable for both NFκB and IRF7 activation. Kawai, T. and Akira, S. (2007) Antiviral signaling through pattern recognition receptor. *Journal of biochemistry*, 141, pp. 137-145, by permission of Oxford University Press.**

The signalling pathways activated through engagement of TLR7 and 9 within the pDC are presented in Figure 2.3 (Kawai and Akira, 2007). Signalling for both receptors is dependent on the cytoplasmic adaptor molecule myeloid differentiation primary response gene 88 (MyD88), which forms a complex with TNF receptor associated factor (TRAF)6, TRAF3, Interleukin-1 receptor-associated kinase (IRAK)4, IRAK1, IκB kinase (IKKα) and IRF7 to produce IFNα. TLR7 and TLR9 also signal through the nuclear factor kappa-light-chain enhancer of activated B cells (NFκB) pathway, which requires the activation of a signalling complex of MyD88, TRAF6, and IRAK4. This subsequently activates the IKK complex, which catalyses the phosphorylation of inhibitor of kappa B (IκBα) protein allowing NFκB to access the nucleus resulting in induction of transcription for a number of pro-inflammatory genes and cytokines including IL6 and TNFα. Like IRF7, NFκB is maintained inactive in the cytosol through association with IκB. Upon phosphorlyation, IκB is targeted for ubiquintination and NFκB is released to translocate to the nucleus (Bonjardim, 2005). The intermediates involved in TLR7 and 9 signalling have been elucidated in various mouse models. Mice deficient in MyD88, IRAK4 and TRAF6 have defects in both the IRF7 and NFκB pathways with subsequent impairment in the production of both IFNα and pro-inflammatory cytokines highlighting that these are important molecules for both pathways. However a deficiency in IRAK1 only results in the loss of IRF7 without affecting NFκB. A number of other molecules have been identified to play a role in the IRF7 signalling pathway but in most cases an exact role has yet to be elucidated. For example, a deficiency in a precursor of osteopontin called oestopontin-I, which co-localizes with MyD88 in the pDCs diminishes the translocation of IRF7 into the nucleus, providing evidence that this is a required component of the MyD88-IRF7 complex in pDC (Kawai and Akira, 2007).

Although IFNα is often the primary focus when considering the cytokines produced by pDCs it is worth touching on the other pro-inflammatory cytokines produced following TLR activation in pDCs. IL6 promotes the activation and/or differentiation of T cells, B cells macrophages and neutrophils, in patients with SLE, elevated levels correlate with disease activity (Jacob and Stohl, 2011). TNFα can trigger either pro-inflammatory or anti-inflammatory pathways depending which one of two receptor subtypes it binds to. Evidence for a role of TNFα in SLE is conflicting with some researchers demonstrating elevated levels correlating with disease activity while other researchers reported lower TNFα levels in SLE patients compared to healthy controls (Jacob and Stohl, 2011). This distinguishes the condition from other chronic autoimmune diseases such as Rheumatoid

arthritis (RA) and inflammatory bowel disease (IBD) where TNFα is a major cytokine in driving the disease pathogenesis.

There are a number of negative regulators of the TLRs which control TLR activation and subsequently the immune response. Intracellular regulators that inhibit the TLR signalling pathways may be expressed constitutively to control TLR signalling or alternatively up-regulated following TLR signalling and attenuate the response in a negative feedback loop. Regulation can also occur by reducing the synthesis of TLRs or degradation of the receptor. If all these fail, activation induced cell death ensures that the hyper-responsive cells are eliminated through apoptosis (Liew et al, 2005). It should be noted that pDCs also express the c-type lectin receptors BDCA-2 and BDCA-4 which have been implicated in cell adhesion and the regulation of signalling events. These receptors have gained interest as potential therapeutic targets as ligation of BDCA-2 with anti-BDCA-2 antibody significantly inhibits IFN secretion by pDCs in response to viral stimulation via TLR activation. BDCA-2 is down-regulated after pDCs mature, and following maturation, pDCs produce less IFNα/β following viral stimulation (McKenna, Beignon and Bhardwaj, 2005). Together these data suggest a role for BDCA-2 and potentially BDCA-4 in the production of IFNα from pDCs and that it may be a critical requirement for optimal signalling via the TLRs.

TLR7 has been shown to play an important role in several mouse models of SLE. Mice deficient in TLR7 were protected from disease progression, organ pathology and motility, which correlated with a decrease in autoantibodies specific for RNA containing complexes (Sun et al, 2007). In contrast, BXSB/Yaa mice lupus prone mice were found to have increased expression of the gene that encodes TLR7, which is regarded as a major functional contributor to the Yaa phenotype (Perry et al, 2011). In addition, it has been demonstrated in transgenic mouse models that TLR7 mediates the activation of autoreactive B cells. Human studies also support findings in mouse models. A human allele of the TLR7 gene with associated risk for SLE development in human males has also been reported (Perry, et al 2011). The role for TLR7 in the pathogenesis in SLE is supported by evidence that an SLE patient who acquired a genetic defect in TLR signalling experienced disease remission with disappearance of anti-DNA antibodies. The TLRs in the B cells act in synergy with the antigen receptor to induce proliferation, isotype switching and plasma cell differentiation (Deane et al, 2007).

2.2.8. The Type I Interferons

Cytokines are soluble factors which mediate the differentiation, maturation and activation of the various immune cells (Yap and Lai, 2013). The pathways involved are very complicated as the effects of cytokines are pleiotropic and include both synergistic and antagonistic effects on other cytokines (Jacob and Stohl, 2011). One such family of cytokines are the type I IFN family which comprises 13 IFNα subunits and one copy of IFNβ, IFNε, IFNκ and IFNω. Evidence is emerging that the different IFNα subtypes may have different actions and differentially regulate some of the IFN regulated genes. For example, while IFNα1, 2 and 21 all induced genes involved in the antiviral response, IFNα2 and 21 but not IFNα1 and IP10 in DCs (Schmidt and Ouyang, 2004). The production of IFNα is rapid with 60% of newly induced transcriptome genes being activated within 6 h after stimulation (Meyer et al, 2009). The majority of IFN is produced within 24 h following stimulation after which little is produced as pDCs become refractory to the same virus or different virus (Liu et al, 2005). IFNα plays an essential role in antiviral innate immunity by directly inhibiting viral replication in infected cells. IFNs are also considered to be important components linking innate and adaptive immunity (Asselin-Paturel et al, 2005). As a result, they affect the function of a large number of cell types in the immune system, including macrophages, NK cells and T cells, initiating and dictating the adaptive immune response (Kadowaki et al, 2000).

There is a large body of evidence that implicates IFNα in the pathogenesis of SLE and dates back to 1979 when increased levels of this cytokine were found in SLE sera (Kirou and Gkrouzman, 2013). In cross-sectional studies, IFNα activation is associated with activity and severity of the disease, however, this has not been shown in longitudinal studies. Interestingly high levels of serum IFNα in quiescent SLE patients predicted SLE flares in follow up visits suggesting it may be an important biomarker for disease prognosis (Kirou and Gkrouzman, 2013). The increased serum concentrations observed in SLE patients have been correlated with both disease activity and key markers, such as anti-DNA antibodies (Marshall et al, 2007; Barrat and Coffman, 2008). Further studies supporting the role of IFNα in SLE have suggested that SLE sera can promote differentiation of quiescent monocytes to fully proficient antigen presenting cells (APC), and this activity was neutralised with blocking antibodies against IFNα. The observation that a single injection of an anti-IFNα antibody could give sustained neutralisation of genes regulated by IFN is of

particular interest and supports the view that the ongoing production of IFN in lupus is at least partly a result of a self perpetuating vicious cycle (Rönnblom, 2010).

Supporting the role of IFNα in the development and progression of SLE comes from cases (~1%) where IFNα therapy for antiviral or anti-tumour purposes has induced lupus like syndrome. In these cases, 30 to 60% of patients produced antinuclear antibodies while 10% produced anti-dsDNA antibodies (Meyer, 2009). In many cases these symptoms disappeared after stopping the IFNα therapy, however, in <1% of patients these symptoms are not reversible and the patients develop SLE (Niewold, 2008).

Interestingly, *in vitro* investigation has shown that the depletion of pDCs in the blood of SLE patients only partially reduce IFNα production (Meyer, 2009). Therefore other cells may contribute to the IFNα concentrations in SLE. One such example could be the granulocytes as microarray analysis suggests that these are involved in SLE pathogenesis (Decker, 2011). Granulocytes, also known as polymorphonuclear leukocytes (PMNs) are capable of producing IFNα, are about 200 times more abundant than pDCs and can activate DCs. These cells are the first to be recruited to the site of action and may be responsible for the early production of IFNα in SLE prior to initiation of the more established pathways of autoantibodies and immune complexes (Decker, 2011). In addition, TLR2 derived IFNα from monocytes has been demonstrated to be a major source of IFN *in vivo* in animal lupus. Like granulocytes monocytes vastly outnumber pDCs and therefore may be at least partly responsible for the elevated levels of IFNα in SLE (Kalliolas and Ivahkiv, 2010).

2.2.9. Downstream effects of IFN

All the type I IFNs signal through the type I IFN receptor (IFNAR) which is expressed in all nucleated cells (Meyer et al, 2009; Pascual, Chaussabel and Banchereau, 2010). The receptors are high affinity low/number receptors with approximately $2x10^2$ to $3x10^3$ receptors per cell (although this is not fixed) and binding of IFNα to cells is saturable (Pestka and Langer, 1987). The receptor consists of two subunits IFNAR1 and IFNAR2 that are constitutively associated with Janus Kinase 1 (JAK1) and non-receptor tyrosine kinase 2 (TYK2) (González-Navajas et al, 2012). The JAK/STAT pathway is the major signalling cascade downstream of a number of receptor types including those for cytokines and chemokines, and consists of the JAK family of non-receptor tyrosine kinases and signal transduction and transcription (STAT) family of transcription factors. Stimulation of cells with a cytokine for

example results in the activation of JAKs which phosphorylate and activate STATs promoting their dimerization and nuclear transcription where they regulate transcription of STAT dependent genes (Seavey and Dobrzanski, 2012). For the type I IFNs, signalling through the IFNAR receptor involves the phosphorylation of JAK1 and TYK2, and subsequently STAT 1 and 2. A complex of STAT1 and 2 together with IRF9, which is known as the IFN-stimulated gene factor 3 (ISGF3) complex (González-Navajas et al, 2012), translocates to the nucleus where it binds to IFN regulatory elements and triggers the transcription of several hundreds of type I IFN-stimulated genes (ISGs) (Eloranta and Rönnblom, 2016).

The binding of IFN primarily occurs through IFNAR2, however, both receptor chains are required for signal transduction. The antiviral activity of IFNs correlates with their binding affinities to IFNAR2 while anti-proliferative activity depends rather on the affinity to IFNAR1 (Delgardo-Vega, Alarcon-Riquelme and Kozyrev, 2010). The signalling pathways for the type I and type II IFNs are presented in Figure 2.4 (González-Navajas et al, 2012). Whilst both type I and type II interferons bind to their independent receptors, they can induce the expression of the same genes by the same elements such as the IFNγ activated binding site (GAS) enhancing element. Type II interferon cannot induce the formation of the ISG3 complex and therefore is not able to promote the engagement of IFN stimulated response elements (ISRE) sites and the activation of corresponding genes (González-Navajas et al, 2012).

Interestingly the pDC express the IFNAR and therefore the type I IFNs have the capability to stimulate pDCs in both an autocrine and paracrine manner leading to augmentation of the type I IFN response (Reizis et al, 2011). The role of this self priming of IFNα is to activate neighbouring cells to viral infection and accelerate the antiviral response (Gary-Gouy, Lebon and Dalloul, 2002). Also, IFNα induces the expression of TLR1, 2, 3 and 7 on APCs including pDCs, mDCs and monocytes (Schmidt and Ouyang, 2004) and induces the expression of IRF7 (Kalliolas and Ivahkiv, 2010) in pDCs. Ultimately these all lead to the amplification of type I IFN production (Kalliolas and Ivahkiv, 2010). As well as positive feedback mechanisms there are a number of mechanisms that provide negative regulation of IFN signalling including receptor internalisation and degradation, dephosphorlyation of JAKs and STATs, induction of suppressors of cytokine signalling (SOCS) and regulation of

STAT1 activation by TNF receptor 1-associated death domain proteins (TRADD) (Baccala, Kono and Theofilopoulos, 2005).

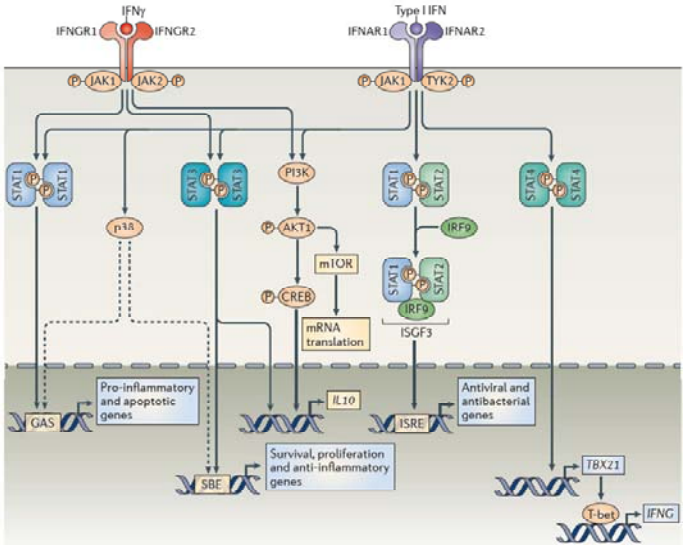

Figure 2.4 **Signalling pathways activated by Type I and Type II IFNs. Different STAT family members can be activated by IFNs. STAT1 STAT2 heterodimers, which are activated by Type I IFNs, bind to IRF9 in the cytosol to form the ISGF3 complex, which in turn migrates to the nucleus to bind to ISREs and activate antiviral and antibacterial genes. Reprinted by permission from Macmillan Publisers Ltd: Nature Reviews Immunology 12: 125-135, © 2012.**

The main role of the interferons it to act as an early line of defence against viral infections, and it has been demonstrated that they can have an action at almost any stage of viral replication. Binding of IFNα to the IFNAR results in both the up regulation and down regulation of a large number of genes that regulate a number of functions including, defence mechanisms against viruses, apoptosis, cell cycle, inflammation, innate immunity and adaptive immunity (Birmachu, 2007; Meyer, 2009). Some of most commonly discussed genes include the classical antiviral proliferative transcripts (2'-5' oligoadneylate (OAS), myxovirus resistance 1(Mx1)), IFN regulatory factors (IRF5 and IRF7), pro-apoptotic molecules (FAS and TNF related apoptosis inuding ligand (TRAIL)), B cell differentiation factors (B lymphocyte stimulator (BlyS)) and chemokines and cytokine receptors (CCL2 and CXCL10) (Pascual, Chaussabel and Banchereau, 2010). The best characterised IFN-induced

antiviral pathways utilize the dsRNA-dependent protein kinase R (PKR), the 2-5 A system and the Mx proteins (Stark et al, 1998; Horscroft, Pyrde and Bright, 2012).

The gene profile induced by the type I IFNs is known as the IFN gene signature and has been utilised as a biomarker for the diagnosis, analysis of disease progression and effects of treatment in IFNα mediated autoimmune diseases. The type I IFN gene signature has been demonstrated in the PBMC of SLE patients and has been correlated with disease activity, renal manifestations and increased damage index (Jacob and Stohl, 2011). A common treatment for auto-immune disease is high-dose intravenous steroids, which cause pDC depletion resulting in inhibition of the IFN signature, however both the pDC numbers and the IFN signature return less than one week after steroid administration (Pascual, Chaussabel and Banchereau, 2010).

IFNα also affects the function of cell types of both the innate and adaptive immune system. A simplified pathway of the affects of Type I IFNs on immune cells including the induction of various cytokines is presented in Figure 2.5.

IFNα enhances innate immunity through the activation of the NK cells which leads to an increase in cell mediated cell cytotoxicity enabling the NK cells to kill virus infected cells (Schmidt and Ouyang, 2004; Asselin-Paturel et al, 2005). Following IFNα activation, NK cells produce IFNγ (Rönnblom and Pascual, 2008) which has a key role in the activation of macrophages. Interestingly, IFNα has been demonstrated to inhibit IL12, which is an important cytokine for NK cell activation and IFNγ production (McKenna, Beignon and Bhardwaj, 2005) suggesting that IFNα can have both stimulatory and inhibitory effects on NK derived IFNγ. Activation of the NK cells results in enhanced apoptosis, which leads to increased levels of cellular debris in the circulation resulting in elevated levels of autoantibodies and subsequently immune complex formation (Schmidt and Ouyang, 2004). This provides another positive feedback loop to augment the production of IFNα and could lead to tissue damage and antigen overloading, which is one of the major contributors in the development of SLE (Kim et al, 2015). One of the IFN inducible genes is ISG15, which has been shown to act as a cytokine to stimulate IFNγ production and increased proliferation of NK cells and enhanced cytotolic activity (Birmachu et al, 2007).

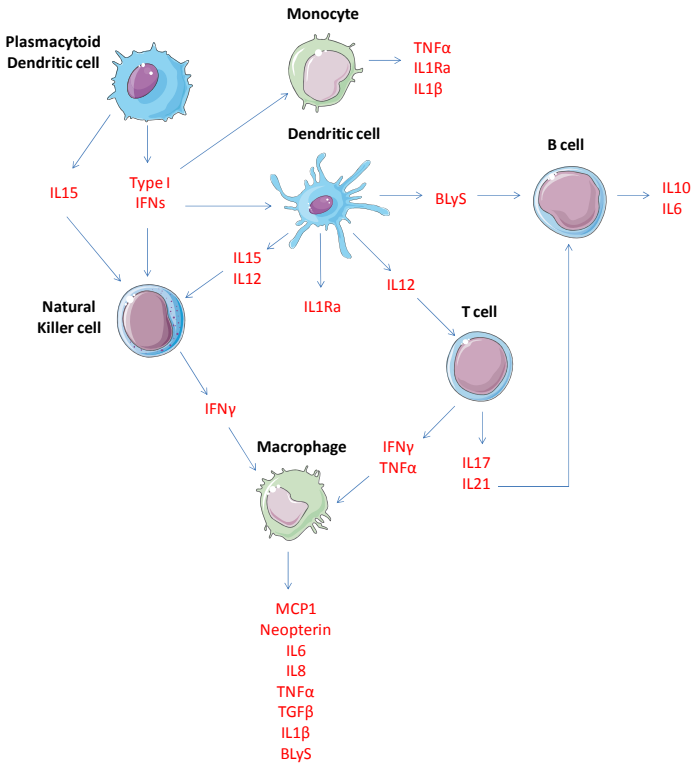

Figure 2.5 **A simplified pathway of the affects of IFNα on various immune cells and subsequent induction of cytokines /chemokines. Type I IFNs released from pDCs directly sitmulates monocytes, dendritic cells and NK cells. Stimulated dendritic cells through the release of various other cyotkines/chemokines can activate B cells, T cells and NK cells, while both activated NK cells (directly via Type I IFNs or indirectly via dendritic cells) and T cells release IFNγ which activates macrophages.**

IFNα also has an action on $CD8^+$ T cells keeping them alive and enhancing their proliferation. These actions can occur both directly or indirectly via the release of the cytokine IL15 from IFNα activated DCs (Baccala, Kono and Theofilopoulos, 2005), which is a strong and selective stimulator of memory-phenotype $CD8^+$ T cells (Theofilopoulos et al, 2005). The activation of naive $CD8^+$ T cells is also dependent on IFNα induced IP10 and the chemokine CXCR3 (Theofilopoulos et al, 2005). DCs derived from SLE patients have been demonstrated to promote the differentiation of $CD8^+$ T cells into cytotoxic T cells (Baccala et al, 2007) and sera from SLE patients promotes the differentiation of CD8+ T cells (Pascual, Farkas and Banchereau, 2006).

IFNα stimulates the maturation of conventional DCs resulting in the up regulation of MHC I and MHC II, co-stimulatory molecules such as CD40, CD80 and CD86 and chemokine and cytokine receptors (Rönnblom, 2010). It also induces the production of the cytokines TNFα, IL6, IL10, IL12, IL15, IL18, IL23, BLyS and A proliferative inducing ligand (APRIL) and the chemokines CCL3, CCL4, CCL5 and CXCL10 (Delgado-Vega, Alarcon-Riquelme and Kozyrev, 2010). Ultimately, the maturation of DCs results in up regulation of the chemokines and their receptors leading to efficient homing of DCs in secondary lymphoid organs and the subsequent activation of T cells (Baccala, Kono and Theofilopoulos, 2005). In addition the increased IL15 production by DCs causes a strong and selective stimulation of memory-phenotypes $CD8^+$ T cells (Theofilopoulos et al, 2005).

The sera from SLE patients promotes the differentiation of quiescent monocytes to fully proficient APCs (Schmidt and Ouyang, 2004). This results in the up regulation of MHC and other co-stimulatory molecules which enables them to capture antigens and present them to autoreactive $CD4^+$ T cells (Kirou and Gkrouzam, 2013) and $CD8^+$ T cells (Marshak-Rothstein, 2006). Also the monocyte derived DCs produce the Th1 promoting cytokine IP10 (McKenna, Beignon and Bhardwaj, 2005) in addition to BlyS and APRIL promoting the Th1 immune pathway and having the potential to activate B cells (Theofilopoulos et al, 2005). The induction of monocyte derived DCs enables the presentation of viral antigens to T cells which induces a strong T cell mediated antiviral response (Liu, 2005).

Sera from SLE patients with active SLE promotes the maturation of DCs and blood monocytes derived from these patients *in vitro.* This action has been attributed to IFNα which consequently results in a reduced number of immature DCs. This potentially plays an important role in the pathogenesis of SLE as autoreactive lymphocytes that have escaped from the central checkpoint of the thymus are normally controlled in the periphery by immature DCs lacking co-stimulatory molecules. The reduced numbers of immature DCs results in impaired regulation of autoreactive T cells, which is one of the key cell types implicated in SLE (Kalliolias and Ivahkiv, 2010). Immature T cells are also important for the maintenance of regulatory T cells (Tregs) which have an immunosuppresive role and maintain tolerance to self-antigens (Eloranta and Rönnblom, 2016).

IFNα has a number of effects on T cells however the main effect is to drive the differentiation of naive T cells down the T helper cell 1 (Th1) pathway whilst inhibiting the development of Th2 responses. Activated or mature DCs produce IL12 which directs Th cell

differentiation into Th1 effector cells (Medzhitov, 2001). Through the up-regulation of the co-stimulatory molecules CD80 and CD86 on APCs, IFNα can directly increase the number of T cells including autoreactive T cells (Ohl and Tenbrock, 2011). IFNα promotes the survival of T cells both directly and indirectly by exerting pro-apoptotic and anti-proliferative effects. Indirect actions include the IFNα driven production of IL15 from DCs which promotes the survival and proliferation of T cells (Baccala, Kono and Theofilopoulos, 2005). The activation of T cells induces the production of IFNγ, a key cytokine in the Th1 response, and IL10 thereby theTh1 response (Theofilopoulos et al, 2005). As well as driving the Th1 pathway the type I IFNs also promote Th17 responses by inducing IL6 and IL23 production by pDCs. The resulting Th17 T cells produce the cytokine IL17 which alone or in conjunction with BLyS can induce B cell hyperactivity and differentiation into antibody producing cells (Kim et al, 2015). IFNα also enhances autoimmunity including, in SLE, by inhibiting regulatory T cells (Tregs) which have an immunosuppressive activity (Kirou and Gkrouzam, 2013). Overall these effects lead to the expansion of autoreactive T cells and an enhanced inflammatory response (Eloranta and Rönnblom, 2016)

IFNα also has multiple direct and indirect effects on the function of B cells and facilitates humoral autoimmunity. IFNα increases B cell proliferation and can have a direct effect on B cell activation. Studies in mice demonstrate that B cells up-regulate TLR7 and TLR9 20 fold and 3 fold, respectively, following IFNα treatment suggesting that it can increase the ability of nucleic acids to activate B cells (Thibault et al, 2009). IFNα can also lower the threshold required for activation through the B cell receptor (Elorant and Rönnblom, 2016) and increase the sensitivity of B cells to CpG DNA which may be in part due to the up regulation of TLR9. It may also facilitate stimulation of B cells by non CpG DNA (Yap and Lai, 2013). IFNα activated DCs produce BLyS and APRIL which drive the activation of B cells. These have a role of increasing B cell survival including the survival of autoreactive B cells, increasing B cell differentiation and antibody class switching which enhances antibody production and secretion. In the case of SLE, this leads to the generation of pathogenic autoantibodies (Schmidt and Ouyang, 2004, Kim et al, 2015). The activation of B cells is an example of another positive feedback loop in SLE whereby antibodies produced by autoreactive B cells form immune complexes and activate pDCs to release IFNα which can then promote B cell survival, activation and differentiation (Barrat and Coffman, 2008). B cells and plasma cells derived from SLE patients express high levels of BLyS and APRIL mRNA and elevated circulating BLyS levels are observed in as many of 50% of SLE patients (Jacob and Stohl,

2011) and these levels correlate with disease activity and levels of autoantibodies. Other pDC and IFNα induced cytokines can also have an influence on the activation of B cells. pDC derived IFNα and IL6 induces CD40 activated B cells to develop into plasmablasts and differentiate into antibody secreting cells (McKenna, Beignon and Bhardwaj, 2005; Fitzgerald-Bocarsly, Dai and Singh, 2008). T cell derived IL10 can directly promote autoreactive B cell proliferation and Ig class switching (Schmidt and Ouyang, 2004) and elevated levels of IL10 have been observed in SLE patients (Chun et al, 2007).

The actions of IFNα discussed above highlight the wide reaching the effects of this cytokine, encompassing cells of both the innate and adaptive immune system. It also highlights the number of different cell types and cytokines that are implicated in the pathogenesis of SLE and the cyclic nature of the disease with many positive feedback loops resulting in the continued activation of the immune system. There is ample evidence to suggest that IFNα plays a central role in the development and ongoing pathogenesis in SLE.

2.3. Diagnosis and biomarkers in SLE

2.3.1. Introduction

As well as the challenges in understanding the complex and numerous immunological pathways that drives the pathogenesis of SLE. There are additional challenges in diagnostic assessment of the disease and suitable biomarker identification. Diagnosis tests are judged by their ability to accurately distinguish individuals with a particular disease, regardless of the level of disease activity, from those who do not have the disease whilst not missing those patients with inactive disease (Tektonidou and Ward, 2011). A variety of indices, instruments and other assessment tools based on clinical signs, with serological and histological evaluations (Kazemipour et al, 2015) are available for monitoring disease activity and response to therapy in patients with SLE (Parodis, Axelsson and Gunnarsson, 2013). The most commonly used index is the SLEDAI (Systemic Lupus Erythamtosus Disease Activity Index) which is based on the presence of 24 features in nine organ systems. It measures disease activity in patients with SLE in 10 days preceding the assessment. Alternative/revised versions include SLEDAI-2000 and the SELENA-SLEDAI (Safety of Estrogen in Lupus National Assessment – SLEDAI). The BILAG (The British Isles Lupus Assessment Group) and revised BILAG 2004 are other commonly used disease assessment tools where nine organ systems are evaluated and weighted for disease severity (Parodis, Axelsson and Gunnarsson, 2013). There is no gold standard disease index to use in the clinic

and clinical trials and the current trend is towards composite responder indices such as the SRI which is a combination of the SELENA-SLEDAI, BILAG and physicians global assessment (PGA), as well as the development of flare assessment tools (Rao and Gorden, 2014).

The EMA (2013) suggest one reason that clinical trials investigating the efficacy and safety of new treatments for SLE are unsuccessful is the lack of predictive biomarkers and surrogate endpoints. A large number of biomarkers have been investigated but only a few of these have been fully validated (Chun et al, 2007; EMA, 2013). Tektonidou and Ward (2011) define biomarkers as "*characteristics that are objectively measured and evaluated as indicators of normal and pathogenic biological processes or pharmacologic responses, can be used to help diagnose disease, to assess disease activity and response to treatment, or to predict prognosis*". These differ from the clinical endpoints, which are defined as "*characteristics or variables that reflect how a patient feels, functions or survives*" and surrogate endpoints which are defined as "*biomarkers that are intended to substitute for a clinical endpoint*". These are more applicable to outcomes in clinical studies (Mittleman, 2004). Taking these definitions into account, biomarkers may be used in preclinical studies, as well as in the clinic (including clinical trials) where they may be used to diagnose disease, monitor disease activity, predict flares, predict and describe damage and predict and monitor response to therapy. In contrast clinical end points and surrogate markers are only applicable to the outcomes of clinical studies and to enable treatment decisions in clinical practice (Illei et al, 2004)

The selection of a biomarker for use in the clinic and/or clinical trials requires validation of the predictive nature of the biomarker, as a measure of response to treatment or disease progression, and the feasibility and reliability of the measurement procedure in the clinical setting. It is also important to relate the biomarker to a validated disease activity. The search for robust biomarkers in SLE is challenging. In a review of translation studies of potential biomarkers for autoimmune disease, Tektonidou and Ward (2010) found that less than half incorporated design features needed for valid interpretation of clinical associations. These limitations hamper the understanding of the potential of biomarkers in the disease diagnosis, and the assessment of activity and prognosis of disease. Illei et al (2004) give an excellent in-depth review of the various biomarkers both traditional (complement) and prospective (cytokines) investigated in various clinical studies in SLE and

their potential as biomarkers. A number of traditional and prospective biomarkers are discussed below.

2.3.2. Antibodies

The American Rheumatism Association criteria for the diagnosis of SLE include several auto antibodies. Despite this, most antibodies have not proven to be particularly useful biomarkers or surrogate markers in clinical trials (Utz, 2004). Antinuclear antibodies (ANA) although sensitive for SLE as most people with SLE have ANA, are also only detectable in about 1 in 3 healthy individuals and are also common in certain subsets of pateints without SLE such as unwell elderly individuals (Egner, 1999). ANA often precede clinical manifestations, for example, Eriksson and Rantapää-Dahlqvist (2014) found that ANA specificities were detectable approximately 5.6 years before the onset of symptoms in 63% of individuals. Amongst the various ANA, anti-dsDNA antibodies are classic biomarkers of lupus disease (Smith et al, 2009), however, anti-dsDNA does not necessarily fluctuate with disease activity and a substantial portion of SLE patients are anti-dsDNA negative (Elwy, Galal and Hansan, 2008). Table 2.1 shows a summary of the common ANA observed in SLE.

2.3.3. Acute phase proteins

The erythrocyte sedimentation rate (ESR) is a sensitive but non-specific indicator of activity in SLE and is slow to reflect changes in disease activity (Egner et al, 1999). C-reactive protein (CRP) rapidly reflects acute inflammation (Egner et al, 1999); and has been correlated significantly with the BILAG score and neopterin levels (Elwy, Galal and Hansan, 2010).

Table 2.1 Summary of auto-antibodies observed in SLE. Adapted from Egner (2000) and Bertsias, Salmon and Boumpas, (2010)

Auto-antibody	Diagnostic feature	% Positive at any stage of the disease
Anti-double stranded (ds) DNA	• ARA criterion for SLE Correlated with • SLE • Nephritis • Progression to end stage renal disease • Increased disease severity • Damage or poor survival Issues • Can be negative early in disease or after treatment or when patients are in clinical remission	30-70
Anti-phospholipid	Strongly associated with • Antiphospholipid syndrome • Central nervous system involvement • Severe renal involvement • Damage • Death • Titres vary with disease activity Issues • Not all Anti-phospholipid positive patients with SLE have antiphospholipid syndrome • Anti-phospholipid negative patients can have thrombotic complications	40-50
Anti-C1q	Correlated with • Renal disease Issues • Of limited clinical use	90
Anti-Ro Anti-La	• Found in SLE and Sjorgens syndrome. • Useful when anti-dsDNA are absent Associated with • Cutaneous SLE • Congenital heart block Issues • Not specific to SLE • Cannot distinguish drug induced SLE from idiopathic SLE	10-15
Anti-Sm	• ARA criterion for SLE • Rarely seen outside SLE • Appear with disease evolution • Titres can fluctuate with disease activity and treatment Issues • Serial monitoring does not predict relapse	20-40
Anti-histone	Issues • Not specific to SLE • Cannot distinguish drug induced SLE from idiopathic SLE	50-80

2.3.4. Complement proteins

The measurement of C3 and C4 complement proteins has traditionally been used to monitor SLE disease activity. However, their value is questionable in SLE as C4 null alleles

are common so that baseline C4 may be chronically low, and SLE can also be active without causing changes in C3 and C4 concentrations, during inflammation both complement synthesis and complement consumption increase (Egner et al, 1999; Illei et al, 2004). Elevated levels of complement cleavage products, which are produced upon activation of the complement cascade, have been demonstrated to better reflect disease activity than conventional measurements. These include C4d, which binds to various cells, and when bound to erythrocytes has been proposed as a sensitive diagnostic marker for SLE. A longitudinal study over 5 years in 156 patients demonstrated that erythrocyte bound C4d measurements were associated with the Systemic Lupus Acitvity measure (SLAM) and SELENA-SLEDAI (Tektondiou and Ward, 2011). The C4d/Cr1 erythrocyte test was 81% sensitive and 91% specific for SLE versus healthy controls (Lui and Ahearn, 2009). In addition platelet bound C4d and reticulocyte bound C4d have been proposed as potential biomarkers for SLE diagnosis and monitoring disease activity respectively (Lui and Ahearn, 2009). Unfortunately assays to measure the cleavage products are not widely available and require special sample handling. This makes routine clinical use impracticable (Egner, 2013) and suggests that at this time they are not feasible biomarkers.

2.3.5. IFN gene signature

The IFN gene signature comprises a set of characteristic IFNα inducible genes that are expressed at elevated levels in blood cells of both adult and paediatric patients with SLE (Barrat and Coffmann, 2008; Kalunian, 2016). These genes can be conveniently measured by Taqman quantitative PCR or microarray and have better sensitivity and specificity than traditional protein bioassays. In one study, concentrations of IFNα were only determined in the serum of 2 out of 38 SLE patients while an IFN score was determined in approximately half (24) of the SLE patients (Baechler et al, 2003). Several well defined gene signatures have been used to correlate type I IFN gene signature with SLE disease pathogenesis and disease activity in patients in both cross-sectional and longitudinal studies (Tektondiou and Ward, 2011). In addition, the type I IFN gene signature is extinguished with high dose steroids (Smith et al, 2009) and has been used to assess drug target interaction (PK/PD) of anti-IFNα therapy in SLE (Wang et al, 2013). There is variation in the IFN gene signature assessed in SLE patients across various studies and among health individuals over time and by age and sex (Tektondiou and Ward, 2011), however there are some common markers that are generally observed across the studies. These include Mx1, interferon induced

protein with tetratrico peptide repeats (IFIT)1, IFIT4, OAS, lymphocyte antigen 6E (Ly6E) and phospholipid scramblase 1 (PLSCR1) (Smith et al, 2009). Due to patient to patient variation in the expression of individual genes, a comparison of the cumulative IFN response gene score between patients and healthy volunteers has been proposed (Smith et al, 2009). Standardisation of both the analytical methodology and the IFN response gene panels between laboratories and clinical studies will enable the comparison of results between studies.

2.3.6. Cytokines and chemokines

Cytokines and chemokines offer promise as potential biomarkers in SLE, as they play a key role in the pathogenesis of SLE, are easily accessible, and many can be conveniently and specifically quantified (Stpinska and Paradowska-Gorycka, 2015). However, a 2010 review of clinical study design in SLE found that cytokines and chemokines had only been used as biomarkers for diagnosis of disease in 13% and for disease activity in 4% (Tektondiou and Ward, 2010). Caution is required when using cytokines as biomarkers, as factors such as age, sex, stress, diet and sample handling can affect their expression and must be taken into account. These factors have often been overlooked in clinical studies, limiting the interpretation of their value as biomarkers which in turn may explain why they are not routinely used in clinical studies (Tektondiou and Ward, 2010, Stpinska and Paradowska-Gorycka, 2015).

Illei et al (2004) give an in-depth review of the potential of various cytokines as biomarkers for SLE. Given its role in the pathogenesis of SLE, IFNα is a candidate, however, serum concentrations in SLE patients are often very low and hard to detect. Despite this, a number of studies have reported increased serum levels of IFNα in patients suffering from severe SLE. It increases markedly at flares and its levels correlate positively with the SLEDAI score, level of anti-dsDNA antibodies and inversely with IL10, C1q, C3 and leukocytes (Stpinska and Paradowska-Gorycka, 2015).

A whole host of other cytokines have been proposed as biomarkers including the Th1 cytokines IL2, IL12 IFNγ and the Th2 cytokines IL4, IL5, IL6 and IL10 (Chun et al, 2007) and the Th17 cytokines IL17 and IL23 (Stpinska and Paradowska-Gorycka, 2015). One study with 166 SLE patients revealed that serum levels of IL6, IL10, IL12 and IFNγ were elevated in SLE patients and the levels of IL6 and IL10 correlated with disease (Chun et al, 2007). IL6 has

been observed in the serum and urine of SLE patients and correlates with disease activity and anti-dsDNA, ESR and CRP whilst IL10 levels in serum correlates positively with ESR and anti-dsDNA antibodies but negatively with complement fraction C3d (Stpinska and Paradowska-Gorycka, 2015). Despite promise, Illei et al (2004) conclude that for both IL6 and IL10, conflicting data make them unlikely to be valid biomarkers in SLE. Two further cytokine related biomarkers of potential interest are IL1 receptor antagonist (IL1Ra) and the soluble IL2 receptor (SIL2r). IL1Ra blocks IL1, which is an important mediator of tissue damage in several chronic autoimmune diseases, and in a longitudinal study high serum levels have been observed during flares not involving the kidney. A strong correlation was observed with the SLEDAI score in a cohort of 31 patients with both active and inactive disease. Soluble IL2 receptor (SIL2r) has been investigated in numerous studies and elevated levels have been observed in patients with active disease. Several longitudinal studies have demonstrated a strong correlation between sIL2R levels and SLEDAI and ECLAM indices, an increase in levels during flares, and a decrease with treatment and clinical improvement (Illei et al, 2004).

BLyS, also known as B cell activating factor (BAFF), is a key growth factor for B cells and both mRNA and protein levels are higher in SLE patients than healthy controls. Elevated levels are observed in about 30% of patients and generally correlate with anti-ds DNA. Although a change in serum BLyS does not necessarily correlate with a change in disease activity, BLys levels can correlate with a higher disease activity score at a subsequent visit. This suggests a delayed causative relationship between circulating BLyS levels and SLE disease activity, and that BLyS levels may be related to the future development of the disease within a patient (Liu and Ahearn, 2009; Stpinska and Paradowska-Gorycka, 2015).

Increased serum levels of IFN-regulated chemokines and IFN inducible chemokine gene expression scores have been identified in patients with SLE, compared with healthy and disease control groups. The levels correlated with disease activity (Tektondiou and Ward, 2011) and can even be detected in patients with a weak IFN signature (Rönnblom and Eloranta, 2013). A longitudinal study of 267 SLE patients over 1 year demonstrated that the IFN regulated chemokines IP10 and MIP3B were significantly higher in patients with active SLE compared to inactive SLE. Patients with high compared to low chemokine levels had a higher fraction of active disease, higher absolute disease activity (SLEDAI), higher anti dsDNA titres and lower complement CS levels. The authors concluded that chemokine

levels serve as biomarkers for current SLE disease activity. The chemokine levels also increased in patients between pre flares and flare visits suggesting that patients with inactive disease and high chemokine levels are at an increased risk of future flares within 1 year. Interestingly none of the common laboratory tests such as ESR, complement or anti-dsDNA antibodies were significant predictors of flare. This indicates that measuring chemokine levels in the clinic may be a predictor of future activity (Tektondiou and Ward, 2011).

2.3.7. Neopterin

Another potential marker is neopterin which is secreted in large quantities by human monocytes/macrophages upon activation by IFNγ and IFNα (Carstens and Andersen, 1994; Dale and Brilot, 2010). It is a marker of immune cell activation and levels are elevated in the majority of patients with SLE and correlated with disease activity. In patients with inflammatory diseases elevated levels of neopterin are observed earlier than other biomakers such as ESR or cytokine levels suggesting neoptetin could be an early marker of disease (Akgul et al, 2013). Neopterin is removed from the body by the kidneys (Carstens and Andersen, 1994; Akgul et al, 2013) and when serum levels of neopterin change urine levels also change (Akgul et al, 2013). Therefore urine measurements offer a non invasive way to measure biomarker concentrations. Neopterin levels have decreased close to healthy controls in patients treated with corticosteroids therapy (Akgul et al, 2013) and antimalarial therapy (Rho et al, 2011)

2.3.8. Summary

Smith et al (2009) suggest that for SLE pharmaceutical companies and clinical trialists need to commit to the evaluation of multiple exploratory biomarkers within clinical studies. Liu and Aheran (2009) state that some biomarkers may be used to facilitate accurate diagnosis of SLE, some may help identify those prone to develop SLE, some may be used to monitor disease progression and some may be used to evaluate response to therapy. An ideal biomarker/test will be specific (only detecting those with the disease), sensitive (detecting all those with the disease) and have both high positive predictive value and high negative predictive value (Egner, 2013). Biomarkers should also be translatable between preclinical and preclinical models. Agoram and Van der Graaf, 2012, highlight that the successful transition between experiments in highly unreliable animal models of disease to more

focused models based on the target and disease pathways will depend on the availability of reliable biomarker and biomeasure data.

2.4. Current and prospective treatments for SLE

Autoimmune diseases tend to persist for the life of the patient, and due to the chronic nature of these diseases they are currently “managed” rather than “cured”. In the past, a diagnosis of SLE often implied a decreased life span but recent improvements in care have dramatically enhanced survival of SLE patients (FDA, 2010). Increased survival rates are, however, associated with increased costs of care with a mean annual direct medical cost in the UK it is estimated to be £3231 per patient, and higher in patients with severe SLE, patients with renal disease involvement and patients experiencing severe flares (Khamashta et al, 2014).

Treatment for SLE is multifactorial and includes education, such as avoidance of ultra violet (UV) light, and therapies to treat both the disease and other complications, which may be treatment related. Current treatment regimens for SLE include 1) corticosteroids, 2(immunosuppressants and 3) anti-malarials (Strand et al, 2013). The standard treatment regimes for commonly administered therapies in SLE are summarised in Table 2.2.

Dexamethasone, is used to treat underlying conditions in SLE and has been successfully used to validate some of the lupus prone mouse disease models (Seavey, Lu and Stump, 2011). Chronic or acute therapeutic administration of glucocorticoids can lead to significant depression of pDC number and function in peripheral blood (Shodell, Shah and Siegal, 2003). Data from healthy volunteers (aged 29-61) show that a short course of moderate-dose corticosteroid therapy (prednisone 30 mg oral for four days) substantially alters both the numbers and function of circulating pDC. One concern with corticosteroids is the risk of infection as patients with SLE have impaired innate and adaptive immune systems. Infections are important causes of morbidity and mortality (Durcan and Petri, 2016).

Table 2.2 Current treatments used for SLE (Seavey, Liu and Stump, 2011)

Drug	Action	Dose	Regime	Route
Cyclophosphamide	Cytotoxic	0.5-1 g/m^2 BSA	once monthly	iv
Azathioprine	antimetabolite	1-3 mg/kg	daily	orally
Methotrexate	antimetabolite	7.5-25 mg	weekly	orally / im
Mycophenolate mofetil	antimetabolite	1 g	3-5 days	iv
hydroxychloroquine	antimalarial	650 mg	1-2 times a day	orally
Methylprednisolone	corticosteroid	1 g	Once daily for 3 days	iv (over 30 min)
Prednisolone	corticosteroid	10 mg	daily	orally

Hydroxychloroquine (HCQ) has been used to treat some forms of lupus for nearly 180 years and for SLE since the 1950s. Due to its multiple beneficial effects, including control of disease activity, reduction in cardiovascular events and improved survival, it is now recommended in the long term for all SLE patients (Frieri, 2013). HCQ is effective in treating mild SLE manifestations including the prevention of new mild SLE, however, it is ineffective in preventing severe SLE (Yildrim-Toruner and Diamond, 2011). The immune cells from SLE patients treated with HCQ do not produce IFNα or TNFα in response to TLR7 and TLR9 agonist stimulation, which would suggest that HCQ inhibits TLR mediated cellular responses (Kandimalla, et al, 2013). For many years the inhibitory action of HCQ against TLR mediated immune responses has been attributed to the inhibition of endosomal acidification, because pH is a prerequisite of endosomal TLR activation (Willis et al, 2013). However, a recent study investigating the inhibitory action of chloroquine has concluded that the mechanism of action in SLE is due to binding to the nucleic acids which activate TLR7, 8 and 9 (Kužnik et al, 2011).

A number of drugs are routinely used “off label” as steroid-sparing agents or for severe SLE. Cyclophosphamide is an immunosuppressant usually used in conjunction with glucocorticoids. However, the optimal dosing regime has not been determined and it can cause serious adverse events including infertility, malignancy, hemorrhagic cystitis and infection (Stichweh, Pascual and Banchereau, 2006; Yildrim-Toruner and Diamond, 2011).

Mycophenolate mofetil is a potent immunosuppressant that has been used to treat SLE, primarily to reduce the adverse events observed with cyclophosphamide. It is a pro-drug of mycophenolic acid, an inhibitor of inosine monophosphate dehydrogenase that selectively suppresses T and B lymphocytes (Goldblatt and Isenberg, 2005). The main side effects include diarrhoea, nausea, vomiting, minor infections and rare cases of leucopenia. Azathioprine is metabolised to mercaptopurine, which inhibits DNA synthesis and so prevents cell proliferation in the immune system. It has been successful in the treatment of SLE, however, side effects include toxicity to the GI tract, oral ulcers, nausea, vomiting, diarrhoea, epigastric pain, leucopenia, and less commonly thrombocytopenia and anaemia (Yildrim-Toruner and Diamond, 2011). Methotrexate is a folic acid analogue and a potent competitive inhibitor of dihydrofolate reductase that acts by inhibition of both RNA and DNA synthesis.

Despite many treatment options some patients are still refractory and need prolonged high dose corticosteroid therapy and/or a long term immunosuppressive regimen to maintain remission. In many cases the drugs used to treat SLE cause irreversible damage sometimes leading to death (Chice et al, 2012). Consequently, there is a drive to develop new therapeutic agents that target specific components of the disease pathogenesis (Schmidt and Ouyang, 2004). With the complex nature of SLE incorporating a large number of cells in the immune system it is unsurprising that a large number of therapies targeting a wide range of cells and cytokines have demonstrated efficacy in some patient populations. Some of the alternative therapies and potential new therapies for SLE are summarised in Table 2.3.

Table 2.3 New and prospective treatments for SLE

Target	Therapy	Therapy / mechanism of action	References
T cell	Spleen tyrosine Kinase (SYK) inhibition	Reverses aberrant T cell signalling	
	AMG 557	B7RP1 monoclonal antibody inhibits the ICOS-B7RP1 pathways important in T cell-B cell interactions	Comte, Karampetsou and Tsokos, 2015.
	IL2 therapy	IL2 promotes activation induced cell death important for the removal of autoreactive T cells Important role in the development and survival of regulatory T cells.	
	Anti-CD40L	Inhibits T and B cell interactions	Nandkumar and Furie, 2016
B cell	Rituximab atumumab, ocrelizumab, Veltuzumab	Anti-CD20 antibody (B cell specific antigen)	
	Epratuzumab	Anti-CD22 antibody (B cell specific antigen)	Stichweh, Pascual and Banchereau, 2006
	Abetimus	B cell tolergen results in functional inactivation or deletion of B cells.	
	Belimumab	Binds and inhibits BLyS	
	Atacicept	Binds both BLyS and APRIL	
Cytokines / chemokines	Statins	Inhibition of pro-inflammatory mediators (TNFα, IL6, MCP1 etc) promote secretion of Th2 cytokines and suppression of IFN transduction pathways amongst others	Amuro et al, 2010 Abud-Mendoza et al, 2003
	Toculizumab	human IL6 receptor antibody which inhibits IL6 signalling	
	anti IL10 antibody	Inhibition of systemic concentrations IL10 a potent stimulator of B cell proliferation and differentiation	
	Anakinra	IL1 receptor antagonist	
	Anti IFNα antibody Anti IFNα receptor antibody TLR antagonists	Inhibition of systemic concentrations of IFNα	
Cell signalling	JAK inhibitors	Inhibition of innate and adaptive immune cell signalling	

2.4.1. Targeting T and B cells

T cells have a key role in the pathogenesis of SLE, therefore targeting molecules expressed on T cells or molecules that modulate T cell activity could offer therapeutic potential in SLE (Nandkumar and Furie, 2016). A number of targets have been explored, including anti-CD40

ligands, cytotoxic T-lymphocyte associated protein 4 Ig (abatacept), IL2, SYK inhibition and immuomodulatory peptides. To date the investigation of molecules targeted against T cells in the clinic has met with mixed results. For example, the anti-CD40L showed a reduction in disease endpoints but studies had to be terminated due to thromboembolic events. Whist treatment with another anti-CD40L ligand demonstrated no significant differences in SELENA-SLEDAI scores or dose-response relationships. A re-engineered anti-CD40L that does not possess the thromboembolic potential, and has demonstrated efficacy in a Phase I safety and tolerability study in SLE patients, is currently being investigated in Phase II trials (Nandkumar and Furie, 2016).

B cells are at the centre of SLE pathogenesis (Goldblatt and Isenberg, 2005; Stichweh, Pascual and Banchereau, 2006). In addition to secretion of autoantibodies, B cells can take up autoantigens, through cell surface immunoglobulin and present them to T cells, as well as regulate and organise inflammatory response through cytokine secretion and regulation of other immune cells. Autoreactive B cells can present self-antigen to T cells leading to the expansion of autoreactive clones (Stichweh, Pascual and Banchereau, 2006).

Rituximab is a chimeric monoclonal antibody that selectively targets CD20-positive B cells which despite failing to meet its primary endpoints in two prospective Phase III trials for SLE (Chiche et al, 2012), has been used off label in refractory cases (Parodis, Axelsson and Gunnarsson, 2013). Rituximab rapidly depletes peripheral blood CD20 positive B cells via complement-mediated and antibody dependent cell mediated cytotoxicity, induction of apoptosis and inhibition of cell growth (Stichweh, Pascual and Banchereau, 2006; Goldblatt and Isenberg, 2005). CD20 is highly expressed on B cells from the pre-B to the memory B cell stage of differentiation, but is absent in plasma cell precursors and terminally differentiated plasma cells. It has demonstrated efficacy in childhood onset and adult onset active and refractory SLE. Case series with severe refractory SLE suggest that re-treatment with rituximab is safe and clinical response is sustained for up to 12 months on average. Unfortunately, the placebo-controlled Phase II/III EXPLORER and LUNAR trials of rituximab in SLE failed to meet the primary and secondary endpoints. Analysis of the data from these trials led Hui-Yuen et al (2016) to conclude that the role for rituximab is not for induction of disease remission in SLE patients but rather as an adjunct to control severe manifestations (Hui-Yuen, Nguyen and Askanase, 2016).

Belimumab is a mAb that binds to and inhibits the action of B lymphocyte stimulator (BlyS) thus preventing it from binding to receptors. It is the first biological drug to be licensed and approved for the treatment of SLE in over 50 years (Mosak and Furie, 2013). BlyS is a type II transmembrane protein that exists in both membrane-bound and soluble forms, it is expressed at the surface of a wide variety of immune cells and when cleaved from the membrane becomes a soluble trimer that is a ligand for three receptors expressed primarily on B lymphocytes promoting their survival and maturation. (Chice et al, 2012; Mosak and Furie, 2013). BlyS is over expressed in patients with SLE and its levels correlate with concentrations of autoantibodies as well as disease activity (Parodis, Axelsson and Gunnarsson, 2013). Two large Phase III studies demonstrated significant clinical efficacy in seropostive patients, with an improvement in serological activity as early as week 8 (reduction in anti-dsDNA) compared to placebo (Chiche et al, 2012; Mosak and Furie, 2013). Patients treated with belimumab reduced their prednisone dose (Parodis, Axelsson and Gunnarsson, 2013). Belimumab was approved in 2011 for the treatment of autoantibody-positive patients with active SLE, and is currently under investigation for subcutaneous administration. Recent data have confirmed efficacy in regard to BAFF inhibition without any additional safety concerns (Hui-Yuen, Nguyen and Askanase, 2016).

2.4.2. Inhibition of IFNα

It is unsurprising that therapeutic approaches that target IFNα are being pursued for SLE. The scope and progress of the various therapeutics that are being developed to target IFNα are summarised in reviews by Kirou and Gkrouzman (2013) and Kalunian (2016). They include anti-IFNα mAbs, anti-IFNα receptor antibodies and immunisation against IFNα (IFNα Kinoid). There are risks to inhibiting IFNα and therapeutic agents that result in complete IFN blockade should be approached with caution as they may increase susceptibility to infection. Despite this, a number of anti-IFNα mAbs (rontalizumab, sifalimumab and ASG-009) have been investigated in Phase II clinical trials. These mAbs have shown reduced disease activity, although without a clearly positive signal, and also without any increase in serious infection but have not progressed further than Phase II (Rönnblom, 2010; Kirou and Gkrouzman, 2013). The anti-IFNα receptor antibody anifrolumab has progressed into pivotal Phase III studies (Kalunian, 2016).

An alternative option is the use of TLR antagonists. The goal with these antagonists is to preferentially inhibit IFNα production by pDCs without blocking the low levels of IFNα

produced by other cell types, which is important for the host antiviral response (Barrat and Coffman, 2008). In addition TLR7/9 antagonists could inhibit the activation of anti-DNA and anti-RNP specific B cells and consequently production of anti-nucleic acid autoantibodies (Barrat and Coffman, 2008). A number of companies are pursuing TLR antagonist programmes, and duel TLR7 and TLR9 antagonists have shown preclinical efficacy in mouse models of lupus and other autoimmune diseases (Romagne, 2007). At the time of writing a small molecule TLR7 antagonist is not yet commercially but there are a number of TLR7, 8 and 9 antagonists currently in clinical trials for SLE or other indications (Kandimalla et al, 2013). Dynavax has an oligonucleotide-based bifunctional inhibitor of TLR7 and TLR9 receptors, which has been shown to block IFNα symptoms in multiple autoimmune disease models of SLE. In addition, Idera pharmaceuticals have two DNA based antagonists of TLR7, 8 and 9 in clinical trials, and Pfizer have an orally available small molecule quinazoline derivative TLR7, 8 and 9 antagonist which completed a Phase I trial in 2011 (Basith et al, 2011; Connolly and O'Neil, 2012).

As an alternative to TLR inhibition there are a number of potential targets downstream of TLR7 and 9 in pDCs such as phosphatidylinosiyol-4,5-biphosphate 3-kinase (PI3K)δ and IRAK1 and 4 kinase, which may offer potential candidates to deliver anti-IFNα therapies (Kirou and Gkrouzman, 2013). The statins are inhibitors of 3-hydroxy-3-methylglutaryl-coenzyme A (HMG-CoA) reductase and have been widely used in the therapy of ischaemic coronary disease and for the control of hypercholesterolaemia (Abud-Mendoza et al, 2003). The statins have an effect on the pDCs production of IFNα by inhibiting p38 mitrogen-activated protein kinases (MAPK) and PI3K/protein kinase B (Akt) and consequently the translocation of IRF7 into the nucleus of both healthy and SLE obtained pDCs (Amuro et al, 2010). In addition, statins inhibit the production of pro-inflammatory mediators, promote the secretion of Th2 cytokines and reduce the expression of MHC-II in various cell types. Although a small number of studies have demonstrated a reduction in SLE disease activity following atorvastatin and simvastatin therapy Yildrim-Toruner and Diamond (2011) conclude multicentre and prospective studies are required to determine whether statin treatment has an impact on SLE disease.

As IFNα signals through the JAK/STAT pathway it stands to reason that this may offer therapeutic opportunities in SLE. The JAKS are a tractable target as they can be inhibited with small molecule oral inhibitors, and as they are downstream of the receptor they can

inhibit the action of multiple cytokines rather than target one particular cytokine. A number of JAK inhibitors are being used or investigated in the clinic for various indications. However, a number of side effects have been reported, including an increase in bacterial, fungal and viral infections, anaemia, thrombocytopenia and neutopenia, which is likely to be related to JAK2 inhibition (O'Shea et al, 2012). A potential advantage of JAK inhibitors compared to biologics with respect to infection risk is in the relatively short half-life. If infections occur, JAK inhibitors can be stopped and the immunomodulatory effect is transient (O'Shea et al, 2012). GSK recently investigated an orally active, selective JAK1 inhibitor in SLE patients. But since an interim analysis found that no significant effect on mean IFN transcriptional biomarker expression, and there were significant safety findings the trial was halted (Kahl et al, 2016).

Despite many potential opportunities for therapeutic targets, only one new drug has been approved for the treatment of SLE in over 50 years and over $10 billion was spent on failed efforts (Wallace, 2016). A change in mindset may therefore be required into the way targets are selected and preclinical studies and clinical trials are designed and conducted. Wallace (2016) highlighted that poor clinical trial design has played a large part in the lack of progression from clinical studies to the patient. Both the FDA and EMA (2013) have released guidance documents in which they outline acceptable endpoints to assess efficacy, including reduction of disease activity/induction of remission parameters, decrease of cumulative steroid dose, prevention of flares/increased time intervals between flares and prevention of long term damage. It is important to apply the same rigour to preclinical models ensuring that historical *in vivo* models are still appropriate today. One further point to consider is that in a review of the potential for TLR7 and 9 antagonists Fulmer (2010) concluded that monotherapy is generally not the way to proceed with the clinical development of lupus therapies, and given the heterogeneity of the disease, personalised treatment approaches are likely to be required. Consequently, in designing clinical studies beyond Phase I, it is important to consider how best to combine the new therapeutic under investigation with steroids and other approaches for lupus and other autoimmune diseases (Fulmer; 2010). What is most important is that we learn to subset patients with respect to genetic susceptibility, pathogenic mechanism and phase of disease so that we maximise the therapeutic effect of each agent and minimize its toxicity (Yildrim-Toruner and Diamond, 2011).

2.5. Models of Autoimmune Disease – Disease vs. Mechanistic

2.5.1. Introduction to Animal models

"*The best model for human disease research is the human*" (European Commission workshop, 2010), this has led to a precedence of researchers striving to progress compounds of interest into the clinic as soon as possible to establish early PK/PD data from Phase I healthy volunteer studies. Such studies may incorporate a physical or chemical challenge to engage a target mechanism and include a clinical biomarker of a disease relevant end point that is likely to be a key measure of efficacy in later clinical trials. Despite the attractiveness of obtaining early mechanistic efficacy data from the clinic there are time, cost, ethical and practical considerations involved in clinical trials that lead researchers to search for preclinical alternatives to human research in attempt to gain confidence around the safety and efficacy profile associated with a particular target mechanism or lead molecule prior to progressing into the clinic. Models in rodents are particularly attractive because of the availability of genetically similar or identical individuals, relatively low cost and ease of handling (Vodovotz et al, 2006). Mouse models have played a valuable role in increasing our understanding of the respective roles of various cells and molecules in the immune system, and the large number of models of autoimmunity that are available have proved extremely useful in developing our understanding of the mechanisms behind various diseases (Nials and Uddin, 2008; Pathak and Mohan, 2011). Within the pharmaceutical industry, there is a long history of using mice to study disease biology, identify possible drug targets, assess the efficacy and safety of potential therapeutic agents and design clinical trials (European Commission workshop, 2010).

Despite their extensive use in drug discovery and development, mice have not always been reliable preclinical models of human disease. The scientific literature is littered with examples of drugs that worked well in animals but ineffective in clinical trials, which have cost the pharmaceutical industry millions of Euros (European Commission workshop, 2010). The question arises, are we putting too many expectations on the mouse models of human disease to deliver new therapies? Given the complexity of inflammation there is likely to be a difficulty in translating animal studies to clinical trials, and as a result, it is not surprising that therapies that modulate inflammation have yielded disappointing clinical results

despite promising results in animal and early human trials. This poor predictive nature of *in vivo* disease models is clearly a concern for both the pharmaceutical industry and academia and in 2004, prompted the FDA to acknowledge the need for a product development tool kit-containing new, powerful, scientific and technical methods. Requirements for the new toolkit were animal or computer based predictive models, biomarkers for safety and effectiveness, and clinical evaluation techniques to improve predictability and efficiency along the critical path from laboratory concept to commercial product (Vodovotz et al, 2006).

For the purpose of this report, animal models used to investigate human disease situations will be considered to fall into two broad categories, disease models and mechanistic models. Disease models should ideally reproduce the clinical condition in an animal model; this includes spontaneous/genetically predisposed animals and models where the disease is induced in normal animals following administration of a stimulating or challenge agent (physical, toxin, drug stimulation). Mechanistic models do not look to replicate the whole disease, but rather allow investigation of a single or small number of mechanisms implicated in the disease usually after administration of a stimulating or challenge agent.

Although disease models that mimic the human disease are an attractive option, it is generally becoming accepted that due to the complexity of many diseases there is unlikely to be one perfect mouse model for each disease. Instead, a 'toolbox' of models may be better utilised to investigate the different mechanisms and pathways of each disease. Regardless of which type of model is preferred, when selecting and developing an animal model, it is critical to integrate clinical information to understand the validity of the model to the human disease situation. Selecting a mouse model and appropriate readouts is critical for the design of appropriate assays for evaluation of potential therapeutic agents (Seavey, Lu and Stump, 2011). Mouse models have undoubtedly contributed to our understanding of the mechanisms of SLE, and unlike many other models of autoimmunity and inflammation, SLE in mice closely resembles human SLE. As there are many models of SLE, choosing the most appropriate model to answer a question of interest requires an understanding of the clinical, pathological and genetic features of each model (Rottman and Willis, 2010).

2.5.2. Mouse disease models of SLE

There are a number of mouse models which have been used to develop an understanding of the cellular and genetic mechanisms behind human SLE pathogenesis, including the interplay between the innate and adaptive immune system (WHO, 2006; Pathak and Mohan, 2011). SLE in mice closely resembles human SLE, including autoantibody production and renal disease (Rottman and Willis, 2010). Investigative studies using these mouse models have been pivotal in understanding the complex nature of the disease, for example the roles that Type I IFNs, dendritic cells and genetic susceptibility play in the pathogenesis of the disease (Tron, 1990; Schmidt and Ouyang, 2004; Pathak and Mohan, 2011). As well as being used to dissect the disease mechanisms behind SLE, mouse models have also proved indispensable to testing potential therapies prior to clinical trials (Perry et al, 2011).

The two categories of mouse disease models of SLE are spontaneous and induced models. Various mouse models of spontaneous lupus (lupus prone mice) exist, which portray their own iterations of lupus-like diseases with a subset of symptoms akin to those observed in human SLE (Perry et al, 2011). Examples of spontaneous lupus mouse strains include the classic mouse model NZB/W F1 used since the early 1960s, the MRL/lpr model and the BXSB/Yaa model. These mice express symptoms similar to the human situation, including hyperactive B and T cells, high titres of several autoantibodies directed against nuclear antigens and defective clearance of immune complexes (Rottman and Willis, 2010) but do not predict that Type I IFN might be an important mediator in human SLE (Pascual, Chaussabel and Banchereau, 2010). Although SLE observed in spontaneous mice resembles the human disease situation there are differences between the two. For example, in BXSB/Yaa mice the condition occurs only in males, due to translocation of the TLR7 gene into the Y chromosome, whereas human SLE has a female to male ratio of 9:1 (Hayashi, 2010; Seavey, Lu and Stump, 2011). In addition, SLE targets the skin, joints, kidneys and many other organs in humans, whereas mouse models of SLE are characterised mainly by the development of nephritis (Perry et al, 2011). One other point to consider is that in mice the course of disease is steadily downhill and fatal, whereas human disease is cyclic, characterised by exacerbation and remission (Hayashi, 2010).

There are a number of *in vivo* mouse models where the administration of a challenge agent produces disease symptoms similar to that observed in humans or spontaneous /

genetically prone mice. An example of an induced mouse lupus model is the pristane model (Rottman and Willis, 2010; Perry et al, 2011). In this model, a single injection of pristane (hydrocarbon oil) in almost any strain of mice results in a disease with most of the features of human lupus. Importantly, it is the only murine model of lupus to exhibit the characteristic Type I IFN signature (Via, 2010). It should be noted that in contrast to spontaneous or genetically prone autoimmune models, chemically-induced autoimmune models, such as SLE models, are actually uncommon. Based on the multifactorial and idiosyncratic nature of autoimmune diseases, few compounds have been shown to induce clinically apparent autoimmune or autoimmune-like allergic phenomena in animals (WHO, 2006). As well as the pristane-induced lupus, certain drugs such as hydralazine, procainamide, isoniazid, chloropromazine and minocycline can provoke lupus-like symptoms, which is known as drug-induced lupus. Although drug induced lupus produces symptoms that overlap with SLE, they are considered different. SLE is a chronic disease where the symptoms can last for years and the exact aetiology has yet to be defined, whereas with drug induced lupus the symptoms normally disappear within weeks of discontinuing the medication suspected to be the cause.

The limitation with using the types of model described above is that very few mouse models faithfully model all the pathology and symptoms of the human disease and, more importantly, accurately predict treatment efficacy. There are even examples where the same treatment has variable effects between the different mouse models of SLE (Perry et al, 2011), which makes it very difficult to translate efficacy observed in the mouse to the human situation. It also potentially means that drugs that are progressed based on efficacy in a single preclinical mouse model of SLE may only be effective for a subset of symptoms or patients. To counteract this it has been suggested that the best way to mimic the genetic pathological heterogeneity in humans, is to use a number of different mouse models in therapeutic studies (Perry et al, 2011).

2.5.3. Mechanistic Challenge models of SLE

An important aspect to consider when selecting a drug screening system such as an *in vivo* model is whether the goal is to develop a symptomatic or a disease-modifying treatment (Sams-Dodd, 2006). It is generally considered that in the normal pattern of disease, a defect or change in a mechanism or pathway results in the abnormal functioning of that pathway. The defective functioning of the pathway then affects the normal functioning of the

organism and gives rise to a wide range of symptoms that can be observed (Figure 2.5A). For many diseases, the underlying mechanisms are unknown, and therefore disease models in drug discovery may be selected, developed and validated based on symptom-similarity to the clinical condition. An example of this, is the selection of a spontaneous lupus mouse strain for the disease model of SLE depending on the particular symptom of the disease an investigator may wish to treat. It is argued that models that target the replication of clinical symptoms will only deliver symptom reducing treatments and will rarely identify disease-modifying treatments (Sams-Dodd, 2006). The reason for this, as described in Figure 2.5B, is that a specific symptom is likely to be due to several underlying function changes, each of which might be attributed to an even wider array of defects at the mechanistic level (Sams-Dodd, 2006).

An alternative option is to use a mechanistic challenge model. For the purpose of this thesis, mechanistic models will be considered to be those where the administration of the challenge agent may only stimulate a single or a small number of pathways and mechanisms implicated in the disease. Challenge models using potent immunomodulatory molecules are frequently used in rodents as models to investigate innate immune response mechanisms (Patrignani et al, 2010). Two examples of inflammatory challenge mouse models are the carrageenan and LPS induced inflammation models. These models allow investigation of cytokine release, inflammatory pain and gene expression in mice challenged with carrageen or LPS (Patrignani et al, 2010). Interestingly, the cases where mouse models have been successfully used to validate drug targets and to determine efficacious and safe dosage schemes for combination treatments in humans have all had one factor in common, they do not aim to fully model a disease or disease mechanisms, but rather set out to obtain specific functional information (European Commission workshop, 2010).

Figure 2.6 **Relationship between disease mechanisms and symptoms. (A) The cause of a disease is a perturbation of a certain mechanism, which leads to a set of functional deficits. These give rise to several primary and secondary changes that result in the symptoms that can be observed in the patient. (B) A specific symptom can be attributed to several underlying primary and secondary causes, which again might be caused by different functional and mechanistic changes, Recreated with permission from Sams-Dodd (2006)**

Mechanistic models are becoming more of an option as the understanding of diseases increases and the key mechanisms involved are identified. As with all models, when developing a mechanistic *in vivo* model it is important to integrate clinical information to ensure the mechanism is translatable to humans. A validated mechanistic animal model that can be translated to the human mechanism may be used to firstly demonstrate that the compound affects the mechanism and then hopefully later will enable an understanding of the exposures required for efficacy on the mechanism. These types of mechanistic model may form part of a toolbox approach, with a number of models that fit to a two- or multiple-tiered approach (WHO, 2006). A toolbox strategy has been successfully utilised for the investigation of asthma. Asthma is a complex multifactorial inflammatory disease, and it is unlikely that a single animal model of asthma that replicates all of the morphological and functional features of the chronic human disease will ever be

developed (Nials and Uddin, 2008). It is, however, possible to use allergen challenge animal models to model specific features of the disease.

2.5.4. Mouse Resiquimod Challenge model

A review of the literature for SLE implicates a number of potential pathways and mechanisms that may be involved in the aetiology of the disease, one of which is the production of IFNα from pDCs following the stimulation of TLR7. Studies have shown that administration of bacterial or viral TLR ligands to SLE prone mice lead to an increase in IFNα production and disease exacerbation (Jacob and Stohl, 2011). Based on this knowledge, a TLR7 agonist may be a suitable chemical challenge agent to enable the investigation of this mechanism *in vivo*. The first small molecule TLR7 agonists were discovered in the 1980s following investigation of nucleoside analogue structures, and belong to a chemical family called the imidazoquinolines (Wu et al, 2004; Czarniecki, 2008). However, the gene encoding the human TLR7 was not identified until 2000 (Du et al, 2000). The imidazoquinolines are potent antiviral and anti tumour agents (Imbertson et al, 1998;) that have been investigated for the treatment of cancer, allergies and viral infections (Basith et al, 2011). They are immune system modifiers (IRMs) and their activity is mediated through the induction of cytokines, in particular IFNα and TNFα (Imbertson et al, 1998; Wagner et al, 1999).

The induction of cytokines is important in driving cell-mediated immune response (Tomai et al, 2007), and the observed induction of cytokine levels following resiquimod treatment observed in the preclinical and clinical studies is mediated through activation of the TLR7 pathway. In humans, resiquimod signals through both the TLR7 and TLR8 pathways, inducing the cytokines IFNα, TNFα and IL12 from innate immune cells (Pockos et al, 2007). Studies have shown that TLR7 deficient mice and MyD88 deficient mice were unresponsive to resiquimod, with no observed induction in cytokine levels following resiquimod challenge (Wu et al, 2004; Jurk et al, 2002). These data show that TLR7 is an essential receptor for resiquimod and other imidazoquinoline-induced immune responses and activation of signalling cascades *in vivo* (Hemmi et al, 2002). TLR8 in mice is non-functional and as such activation by resiquimod in the mouse is solely through TLR7 (Tomai et al, 2007).

The most important cell types activated by resiquimod through the TLR7 pathway are the pDC. TLR7 agonists such as resiquimod act directly on DCs, inducing the up-regulation of cytokines (IL12, IL6, TNFα and IFNα), MHC class II (interferons) and co-stimulatory molecules, and promoting DC migration to the lymph nodes (Schiller et al, 2006; Igartua and Pedraz, 2010). Resiquimod stimulates pDCs to produce large amounts of IFNα and other pro inflammatory cytokines, and *in vitro* studies have shown that pDC-enriched cultures produced 2-20 times more IFNα than similarly treated PBMCs following resiquimod (Gibson et al, 2002). As well as stimulating the DCs and pDCs, resiquimod affects many other immune cells. It enhances the antigen presenting function of monocytes and macrophages, stimulates B-cell proliferation and antibody production, stimulates NK cell activity and enhancement of Th1 responses, while at the same time inhibiting Treg function (Tomai et al, 2007).

A number of imidazoquinoline molecules have progressed to clinical development, where, depending on the therapeutic purpose, they have been administered systemically via oral or intravenous (iv) administration, and locally as a topical cream or a subcutaneous (sc) injection (Engel, Holt and Lu, 2011). Imiquimod was the first commercially available imidazoquinoline for the treatment of anogenital warts, actinic keratosis and superficial basal cell carcinoma (Miller et al, 1999). The second generation drug resiquimod (R-848, S-28463, 4-amino-2-ethoxymethyl-α,α-dimethyl-1H-imidazo[4,5-c]quinolin-1-ethanol) was shown to be both more potent and soluble than imiquimod (Wu et al, 2004), producing a 50-to 100 fold greater cytokine response *in vivo* (Dockrell and Kinghorn, 2001). Resiquimod was developed as a potential antiviral for the topical treatment for genital herpes (Czarniecki, 2008; Engel, Holt and Lu,2011), and reached Phase III before being discontinued due to lack of efficacy. Resiquimod was also investigated as a potential therapy for hepatitis C virus (HCV) infection (Engel, Holt and Lu, 2011 but showed limited (Pockros et al, 2007), and the development of resiquimod as a treatment for HCV infection was halted.

The antiviral action of resiquimod is attributed to the induction of cytokines and elevated levels of cytokines were observed in subjects following oral administration. As part of preclinical development, *in vivo* studies in mice were conducted to investigate the relationship between doses of resiquimod and the induction of IFN and TNF following oral administration (Tomai et al, 1995). A dose dependent increase in serum IFN concentrations was observed when resiquimod was increased from 0.003 mg/kg to 0.3 mg/kg. Maximum

IFN serum concentrations (C_{max}) for all doses were observed at a time (T_{max}) of 2 h post oral resiquimod administration. The highest IFN C_{max} of 8900 U/mL was observed following oral administration of 0.3 mg/kg. Interestingly, a further increase in the dose up to 10 mg/kg resulted in lower concentrations of serum IFN and the systemic exposure of IFN was comparable to that observed following oral administration at 0.03 mg/kg. Later studies investigated the capacity of resiquimod to induce IFNα serum concentrations in mice following intraperitoneal (ip) injection (Hemmi et al, 2002) and iv administration (Asselin-Paturel et al 2005). Doses of 0.8 mg/kg ip and 0.25 mg/kg iv, achieved mean maximum IFNα serum concentrations of *ca* 3000 pg/mL and *ca* 8900 pg/mL respectively at 1 h and 2 h post resiquimod challenge.

Following a review of the literature, the question is whether resiquimod is a suitable challenge agent for an *in vivo* PK/PD model. The process of integrating clinical and preclinical information, and the generation of a hypothesis around model suitability is described below and summarised in Figure 2.6. The induction of IFNα from pDCs via activation of the TLRs has been implicated in the aetiology of SLE. Given that administration of resiquimod in the clinic resulted in an elevation of cytokines, particularly IFNα, and that most studies evaluating the function of human TLR7 have used resiquimod (Gorden et al, 2005), it can be concluded that resiquimod may be a suitable challenge for investigating the pDC related pathways implicated in SLE in healthy volunteers in the clinic. From a preclinical perspective, studies have shown that the stimulation of mouse pDCs via synthetic TLR7-9 ligands trigger events that lead to pDC differentiation into conventional-like DC and Type I IFN cytokine production (Fuchsberger, Hochrein and O'Keeffe, 2005). Further *in vivo* studies have successfully demonstrated an increase in IFNα serum concentrations following resiquimod treatment in the mouse (Asselin-Paturel et al, 2005). This indicates that the effects of resiquimod on the target mechanisms observed in the clinic are replicated in preclinical species. Based on this information, a mouse *in vivo* resiquimod challenge model may offer a translatable model that can be used to investigate the induction of serum cytokine levels by pDCs through the TLR7 mediated pathway.

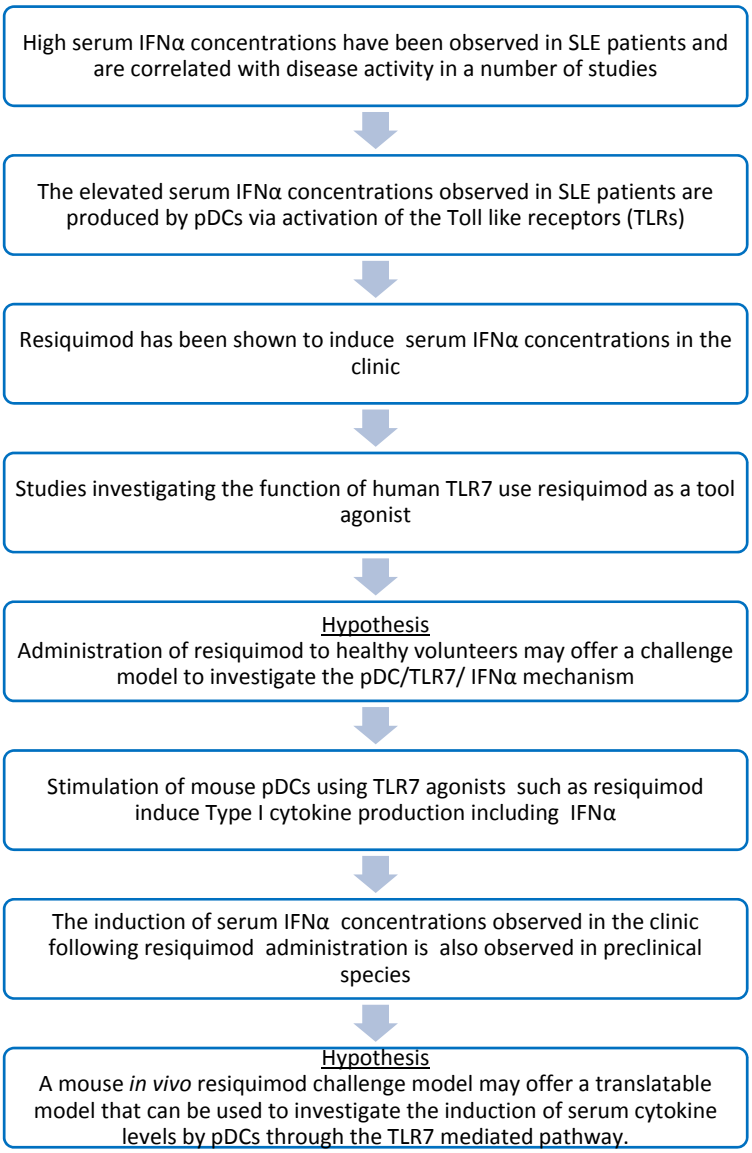

Figure 2.7 The process of integrating clinical and preclinical information, to generate hypotheses around the suitability of a PK/PD model.

2.5.5. Primate Challenge model

During the drug development process it is often desirable and/or necessary to investigate compounds of interest in PK/PD or disease models in larger species. SLE is a chronic illness in both dogs and cats and a number of induced disease models have been investigated in a number of species including dogs, rabbits and primates (Rottman and Willis, 2010). Spontaneous SLE rarely occurs in nonhuman primates, although SLE-like disease can be induced in nonhuman primates by feeding the animals alfalfa seeds or L-canavanine sulfate (Rottman and Willis, 2010) The primate offers an interesting species to consider for a

translatable mechanistic challenge model as many of the potential biomarkers are cross-reactive between human and primate.

In the clinic, the IFNs have been administered in a number of approved and off label indications which are summarised in a review by Burdick, Somani and Somani (2009). The IFNs have been administered via intravenous injection and infusion, intra-muscular, subcutaneous, intra-lesional, intra-nasal, intra-dermal and trans-cutaneous application. Recombinant IFNs are produced by recombinant DNA technology using genetically engineered *E. coli* containing DNA that codes for that protein. While natural IFNα induced, for example, by activation of the TLRs can be mixture of at least 13 subtypes, the recombinant IFNs consist of a single species of authentic or hybrid IFN. Both antiviral and antiproliferative activities induced by recombinant IFNs vary among the different subtypes and the pharmacokinetics of the IFNs may change depending on the sugar residues (Bannai, 1986). For example, IFNα2b is a highly purified protein containing 165 amino acids with an approximate molecular weight of 19,000 daltons and it is in commercial development under the brand name IntronA.

The administration of IFNs that are approved for administration in the clinic offer and interesting option to investigate the pathways and targets downstream of the IFN receptor, such as components of the JAK/STAT pathway including potential therapeutic intervention against these targets in humans. For example it may be possible in early clinical trials to see if a new therapeutic can inhibit IFNα challenge induced biomarkers thus delivering confidence that the therapeutic under investigation engages the target mechanism.

In general, the pharmacokinetics of IFNs decline in a biphasic manner, characterised by an initial rapid disposition phase followed by a slower elimination phase. Following subcutaneous administration IFNβ1a results in a prolonged absorption phase and “flip flop kinetics” where the absorption rate is controlling the terminal phase resulting in prolonged drug exposure (Mager et al, 2003). This has also been observed in studies investigating IFNα in the cynomolgus monkey where the initial half life is approximately 5-7 times longer after intra muscular administration compared to that observed following iv bolus administration (Bannai et al, 1985).

The PK for the IFNs like many therapeutic proteins is nonlinear and is best described by the target mediated drug disposition (TMDD model). In this concept the interaction of the drug

with its high affinity receptor has major influences on the drug distribution and elimination patterns (Kagan et al, 2010). It has already been mentioned that the binding of IFN to the IFNAR is saturable, and following low dose administration the majority of the IFN will be bound to the receptor which results in a high apparent volume of distribution high systemic clearance. When higher dose levels are administered as in studies with IFNβ1a in the monkey (Jusko et al, 2003) the receptors become saturated and more IFN is available in its unbound form in the systemic circulation resulting in a lower predicted systemic clearance (Kagan et al, 2010). Jusko and Mager (2002) and later Jusko et al (2003) investigated the PK/PD relationship of the IFNβ1a induction of serum neopetrin concentrations in humans and monkeys respectively over a range of doses. They investigated single and multiple dosing and different routes of administration (iv and sc) and related the monkey and human TMDD models to each other. They also include a secondary elimination pathway which is always present but becomes more important once the receptor mediated elimination becomes saturated for example at high iv doses. Later work by Kagan et al (2010) looked to use a single PK/PD model incorporating TMDD and allometric scaling to describe the same data set used in the earlier modelling. Kagan concluded that the PK/PD model with TMDD combined with allometric scaling demonstrated a good predictive performance of the PK/PD relationship of IFNβ1a induction of neopterin in human and monkey. In addition they used single dose data from studies investigating other IFN subtypes and demonstrated that a number of the parameters predicted for IFNβ1a can be shared to predict the kinetic behaviour of other IFN subtypes in different species. This suggests that the PK/PD relationship for at least IFN induction of neopterin is translatable between human and monkey.

The translatability of the PK and PD effects between human and primates suggests that a preclinical IFNα challenge PK/PD model may enable the design and selection of compounds with a desirable PK/PD profile and ultimately, may be used to predict efficacious clinical doses. Supporting this is evidence that suggests monkeys are preferable animals for studying pharmacokinetic characteristics of IFNs (Cai et al, 2012), since human IFNs lack activity in mouse cells but are active in different monkey species (Kagan et al, 2010). The administration of recombinant IFNα to various strains of monkeys using a variety of doses and routes of administration has been comprehensively investigated. In many studies, particularly early ones, the version of IFNα which was used i.e IFNα2a or IFNα2b is often not detailed, making it difficult to compare between studies. As it is documented that the

different IFN subtypes have different binding affinities to the IFNAR and can have different anti-viral and anti-proliferative effects, when discussing previous studies from the literature the exact type of IFNα used in those studies has been documented to avoid speculation that the PK and PD are the same between the various types.

Clinical studies show that IFN concentrations are linked to a high incidence of side effects, which are usually mild and reversible, yet compromise the tolerability of IFN (Cai et al, 2012). These side effects resemble flu-like symptoms and include fever, chills, headaches, myalgia and dizziness (Reddy, 2004). Studies have shown that these symptoms are observed approximately 8 h after sc administration of IFN and coincide with peak plasma concentrations (Reddy, 2004). Within GSK, a dose dependent increase in body temperature has been observed in studies investigating the intranasal administration of TLR7 agonists to cynomolgus monkeys. The increase in body temperature was observed from 5 h post dose and had returned to baseline by the 20 h post dose and was attributed to the cytokine profile alterations seen over the same time period. A similar increase was also observed in the clinic following intranasal administration of the TLR7 agonist to healthy volunteers with a small increase in body temperature observed in some subjects at doses ≥40 ng. However, the IFNα were below the assay LLQ (Tsitoura et al, 2015). A similar increase in body temperature has also been observed in other clinical studies investigating recombinant IFNαA following iv infusion, intramuscular and subcutaneous administration (Wills et al, 1984). And again is attributed to increased serum concentrations of IFNα. However, studies indicate that the relationship is more complicated than just a simple function of magnitude of the serum concentration to effect and appear to be a function of exceeding and maintaining serum concentrations above a certain level (Wills et al, 1984).

There is extensive published toxicity information for the marketed recombinant IFNs used in the clinic (Roferon-A / IFNα2a and Intron-A/IFNα2b). Monkeys are considered an adequate species for characterisation of the toxicity of IFNα2b as most findings can be related to those observed in humans. No signs of toxicity were observed following a single intramuscular or intravenous administration of a high dose (approximately 7 times the therapeutic dose) of IFNα2b to rhesus monkeys. Daily administration of IFNα2b in cynomolgus at 20 x 10^6 IU/kg/day for three months caused no remarkable toxicity, although toxicity was shown in monkeys administered the daily with 100 x 10^6 IU/kg/day for three months (EMA, 2005). Irritation at the injection site in repeat dose toxicity studies has been

reported in both rats and monkeys. The potential for irritation appeared to be mild to moderate and, at least part, dependent on tonicity of the formulation (EMA, 2005).

Following IFN challenge neopterin has been described as a translatable biomarker for immune cell activation between human and monkey (Mager and Jusko, 2002; Mager et al, 2003; Kagan et al, 2010) and has routinely been measured in studies investigating recombinant human IFNs in monkeys. Although in the clinic a significant relationship exists between neopterin and IFNγ concentrations there are examples where IFNα2b treatment in patients with chronic hepatitis C led to increased neopterin concentrations were observed without an elevation in IFNγ concentrations. This may indicate that IFNα is directly stimulating neopterin production, engaging an alternative immune response pathway or a combination of the two.

It appears that primate offers and excellent species to mirror the IFNα challenge study design conducted in the clinic to some extent based on available PK and biomarker data. The evidence that the PK/PD relationship for number of different IFNs can be translated from the primate to human really highlights how valuable a primate model could be for a drug discovery programme. It will allow an assessment of the efficacy of a compound that can be translated with a degree of confidence into the clinic enabling the optimal design of expensive clinical studies.

2.6. PK/PD modelling

Modelling can be explained as the use of mathematical means to describe aspects of a system and/or process, thereby focusing on the factors believed to be important (Zhang, Pfister and Meibohm, 2008). Pharmacokinetics describe the concentration-time course of a drug in different body fluids and tissues, and includes drug administration, distribution and elimination (Sharma and Jusko, 1998). Pharmacodynamics characterise the intensity of the effect resulting from certain drug concentrations at the assumed effect site (Derendorf and Meibohm, 1999). The goal of PK/PD modelling is to link the change in concentration of the drug over time to the intensity of the observed response to derive an effect vs time profile in response to a dosing regimen as presented in Figure 2.7. Derendorf and Meibohm, (1999) comment that the ultimate goal of PK/PD analysis is predictive rather than descriptive modelling, and to achieve this, mechanism based models should be preferred as

they not only describe observations but also offer some insight into the underlying biological processes involved.

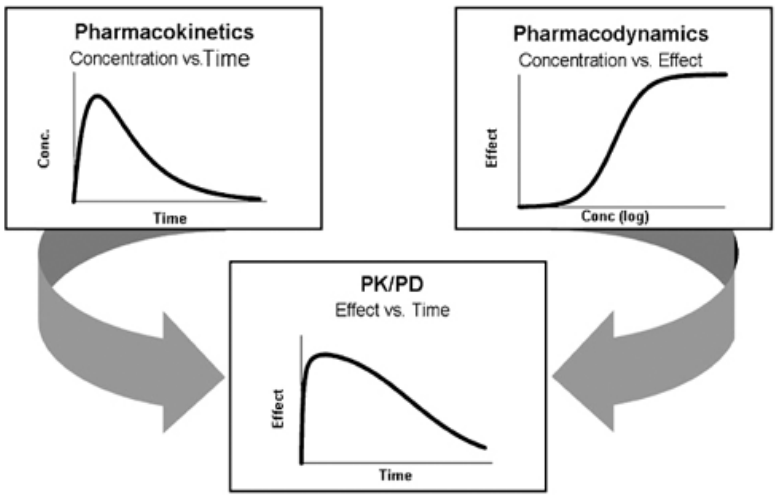

Figure 2.8 Modeling of Pharmacokinetic/Pharmacodynamic (PK/PD) Relationships: Concepts and Perspectives. Recreated with permission Derendorf and Meibohm (1999)

Using mechanism based PK/PD models offer flexibility in extrapolating the model from preclinical to clinical and/or across clinical situations. One of the focuses in drug discovery in recent years is to reduce attrition due to lack of efficacy in proof-of-mechanism/concept studies (Van Der Graaf and Gabrielsson, 2009). Using PK/PD modelling to provide confidence that the efficacy observed in preclinical studies can be translated to the clinic may improve the overall efficiency and success of drug discovery programmes. With regard to translation, studies have demonstrated that PK and physiological turnover parameters can often obey allometric principles and pharmacological capacity and sensitivity parameters are essentially species-independent giving confidence that PK/PD models should be translatable between species (Mager and Jusko, 2008). As biological system specific parameters, such as the expression of a target protein, can vary between species, individuals and disease states, intra and inter individual variability in these parameters must be considered (Danhof et al, 2008).

To derive the PK of a drug, non-compartmental analysis can be used as a starting point to estimate clearance (CL) and steady-state volume of distribution (V_{ss}) (Jusko, 2013). Compartmental models are then commonly used as they provide a continuous description

of the concentration that can easily serve as input function for the pharmacodynamic model (Derendorf and Meibohm, 1999). As an alternative, physiologically based pharmacokinetic models (PBPK) incorporate physiological pathways and processes such as blood flow, tissue weights and composition with a series of mass balance equations to describe the plasma and tissue drug concentrations following a range of routes of administration (Mager and Jusko, 2008). These models provide an option to potentially translate the PK between species based on the understanding of the impact of certain physiology on the kinetics of the drug and difference in the physiology between species.

PK/PD models relate the concentration provided by the PK model to the observed effect, and many PK/PD models look to link the PK, which are derived from analysis of drug concentrations in blood or plasma and are readily measurable, to the observed intensity of the effect. Different commonly used PK/PD models are summarised in a review by Mager, Wyska and Jusko (2003) and the model should, if possible, be selected based on the mechanisms of the action of the drug and an understanding of the biology (Sharma and Jusko, et al 1998). The simplest PK/PD models are where the observed effect is directly linked to concentrations at the effect site, and the concentrations in the effect site and blood/plasma are in equilibrium (Derendorf and Meibohm, 1999). For many drugs, the effect may not be directly associated with blood concentrations but rather to the drug concentrations at the site of action. Often a delay in the effect compared to the blood concentrations can be observed which results in counter-clockwise hysteresis when the effect is plotted against the blood concentrations. This delay may be attributed to a delay in distribution of the drug from the plasma to the effect site, or the time needed for synthesis or degradation of an endogenous substance. The former can be described using an effect-compartment model, which incorporates a hypothetical effect compartment attached to the pharmacokinetic model that describes the concentration-time course at the effect site and does not account for the mass balance of the drug (Derendorf and Meibohm, 1999). If the delay is not due to the distribution of the compound but rather a biological pathway, then an indirect response model should be used which takes into account that there is a lag time for development of the response even after the drug reaches the site of action (Sharma and Jusko, 1998). Dayneka Garg and Jusko, (1993) proposed four basic indirect response models that account for drug inhibition or induction of the response, by the inhibition or stimulation of either the zero order rate constant for the production of the

response (k_{in}) or the first order rate constant for the loss of the response (k_{out}) (Dayneka, Garg and Jusko, 1993).

PK/PD modelling requires measurement of both the drug concentration and the response. Ideally the measure of drug concentration would be in the biophase responsible for the drug effect, however, this is often challenging and for the majority of PK/PD modelling plasma or blood concentrations are used as a surrogate measure of concentrations at the effect site. In that case, the effect compartment model described above can be used to account for the site of action in an unmeasured compartment (Jusko, 1994). The response can be any type of response such as a pharmacological marker, a physiological parameter, and index of efficacy or a measure of safety (Zhang, Pfister and Meibohm, 2008). Traditionally PK/PD models have often relied on a single end point as a measure of drug activity. Iyengar et al (2012) suggest that this practice is a disadvantage as drugs often have multiple targets that are parts of networks that comprise multiple components that determine drug activity. Taking this into account, more complicated systems pharmacology models which look to understand the behaviour of the system as a whole are proposed to be an option for the future (Van de Graaf and Benson, 2011). These models should provide a network view of drug action and consider both on and off target effects that likely will affect multiple interconnected pathways (Iyengar et al, 2012).

PK/PD modelling can be approached in a number of ways. Data can be evaluated by a naive pooled approach, where data from all individuals are pooled and fitted simultaneously, ignoring individual differences in exposure and response (Upton and Mould, 2014). The issue with this approach is that it does not include an assessment of inter-individual variability and can produce biased parameter estimates (Kiang et al, 2012). Another option is to use what is known as the two step method where each individual's data are modelled, and summary statistics including mean and covariance for the parameter estimates are determined from the individual values. The issue with this method is that while the mean estimates of parameters are not necessarily biased, random effects (variance and covariance) most likely demonstrate bias and are imprecise (Kiang et al, 2012). The final option is population, or mixed effects, PK/PD modelling which enables characterization of the dose concentration effect relationships in populations rather than individuals, whilst taking into account differences between individuals (Derendorf and Meibohm, 1999). This

provides the opportunity to identify and account for sources of inter-individual pharmacokinetics and/or pharmacodynamic variability.

Population PK/PD modelling is primarily based on nonlinear mixed effect regression models introduced by Sheiner and co-workers (Sheiner and Grasela, 1991) which explains both fixed and random effects. Fixed effects are the population averaged PK/PD parameters whereas random effects describe variability not characterised by fixed effects including inter-individual variability (IIV), which is the variance of a particular parameter between individuals, and residual variability which is unexplained variability (errors in dosing, sampling time, assay errors, etc.) (Kiang et al, 2012). In some instances there may also be inter-occasion variability (IOV) where a drug administered to the same individual after a period of time may demonstrate variability in the parameters between the different dosing occasions (Mould and Upton, 2013). Population models are composed of several components; structural models, stochastic models and covariate models. Structural models are functions that describe the time course of a measured response and can be represented as algebraic or differential equations. Stochastic models describe the variability or random effects in the observed data and covariate models describe the influence of factors such as demographics or disease on the individual time course of the response (Mould and Upton, 2012). A number of software packages are available for population modelling, however NONMEM was the first and remains the most frequently used for both modelling and simulation (Kiang et al, 2012; Kelzer, Karlsson and Hooker, 2013). When conducting population PK/PD modelling, PK and PD models can be fitted simultaneously or the PK model can be developed first, then parameters from this model can used to develop the PD model (Upton and Mould, 2014). For the second option the PK parameters can either be fixed to population parameter estimates, including any variability or to the individual (“post hoc”) parameter estimates.

Gabrielsson and Weiner (2000) commented that a model needs to be challenged and validated. A good way to challenge a model is to test the model on a new set of experimental data or alternatively the model can be used to run numerous simulations. Whereas modelling looks to describe the system from the data already generated, simulation allows prediction of an expected distribution of response under different scenarios (Mould and Upton, 2012). Within drug development, simulations are important as they allow the evaluation of many different study designs and strategies before

conducting the actual *in vivo* or clinical study. This is analogous to many other industries that use modelling and simulation extensively, particularly when the costs of development are high and the risks are considerable (Lalonde et al, 2007)

Chapter 3: *in vivo* study design and sample analysis

3.1. Introduction

The delivery of a robust *in vivo* pharmacokinetic and pharmacodynamic (PK/PD) model requires accurate measurement of concentration time data. The parameter that is measured to determine the effect is normally termed a biomarker which can be defined as a physical sign or cellular, biochemical, molecular or genetic alteration by which normal or abnormal biologic process can be recognised and or monitored and that may have diagnostic or prognostic utility (Illei et al, 2004). Other important factors are the *in vivo* study design, the biomarkers to be investigated, analytical assays to determine the concentrations of therapeutic agents, challenge agents and biomarkers in samples of interest.

The selection and design of an *in vivo* PK/PD model is principally governed by its relevance to the target mechanism and/or disease and legislation. The legislation for working with animals differs between countries. Within the UK, an *in vivo* model must be approved by the Home office within a specified establishment, project and personal licence. Prior to any in life experiments a proposed model will undergo an ethical review of the chosen species, numbers of animals, severity of techniques, number of samples and competency of staff to conduct relevant techniques. A model may have to undergo a 3Rs (Replacement, Reduction and Refinement of animals in experimentation) review and demonstrate that no suitable animal alternative is available prior to in life experimentation. New models are typically designed following a review of the literature to ensure, in the case of a challenge model, a suitable dose of challenge to elicit a measurable response is selected and that an adequate sampling regime is put in place to capture both PK and PD measurements. A pilot study with a small number of animals may then be conducted to test a hypothesis and investigate the suitability of a model. A model may go through several iterations to optimise the study design before it can confidently be used to interrogate the PK/PD relationship.

Sample analysis may require the determination of small molecules and biological end points, such as cytokines in blood and serum samples. A range of analytical methodologies including Liquid chromatography linked to tandem mass spectrometry (LC-MS/MS), Enzyme-linked immunosorbent assay (ELISA) and Luminex bead technology may be utilised. LC-MSMS is preferred for the analysis of small molecule drugs, metabolites and other xenobiotic biomolecules in biological matrices. The ELISA is used to detect a substance of interest using antibodies, and is one of the most common methods for measuring serum

cytokines (Seavey, Lu and Stump, 2011). A typical ELISA is the sandwich ELISA where an antibody attached to the bottom of a well provides both antigen capture and immune specificity with the antigen being the substrate of interest. Another antibody linked to an enzyme provides detection and an amplification factor which enables accurate and sensitive detection of the antigen (Leng et al, 2008). An alternative is the competitive ELISA which is based upon the competition of labelled and unlabeled ligand for a limited number of antibody binding sites. One disadvantage of the ELISA is that it can only measure one analyte at a time, whereas the Luminex bead technology allows the measurement of multiple analytes from the same sample at the same time. This technology uses beads that have specific capture antibodies that bind the substrate following which fluorescence detection antibodies, which are distinguishable using flow cytometry, bind to the specific substrate-capture antibody complex on the bead set (Leng et al, 2008). All three assays determine the concentration of the analyte of interest by comparing the response in that sample to a standard curve derived from analysing a range of prepared standards.

This project will investigate, optimise and validate two in vivo challenge PK/PD models, one in the mouse using a small molecule challenge agent and one in the primate using a recombinant human cytokine as a challenge agent. This chapter will describe the in life methodologies used in these studies. In addition, this chapter will also describe the technology, method development and sample preparation conducted to provide robust concentration data for both the challenge agents and biomarkers in samples.

For the mouse model, both the *in vivo* work and sample analysis were conducted in the UK. The *in vivo* primate model was conducted and samples were analysed in the USA on behalf of the author. The author designed and submitted a study design, sourced and communicated with local experts in the US around the requirements of the in life phase and sample analysis and co-ordinated the successful delivery of the primate IFN challenge model and sample analysis.

3.2. In life and Analytical Methodology

3.2.1. Mouse Resiquimod challenge PK/PD model

3.2.1.1. Compound

Resiquimod was synthesized by GlaxoSmithKline R&D, Stevenage. The structure of resiquimod is shown in Figure 3.1.

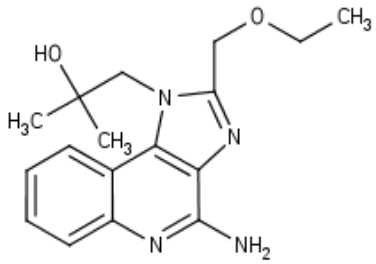

Figure 3.1 Chemical structure for Resiquimod

3.2.1.2. Animals

All *in vivo* experiments were ethically reviewed and carried out in accordance with Animal (Scientific Procedure) Act 1986 and the GlaxoSmithKline (GSK) policy on the Care, Welfare and Treatment of laboratory animals.

Male CD1 mice, weight 34-51g, were supplied by Charles River UK Ltd. Each mouse was individually housed in a plastic solid bottom cage and had free access to food (5LF2 EURodent Diet 14% supplied by PMI Labdiet, Richmond, Indiana, USA) and water. There were no known contaminants in the diet or water at concentrations that could interfere with the outcome of this study. Temperature and humidity were nominally maintained at 21°C ± 2°C and 55% ± 10%, respectively. Mice were allowed to acclimatise for at least 13 days and up to 8 weeks prior to the start of the study.

Body weight was the primary selection criterion for inclusion of mice into a study group. Following a change in working practice within the Quantitative Pharmacology group; the age of mice was also incorporated into the selection criteria. Mice in study groups 2, 3 and

4 were approximately 40 g and were older than 12 weeks of age on the study day. Table 3.1 shows the number, weight range and age of mice included in each study group.

Table 3.1 Number of mice, weight range and age of mice for included on study days 1-5

Study Group	Number of Mice	Weight Range (g)	Age of mice (weeks)
1	5	34-41	NR
2	32	40-51	17-18
3	8	42-49	17-18
4	8	45-48	17-18

NR – Not recorded

3.2.1.3. Pharmacokinetics of resiquimod in male CD1 mice

Mice were surgically implanted with a jugular vein cannula for drug administration under isoflurane anaesthesia using an established protocol. Prior to surgery, each mouse received penicillin and carprofen as a preoperative antibiotic and analgesic, respectively. Anaesthesia was induced, and then maintained with isoflurane 2.5-4% in 500-1000 mL/min oxygen. The fur was shaved from the back of the neck and front right of the neck, and the shaved area was cleaned with dilute Hibiscrub and Videne antiseptic solution. An incision (ca. 0.75 cm) was made at the front of the neck and the right jugular vein was exposed. A plastic strip was placed under the vessel, and two ligatures (Mersilk™ 5/0) were placed around the vein, one anteriorly and one toward the heart.

The jugular vein cannulae were made in house using 40 cm polyurethane tubing with a Silastic retention ring placed 1 cm from the tip. Prior to cannulation the anterior ligature was tied tightly and had tension applied. The cannula, which had been pre-soaked in sterile saline for 24 h, was inserted 1.0-1.2 cm into a small incision made in the vein wall. It was then secured on either side of the retention ring using the ligatures and exteriorised at the back of the neck using a trocar. The jugular vein incision was closed using continuous suture (Vicryl ™ 6/0), following which mice were placed in harnesses with protective tethers attached to a single channel swivel and anchored outside the cage to a counter balance system. The mice were allowed to recover for at least 6 days prior to dosing.

The target dose of resiquimod was based on the dose previously administered to mice (Asselin-Paturel et al, 2005). In the published study, 0.005 mg of resiquimod was dissolved and administered in 0.2 mL of phosphate buffered saline (PBS). Assuming a mouse was

approximately 0.02 kg (weights of mice not published) the administered dose would have been 0.25 mg/kg, therefore the target dose administered by iv infusion to male CD1 mice was 0.25 mg/kg.

For intravenous administration, resiquimod was dissolved in dimethyl sulfoxide (DMSO) to give a 0.8 mg/mL solution which was then made to the required total volume to achieve a concentration of 0.035 mg/mL with 10% (w/v) Kleptose™HPB in saline. The dose was filtered and administered as a 5 min constant rate iv infusion at 1.4 mL/kg/min using a syringe pump to achieve a target dose of 0.05 mg/kg/min (0.25 mg/kg).

3.2.1.4. Investigation of the induction of serum concentrations of IFNα (response) over a resiquimod dose range in the male CD1 mouse.

Six dose solutions at concentrations of 0.006, 0.014, 0.02, 0.06, 0.14 and 0.2 mg/mL were prepared from a 10 mg/mL resiquimod DMSO stock solution. An additional 0.6 mg/mL dose solution was prepared by dissolving 8.3 mg of resiquimod in DMSO to give a 12 mg/mL DMSO solution. The DMSO solutions were made to the required total volume with the addition of DMSO (where required to ensure the volume of DMSO in the final dose solution was 5% (v/v) of the total volume) and 10% (w/v) Kleptose™HPB in saline. The exact dilution scheme used to prepare the dose solutions on both dosing occasions can be viewed in Appendix 1.1.

In group 2 mice were sub divided into 8 groups of 4 mice. All doses were administered as a single iv bolus via the tail vain at a dose volume of 5 mL/kg. One group received administration of vehicle [DMSO 10% (w/v) Kleptose™HPB in saline (5:95% v/v)] as a control, the remaining 7 groups received target resiquimod doses of 0.03, 0.07, 0.1, 0.3, 0.7, 1 and 3 mg/kg respectively.

Mice were placed into a warming cabinet set at a temperature of 39°C 5 min prior to dose administration, and 5 min before each blood sample. The tail vein that was used for dose administration was noted and the vein on the opposite side of the tail was used for blood sampling.

3.2.1.5. Reproducibility of the response between study days.

This study was conducted over two separate days with group 3 dosed on one day and group 4 dosed on a second day. On each study day a fresh dose solution was prepared. For intravenous bolus administration, resiquimod was dissolved in DMSO to give a 1.2 mg/mL DMSO solution. The DMSO solution was then made to the required total volume with 10% (w/v) Kleptose™HPB in saline to achieve a concentration of 0.06 mg/mL.

Groups 3 and 4 were comprised of eight mice sub divided into 2 groups of 4 mice. One of these sub groups received administration of vehicle [DMSO 10% (w/v) Kleptose™HPB in saline (5:95% v/v)] as a control, the other group received resiquimod treatment at 0.3 mg/kg. All doses were administered as a single iv bolus via the tail vein at a dose volume of 5 mL/kg.

3.2.1.6. Collection of dose aliquots

All dose syringes were weighed pre and post dose using a precision balance to determine the exact weight of dose administered to each mouse. All doses were filtered prior to administration using a 0.22 µm syringe filter unit. For analysis of the concentration of resiquimod in the dose solution, three 0.05 mL aliquots of the pre and post filter dose solutions were collected into blank matrix tubes and stored at approximately -20°C prior to analysis. The pre and post filter aliquots were taken to determine if there was any loss of compound during the filtration process.

3.2.1.7. Collection and preparation of blood samples

The protocols used for sample collection and processing were comparable across all studies. Serial blood samples (0.087 mL) were collected for analysis of IFNα and resiquimod concentrations at 0.75 h, 1 h, 1.5 h and 2 h post dose via direct venepuncture of the tail vein. An additional 0.015 mL sample was collected via direct venepuncture of the tail vein at 5 min post dose for analysis of resiquimod concentration only. At 3 h post dose, mice were anaesthetised with isoflurane 2.5-4% in 500-1000 mL/min oxygen and exsanguinated via cardiac puncture to obtain a terminal blood sample. Mice receiving the iv infusion administration of resiquimod (study 1) had an additional blood sample (0.087 mL) collected via direct venepuncture of the tail vein at 2.5 h. Mice receiving resiquimod as an iv bolus

(studies 2-4) had an additional blood sample (0.072 mL) collected prior to challenge administration for analysis of IFNα concentration only.

The 0.087 mL blood samples were separated into 0.072 mL for analysis of IFNα concentrations and 0.015 mL for analysis of resiquimod concentrations. The blood samples collected for IFNα analysis were allowed to clot at room temperature for at least 1 h. Following this, the samples were centrifuged for 10 min at 12500 RPM using a microlitre centrifuge to separate the serum from the blood cells/clot. The separated serum samples were aspirated into 96 well V bottomed plates. The 0.015 mL blood samples for resiquimod analysis were collected into matrix tubes and diluted with an equal volume of water for injection. Both diluted blood samples and serum samples were stored at approximately -20°C prior to analysis.

3.2.1.8. Analysis of the resiquimod dose concentration

The actual concentrations of the resiquimod dose solutions were determined on each study day. The dose solution administered by iv infusion, and the dose solutions used to assess the inter study day variability were analysed using a Photodiode Array (PDA) detector. The dose solutions prepared to investigate the resiquimod dose response were analysed using LC-MS/MS. The methods used on each occasion are briefly described below.

3.2.1.9. Determination of the concentration of the resiquimod dose solutions for groups 1, 3 and 4 using a Photodiode Array (PDA) detector

For the resiquimod dose solution prepared for iv infusion administration to group 1, aliquots (0.1 mL) of the pre and post filter iv dose solution (0.035 mg/mL) were diluted in matrix sample tubes with 0.9 mL of water containing 0.1% (v/v) formic acid to achieve a nominal concentration of 0.0035 mg/mL. Three resiquimod analytical reference solutions were prepared by creating three 10 mg/mL resiquimod stock solutions in DMSO. Aliquots of each of the DMSO stock solutions (0.002 mL) were diluted in 0.569 mL of 10% (w/v) Kleptose™HPB in saline to achieve a concentration of 0.035 mg/mL. Aliquots (0.1 mL) of the 0.035 mg/mL reference solutions were diluted with 0.9 mL of water containing 0.1% (v/v) formic acid to achieve a nominal concentration of 0.0035 mg/mL.

For the resiquimod dose solution prepared for iv bolus administration to groups 3 and 4, aliquots (0.05 mL) of the pre and post filter iv dose solution (0.06 mg/mL) were diluted in

matrix sample tubes with 0.450 mL of water containing 0.1% (v/v) formic acid to achieve a nominal concentration of 0.006 mg/mL. Three resiquimod analytical reference solutions were prepared by creating three 10 mg/mL resiquimod stock solutions in DMSO. 0.002 mL aliquots of each of the DMSO stock solutions were diluted in 0.333 mL of 10% (w/v) Kleptose™HPB in saline to achieve a concentration of 0.06 mg/mL. 0.1 mL aliquots of the 0.06 mg/mL reference solutions were diluted with 0.9 mL of water containing 0.1% (v/v) formic acid to achieve a nominal concentration of 0.006 mg/mL.

The reference standards were prepared in 1.5 mL Eppendorf tubes, and both the dose solutions and reference solutions were prepared in triplicate. Aliquots (0.01 mL) of samples, reference standards and blanks were injected onto an ultra performance liquid chromatography (UPLC™) system with a PDA detector. The system was controlled using MassLynx software for data acquisition. Prior to sample analysis, a single 0.01 mL aliquot of one of the reference standards was injected onto the system and an analytical method was created using the MassLynx software. The chromatographic conditions and gradient are detailed in Appendix 1.2 and 1.3 respectively. The ultra-violet spectrum of the resiquimod reference solution was obtained, and based on this spectrum a target wavelength was selected (247 nm). To create the analytical method a wavelength range of ± 5 nm of the target wavelength was entered (242-252 nm) into the software. The accuracy of the analytical method was confirmed by injection of a second 0.01 mL aliquot of one of the reference standards and integration of the chromatogram using a single integration method within the QuanLynx software.

Each replicate of the samples, or reference standards was injected three times during the analysis. The generated peak area for each sample was used for comparison. The median of the three prepared reference solutions was chosen as the reference solution for data analysis. The accuracy of the resiquimod dose solutions was confirmed by comparing the average peak area determined for each of the dose solution samples to the average peak area determined for the selected reference solution.

3.2.1.10. Determination of the concentration of the resiquimod dose solution for group 2 using Liquid Chromatography Mass Spectrometry (LC-MS/MS)

For the analysis of the dose solutions administered to group 2, aliquots (0.05 mL) of the pre and post filter iv dose solution for all doses were diluted in matrix sample tubes with 1:1

(v/v) acetonitrile:water. The dose solutions were prepared by diluting 50 µL of each sample in 450 µL 1:1 (v/v) acetonitrile:water to give a 1:10 dilution. All dose solutions except the 6 µg/mL dose solution were subsequently further diluted in multiples of 10 depending on the initial dose concentration. The exact dilution scheme used to prepare the dose solutions for analysis can be viewed in Appendix 1.4.

Three aliquots (50 µL) of each diluted dose solution were aliquotted into blank matrix tubes. The dose samples were then matrix matched to the blood samples with the addition of 0.1 mL of control 1:1 (v/v) CD1 mouse blood:water. The dose samples were extracted using protein precipitation with 0.3 mL of acetonitrile containing labetalol as an analytical internal standard. The internal standard was prepared by diluting 12.5 µL of a 5 mg/mL DMSO labetalol stock solution in 1000 mL of acetonitrile to give a final internal standard solution at an approximate concentration of 62.5 ng/mL. Once the internal standard or acetonitrile was added to all dose samples, all matrix tubes were capped with pierceable caps, and shaken for 10 minutes with a mechanical shaker then centrifuged at 3000g for 30 minutes using a Heraeus centrifuge.

1.5 µL of each dose sample were injected onto a LC-MS/MS system then the concentration of resiquimod in the dose samples was determined by comparing the peak area ratio determined for each sample to the calibration line. The acceptance criteria for the assay were that dose samples had to be within +/-20% of the nominal concentration. The internal standard signal variability was analysed using the peak area, to ensure consistency in the peak area across all samples.

3.2.1.11. Analysis of resiquimod whole blood concentrations

The concentration of resiquimod in blood sampled from individual mice following both iv infusion and iv bolus administration of resiquimod, was determined using LC-MS/MS. Sample analysis was undertaken in accordance with the II TAU Quantitative Pharmacology (GlaxoSmithKline) sample analysis guidelines. Prior to preparation and analysis, blood samples were thawed unassisted at room temperature, and a fresh set of calibration standards were prepared.

The calibration standards were prepared in blank matrix tubes over a concentration range of 1-10000 ng/mL. Initially a 0.1 mg/mL resiquimod stock solution in 1:1 (v/v) acetonitrile:water was prepared and labelled as A0. This stock solution was then diluted to

prepare four resiquimod stock solutions at 0.01, 0.001, 0.001 and 0.00001 mg/mL (A1-A4) in 1:1 (v/v) acetonitrile:water. The dilution steps are detailed in Appendix 1.5. Individual standards were prepared by the addition of one of the resiquimod stock solutions (A1 to A4) depending on the required standard concentration. An additional amount of 1:1 (v/v) acetonitrile:water was added where required to ensure that the total volume of 1:1 (v/v) acetonitrile:water in all matrix tubes was 15 µL. The calibration standards were then matrix matched to the blood samples with the addition of 30 µL of control 1:1 (v/v) CD1 mouse blood:water. The exact dilution scheme used to prepare the calibration standards can be viewed in Table 3.2.

Blank standards were prepared in blank matrix tubes by combining 0.015 mL of 1:1 (v/v) acetonitrile:water with 0.03 mL of control 1:1 (v/v) CD1 mouse blood:water. Blank samples were extracted using protein precipitation with 0.3 mL of pure acetonitrile.

Diluted blood samples and calibration curve standards were extracted using protein precipitation with 0.3 mL of acetonitrile containing labetalol as an analytical internal standard. The labetalol solution was prepared by diluting 12.5 µL of a 5 mg/mL DMSO labetalol stock solution in 1000 mL of acetonitrile to give a final internal standard solution at an approximate concentration of 62.5 ng/mL. A blank sample with internal standard (blank +internal standard) was prepared by extracting one of the prepared blank samples with 0.3 mL of the labetalol internal standard. Once the internal standard or acetonitrile was added, matrix tubes were sealed with pierceable caps and shaken for 10 minutes with a mechanical shaker then centrifuged at 3000g for 30 minutes using a Heraeus centrifuge.

Table 3.2 Resiquimod calibration standard dilution scheme

Standard Concentration (ng/mL)	Volume of A4 stock solution added to standard (µL)	Volume of A3 stock solution added to standard (µL)	Volume of A2 stock solution added to standard (µL)	Volume of A1 stock solution added to standard (µL)	Volume of 1:1 (v/v) (Acetonitrile:Water) added to standard (µL)	Volume of control 1:1 Blood:Water added to standard (µL)
Total Blank	-	-	-	-	15	30
Blank+internal standard	-	-	-	-	15	30
1	1.5	-	-	-	13.5	30
2	3	-	-	-	12	30
5	7.5	-	-	-	7.5	30
10	15	-	-	-	-	30
20	-	3	-	-	12	30
50	-	7.5	-	-	7.5	30
100	-	15	-	-	-	30
200	-	-	3	-	12	30
500	-	-	7.5	-	7.5	30
1,000	-	-	15	-	-	30
2,000	-	-	-	3	12	30
5,000	-	-	-	7.5	7.5	30
10,000	-	-	-	15	-	30

2 µL of samples, calibration standards and blanks were injected onto a LC-MS/MS system and analysed by MS/MS using a heat assisted electrospray interface in positive ion mode. The LC system was controlled by Jasco analyst companion software. The LC methodology and gradient used for sample analysis are detailed in Appendix 1.6 and 1.7 respectively. The mass spectrometer was controlled by Analyst software, using an optimised multiple reaction monitoring (MRM) for data acquisition. The MRM transitions selected for analysis of resiquimod and the labetalol were 315 to 251 and 329 to 162, respectively.

For data analysis the chromatograms were integrated using the IntelliQuan algorithm and a single integration method within the Analyst software. The assay LLQ was set at lowest calibration standard with a peak greater than the height of the peak observed in the total blank sample plus 5 times the average background noise. The peak area ratio was determined for each of the calibration standards by dividing the resiquimod peak area by the labetalol peak area. The peak area ratios were then used to create a calibration line using linear regression with a weighting of $1/(x^2)$. The acceptance criteria for the assay were that samples had to be within +/-20% of the nominal concentration. The concentration of resiquimod in the samples was determined by comparing the peak area ratio determined for each sample to the calibration line and calculating the corresponding resiquimod concentration. The internal standard signal variability was analysed using the peak area, to ensure the consistency in the peak area across all samples.

The analysis of samples was conducted as previously described above except for the following amendments

- For the analysis of samples from Group 2, two 0.1 mg/mL resiquimod stock solutions in 1:1 (v/v) acetonitrile:water were prepared and labelled as A0 and B0. The A0 solution was used to prepare the calibration standards as previously described. The B0 solution was used to prepare analytical quality controls (QCs) which were included in the analysis of samples. The quality control samples were prepared using the same method as for the analytical standards at the following concentrations 0.5, 2, 20, 200 and 1000 ng/mL on study day 2.
- For the analysis of samples from Group 2, an increased range of analytical standards was prepared including 0.1, 0.2 and 0.5 ng/mL. The exact dilution

scheme used to prepare the 0.1-1 ng/mL calibration standards can be viewed in Table 3.3.

Table 3.3 Resiquimod calibration standard 0.1- 1 ng/mL dilution scheme

Standard Concentration (ng/mL)	Volume of A5 stock solution added to standard (µL)	Volume of A4 stock solution added to standard (µL)	Volume of A3 stock solution added to standard (µL)	Volume of A2 stock solution added to standard (µL)	Volume of A1 stock solution added to standard (µL)	Volume of 1:1 (v/v) (Acetonitrile: Water) added to standard (µL)	Volume of control 1:1 Blood:Water added to standard (µL)
0.1	1.5	-	-	-	-	13.5	30
0.2	3	-	-	-	-	12	30
0.5	7.5	-	-	-	-	7.5	30
1	15	-	-	-	-	-	30

- Diluted blood samples and calibration curve standards on study days 2, 3 and 4 were extracted using protein precipitation with 0.2 mL of acetonitrile containing labetalol as an analytical internal standard.
- On study day 2, 1.5 µL of each sample were injected onto a LC-MS/MS system as part of the analytical run to determine the concentration of resiquimod in the mouse blood and dose samples.
- On study day 3 and 4, 3 µL of each sample were injected onto a LC-MS/MS system as part of the analytical run to determine the concentration of resiquimod in the mouse blood samples.

3.2.1.12. Analysis of IFNα serum concentrations

IFNα serum concentrations were determined using a VeriKine™ mouse IFNα ELISA kit.

The IFNα ELISA assay was conducted over two days. On day one all incubations were performed at room temperature (22-25˚C). An IFNα standard curve constructed over a range of 20 - 1000 pg/mL was prepared by diluting the 10000 pg/mL mouse IFNα stock solution supplied with the kit. Initially a 1000 pg/mL stock solution was prepared by diluting 80 µL of the 10000 pg/mL stock solution in 720 µL of the supplied sample buffer solution. The 1000 pg/mL stock solution was then diluted to prepare the IFNα standards at the following concentrations 20, 50, 100, 300, 500, 625 and 800 pg/mL.

The mouse serum samples were prepared by diluting 10 µL of each sample in 90 µL of the sample buffer solution to give a 1:10 dilution. As the standards do not contain any matrix (serum), matrix controls at 100 and 300 pg/mL were prepared to determine whether the

matrix had an effect on the IFNα concentrations. Aliquots of the supplied sample buffer solution were used for blanks. For analysis, 7070 µL of the secondary antibody solution is required per plate of samples/standards. The secondary antibody was prepared by diluting 70 µL of the supplied antibody solution in 7000 µL of the sample buffer solution.

Aliquots (100 µL) of the standards, matrix controls, blanks or samples were transferred into individual wells in the supplied 96 well pre-coated plate. Standards and matrix control samples were run in duplicate. 50 µL of the diluted antibody solution was then added to each well in the plate, following which the plate was covered with the supplied plate sealers and incubated for 1 h at room temperature with mechanical shaking at 450 RPM using a mini orbital shaker. After 1 h the plate was placed in the fridge and incubated at +4 °C for 16-20 h.

On Day 2, a wash solution was prepared by diluting 50 mL of the supplied wash solution concentrate in 950 mL of deionised water. The contents of the plate were emptied, and the plate was washed four times using the prepared wash solution. A horseradish peroxidase (HRP) solution was prepared by diluting 40 µL of the supplied HRP conjugate concentrate in 1200 µL of the sample buffer solution. Following this, 100 µL of the HRP solution was added to each well in the plate, which was then covered with the supplied plate sealers and incubated for 2 h at room temperature with mechanical shaking at 450 RPM.

Following the 2 h incubation period, the plate was emptied and washed four times using the prepared wash solution. 100 µL of the supplied tetramethyl benzidine (TMB) substrate solution was added to each well, and the plate was incubated in the dark at room temperature for 15 min. After the 15 min incubation, 100 µL of the supplied stop solution was added to each well. The absorbance at 450 nm was determined using a SpectraMax micro-plate reader and Softmax software. The optical densities determined for the calibration standards were used to plot a standard curve in GraphPad using a 4-parameter logistic fit. The Dixon's Q test was used to examine whether standards were considered outliers compared to the blanks. The limit of detection was set as the lowest standard that was statistically different from the blank as determined by the Dixons Q test and within ± 20% of the nominal concentration. The final standard curve was then used to determine the IFNα concentration in the mouse serum samples.

The serum samples from each study were run as separate assays, the analysis of all samples was conducted as detailed above except for the following amendments

- Following iv infusion administration (group 1) due to a low sample volume, the 2 h sample from Mouse 3 was prepared by diluting 5 µL of each sample in 95 µL of the sample buffer solution to give a 1:20 dilution.
- Following iv bolus administration (group 4) There was insufficient serum sample volume for the mouse 8 1.5 h sample, so this sample was diluted 1:20.
- For the analysis of samples from groups 2, 3 and 4, any samples where the determined IFNα concentration was above the assay higher limit of quatification (HLQ) were repeated. For the repeat analysis the mouse serum samples were prepared by diluting 10 µL of each sample in 490 µL of the sample buffer solution to give a 1:50 dilution.

3.2.2. Primate IFNα2b challenge PK/PD model

3.2.2.1. IFN

Recombinant Interferon α2b (INTRON® A) for intramuscular, subcutaneous, intralesional or intravenous injection was purchased for use in this study. The recombinant Interferon α2b was supplied as vials containing 50 million IU of powder for injection with a specific activity of approximately 2.6 x10^8 IU/mg protein as measured by HPLC.

3.2.2.2. Animals

All studies were conducted in accordance with the GSK Policy on the Care, Welfare and Treatment of Laboratory Animals and were reviewed by the Institutional Animal Care and Use Committee either at GSK or by the ethical review process at the institution where the work was performed. All in life procedures were carried out on behalf of the author by GSK laboratory animal staff at the Upper Providence site, Pennsylvania, US.

Male cynomologus monkeys, weight 6.2-9.5 kg, aged between 5.5 and 8.7 years were used in this study. The monkeys were supplied by Charles River Ltd or Covance and had resided at GSK for at least 3 years prior to the start of the study. None of the monkeys were naive at the start of the study and had been used in up to 5 previous experiments. Prior to the start of the study, monkeys underwent a complete blood cell count, blood chemistry analysis and a health check by a veterinarian to confirm eligibility to be placed on the study.

Monkeys were either individually housed or house in compatible pairs, in stainless steel cages, had free access to water and were offered 8 biscuits of Monkey diet (5038, supplied by PMI Nutrition International, Richmond, Indiana, USA) and a daily allocation of fresh fruits twice a day. There were no known contaminants in the food or water at concentrations that could interfere with the outcome of this study. Temperature and humidity were nominally maintained at 18°C to 29°C and 30% to 70%, respectively with an approximate 12 h light 12h dark cycle. All monkeys were acclimatized to restraint chairs and visual enrichment in the form of videos was provided while monkeys were in the chairs.

Monkey 6 (M05212) was involved in a fight prior to the third dosing occasion (10MIU/kg) and sustained injuries which required treatment with antibiotics. The decision was taken to postpone the treatment to a later date, however his condition deteriorated and the decisions was taken to euthanize him for humane reasons.

3.2.2.3. IFNα2b preparation and administration

This study was conducted as a Latin square design utilizing a total of nine animals, consisting of three animals per dose group and three dosing occasions per group. Each animal received subcutaneous administration of a low dose of Interferon α2b at 3 MIU/kg, a high dose of Interferon α2b 10 MIU/kg and vehicle. On each study day three monkeys received either interferon α2b or vehicle, following the last blood sample monkeys had at least a three week wash out period prior to the next dosing occasion. The proposed dosing schedule is shown in Table 3.4.

Table 3.4 Monkeys assigned to each dose group and dosing schedule

Dose Group	Monkey Number	Monkey ID	First Dosing Occasion	Second Dosing Occasion	Third Dosing Occasion
1	1	129-184	10 MIU/kg	3 MIU/kg	Vehicle
	2	129-208	10 MIU/kg	3 MIU/kg	Vehicle
	3	M05814	Vehicle	10 MIU/kg	3 MIU/kg
2	4	129-204	Vehicle	10 MIU/kg	3 MIU/kg
	5	70-207	10 MIU/kg	Vehicle	3 MIU/kg
	6	M05212	3 MIU/kg	Vehicle	10 MIU/kg
3	7	129-116	10 MIU/kg	Vehicle	3 MIU/kg
	8	129-81	3 MIU/kg	Vehicle	10 MIU/kg
	9	M05848	3 MIU/kg	Vehicle	10 MIU/kg

For subcutaneous administration, the required number of vials containing 50 million IU of Interferon α2b as a powder were reconstituted on each study day with 1 mL of sterile water for injection per vial to give a concentration of 50 million IU/mL. Prior to administration the animals were weighed, the hair on the left forearm was shaved and the underlying skin was cleaned with alcohol wipes. IFNα2b was administered as a single subcutaneous injection to achieve a dose of 3 MIU/kg or 10 MIU/kg but not exceeding a dose volume of 5 mL/kg. On vehicle treatment legs, monkeys received a single subcutaneous (sc) administration of saline at a dose of 0.2 mL/kg.

3.2.2.4. Collection and preparation of blood samples

Serial blood samples (1 mL) were collected for analysis of IFNα2b, neopterin and cytokine concentrations predose and at 0.5 h, 1 h, 2 h, 4 h, 6 h, 8 h, 10 h, 24 h, 27 h, 30 h, 33 h, 48 h, 72 h, 96 h, 120 h, 168 h and 240 h post dose via femoral venepuncture for each sample. The blood samples were aliquoted into serum collection tubes, and allowed to clot at room temperature for at least 1 h. Following this, the samples were centrifuged for 10 min at 5000 RPM to separate the serum from the blood cells/clot. The separated serum samples were aspirated using a pipette into eppendorfs and stored at approximately -80°C prior to analysis.

An additional 0.5 mL sample was collected via femoral venepuncture predose and at 0.5 h, 1 h, 2 h, 4 h, 6 h, 8 h, 10 h, 24 h, 27 h, 30 h, 33 h, 48 h and 72 h for analysis of the induction of a number of interferon inducible genes. The blood samples were aliquoted into RNAprotect® animal blood tubes, gently inverted 8-10 times and allowed to sit at room temperature for at least 6 h but not more than 24 h. Following this the samples were stored at approximately -80°C prior to analysis.

3.2.2.5. Analysis of body temperature

The body temperature of the monkeys was obtained predose and at 0.25 h, 0.5 h, 1h, 1.25h, 1.5 h, 1.75 h, 2 h, 4 h, 6 h, 8 h, 10 h, 24 h, 27 h, 30 h, 33 h, 48 h and 72h post dose using a rectal thermometer.

3.2.2.6. Analysis of serum neopterin concentrations

The analysis to determine the concentrations of neopterin in the serum samples was conducted on behalf of the author by Quantitative Pharmacology, II TAU, GSK, Upper Merion site, Pennsylvania, US. Serum samples (50 µL per sample) were analysed using a B·R·A·H·M·S competitive ELISA assay for the quantitative determination of neopterin in serum, plasma and urine using coated microtitre plates. The assay was conducted as per the manufacturer's instructions and the absorbance at 405 nm was determined using an EnVision micro-plate reader and EnVison workstation software (version 1.12).

3.2.2.7. Analysis of serum cytokine/chemokine concentrations

The concentrations of multiple cytokines/chemokine in the serum samples were determined on behalf of the author by Quantitative Pharmacology, II TAU, GSK, Upper Merion site, Pennsylvania, US. Serum samples (25 µL per sample) were analysed using a Milliplex® Human cytokine/chemokine magnetic bead panel kit 96 well plate assay. The assay allows for the simultaneous quantification of the following 29 human cytokines and chemokines; EGF, Exotaxin, GCSF, GMCSF, IFNα2b, IFNγ, IL10, IL12P40, IL12P70, IL13, IL15, IL17A, IL1Ra, IL1α, IL1β, IL2, IL3, IL4, IL5, IL6, IL7, IL8, IP10, MCP1, MIP1α, MIP1β, TNFα, TNFβ, VEGF. The assay was conducted as per the manufacturer's instructions and the fluorescent intensity was determined using a BioRad BioPlex-200 instrument with BioPlex manager software (version 6.1).

The samples were analysed over 3 different occasions with 6 separate assays / plates across the 3 occasions the samples analysed on each occasion are presented in Table 3.5. Any samples on analytical occasion 2 that were above the IFNα2b assay HLQ were diluted 1:10 and included in the analysis as part of plate 3 on occasion 3. In addition, a number of samples on plates 1-3 on analytical occasion 3, that were anticipated to have serum IFNα2 concentrations above the IFNα2b assay HLQ, were also diluted 1:10 and re-assayed on that plate.

Following the completion of assays on occasion 1 and occasion 2 the serum concentrations from all analytes were reviewed and the number of analytes was triaged to select a smaller number of analytes to be progressed in future assays. The analytes were selected as 1) the ones that appeared to demonstrate a response to IFNα2b, 2) analytes that appeared to

show no response to IFNα2b to confirm this lack of response in all subjects and 3) analytes that may be of interest to other research programmes within GSK.

Table 3.5 Samples analysed on each day of analysis

First Analytical Occasion	Second Analytical Occasion		Third Analytical Occasion		
Plate 1	Plate 1	Plate 2	Plate 1	Plate 1	Plate 2
Monkey 1 10 MIU/kg	Monkey 1 Vehicle	Monkey 3 3 MIU/kg	Monkey 4 10 MIU/kg	Monkey 5 3 MIU/kg	Monkey 8 10 MIU/kg
Monkey 2 10 MIU/kg	Monkey 1 3 MIU/kg	Monkey 3 10 MIU/kg	Monkey 4 3 MIU/kg	Monkey 7 Vehicle	Monkey 9 Vehicle
Monkey 3 Vehicle	Monkey 8 3 MIU/kg	Monkey 9 3 MIU/kg	Monkey 5 Vehicle	Monkey 7 3 MIU/kg	Monkey 9 10 MIU/kg
		Monkey 5 10 MIU/kg	Monkey 6 Vehicle	Monkey 8 Vehicle	
		Monkey 6 3 MIU/kg			

3.3. Results

3.3.1. Mouse Resiquimod challenge PK/PD model

3.3.1.1. Quantification of the resiquimod dose administered to mice

There was no peak corresponding to resiquimod observed in any of the blank injections. The mean peak areas, standard deviation and CV (%) of the reference solutions A, B and C are presented in Appendix 1.8 (group 1) and Appendix 1.10 (groups 3 and 4). For both dose checks, reference standard B was selected as the analytical reference standard. A comparison of the mean peak areas determined for reference solutions A and C to that determined for reference solution B was within the ± 20% acceptance range.

All dose solution concentrations for the pre and post filter aliquots prepared for administration to group 1 were within ± 20% of the reference solution, while the pre and post filter aliquots prepared for administration to groups 3 and 4 were outside ± 20% of the reference solution. Based on this the nominal dose concentration was used to determine the actual dose administered to group 1, while the analytically measured dose concentration for the post filter dose solutions administered to groups 3 and 4, calculated

as 0.076 and 0.078 mg/mL respectively, were used to determine the actual dose administered to mice in groups 3 and 4.

For group 2 the analytically measured dose concentrations were outside ± 20% of the nominal dose concentration (Appendix 1.10). The 0.006-0.2 mg/mL dose concentrations were all 16-53% higher than the nominal dose concentration for both the pre and post filter aliquots. The pre and post filter aliquots of the 0.6 mg/mL dose solution, which was made from a separate stock solution, were 44% and 51% higher than the nominal concentration respectively. The analytically measured concentrations for each dose were calculated and used to determine the actual dose administered to mice in group 2.

3.3.1.2. Quantifying the concentration of resiquimod in blood samples

A summary of the LC-MSMS analysis including the analytical range analysed, the final accepted analytical range and any standards that were not included in the calibration line for all 4 groups is presented in Table 3.6. For group 1, the analytical range was sufficient to determine the concentrations of resiquimod in all but the 3 h samples and so was considered fit for purpose for this study. As part of the analysis for group 2 QCs were included. The 2, 20, 200 and 1000 ng/mL QCs were within ± 20% of the nominal concentration and linear range of the calibration curve but the 0.5 ng/mL QCs were outside. The analytical range was therefore set from 1 ng/mL (LLQ) to 2000 ng/mL (higher limit of quantification, HLQ).

In the first analytical run for samples from group 2, the peak area of the internal standard observed in all dose samples was outside of ± 20% of the mean internal standard peak area and these samples were rejected. To counteract any ion suppression effects in these samples the heat assisted electrospray interface was replaced with an atmosphere pressure chemical ionisation interface and these dose aliquots were reanalysed. Standards were not injected as part of the standard curve as the range was not required.

Table 3.6 Analytical assay performance

Group	Standards Injected as part of standard line	Samples rejected as outside ± 20% of nominal concentration	Samples rejected as indistinct from background	Final analytical range
1	1 to 10000 ng/mL	2000, 5000 and 10000 ng/mL	1 ng/mL	2 to 1000 ng/mL
2 (Run 1)	0.1 to 5000 ng/mL	5000 ng/mL	0.1, 0.2, and 0.5 ng/mL	1 to 2000 ng/mL
2 (Run 2)	0.1 to 1000 ng/mL	1 and 2 ng/mL	0.1, 0.2, and 0.5 ng/mL	5 to 1000 ng/mL
3	1 to 2000 ng/mL	1 and 10 ng/mL		2 to 2000 ng/mL
4	1 to 2000 ng/mL		1 ng/mL	2 to 2000 ng/mL

3.3.1.3. Analysis of IFNα in serum samples

The concentration of IFNα in serum sampled from individual mice following administration of resiquimod, was determined using an ELISA assay on four separate occasions. The LLQ and HLQ for the ELISA assay were 200 pg/mL and 8000 pg/mL respectively for all four assays.

The serum IFNα concentration determined at 2 h for mouse 1 and 1.5 h for mouse 3 in Group 1 were above the assay HLQ (8000 pg/mL). To enable data analysis, the IFNα serum concentrations (8263 and 8626 pg/mL for mouse 1 and 3 respectively) were used for these samples as they were within 10% of the HLQ.

3.3.2. Primate IFNα2b challenge PK/PD model

3.3.2.1. Dose of IFN administered

The weight of monkeys and dose of IFNα administered on each dosing leg are detailed in Table 3.7

Table 3.7 Individual monkey body weights and actual doses of IFNα2b administered to each monkey on each dosing occasion.

Monkey Number	Monkey ID	Dose (MIU/kg)	Body weight (kg)	Volume of 50 MIU/mL IFNα or saline administered (mL)	Amount of IFNα administered (MIU)
1	129-184	Vehicle	7.9	NR	N/A
		3 MIU/kg	7.8	0.468	23.4
		10 MIU/kg	6.8	1.36	68
2	129-208	Vehicle	6.9	NR	0
		3 MIU/kg	6.0	0.36	18
		10 MIU/kg	6.6	1.32	66
3	M05814	Vehicle	8.9	NR	N/A
		3 MIU/kg	9.3	0.56	27.9
		10 MIU/kg	9.3	1.86	93
4	129-204	Vehicle	9.5	NR	N/A
		3 MIU/kg	9.0	0.54	27
		10 MIU/kg	9.2	1.84	92
5	70-207	Vehicle	6.4	1.28	N/A
		3 MIU/kg	6.3	0.38	15
		10 MIU/kg	6.2	1.24	62
6	M05212	Vehicle	8.2	1.64	N/A
		3 MIU/kg	8.5	0.51	25.5
		10 MIU/kg		Monkey not dosed	
7	129-116	Vehicle	8.7	0.50	N/A
		3 MIU/kg	9.1	0.55	27.5
		10 MIU/kg	8.4	1.68	84
8	129-81	Vehicle	6.6	0.40	N/A
		3 MIU/kg	7.0	0.42	21
		10 MIU/kg	6.9	1.38	69
9	M05848	Vehicle	8.8	0.50	N/A
		3 MIU/kg	9.0	0.54	27
		10 MIU/kg	9.0	1.80	90

NR –Not recorded

3.3.2.2. Analysis of body temperature

The body temperature of the monkeys was successfully obtained predose and at the target time points of 0.25 h, 0.5 h, 1h, 1.25h, 1.5 h, 1.75 h, 2 h, 4 h, 6 h, 8 h, 10 h, 24 h, 27 h, 30 h, 33 h, 48 h and 72h post dose using a rectal thermometer. On occasions during the early part of the sampling regime some body temperatures were not obtained due to close proximity of multiple temperature readings. These time points are detailed in Appendix 1.11. Based on consideration of the monkeys welfare following the first dosing occasion which incorporated 20 body temperature readings, the sampling regime was reduced to 15 readings with reading taken every 0.5 h in the first 2 h rather than every 0.25 h.

3.3.2.3. Determination of serum neopterin concentrations

Samples were analysed over 3 different occasions with 6 separate assays / plates across the 3 occasions. The neopterin concentrations determined in samples fell within the dynamic range (0.5-63 ng/mL) of the standard curve and so the assay was considered fit for purpose for this study.

3.3.2.4. Determination of serum Cytokine / Chemokine concentrations

Samples were analysed over 3 different occasions with 6 separate assays / plates across the 3 occasions. The samples analysed in each assay together with the assay LLQ and HLQ are presented in Appendix 1.12 and Appendix 1.13 respectively. Measurable levels of 26 of the 29 cytokines were observed in a least one or more of the monkeys. Serum concentrations of IL3, IL4 and IL5 were below the assay LLQ for all monkeys following all three treatments. The concentration data for the various cytokines/chemokines will be discussed in depth as part of the non-compartmental analysis in Chapter 6.

Following the selection of the analytes to be progressed, a specific Milliplex® Human cytokine/chemokine magnetic bead panel kit was created with the following analytes included IFNα2b, IL15, IFNγ, MCP1, IL6, IL7, IL17A, Eotaxin, GMCSF, IP10, IL1Ra and IL12p70 for the analysis of subsequent samples.

The assay LLQ was consistent across all the plates on all three analytical occasions for 8 of the analytes. A further 9 analytes demonstrated a consistent LLQ on all but the first analytical occasion on which the determined assay LLQ was considerably higher than in subsequent assays. The remaining 9 analytes showed variable assay LLQ across the plates and analytical occasions. In total 16 of the analytes demonstrated a considerably higher assay LLQ on the first and in some cases second analytical occasion to subsequent analytical occasions.

Due to equipment malfunction a number of samples from Monkey 4 following 3 MIU/kg and 10 MIU/kg IFNα2b treatment and Monkey 5 following vehicle treatment were not analysed during analytical occasion 2. The exact samples that were not analysed for each analyte are detailed in Appendix 1.13. In addition due to analytical resource constraints the samples from monkey 2 and monkey 4 following vehicle treatment were not analysed. Following IFNα2b treatment at 10 MIU/kg concentrations of IFNα2b in the following samples were all above the assay HLQ; Monkey 1 (4, 6, 8, 10 h), Monkey 2 (1, 2, 4, 6, 8, 10

h), Monkey 3 (2, 4, 6, 8, 10 h), Monkey 4 (2, 4, 6, 8 h), Monkey 5 (2, 4, 6, 8, 10 h), Monkey 7 (4, 6, 8, 10 h), Monkey 8 (2, 4, 6 h) and Monkey 9 (4, 6, 8 h). Based on this the serum samples presented in Table 3.10 were diluted and re-analysed for all analytes. The determined concentrations from the re-assay of diluted samples that were originally above the IFNα2b HLQ were incorporated in the concentration-time profile where applicable. The samples above the HLQ for Monkey 1 and Monkey 2 were not diluted and reanalysed with the other samples.

Table 3.10 Higher limits of quantification (HLQ) for individual cytokines determined across separate plates and analytical occasions

	Sample time (h) IFNα2b dose	
Monkey	3 MIU/kg	10 MIU/kg
1	2, 4, 6	
2		
3	2, 4, 6	2, 4, 6, 8, 10
4	2, 4, 6, 8, 10	2, 4, 6, 8, 10
5	2, 4, 6, 8, 10	2, 4, 6, 8, 10
6	2, 4, 6	
7	2, 4, 6, 8, 10	2, 4, 6, 8, 10
8	2	2, 4, 6, 8, 10
9		2, 4, 6, 8, 10

3.4. Discussion

3.4.1. Mouse Resiquimod challenge PK/PD model

3.4.1.1. In vivo study design

As part of the delivery of an optimised mouse PK/PD challenge model, the relevant literature was reviewed and an initial pilot study was designed to investigate the induction of serum IFNα concentrations following iv infusion administration of resiquimod to the male CD1 mouse. Administration of resiquimod as an iv infusion was selected to ensure controllable exposure because the solubility of resiquimod is relatively poor so oral bioavailability was predicted to be low and variable. The pharmacokinetics of resiquimod in the mouse have not previously been reported so administration of resiquimod as an iv infusion would also allow the determination of the definitive pharmacokinetic parameters. The administration of resiquimod via iv infusion was successfully conducted and tolerated in all animals. There is a finite number of mice that can be surgically prepared on each day (up to 10) and resources for after surgery care and monitoring are limited. To investigate a

dose response where larger numbers of mice are required it becomes unfeasible to use surgically cannulated mice and so iv bolus administration via the tail vein was used. The administration of the dose via the tail vein was successfully conducted and well tolerated in mice. Following the first study, where resiquimod was administered as an iv infusion, a vehicle group of n=4 animals was included on all other dosing occasions. The purpose of this group was to understand if the administration technique, vehicle or sampling on serum IFNα concentrations had any impact on the understanding of the PK/PD relationship. In addition, the presence of measurable serum IFNα concentrations prior to challenge may be an indicator of an immune response to an illness which may explain why some mice may have demonstrated a different serum IFNα concentration-time profile to other mice receiving the same resiquimod treatment.

The sampling regime selected for the pilot study was based on the data presented by Asselin-Paturel et al (2005) where following iv bolus administration of resiquimod the maximum serum IFNα concentrations were observed approximately 2h post dose and were close to baseline levels at 6 h post dose. Since the sampling regime adequately captured both the resiquimod blood concentration-time profile following iv administration and the serum IFNα concentration-time profile, it was used for all studies. Generally the sample at each time point was used to determine both the resiquimod and IFNα concentration except for the sample taken at 5 min post dose which is to capture the maximum resiquimod blood concentrations, or in the case of iv bolus administration as feasibly close to the maximum concentration as possible. It was not deemed necessary to analyse this sample to investigate if concentrations of IFNα were observed in these samples as it was felt that it may be too early to observe a response. Subsequent studies in house have demonstrated that measurable serum IFNα concentrations are not observed until 30-45 min post resiquimod treatment (data not reported). In general the sampling regime appears to have been suitable to obtain sufficient measurable concentrations of both resiquimod and IFNα to investigate the PK/PD relationship.

3.4.1.2. Analysis of resiquimod dose concentration

The dose solutions were analysed on each study day to confirm that they had been made to an acceptable level of accuracy with respect to the target concentration. In general, the PDA is the preferred methodology for the analysis of the concentration of dose formulations as it is easy to use, quick to run and relatively cheap. However when a large

number of dose aliquots are to be analysed, it can be more effective analyse them using LC-MSMS. Another consideration is that LC-MSMS is generally more sensitive than the PDA with typical lower confidence limits of quantification of 1 ng/mL and 10000 ng/mL respectively. As lower doses were investigated as part of the dose response together with the number of doses, it was felt that LC-MSMS offered the best platform to determine the concentrations.

The analysis indicated that the dose solution for group 1 (iv infusion) was prepared to an acceptable level of accuracy, however the prepared iv bolus dose solutions for group 2, group 3 and group 4 were outside the acceptance criteria and so the analytically measured dose concentration was used to determine the actual dose of resiquimod administered to individual mice.

3.4.1.3. Analysis of resiquimod whole blood concentration

The concentrations of resiquimod in blood samples were successfully determined using LC-MSMS following extraction using protein precipitation. A specific LC-MSMS analytical method was developed using a state-of-the-art triple quadrupole mass spectrometer coupled to a HPLC system. The analysis had an adequate dynamic range, with an LLQ of 1 ng/mL, to enable the determination of resiquimod concentrations in the majority of the samples. Although the analytical method was deemed as suitable for the purpose of the project, for future studies it may be of value to have the capacity to determine lower concentrations of resiquimod. Protein precipitation is a quick but relatively crude sample extraction technique and as such the sample extraction and preparation could be further optimised to deliver increased sensitivity if required. Solid phase extraction techniques may offer options to improve the sample preparation and may offer improved sensitivity if required. Sample size can also have a big impact on the analysis and a small sample volume such as in this study does not help when trying to achieve greater sensitivity. Based on guidelines around the blood volumes that can be ethically removed from a mouse during a study this is feasibly the largest sample that could be obtained with this study design.

3.4.1.4. Analysis of IFNα serum concentration

Approximately 20 µL of serum was obtained from each blood sample and as the ELISA assay required 100 µL it was necessary to dilute the serum samples 1 in 10 with the buffer solution to enable analysis. In addition the IFNα concentrations of a number of samples at

and around the C_{max} were above the assay HLQ and so it was necessary to dilute these samples up to 1 in 50 to enable a concentration to be determined. It has been reported that dilution particularly of serum samples can exaggerate the differences between samples that have cytokine concentrations with the dynamic range and samples that have cytokine concentrations above the dynamic range and require dilution (Leng et al, 2008). As all the samples were diluted for analysis in this study it is not possible to comment on the impact that the dilution may have had on the observed cytokine levels, although it may be worth investigating whether the extent of dilution i.e. 1:10 vs. 1:50 has an impact on the observed cytokine concentrations. As part of the analysis the effect of the matrix (serum) on the observed IFNα concentrations was investigated by spiking control serum with IFNα standard to create control samples of known concentration. This demonstrated that the serum had no impact on the performance of the assay and the observed IFNα concentrations.

3.4.2. Primate IFNα2b challenge PK/PD model

3.4.2.1. *In vivo* study design

The delivery of a monkey IFNα2b challenge PK/PD model presented a different situation to the mouse model as the dosing, sampling and sample analysis had to be conducted in the US where the GSK primate colony is located. As with the mouse model a study design based on an extensive review of the literature was submitted to colleagues in the US, and following discussion with local experts around the number of sampling points, a final study protocol was formed. Developing a model in this manner presented a number of challenges such as the different time zones, local working practices, communication issues and co-ordinating colleagues with different areas of expertise who had not worked together previously.

Both the IFNα2b dose and the sampling regime were selected to ensure that the dose would elicit a measurable response and would not cause any toxicity and would be suitable to adequately characterise both the IFNα2b concentration-time profiles (PK) and the biomarker-concentration time profile (PD). Based on the reported experimental medicine clinical endpoints and the literature for administration of IFNα2b to both humans and monkeys neopterin and body temperature were selected as the primary biomarkers of interest. Originally a sampling regime of 20 samples out to 240 h post dose was proposed

based on that reported in the literature (Zhang et al, 2008). Following the first in life dosing occasion interim concentration time data for both cytokines/chemokines and neopterin was generated and reviewed. Based on these data and the observations and recommendations of the animal technicians the sampling regime was refined to develop the most optimal sampling regime for future studies.

3.4.2.2. Analysis of body temperature

Administration of IFNα can result in flu like symptoms, including an increase in body temperature, and as a result body temperature has the potential to act as a biomarker for anti- IFNα therapies or therapies that target pathways downstream of IFNα. In a clinical experimental medicine study investigating an inhibitor of a target downstream of the IFNα receptor, body temperature was included as a potential clinically relevant biomarker that could demonstrate a direct inhibition of the response following an IFNα response. Based on this body temperature was included as a measure /biomarker to be recorded in the monkeys in this study. The sampling regime for body temperature was selected based on that previously reported in the literature (Tsitoura et al, 2015) to capture the IFNα mediated increase in body temperature in the monkey following administration of a TLR7 agonist.

3.4.2.3. Analysis of serum neopterin concentrations

Serum neopterin concentrations were successfully determined using a competitive ELISA. It is possible to determine the concentrations of neopterin in samples using LC-MSMS (Dale and Brilot, 2010), however, as the other samples were being analysed using a bioassay the neopterin samples were also analysed in this manner rather than incorporating another technology. The neopterin ELISA was for a single analyte, however in the monkey as a larger blood samples could be taken, there was enough sample available for this assay and subsequent cytokine/chemokine analysis without diluting the samples. Competitive ELISAs are generally used for small analytes such as neopterin, however a number of drawbacks have been reported (Cox et al, 2012). Generally these assays are not considered as sensitive as a sandwich ELISA, they are more sensitive to matrix issues especially serum, and the IC_{50} of a standard curve will shift with minor changes in incubation of the various steps of the immunoassay. It was considered that the performance of the assay was fit for purpose and there was no discernible difference between the assay on the different analytical occasions.

3.4.2.4. Analysis of serum cytokine/chemokine concentrations

For the analysis of the cytokines and chemokines a human multiplex plate was used that allowed for the simultaneous analysis of 29 cytokines. The kit was primarily selected to determine concentrations of IFNα2b but enabled the investigation of the impact of IFNα2b challenge on a large number of cytokine and chemokines. In this manner it enables one to "fish" for potential valuable biomarkers which may be disease relevant but equally may be good markers for that mechanism which may not have been considered previously. There is the option to customise the kit to the cytokines of interest, therefore an interim sample analysis was conducted and the number of cytokines/chemokines was triaged down to 12 cytokines of interest for the final analysis.

The multiplex kit is clearly a valuable tool that can provide an extremely rich data set from a small amount of sample, however, there are a number of points that are worth considering when using this assay format to analyse preclinical samples. Firstly, it is assumed that all the cytokines and chemokines induced in the monkey are cross reactive with the human assay. At least 3 cytokines demonstrated no measurable concentrations and were either not induced following IFNα2b challenge or the kit was unable to measure them. For a number of other cytokines, measurable concentrations were determined but there was no difference between vehicle and challenge. The measurable concentration could therefore be analytical noise rather actual determined concentrations. The manufacturers do not provide any information around the cross reactivity between species, but it can be assumed that for many of the cytokines the kit should be able to determine the concentrations of monkey cytokines. For example, it has been demonstrated that the nonhuman primate cytokines IL1α, IL1β, IL2, IL4, IL5, IL6, IL8, IL10, IL12α, IL12β, IL15, IFNα, IFNγ and TNFγ share 93-99% homology at the nucleic acid and protein levels with the human equivalents (Villinger et al, 1995). A second consideration is that the current analysis is only measuring the single subtype of IFNα that was administered as the challenge. IFNα induces its own production from neighbouring cells so it may be that administration of human recombinant human IFNα2b induces the production of endogenous monkey IFNα of various subtypes. These in turn may contribute to the observed response following IFNα2b challenge. It would be interesting to investigate this, however, it may not be possible to distinguish between IFNα with the current assays available. Thirdly, it is worth considering the potential for variability in the assay between analytical occasions. Taking IFNα2b as an

example the HLQ was comparable across the analytical occasions and plates however the LLQ was highest on the first analytical occasion and was approximately 36 fold lower on the second. It should be noted that a comparable LLQ was observed between the remaining analytical occasions although still 5 fold lower than that observed on the first occasion. This does raise questions as to the robustness of the assay and whether data generated across multiple analytical occasions can reliably be compared to one another. However in a large study such as this it is difficult to analyse all the samples on the same study day. In addition the concentrations of the various cytokines observed following the dilution of samples when concentrations were above the assay HLQ also raises question around the behaviour of the assay. As part of this repeat analysis some samples that were not above the assay HLQ when run undiluted were re-assayed and considerably different concentrations were observed between the two assays. In general it was felt that if there was no reason to reject the undiluted samples and despite these caveats it was felt that the multiplex assay provided robust serum concentration-time data for IFNα2b and a number of other cytokines of interest to enable the interrogation of the PK/PD relationship within this model.

3.5. Conclusion

The *in vivo* study designs investigated in this chapter have demonstrated how valuable it is to review the available literature to get an indication of appropriate doses, sampling regimes and potential biomarkers for early pilot studies. It has also demonstrated how, as well as scientific requirements, ethical, cost and time factors need to be considered and balanced together to deliver a suitable design for an *in vivo* study. There is also a need to be flexible with the design as a study design may go through several iterations and refinements as part of the validation and optimisation before a final optimal study design is derived. It is important to incorporate statistical analysis into the study design where possible to ensure that studies are appropriately powered to test the hypothesis

A range of analytical techniques including LC-MSMS, for the analysis of small molecules, and bio-assays, such as ELISA for cytokines, were incorporated in this study to successfully determine the concentrations of analytes of interest in blood and serum samples from both the mouse and monkey. Across the different assay formats, the analytical range in most cases was sufficient to determine the concentrations of the key analytes of interest in the majority of samples. Although the concentrations of some samples sat outside of the assay

LLQ and HLQ, measures were put in place to ensure a quality data set for all analytes of interest. The data are therefore suitable quality to determine the pharmacokinetics of the challenge agents and to assess the pharmacokinetic and pharmacodynamic relationship of the challenge agents and key biomarkers of interest in both the mouse and monkey.

Chapter 4: Investigation and validation of an *in vivo* PK/PD mouse model using resiquimod as a challenge agent

4.1. Introduction

A mouse *in vivo* resiquimod challenge model may offer a translatable model that can be used to investigate the induction of serum cytokine levels by pDCs through the TLR7 mediated pathway. Investigations of the mouse model were designed to develop an understanding of the utility of this model in the drug development environment to select the most suitable compounds for progression to the clinic. The analysis will broadly focus on the optimisation, validation and testing of the model with the objective to answer the following questions. Firstly, "What is the optimal dose of resiquimod to give a reproducible IFNα response?" and secondly "How reproducible is the response over multiple studies?" The later is important as it will allow comparison of data between different studies. This is of interest in drug discovery environment, when a number of compounds may be screened across different studies. A reproducible model will give a scientist confidence in selecting the most suitable compound for progression to candidate selection.

Although the administration of resiquimod to the mouse has been investigated in a number of studies, the pharmacokinetic (PK) parameters of resiquimod in the mouse have not previously been reported. The pharmacokinetic parameters are considered vital to understand the challenge (resiquimod) and its action in an *in viv*o model of acute inflammation. This chapter will describe the non compartmental analysis of resiquimod blood concentration data in the mouse following both iv infusion and iv bolus administration of resiquimod. Non-compartmental analysis of the serum IFNα concentration data determined following administration of resiquimod was also conducted to determine parameters that describe the induction of IFNα (response) by resiquimod in the mouse. The non-compartmental analysis was conducted for resiquimod and IFNα concentration data following a single iv infusion administration of resiquimod, following iv bolus administration of resiquimod over a dose range and following iv bolus administration at a single dose over two study days to investigate the reproducibility of the response between study days.

4.2. Methods

The in life and analytical protocols are presented in Chapter 3

4.2.1. Resiquimod pharmacokinetic analysis

Pharmacokinetic (PK) analysis of the resiquimod blood concentration data was performed to determine the maximum blood concentration (C_{max}), the area under the blood concentration-time curve (AUC), the terminal half-life ($t_{1/2}$), the blood clearance (CL_b) and the volume of distribution at steady-state (V_{ss}). The pharmacokinetic parameters were determined using non-compartmental analysis (NCA) in the WinNonlin Phoenix software (Pharsight, version 6.2).

For NCA of the blood concentration time profile determined following iv infusion administration, a blood/plasma iv infusion model (Model 202) was selected within WinNonlin. The data inputs for this model included the dose, length of infusion, time of last dose, time for each sample and blood concentrations for each mouse. Blood concentration data from the 0.75 h time point to the last blood sample (2-2.5 h) were included in the estimation of the rate constant associated with the terminal elimination phase, which enabled PK parameters to be extrapolated to infinity.

For NCA of the blood concentration time profile determined following iv bolus administration, a blood/plasma iv bolus model (Model 201) was selected within WinNonlin. The data inputs for this model included the dose, time of last dose, time for each sample and blood concentrations for each mouse. Following iv bolus administration, at least the last three and where possible the last four quantifiable blood samples were included in the estimation of the rate constant associated with the terminal elimination phase, which enabled PK parameters to be extrapolated to infinity.

WinNonlin estimated the elimination rate constant by performing a regression of the natural logarithm of the concentration values in the selected range against sampling time. The AUCs from the time of dosing to the last measurable blood concentration (AUC_{last}) were defined using the linear log trapezoidal rule with uniform weighting. Following iv infusion administration, the rule uses the linear trapezoidal rule from the start of the iv infusion to C_{max} and the log trapezoidal rule after the C_{max} to the last measurable blood concentration. Following iv bolus administration, the rule uses the log trapezoidal rule after the C_{max} to the

last measurable blood concentration or after C_0 if C_0 is greater than C_{max}. The equations used to derive the AUC_{last} for both the linear trapezoidal rule and the logarithmic trapezoidal rule were

Linear trapezoidal rule

$$AUC_{t_1}^{t_2} = \delta t * \frac{C_1 + C_2}{2}$$

Logarithmic trapezoidal rule

$$AUC_{t_1}^{t_2} = \delta t * \frac{C_2 - C_1}{\ln\left(\frac{C_2}{C_1}\right)}$$

where δt is (t_2- t_1), t_1 and t_2 represent the first and last time points of the time interval, C is the concentration.

The AUC_{last} was extrapolated to give an AUC to infinity (AUC_∞). The AUC_∞ was estimated using the last measurable blood concentration and λ_z and were defined by

$$AUC_\infty = AUC_{last} + \frac{C_{last}}{\lambda_z}$$

Where C_{last} is the last measurable blood concentration and λz is the elimination rate constant.

4.2.2. IFNα concentration data analysis

Analysis of the IFNα serum concentration data was performed to determine the maximum serum concentration (C_{max}) and the area under the serum concentration time curve (AUC). The parameters were determined using non-compartmental analysis (NCA) in the WinNonlin Phoenix software (Pharsight, version 6.2).

For NCA a blood/plasma extra vascular model (Model 200) was selected within WinNonlin. The data inputs for this model included time for each sample and serum concentrations for each mouse. The estimation of the rate constant associated with the terminal elimination phase was not conducted for this data so determined parameters could not be

extrapolated to infinity. The AUC from the time of dosing to the last measurable blood concentration (AUC_{last}) was defined using the linear trapezoidal rule with uniform weighting.

4.2.3. Statistical Analysis

Serum IFNα C_{max} and AUC values determined in mice administered with resiquimod at a dose of 0.4 mg/kg in three separate study groups (groups 2, 3 and 4, n= 4 mice per group) were analysed using a one-way analysis of variance (ANOVA) test within the JMP software (SAS Institute Inc, version 11.0.0) to test the null hypothesis that either the mean C_{max} or AUC were the same between the three study groups receiving the same dose of resiquimod. Following the one-way ANOVA test the same data was subsequently analysed using the restricted maximum likelihood (REML) method, also within the JMP software, with study day as a random effect term, to determine the variance between serum IFNα C_{max} and AUC on each study day, and the contribution of the intra-study day variance.

4.2.4. Power Analysis

Power analysis was conducted using PASS software (NCSS, version 12.0.2) incorporating the grand mean and CV for both C_{max} and AUC to determine what sample size is likely to be required to detect 10 to 90% inhibition in serum IFNα C_{max} and AUC in mice dosed with resiquimod at 0.4 mg/kg. The sample size calculations were performed with the specification of power > 0.9 and the criterion for statistical significance being a one sided two sample t test with threshold value $\alpha = 0.05$.

4.3. Results

4.3.1. Resiquimod Pharmacokinetics

4.3.1.1. Pharmacokinetics of resiquimod in male CD1 mice

The actual doses administered to each mouse as presented in Table 4.1 and the blood concentration time profiles of resiquimod following a 5 min iv infusion of resiquimod hydrochloride salt are presented in Figure 4.1.

Table 4.1 **Individual mouse body weights and actual doses of resiquimod administered as a 5 min iv infusion to each mouse**

Mouse Number	Body weight (kg)	Dose administered (mg)	(mg/kg)	(mg/kg/min)
Mouse 1	0.044	0.012	0.28	0.055
Mouse 2	0.043	0.012	0.28	0.056
Mouse 3	0.038	0.011	0.29	0.058
Mouse 4	0.041	0.011	0.27	0.055
Mouse 5	0.041	0.011	0.27	0.053

For all mice the maximum resiquimod blood concentration (C_{max}) was observed at the end of the iv infusion, at a time (T_{max}) of 0.08 h. Measurable blood concentrations of resiquimod were observed up to 2 h for mice 1 and 3, and up to 2.5 h for mice 2, 4 and 5. During the study, it was not possible to obtain a blood sample for pharmacokinetic analysis from mouse 2 at the 2 h time point due to difficulties with tail vein bleeding. The decision was taken to anaesthetise this animal at the 2.5 h time point and take the terminal blood sample via cardiac puncture. It was also necessary to take the terminal blood sample from mouse 3 at 2.5 h rather than 3 h due to the lower body weight of this mouse. No measurable blood concentrations were observed in the 3 h blood samples obtained from mice 1, 4 and 5.

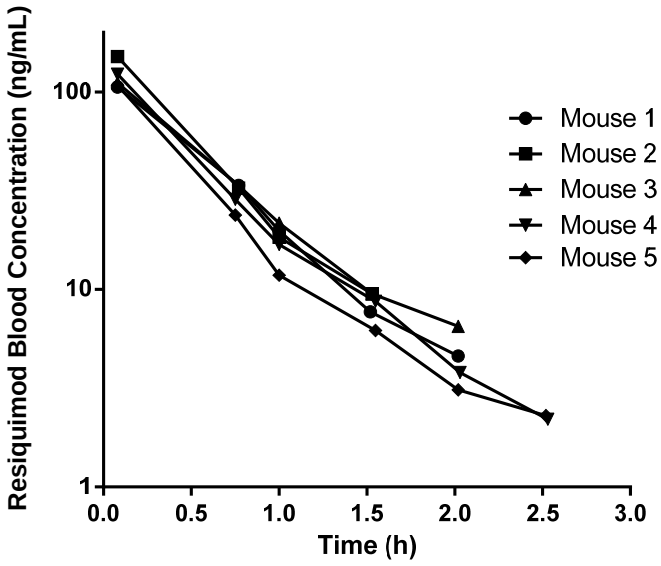

Figure 4.1 **Individual blood concentration time profiles for resiquimod in conscious male CD1 mice following a 0.08 h constant rate iv infusion of 0.27-0.28 mg/kg resiquimod hydrochloride salt**

The pharmacokinetic parameters determined for resiquimod in the male CD1 mouse are shown in Table 4.2. The pharmacokinetic parameters show low variability among the five mice with the highest CV (%) being determined for C_{max} at 16%. The blood clearance (CL_b) was 69 ± 7 mL/min/kg, the volume of distribution at steady-state (V_{ss}) was 2.4 ± 0.3 L/kg and the terminal half-life ($t_{1/2}$) was 0.5 ± 0.04 h.

Table 4.2 Individual and mean (SD and CV) pharmacokinetic parameters of resiquimod in the male CD1 mouse following 0.08 h constant rate iv infusion of 0.27-0.28 mg/kg resiquimod hydrochloride salt

	Parameter				
Mouse ID	CL_b (mL/min/kg)	V_{ss} (L/kg)	$t_{1/2}$ (h)	C_{max} (ng/mL)	AUC_∞ (ng*h/mL)
1	70	2.5	0.4	106	66
2	60	1.9	0.5	151	78
3	67	2.7	0.5	111	71
4	69	2.4	0.5	123	66
5	80	2.7	0.5	108	56
Mean	**69**	**2.4**	**0.5**	**120**	**67**
SD	**7**	**0.3**	**0.04**	**19**	**8**
CV (%)	**10**	**13**	**9**	**16**	**12**

4.3.1.2. Induction of serum IFNα concentrations over a resiquimod dose range in the male CD1 mouse.

Table 4.3 shows the doses administered to each mouse determined using the analytically measured dose concentrations.

Table 4.3 Individual mouse body weights and actual doses of resiquimod administered as an iv bolus to each mouse in group 2

Treatment Group	Mouse Number	Body weight (kg)	Weight of dose administered (g)	Resiquimod dose administered (mg)		Mean Resiquimod dose administered (mg/kg)
				(mg)	(mg/kg)	
Vehicle	Mouse 1	0.048	0.260	NA	NA	NA
	Mouse 2	0.045	0.246	NA	NA	
	Mouse 3	0.043	0.236	NA	NA	
	Mouse 4	0.045	0.253	NA	NA	
0.03 mg/kg Resiquimod	Mouse 5	0.046	0.243	0.0019	0.041	0.041
	Mouse 6	0.045	0.236	0.0018	0.041	
	Mouse 7	0.040	0.218	0.0017	0.043	
	Mouse 8	0.043	0.221	0.0017	0.040	
0.07 mg/kg Resiquimod	Mouse 9	0.047	0.247	0.0041	0.089	0.091
	Mouse 10	0.045	0.235	0.0039	0.088	
	Mouse 11	0.044	0.240	0.0040	0.091	
	Mouse 12	0.043	0.246	0.0041	0.096	
0.1 mg/kg Resiquimod	Mouse 13	0.047	0.245	0.0075	0.160	0.16
	Mouse 14	0.045	0.237	0.0072	0.162	
	Mouse 15	0.042	0.235	0.0072	0.169	
	Mouse 16	0.042	0.223	0.0068	0.163	
0.3 mg/kg Resiquimod	Mouse 17	0.043	0.229	0.019	0.437	0.40
	Mouse 18	0.047	0.200	0.016	0.351	
	Mouse 19	0.043	0.197	0.016	0.376	
	Mouse 20	0.043	0.236	0.019	0.453	
0.7 mg/kg Resiquimod	Mouse 21	0.045	0.234	0.048	1.07	1.10
	Mouse 22	0.043	0.227	0.047	1.10	
	Mouse 23	0.050	0.266	0.055	1.10	
	Mouse 24	0.044	0.238	0.049	1.11	
1 mg/kg Resiquimod	Mouse 25	0.041	0.218	0.061	1.49	1.50
	Mouse 26	0.044	0.233	0.065	1.50	
	Mouse 27	0.051	0.283	0.080	1.56	
	Mouse 28	0.042	0.216	0.061	1.45	
3 mg/kg Resiquimod	Mouse 29	0.047	0.253	0.23	4.87	4.79
	Mouse 30	0.042	0.226	0.20	4.83	
	Mouse 31	0.043	0.215	0.20	4.55	
	Mouse 32	0.043	0.234	0.21	4.90	

The individual blood concentration time profiles of resiquimod in male CD1 mice following a iv bolus administration of resiquimod hydrochloride salt over a dose range of 0.04 to 4.8 mg/kg are presented in Figure 4.2.

In the vehicle dosed mice, measurable blood concentrations of resiquimod were observed in mouse 1 at the 1.5 h time point and mice 3 and 4 at the 2 h time point. All other resiquimod blood concentrations in the vehicle dose group were below the assay LLQ of 1 ng/mL. The blood concentration time profiles presented in Figure 4.2 demonstrate that at all doses C_{max} was observed at 0.08 h (T_{max}), which was the time of the first blood sample following iv bolus administration. Following the C_{max} the blood concentrations declined in a log-linear manner to the last quantifiable concentration in most cases. There are a number of mice (mouse 6, mouse 7, mouse 9, mouse 10, mouse 12 and mouse 25) where a blood concentration observed at a time point was greater than the blood concentration observed at a previous time point. For example, the blood concentration determined at 1 h for mouse 7 dosed at 0.04 mg/kg was greater than the blood concentration observed at 0.08 h. The time of the last quantifiable blood concentration (T_{last}) broadly increased with increasing dose to a maximum of 3.0 h for doses of 0.4 mg/kg and above.

The individual and mean pharmacokinetic parameters determined for resiquimod are presented in Table 4.4. The blood concentration time profile observed for mouse 7 (0.04 mg/kg) and mouse 9 (0.09 mg/kg) did not enable characterisation of a terminal half-life and therefore only a C_{max} was reported for these animals. CL_b and V_{ss} varied approximately 10 fold between the highest value (observed for mouse 20) and the lowest value (observed for mouse 11). Mean values of CL_b and V_{ss} were 53 mL/min/kg and 1.9 L/kg, respectively, with comparable variability of 37-38% CV.

A) 0.04 mg/kg

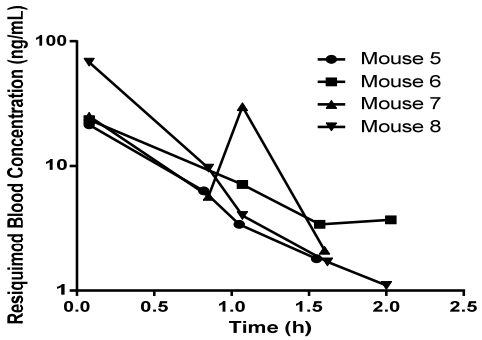

B) 0.09 mg/kg

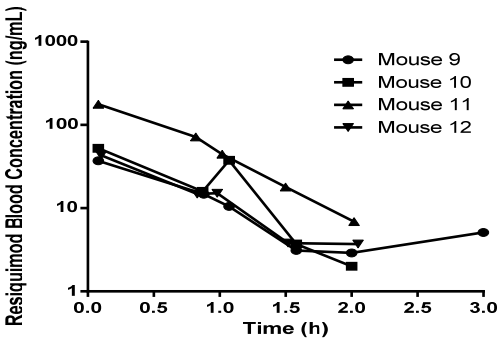

C) 0.16 mg/kg

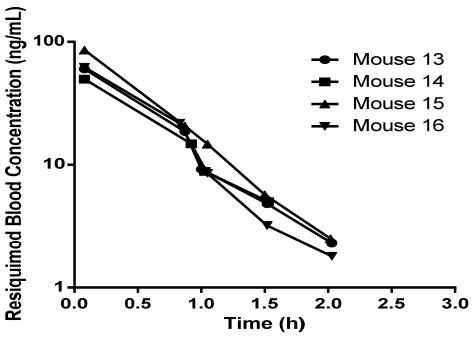

D) 0.4 mg/kg

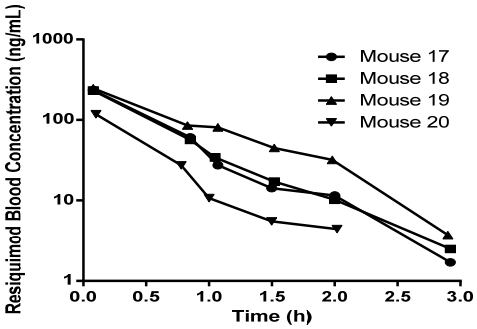

E) 1.1 mg/kg

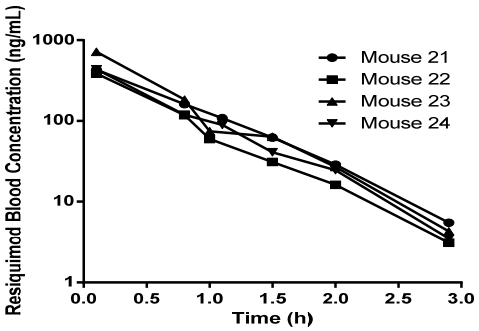

F) 1.5 mg/kg

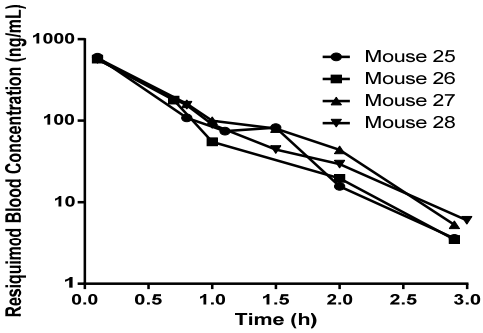

G) 4.8 mg/kg

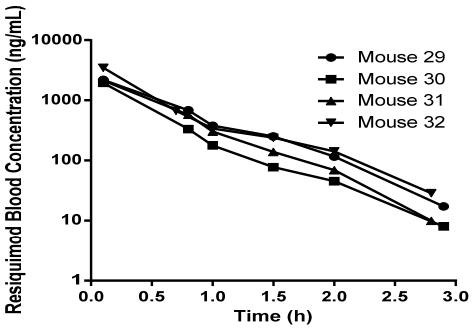

Figure 4.2 Blood concentration time profiles for resiquimod in conscious male CD1 mice following iv bolus administration of resiquimod hydrochloride salt at a dose of A) 0.04 mg/kg, B) 0.09 mg/kg, C) 0.16 mg/kg, D) 0.4 mg/kg, E) 1.1 mg/kg, F) 1.5 mg/kg and G) 4.8 mg/kg

Table 4.4 Individual and Mean Pharmacokinetic Parameters of resiquimod in conscious male CD1 mice following iv bolus administration of resiquimod hydrochloride salt over a dose range of 0.04 –4.8 mg/kg

Resiquimod Dose (mg/kg)	Mouse ID		Parameter				
		CL_b (mL/min/kg)	V_{ss} (L/kg)	$t_{1/2}$ (h)	C_{max} (ng/mL)	AUC_∞ (ng*h/mL)	AUC_∞ /D (min*kg/L)
0.04	5	47	1.7	0.42	21.4	14.4	20.9
	6	28	2.0	1.00	23.5	24.4	35.5
	7	ND	ND	ND	29.9	ND	ND
	8	20	0.5	0.50	67.9	33.1	49.3
0.09	9	ND	ND	ND	37.0	ND	ND
	10	34	1.3	0.29	52.4	43.1	29.3
	11	11	0.4	0.36	177	136	89.4
	12	46	2.0	0.53	43.3	34.9	21.9
0.16	13	62	2.3	0.52	60.2	41.8	15.7
	14	73	2.7	0.44	49.8	36.1	13.4
	15	51	1.7	0.37	85.9	54.3	19.3
	16	63	2.0	0.44	62.2	42.1	15.5
0.4	17	49	1.7	0.47	235	150	20.4
	18	39	1.4	0.50	231	149	25.5
	19	29	1.4	0.41	247	214	34.2
	20	108	4.0	0.80	117	70.1	9.3
1.1	21	51	2.1	0.40	430	349	19.5
	22	71	2.4	0.42	385	260	14.1
	23	41	1.3	0.44	716	447	24.4
	24	61	2.2	0.38	437	303	16.4
1.5	25	70	2.3	0.38	602	357	14.4
	26	73	2.3	0.48	568	342	13.7
	27	63	2.5	0.44	585	416	16.6
	28	64	2.3	0.51	564	377	15.7
4.8	29	53	1.9	0.36	2180	1540	19.0
	30	79	2.2	0.42	1942	1023	12.7
	31	57	1.8	0.34	2127	1333	17.6
	32	43	1.4	0.42	3478	1878	23.0
Mean	Mean	53	1.9	0.46			
	SD	20	0.7	0.14	ND	ND	ND
	CV (%)	38	37	31			

ND – Not determined

The mean C_{max} increased from 36 ng/mL to 2432 ng/mL over the administered dose range, and roughly increased in proportion to the increase in dose. The mean C_{max} observed following administration of 0.16 mg/kg was lower than that observed following administration of resiquimod 0.09 mg/kg. The resiquimod blood C_{max} observed for mouse 11 dosed at 0.09 mg/kg was up to 5 fold greater than that observed for the other 3 mice in this group.

The resiquimod blood AUC_∞ roughly increased in proportion to the increase in dose between 0.04 and 4.79 mg/kg, and this is reflected in the comparable values determined

for the dose normalised AUC (AUC/D). As with the C_{max}, the observed resiquimod blood AUC_{∞} for mouse 11 (dosed at 0.09 mg/kg) was approximately 3 fold greater than the next highest resiquimod blood AUC_{∞} observed for the other mice in this group.

4.3.1.3. Reproducibility of the response between study days

The analytically measured dose concentration for the post filter dose solutions administered to groups 3 and 4 were calculated as 0.076 and 0.078 mg/mL respectively, and were used to determine the actual dose administered to each mouse in groups 3 and 4 as presented in Table 4.5. The resiquimod concentration-time profiles arising from these doses are shown in Figure 4.3

Table 4.5 Individual mouse body weights and actual doses of vehicle or resiquimod administered as an iv bolus to each mouse in groups 3 and 4.

Group	Treatment	Mouse Number	Body weight (kg)	Weight of dose administered (g)	Resiquimod dose administered (mg)	
					(mg)	(mg/kg)
3	Vehicle	Mouse 1	0.045	0.240	NA	NA
		Mouse 2	0.045	0.197	NA	NA
		Mouse 3	0.042	0.210	NA	NA
		Mouse 4	0.049	0.248	NA	NA
	Resiquimod	Mouse 5	0.048	0.255	0.019	0.41
		Mouse 6	0.042	0.226	0.017	0.42
		Mouse 7	0.043	0.216	0.016	0.38
		Mouse 8	0.044	0.220	0.017	0.38
4	Vehicle	Mouse 9	0.046	0.245	NA	NA
		Mouse 10	0.047	0.246	NA	NA
		Mouse 11	0.048	0.258	NA	NA
		Mouse 12	0.045	0.248	NA	NA
	Resiquimod	Mouse 13	0.045	0.234	0.018	0.41
		Mouse 14	0.046	0.248	0.019	0.42
		Mouse 15	0.047	0.213	0.017	0.36
		Mouse 16	0.045	0.251	0.020	0.43

No measurable blood concentrations of resiquimod were observed in the vehicle dosed mice in either group. In all mice that received resiquimod treatment, C_{max} was observed at 0.08 h (T_{max}). Blood concentrations then declined in an approximately log-linear manner to the last quantifiable concentration, which was observed at 2 h for all mice. The blood concentration time profiles observed in group 4 are comparable among the four mice,

whereas the profiles observed in group 3 are comparable for 3 mice but greater systemic exposure is observed for mouse 8.

The pharmacokinetic parameters of resiquimod are presented in Table 4.6. For comparison, the PK parameters determined for mice administered 0.4 mg/kg in group 2 have also been included in the table. The mean CL_b, V_{ss} and $t_{1/2}$ were comparable among all three groups. The lowest variability in parameters was observed for group 4 with a range of between 10-25%. The variability in PK parameters in group 3 was comparable to the variability observed in group 2.

Both C_{max} and AUC_∞ observed for group 4 were comparable to that observed in mice administered 0.4 mg/kg in group 2, with comparable intra-group variability for C_{max} between the two groups. The mean C_{max} observed for group 3 was approximately three fold greater than that observed for group 4, with an intra group variability of 136%. The resiquimod C_{max} value for Mouse 8 was up to 13 fold greater than the resiquimod blood C_{max} observed for the other mice in this dose group. The mean AUC_∞ observed for group 3 was approximately two fold greater than that observed for group 4, with an intra group variability of 116%. The observed resiquimod blood AUC_∞ value for Mouse 8 was up to 8 fold greater than the resiquimod blood AUC_∞ observed for the other mice in this dose group.

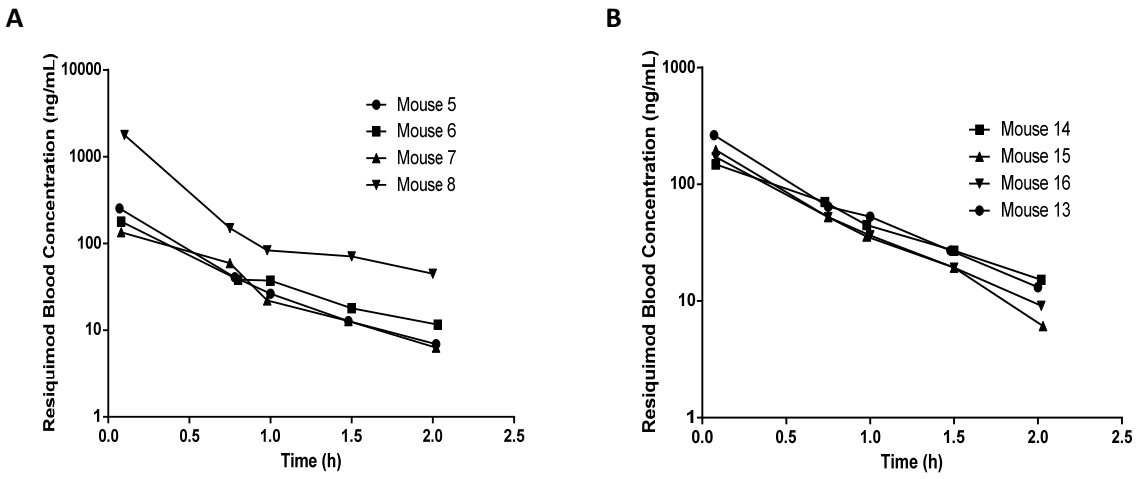

Figure 4.3 **Blood Concentration time profiles for resiquimod in conscious male CD1 mice following iv bolus administration of resiquimod hydrochloride salt at a dose of 0.4 mg/kg in A) Group 3 and B) Group 4**

Table 4.6 Pharmacokinetic Parameters of resiquimod in conscious male CD1 mice following iv bolus administration of resiquimod hydrochloride salt at a dose of 0.4 mg/kg on three separate study days

Study	Mouse ID	Parameter				
		CL_b (mL/min/kg)	V_{ss} (L/kg)	$t_{1/2}$ (h)	C_{max} (ng/mL)	AUC_∞ (ng*h/mL)
Group 3	5	53	1.6	0.49	254	128
	6	57	2.6	0.66	179	121
	7	64	2.4	0.58	135	100
	8	8	0.2	0.40	1784	758
	Mean	**46**	**1.7**	**0.52**	**588**	**277**
	SD	**25**	**1.1**	**0.13**	**799**	**321**
	CV (%)	**55**	**64**	**26**	**136**	**116**
Group 4	13	40	1.6	0.53	264	169
	14	52	2.6	0.61	148	136
	15	48	1.7	0.43	197	124
	16	60	2.4	0.51	171	120
	Mean	**50**	**2.1**	**0.55**	**195**	**138**
	SD	**8**	**0.5**	**0.05**	**50**	**22**
	CV (%)	**17**	**25**	**10**	**26**	**16**
Group 2 0.4 mg/kg administered in dose response study	17	49	1.7	0.47	235	150
	18	39	1.4	0.50	231	149
	19	29	1.4	0.41	247	214
	20	108	4.0	0.80	117	70.1
	Mean	**56**	**2.1**	**0.55**	**208**	**146**
	SD	**35**	**1.3**	**0.17**	**60.6**	**59.0**
	CV (%)	**63**	**60**	**32**	**29**	**40**

4.3.2. IFNα pharmacokinetics

4.3.2.1. Pharmacokinetics of the resiquimod induced IFNα response in male CD1 mice

The serum concentration time profiles for IFNα following 5 min iv infusion administration of resiquimod hydrochloride to the male CD1 mouse are presented in Figure 4.4. Since fewer blood samples were obtained for mouse 2 and mouse 3, limited IFNα concentration time profiles were available for these mice compared to the other mice. After a delay of approximately 0.5-0.75 h, IFNα concentrations raise from baseline levels to reach a C_{max} between 1.5 and 2 h (T_{max}). Following the $C_{max,}$ serum concentrations of IFNα declined towards baseline levels with the last concentration (C_{last}) observed between 2.5 – 3 h post dose.

PK parameters for IFNα are listed in Table 4.7. As a terminal phase could not be assigned for Mouse 1 and Mouse 3, parameters could not be extrapolated to infinity. Due to the limited numbers of samples obtained, an AUC was not determined for mouse 2. The terminal blood

sample for mouse 3 was taken at 2.5 h post dose. To enable a comparison between the systemic exposure observed for mouse 3 and that observed for mice 1, 4 and 5, AUC values out to 2.5 h post dose were generated for each mouse.

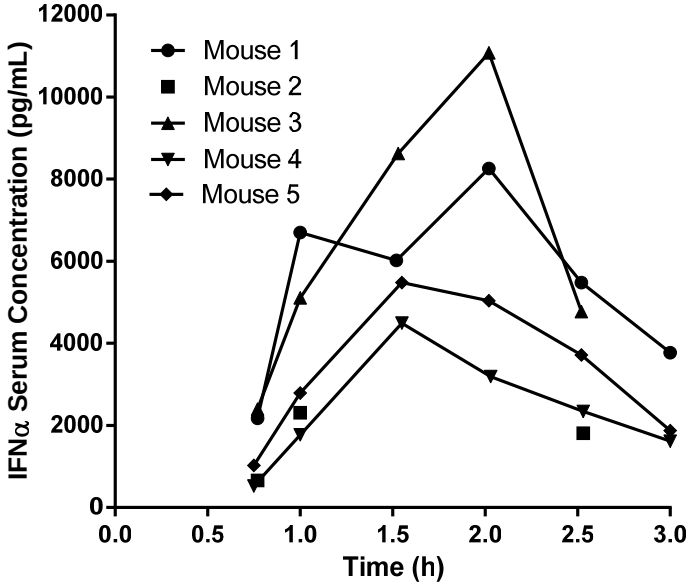

Figure 4.4 **Individual serum concentration time profiles of IFNα in 5 conscious male CD1 mice following a 0.08 h constant rate iv infusion of resiquimod hydrochloride salt at a dose of 0.27-0.28 mg/kg**

The IFNα C_{max} varied approximately 5 fold between the highest value (mouse 3) and the lowest value (mouse 2). Higher IFNα serum concentrations were observed for mice 1 and 3, compared to mice 4 and 5, and this is reflected in the higher values determined for AUC_{last} and $AUC_{2.5}$ for mice 1 and 3. There was approximately a 2.5 fold window between the lowest and highest values of AUC_{last} and $AUC_{2.5}$.

Table 4.7 **Individual pharmacokinetic parameters of IFNα in the male CD1 mouse following a 0.08 h constant rate iv infusion of resiquimod hydrochloride salt at a dose of 0.27-0.28 mg/kg**

	Parameter			
Mouse ID	T_{max} (h)	C_{max} (pg/mL)	AUC_{last} (pg*h/mL)	$AUC_{2.5}$ (pg*h/mL)
1	2.02	8263	14392	112061
2	1.00	2311	ND	ND
3	2.02	11080	14217	14119
4	1.55	4488	6388	5357
5	1.55	5481	9137	7722

ND – Not determined

4.3.2.2. Induction of serum IFNα concentrations over a resiquimod dose range in the male CD1 mouse.

The individual serum concentration time profiles for IFNα in male CD1 mice following iv bolus administration of resiquimod hydrochloride salt over a dose range of 0.04 to 4.8 mg/kg are presented in Figure 4.5. Serum IFNα concentrations in predose samples from all the mice were below the assay LLQ of 200 pg/mL. Quantifiable serum IFNα concentrations could not be determined in samples from the vehicle treated mice.

Figure 4.5 demonstrates that following T_0, an increase in serum IFNα concentrations was observed in all mice in all resiquimod dose groups. Measurable serum IFNα concentrations were observed at the first sampling time point post dose (0.73-0.92 h) and reached a C_{max} between 1.03 and 2.02 h post dose, following which the serum IFNα concentrations declined towards baseline levels. All the dose groups demonstrated intra group variability in the serum IFNα concentrations, however, the serum IFNα concentrations observed for mouse 7 (0.04 mg/kg), mouse 11 (0.09 mg/kg) and mouse 31 (4.8 mg/kg) were much higher than those observed for the other three mice in these dose groups.

PK parameters of IFNα are listed in Table 4.8. The C_{max} and AUC values for mice dosed at 0.04 mg/kg, 0.09 mg/kg and 1.5 mg/kg varied approximately 4 to 6 fold compared to 2-3 fold in other dose groups. At doses greater than 0.09 mg/kg serum IFNα C_{max} and AUC were generally lower that that observed for the 0.09 mg/kg dose group.

A) 0.04 mg/kg

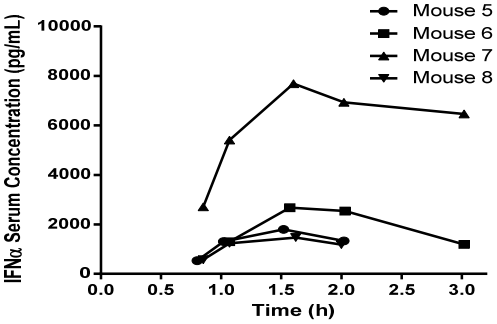

B) 0.09 mg/kg

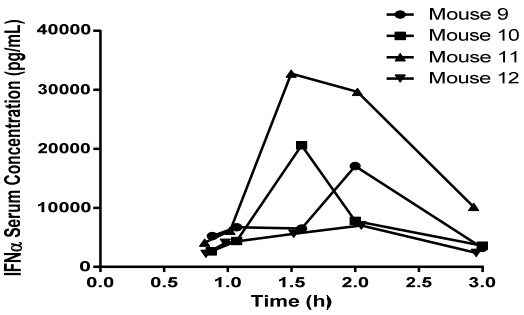

C) 1.6 mg/kg

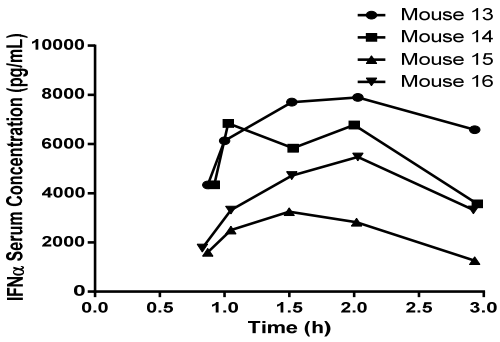

D) 0.4 mg/kg

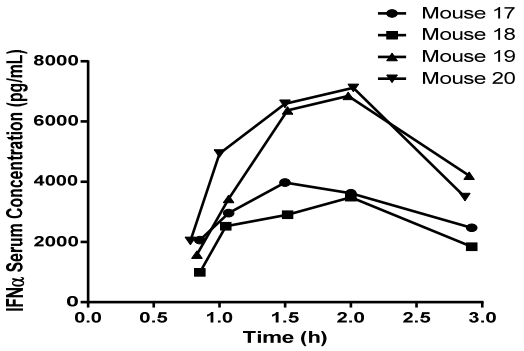

E) 1.1 MG/KG

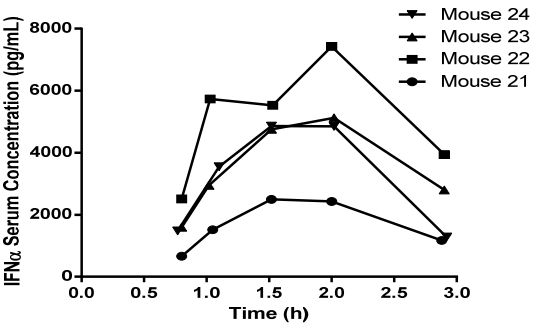

F) 1.5 mg/kg

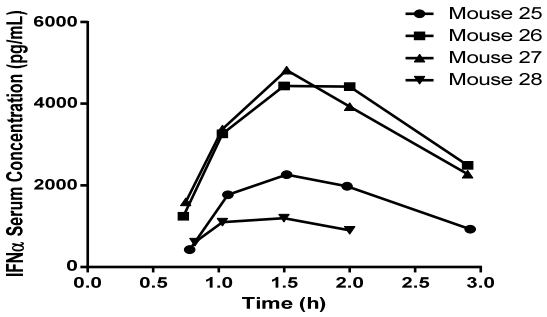

G) 4.8 mg/kg

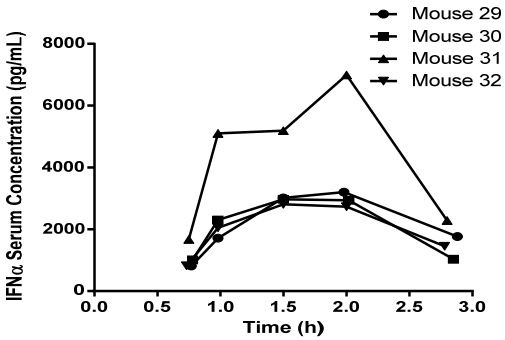

Figure 4.5 Serum concentration time profiles for IFNα in conscious male CD1 mice following iv bolus administration of resiquimod hydrochloride salt at a dose of A) 0.04 mg/kg, B) 0.09 mg/kg, C) 0.16 mg/kg, D) 0.4 mg/kg, E) 1.1 mg/kg, F) 1.5 mg/kg and G) 4.8 mg/kg

Table 4.8 Pharmacokinetic parameters of IFNα in conscious male CD1 mice following iv bolus administration of resiquimod hydrochloride salt over a dose range of 0.04 –4.8 mg/kg

Resiquimod Dose (mg/kg)	Mouse ID	Parameter		
		T_{max} (h)	C_{max} (pg/mL)	AUClast (pg*h/mL)
0.04	5	1.55	1796	1912
	6	1.57	2678	4737
	7	1.60	7684	15280
	8	1.62	1469	1691
0.09	9	2.00	17089	21919
	10	1.58	20607	19877
	11	1.50	32768	46408
	12	2.05	7002	11561
0.16	13	2.03	7895	16658
	14	1.03	6838	13657
	15	1.50	3254	5803
	16	2.03	5481	9700
0.4	17	1.50	3976	7618
	18	2.00	3488	6034
	19	1.98	6852	11585
	20	2.02	7118	12513
1.1	21	1.50	2494	4252
	22	2.00	7426	12927
	23	2.02	5128	9020
	24	1.52	4857	8350
1.5	25	1.52	2261	3705
	26	1.50	4434	8259
	27	1.52	4823	8198
	28	1.50	1198	1492
4.8	29	1.98	3197	5527
	30	1.50	2970	5275
	31	2.00	6992	10831
	32	1.50	2807	4927

Individual serum IFNα AUC vs. resiquimod dose and C_{max} values presented in Figure 4.6 A and B respectively. The serum IFNα AUC peaks at 0.09 mg/kg and then declines to a constant serum IFNα AUC value despite increasing dose, which gives a bell shaped dose response profile. Figure 4.6 demonstrates that both the highest serum IFNα and the greatest range in the serum IFNα AUCs were observed following 0.09 mg/kg.

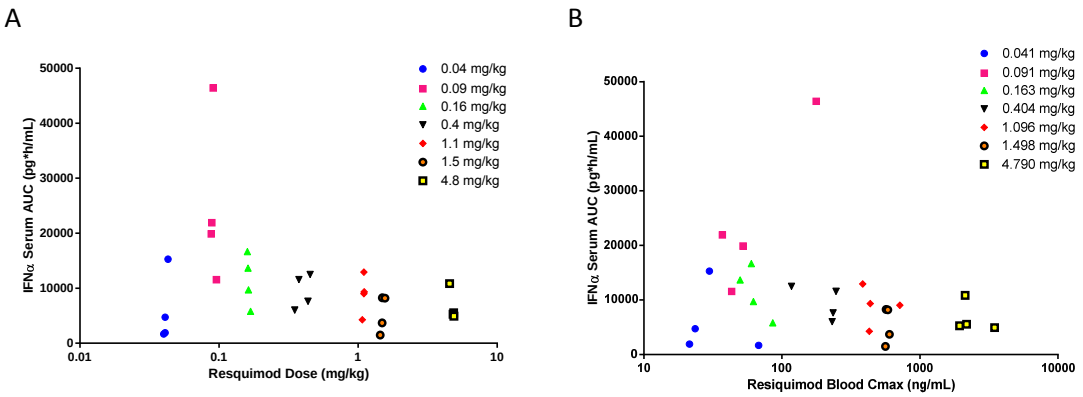

Figure 4.6 **Observed resiquimod Dose (A) and observed C_{max} (B) vs. observed serum IFNα AUC in male CD1 mice following iv bolus administration of resiquimod hydrochloride salt over a dose range of 0.04-4.8 mg/kg**

4.3.2.3. Reproducibility of the response between study days

The individual serum concentration time profiles of IFNα following iv bolus administration of resiquimod hydrochloride salt at a target dose of 0.4 mg/kg to the male CD1 mouse on two separate occasions are presented in Figure 4.7. The serum IFNα concentrations in the samples from vehicle dosed mice and the predose samples from all mice were below the assay LLQ of 200 pg/mL.

Measurable serum IFNα concentrations were observed at the first sampling time point post dose (0.73-0.8 h) reaching a C_{max} between 1.5 and 2 h post dose, then declined towards baseline levels. In group 3 (Figure 4.7 A) two mice had comparable serum IFNα concentrations-time profiles, while two mice had higher IFNα concentrations. For group 4 (Figure 4.7 B) mouse 13 and 15 had comparable serum IFNα concentrations-time profiles, while mouse 14 and 16 demonstrated greater and lower compared to mouse 13 and 15 serum IFNα concentrations respectively. In general the shape of the serum IFNα concentrations-time profiles is comparable between mice in each group and across both groups.

The IFNα PK parameters are listed in Table 4.9. For comparison, the C_{max}, T_{max} and AUC determined for mice administered with 0.4 mg/kg in group 2 have also been included. The mean C_{max} and AUC were comparable among all three groups with comparable intra-group variability observed in all three groups for both parameters.

A

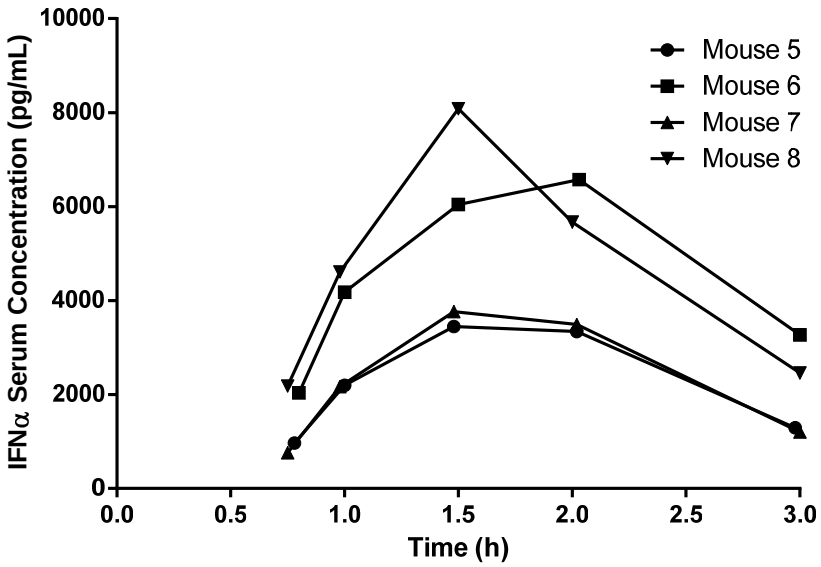

B

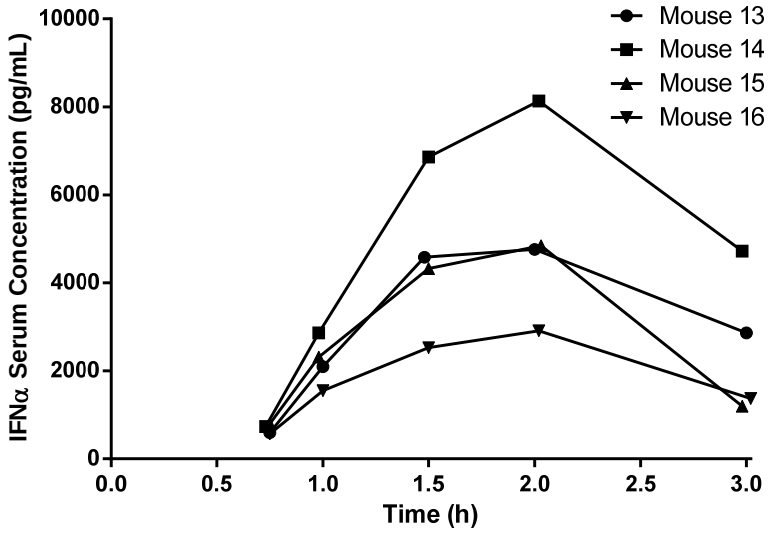

Figure 4.7 **Serum Concentration time profiles for IFNα in conscious male CD1 mice following iv bolus administration of resiquimod hydrochloride salt at a dose of 0.4 mg/kg in group 3 (A) and group 4 (B)**

Table 4.9 Pharmacokinetic Parameters of IFNα in conscious male CD1 mice following iv bolus administration of resiquimod hydrochloride salt at a dose of 0.4 mg/kg on three separate study days

Group	Mouse ID	Parameter		
		T_{max} (h)	C_{max} (ng/mL)	AUC_{last} (pg*h/mL)
3	5	1.48	3449	6142
	6	2.03	6575	12108
	7	1.48	3765	6367
	8	1.50	8081	12397
	Mean	**ND**	**5468**	**9254**
	SD	**ND**	**2238**	**3466**
	CV (%)	**ND**	**41**	**37**
4	13	2.00	4759	8400
	14	2.02	8134	13312
	15	2.03	4844	7681
	16	2.02	2914	5051
	Mean	**ND**	**5163**	**8611**
	SD	**ND**	**2172**	**3449**
	CV (%)	**ND**	**42**	**40**
0.4 mg/kg administered in dose response study	17	1.50	3976	7618
	18	2.00	3488	6034
	19	1.98	6852	11585
	20	2.02	7118	12513
	Mean	**ND**	**5358**	**9438**
	SD	**ND**	**1892**	**3107**
	CV (%)	**ND**	**35**	**33**

The individual resiquimod blood C_{max} values determined for group 3 (Blue Circles), group 4 (Red squares) and in mice dosed with 0.4 mg/kg administered in dose response in group 2 (green triangles) vs. Serum IFNα AUC are presented for comparison in Figure 4.8. The figure demonstrates that 11 out of 12 mice fall into a similar area with a *ca*. 2 fold difference in resiquimod C_{max} and a *ca*. 2.5 fold difference in serum IFNα AUC. Mouse 8 (group 4) demonstrates a *ca*. 7 fold greater resiquimod C_{max} (Table 4.6) compared to the next highest resiquimod C_{max} yet despite this the determined serum IFNα AUC is comparable to that observed in other mice.

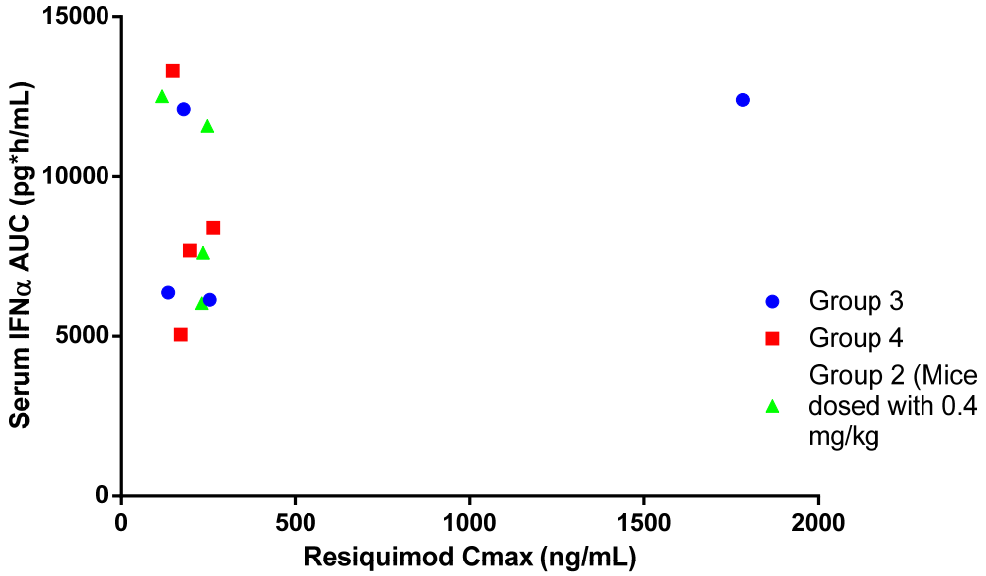

Figure 4.8 **Serum IFNα AUC vs. Resiquimod C_{max} in conscious male CD1 mice following iv bolus administration of resiquimod hydrochloride salt at a dose of 0.4 mg/kg group 3 (Blue circles), group 4 (red squares) and mice dosed with 0.4 mg/kg administered in dose response group 2 (green triangles)**

The individual data for IFNα C_{max} and AUC for each group mean of each parameter for each group and corresponding 95% confidence intervals are presented graphically in Figure 4.9. The individual group means, grand mean and CV for both IFNα C_{max} and AUC are presented in Table 4.10 and the results of the analysis of variance following investigation of the data with a one-way ANOVA test are presented in Table 4.11.

Figure 4.9 suggest that comparable mean IFNα C_{max} and AUC values were obtained for each of the three groups, and also that similar intra-group variability for both parameters was observed for each of the groups. The grand means for both parameters are similar to the means values determined for each group again. The root mean square error and determined CV values captures the variation within a group averaged over the three groups, with IFNα C_{max} and AUC CV values of 40% and 37% respectively.

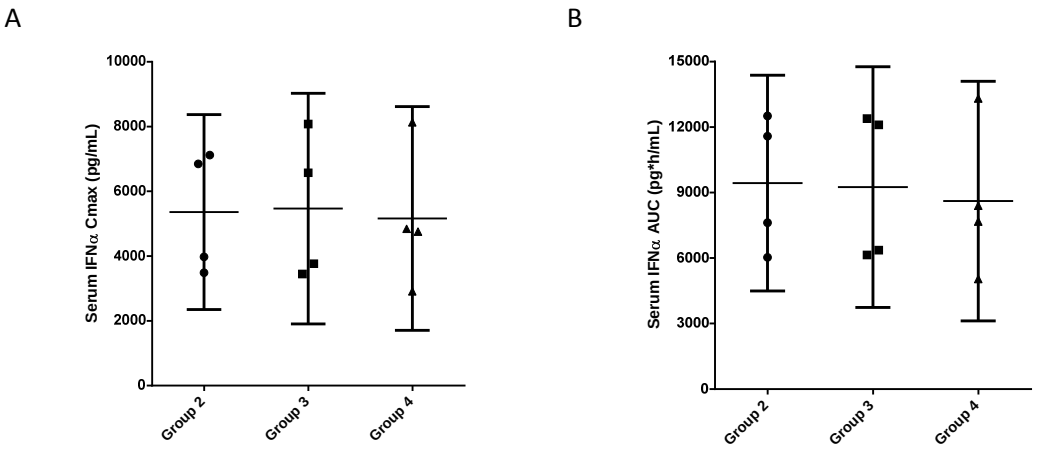

Figure 4.9 **Individual values for resiquimod induced serum INFα C_{max} (A) and AUC (B) with mean and 95% confidence intervals for each group in mice receiving resiquimod treatment at 0.4 mg/kg in three different groups**

Table 4.10 **Individual group means, grand mean, mean root square error and CV of resiquimod induced serum INFα C_{max} and AUC in mice receiving resiquimod treatment at 0.4 mg/kg in three different groups**

Response Variable	Group	Mean	Grand Mean	Mean root square error	CV (%)
C_{max} (pg/ml)	2	5359	5330	2106	40
	3	5468			
	4	5163			
AUC (pg/mL)	2	9438	9101	3345	37
	3	9254			
	4	8611			

Table 4.11 **Analysis of Variance results following investigation of resiquimod induced serum INFα C_{max} and AUC between groups using a one-way ANOVA test**

Response Variable	Source of variation	Degrees of Freedom	Mean Square	F ratio	P Value
C_{max} (pg/mL)	Group	2	95381	0.0215	0.9788
	Residual	9	4435118		
AUC (pg*h/mL)	Group	2	753176	0.0673	0.9354
	Residual	9	11187816		

The results of the analysis of variance are presented in Table 4.11, the P Value determined for the C_{max} and AUC is large and therefore indicates that the null hypothesis cannot be rejected, this therefore does not give any reason to conclude that the means differ, however the data does not allow the conclusion that they are definitely the same. An F ratio of <1 was observed for both C_{max} and AUC and indicates that the null hypothesis cannot be rejected although a value close to 0 can indicate violations of the assumptions that the anova test is based on and so the results should be treated with caution.

The results of the analysis of variance following investigation of the data using REML analysis are presented in Table 4.12.

Table 4.12 Analysis of Variance results following investigation of resiquimod induced serum INFα C_{max} and AUC between groups using REML analysis

Response Variable	Source of Variation	Variance Component	95% CI Lower	95% CI Upper	% of Total
Cmax (pg/mL)	Group	-1084934	-2110441	-59428	0
	Residual	4435118	2098331	14781595	100
AUC (pg/mL)	Group	-2068660	-5219085	1765	0
	Residual	11187816	5293149	37287342	100

The analysis suggests that for both C_{max} and AUC the between group variance accounts for none of the total observed variance, and all the variance is associated with intra group variance. The negative variance component indicates that the agreement between the group means is better than would be expected by chance. The confidence interval for C_{max} estimate does not include zero, so this suggestion is quite strong: nevertheless, there is no obvious explanation for it. The range of the upper and lower boundaries of the confidence interval may indicate that the estimate of group variance is poor, being based on only three groups. The large range in the confidence interval may be due to random error, and an increase in the data may balance out the random error and refine the understanding of between group variance for serum IFNα AUC.

4.3.3. Power Analysis

Power analysis was conducted to determine what sample size is likely to be required to detect inhibition of IFNα in terms of C_{max} and AUC in mice dosed with resiquimod at 0.4 mg/kg. A range of inhibition levels from 10 to 90% was explored, and the sample sizes obtained are presented in Table 4.13.

If for example inhibition of the resiquimod-induced serum IFNα response by an inhibitor compound is measured as inhibition of the serum IFNα C_{max}, then if the inhibitor compound gives 90% inhibition a sample of 2 animals per treatment is predicted to detect this effect with 97% power. If however the inhibitor compound only gives 10% inhibition of the serum IFNα C_{max} a sample of 230 animals per treatment is predicted to be required to detect this effect with 90% power.

Table 4.13 Power calculations for inhibition of resiquimod induced IFNα by a co-administered inhibitory agent

Response Variable	Inhibition (%)[1]	Sample Size[2]	Power[3]
C_{max} (CV=37%)	90	2	0.9822
	80	3	0.9970
	70	3	0.9538
	60	4	0.9369
	50	6	0.9290
	40	10	0.9223
	30	18	0.9001
	20	45	0.9010
	10	199	0.9005
AUC (CV=40%)	90	2	0.9698
	80	3	0.9928
	70	3	0.9277
	60	4	0.9050
	50	7	0.9361
	40	11	0.9120
	30	21	0.9038
	20	52	0.9013
	10	230	0.9004

[1]% inhibition = 100 × (mean (control) – mean (resiquimod))/ mean (control)
[2]Sample size = No. of animals in resiquimod group = No. of animals in control group
[3]Power = precise power given by the sample size, always > 0.9

4.4. Discussion

4.4.1. Determining the Pharmacokinetics of Resiquimod in the mouse

4.4.1.1. Resiquimod Pharmacokinetics

In this study, the pharmacokinetic parameters were determined for resiquimod in the male CD1 mouse. Resiquimod has been reported to have been dosed *in vivo* to mice, rats (Tomai et al, 1995; Graul and Castaner, 1999), guinea pigs (Tomai et al, 1995), monkeys (Tomai et al, 1995; Wagner et al, 1997), and humans (Pockros et al, 2007) using a variety of routes, however limited pharmacokinetic data for resiquimod has been reported in the literature.

Following iv infusion administration the CL_b for resiquimod in the mouse was moderate to high based on reference guidelines (Kerns and Di, 2008). Studies investigating the routes of elimination of resiquimod in the rat following both iv and oral administration using [14C]-labelled resiquimod demonstrated, that resiquimod was the predominant analyte in the serum with approximately 40% of the total radiolabel attributed to unknown metabolites. Following iv administration, 16% of the administered dose was eliminated in the urine as unchanged drug with a further 26% as metabolites (Graul and Castaner, 1999). This indicates that both metabolism and renal elimination may contribute to the total blood clearance of resiquimod observed in the male CD1 mouse.

The V_{ss} determined for resiquimod following iv infusion administration to the mouse was greater than the body water volume (0.7 L/kg Kerns and Di, 2008) indicating distribution into the tissues. This is in agreement with reports in the literature that resiquimod distributes extensively throughout the body from the site of administration (Graul and Castaner, 1999; Tomai and Vasilakos, 2011).The distribution of resiquimod into individual tissues has been investigated in the rat (Graul and Castaner, 1999) where the highest percentages of administered dose were detected in the gastrointestinal tract contents, kidney, liver, skeletal muscle, small intestine, skin and stomach.

The pharmacokinetic parameters of resiquimod in man following oral capsule administration doses of 0.01 and 0.02 mg/kg were of 10 ± 7 mL/min/kg and 18 ± 24 mL/min/kg for serum CL/F, 4.29 ± 1.84 and 6.58 ± 3.83 L/kg for V/F (Pockros et al, 2007). The absolute oral bioavailability of resiquimod determined in the rat was 90% (Graul and Castaner, 1999), assuming the bioavailability of resiquimod is comparable between species,

then the serum CL/F can be adjusted to give a estimation of the total serum CL in human (9 – 16 mL/min/kg). The unbound fractions of resiquimod in human serum and blood are unknown, but assuming they are comparable between man and rodent, the resiquimod clearance in man ranges from 40% - 80% of liver blood flow (taking the liver blood flow in man to be 21 mL/min/kg; Davis and Morris, 1993). The caveats in the estimation of total clearance from oral clearance when incorporating a number of assumptions, are acknowledged, however, the resiquimod clearance in man (40-80% LBF) is considered to be comparable to the clearance observed in this study in CD1 mice (55% LBF). Resiquimod serum concentrations in man declined in a biphasic manner with the terminal phase becoming apparent between 8 and 16 h (Pockros et al, 2007). A biphasic decline of resiquimod serum concentrations has been reported in the in the rat following iv administration (Graul and Castaner, 1999). The decline of resiquimod blood concentrations in this study in the mouse followed a mono-exponential decline. The difference between the decline in resiquimod concentrations between the mouse, rat and human may be due to the difference in the volume of distribution observed between the species. The higher volume of distribution in human compared to that observed in the mouse may account for the longer terminal half-life for resiquimod reported in human (6.8 ± 3.3 h) compared to the terminal half-life determined in the CD1 mouse.

4.4.1.2. Resiquimod induction of serum IFNα concentrations

Following iv infusion of resiquimod to male CD1 mouse, measurable serum IFNα concentrations were observed up to 3 h post dose confirming that resiquimod can induce serum IFNα concentrations. In mice, the imidazoquinalolines, such as resiquimod, stimulate plasmacytoid dendritic cells through the TLR7 dependent pathway to rapidly produce large amounts of IFNα (Schiller et al 2006). Resiquimod has previously been shown to induce serum IFNα concentrations in mice following iv (Asselin-Paturel et al, 2005) oral (Tomai et al, 1995) and topical (Imbertson et al, 1998) administration. Resiquimod has also been shown to induce serum IFNα concentrations in humans (Pockros et al, 2007) and primates (Wagner et al, 1999) following oral administration.

The dose of resiquimod administered to CD1 mice (0.25 mg/kg) was selected to allow comparison to data previously published. Administration of resiquimod as an iv bolus at 0.25 mg/kg to female 129/SvPas mice resulted in a mean maximum IFNα serum concentration of *ca* 8900 pg/mL at a T_{max} of 2 h post resiquimod challenge (Asselin-Paturel

et al, 2005). These values are comparable to those observed in this study. The variability associated with the published IFNα C_{max} was approximately 40% (n=3 mice), which is comparable to the variability reported in group 1 for the IFNα C_{max} (40%). It should be noted that there are a number of differences between the methodology used in this study and that used in the previously published study. The strain, sex and age of mice, the dose route (iv infusion vs iv bolus) and vehicle, and the blood sampling regime were all different between the two studies. The impact of these variables on the observed IFNα concentrations between the two studies is unknown.

Following iv bolus administration of resiquimod Asselin-Paturel et al, (2005) collected serum samples up to 36 h post challenge and demonstrated that IFNα serum concentrations were close to the baseline at 6 h post dose, and remained there to 36. The IFNα serum concentration determined by Asselin-Paturel et al, (2005) at 4 h post challenge was *ca* 2000 pg/mL, and similar to the IFNα serum concentration observed at 3 h in this study. This indicates that the sampling regime implemented in this study was sufficient to characterise the IFNα serum concentration time profile following the 0.25 mg/kg resiquimod challenge.

Following iv infusion of resiquimod a delay of 1.5-2h was observed between the resiquimod blood T_{max} and the IFNα serum T_{max}. Activation of TLR7 or TLR8 expressing cells by IRMs, such as resiquimod, occurs within minutes, eventually leading to direct or indirect activation of both innate and adaptive arms of the immune response (Tomai et al, 2007). The delay between the observed resiquimod blood T_{max} and the IFNα serum T_{max} can probably be attributed to the production and release of IFNα from the pDCs. The resiquimod blood C_{max} values determined in this study following iv infusion was comparable between the five mice (CV 16%). With similar resiquimod blood C_{max} values it is difficult to draw any conclusions around the resiquimod concentration effect relationship, although clinical studies have suggested that there appears to be a relationship between resiquimod C_{max} and IFNα serum concentrations following a single oral dose of resiquimod in subjects with chronic hepatitis C virus infection (Pockros et al, 2007). What can be determined from this study is that the variability of the IFNα serum concentrations (IFNα C_{max} 5 fold) is greater than the variability of the resiquimod blood concentrations (resiquimod C_{max} 1.4 fold). This may indicate that the variability in the IFNα serum concentration data observed in this study is the best it will be for this *in vivo* challenge model.

Following oral administration of 1 mg/kg resiquimod to the monkey, peak IFN serum concentrations were observed at 2-6 h (Wagner et al, 1997). The T_{max} may be later in the monkey compared to that observed in the mouse due to the slower absorption by the oral route compared to iv infusion. The IFNα C_{max} following oral administration at 1 mg/kg was 30108 pg/mL with a CV of 184%. Similar variability was also observed in monkeys following oral administration of resiquimod at 0.01 and 0.1 mg/kg. This is considerably higher and more variable than the C_{max} observed in this study in the mouse. The authors do not provide resiquimod concentration data so it is difficult to assess whether the variability observed in IFNα C_{max} can be explained by the variability of the resiquimod blood concentrations.

The 0.25 mg/kg dose of resiquimod is approximately 10 fold higher than the maximum oral dose administered to man (0.02 mg/kg, Pockros et al, 2007). The serum IFNα C_{max} values observed in the mouse (8900 pg/mL, Asselin-Paturel et al, 2005) and man (7550 pg/mL) were comparable despite the lower dose administered to man. This may imply a reduced sensitivity of resiquimod to activate TLR7 responses leading to IFNα production in mouse compared to man. *In vitro* studies comparing TLR7 responses in rat and human to a number of TLR agonists concluded that rat is more sensitive to TLR7 activation than human (Clarke et al, 2009), and the authors suggest that this could be explained by a number of factors such as the TLR7 agonists having a higher affinity for the rat TLR7 receptor, a difference in expression levels of TLR7 signalling pathway components, a higher proportion of pDCs in rat blood or that expression levels of the TLR7 receptor is higher in rat pDC than human. These factors may explain the lower sensitivity of resiquimod in mice compared to humans, although TLR7 is expressed in mouse immune cells more broadly than in humans (Tomai et al, 2007). Another factor to consider is that resiquimod is a TLR7/TLR8 agonist, human pDCs express TLR7 and TLR8 but TLR8 is thought to be a pseudogene in the mouse, and it may be that the response to resiquimod through the TLR8 pathway accounts for the different sensitivity to resiquimod observed between mice and humans.

The objectives of this study were to determine the pharmacokinetics of resiquimod following iv infusion administration to the male CD1 mouse and to investigate the induction of serum concentrations of IFNα by resiquimod. Both of the objectives were successfully accomplished. The following studies focused on the further optimisation and validation and of the model in an effort to understand its utility in the drug development environment.

4.4.2. Induction of serum IFNα concentrations over a resiquimod dose range in the male CD1 mouse.

4.4.2.1. Resiquimod Pharmacokinetics

Following the "proof of concept" that resiquimod induces IFNα concentrations, the decision was taken to investigate what is the optimal dose of resiquimod is to deliver a robust IFNα response. A resiquimod dose range study has previously been reported in the mouse (Tomai et al, 1995), with the highest IFNα C_{max} observed following oral administration of resiquimod at 0.3 mg/kg, and further increases in the dose to 1, 3 and 10 mg/kg resulting in a lower IFNα C_{max} compared to that observed with 0.3 mg/kg. Taking this into account this study looked to investigate the concentration-effect relationship of resiquimod following the administration of resiquimod over a range of doses.

For this study, and all subsequent studies resiquimod was administered as a single iv bolus dose. The change in the route of administration enabled increased numbers of mice to be included on to a study. Due to the time constraints associated with the surgical implantation of a cannula into mice only a small number of mice can be prepared each day. It is therefore unfeasible to surgically prepare 30 – 40 mice to enable a thorough investigation of the dose response relationship of resiquimod in the mouse. Moving to iv bolus administration enables an increased number of mice to be included onto a study (up to 50 mice per study)

One concern with moving from iv infusion to iv bolus administration is that the pharmacokinetics may change due to saturation of either a metabolic or transport process that is involved in the elimination of a compound since all the drug is administered into the blood in a very short time frame leading to higher peak concentrations. This saturation may not be observed following iv infusion as the dose is administered over a longer time frame resulting in lower maximum blood concentrations and therefore a lower load for the elimination pathways.

The target dose range of 0.03 to 3 mg/kg resiquimod was selected using a dose of 0.3 mg/kg as the midpoint based on the initial study investigating the iv infusion of 0.25 mg/kg. The concentrations of the dose solutions were approximately 20-50% higher than the nominal dose solution, and the actual dose range was 0.04 to 4.8 mg/kg.

The resiquimod CL_b, V_{ss} estimates determined across the dose groups were comparable, although in general the determined values were lower than those observed with iv infusion of 0.25 mg/kg. The terminal half-life between iv bolus and iv infusion was comparable. The variability for CL_b and V_{ss} following iv infusion was towards the lower end of the range following iv bolus administration, and it may therefore be that the change in the administration of resqiuimod from iv infusion to iv bolus increased variability in the pharmacokinetics

4.4.2.2. Resiquimod induction of serum IFNα concentrations

In this study a bell shaped dose response curve was observed in mice with increasing resiquimod dose. The greatest IFNα response was observed at 0.09 mg/kg, with high concentrations also observed at 0.16 mg/kg although the AUC determined at this dose was approximately 2 fold lower than that observed at 0.09 mg/kg.

Tomai et al, (1995) also identified a bell shaped dose response curve between resiquimod dose and serum IFN concentrations (Figure 4.10). They found that the greatest response occurred at a resiquimod dose of 0.3 mg/kg, and that the IFNα response did not return to the low levels observed at very low doses until a dose of 10 mg/kg. This suggests that the dose response curve observed by Tomai et al, (1995) is shifted to the right compared to this study. This may be due to a different strain of mice being used in the published study, CFW mice rather than CD1 mice, or it may be down to the route of administration. In the published study, mice were dosed orally, and therefore a simple explanation for this shift to the right in the dose response curve may be that only a fraction of the dose reached the systemic circulation due to absorption issues or first pass metabolism. If, for example, only 70% of a 1 mg/kg oral dose reaches the systemic circulation then example 1.4 mg/kg would be required to deliver the same systemic concentrations as a 1 mg/kg iv bolus dose, where 100% of the dose reaches the systemic circulation.

A number of potential mechanisms may drive the shape of the dose response relationship. *In vitro* studies in isolated pDCs, have demonstrated that the resiquimod inhibition occurs at the level of the pDC and does not require the presence of secondary cell types to carry out the effect (Marshall et al, 2007). Taking this into account, the hypothesis can focus on the pDC and the components involved in the production of IFNα within these cells.

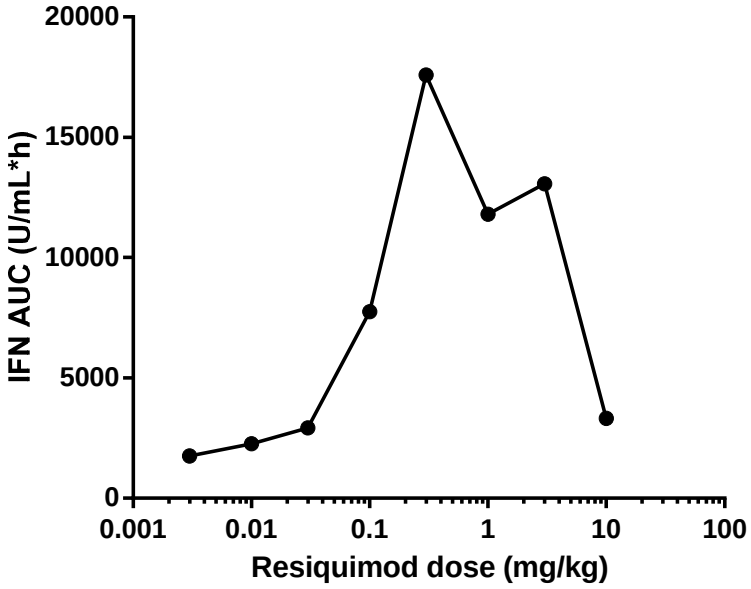

Figure 4.10 **Resiquimod dose vs. Serum IFNα AUC in the male CFW mouse following oral administration of resiquimod free base over a dose range of 0.003 to 10 mg/kg. AUC derived from data presented by Tomai et al (1995) using NCA in WinNonlin Phoneix software (Pharsight, version 6.2)**

Resiquimod has been demonstrated not to by cytotoxic (Forsbach et al, 2012) and whilst other cytokines have been demonstrated to have an inhibitory effect on IFNα production from pDCs (Gary-Gouy, Lebon and Dalloul, 2002) the rapid production of IFNα following resiquimod challenge make it “unfeasible” that these may be produced and available to have an inhibitory action in such short timeframes. It may be that resiquimod is interfering with or inhibiting components of the pathway involved in TLR signalling within the pDC. Supporting the capability of resiquimod to interfere with components of the signalling pathway comes from *in vitro* studies using human PBMC to investigate the impact of resiquimod on the JAK/STAT pathway. In these studies it was demonstrated that the binding of resiquimod to the SH2 phosphorylation site of STAT2, blocked the downstream signalling of Type I IFN (Forsbach et al, 2012). Although this is downstream of the induction and inhibition of IFNα observed in the present study, it provides evidence that resiquimod may be having a dual effect, both activating and inhibiting the response, depending on the concentration.

The induction of IFNα via the activation of the pDC through the TLR receptors initiates a complex network of transcriptional regulation as discussed in Chapter 2 where resiquimod may exert an inhibitory effect. If resiquimod did have an inhibitory action on a component of the cascade it could explain the bell shaped dose response curve observed for serum IFNα concentrations following resiquimod challenge, but this would depend on the selectivity of resiquimod against the TLR7 receptor and the other unknown target. In this scenario, the selectivity between the two targets would enable resiquimod to induce serum IFNα concentrations in a dose dependent manner until a threshold concentration of resiquimod is reached. At this threshold concentration, the inhibitory action of resiquimod would be the predominant pharmacology inhibiting the TLR7 induced production of serum IFNα concentrations. To further explain this hypothesis the target engagement-time profiles at both the TLR7 receptor and an inhibitory mechanism achieved with hypothetical low, optimal and high doses of resiquimod are presented graphically in Figures 4.11 A, B and C respectively. With a low dose of resiquimod (Figure 4.11A), despite low blood concentrations of resiquimod target engagement at the TLR7 receptor of approximately 60% is achieved, resulting in the production of serum IFNα concentrations. With the difference of the selectivity between the two targets at the low resiquimod blood concentrations, the target engagement of the inhibitory response is low at approximately 15% and so little to no inhibition on the serum IFNα concentrations is observed. The optimal dose of resiquimod (Figure 4.11B) would potentially represent the scenario observed for the 0.03 mg/kg or 0.09 mg/kg dose in group 2. With these doses a greater target engagement (~90%) for the TLR7 receptor is achieved compared to the low dose which would result in a greater serum IFNα concentrations observed for the optimal dose compared to the low dose. With the increase in dose and corresponding increase in resiquimod blood concentrations, the target engagement achieved at the inhibitory response increases to approximately 50%, however, in this scenario this target engagement would be hypothesised to be below the threshold required to inhibit the production of IFNα concentrations and so as with the low dose there would be little to no inhibition of the serum IFNα concentrations. The third scenario (Figure 4.11C) represents greater than optimal doses of resiquimod where a reduction in serum IFNα concentrations is observed despite increasing resiquimod blood concentrations. With these doses and corresponding blood concentrations, high levels of target engagement (>90%) of the TLR7 receptor are observed, however greater target engagement (~90%) of the inhibitory response is also

observed. It is hypothesised that in this scenario the threshold target engagement is reached for the inhibitory response, and this response is greater than the production of serum IFNα concentrations, so despite high target engagement for the TLR receptor, the net result is the inhibition of serum IFNα concentrations.

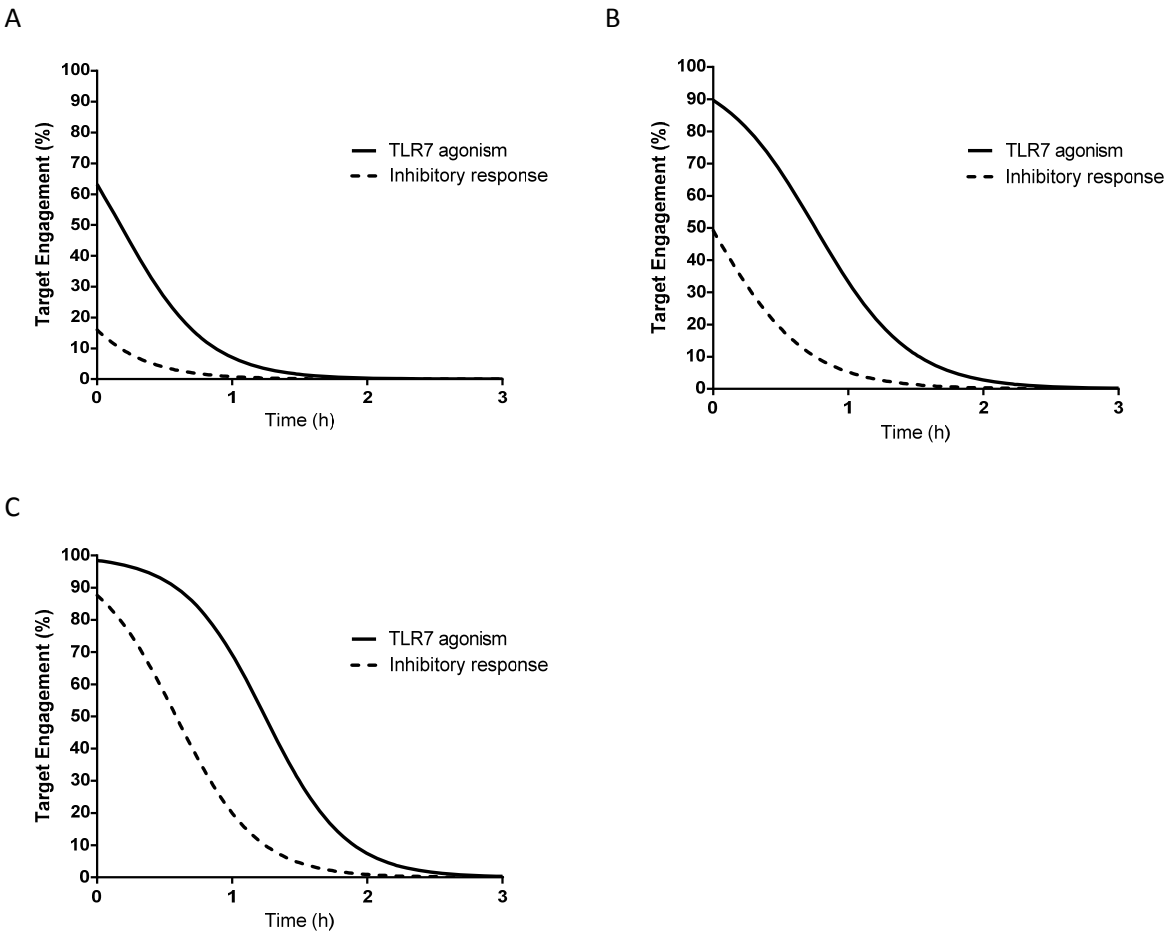

Figure 4.11 Hypothetical target engagement-time profiles at both the TLR7 receptor and an unknown inhibitory mechanism achieved with low (A), optimal (B) and high (C) doses of resiquimod

Even though many signalling molecules are important for the IFN pathway, they rely on their ability to activate IRF7 (Guiducci, Coffman and Barrat, 2008). Studies have shown that Irf7 -/- mice are highly vulnerable to infection by HCV or encephalomyocarditis virus (EMCV) and IFNα induction is markedly inhibited in the sera of IRF7 -/- mice infected with these viruses (Honda et al, 2005). Taking into account the importance of IRF7 in the production of IFNα, it is no surprise that pDCs, the fastest and most potent producers of IFNα, constitutively express large amounts of IRF7 (Kirou and Gkrouzman, 2013). The

inhibition of the translocation of IRF7 into the nucleus or a reduction in the level of IRF7 phosphorylation, which is central to the activation of the IRF7 pathway, may be a method by which TLR7 ligands can interfere with IFNα expression (Marshall et al, 2007). However, with many critical components being involved in the signalling pathway there are a number of other areas where resiquimod could interfere or inhibit the formation of the complex resulting in inhibition or defective translocation of IRF7 into the nucleus and therefore inhibition in IFN production.

It may be that as well as acting as an agonist against the TLR7 receptor resiquimod could also be acting as either an antagonist on one of the components involved in the production of IFNα or as and agonist for a regulatory protein that delivers an inhibitory response on the production of IFNα. There is a bifurcation of the signalling pathway downstream from MyD88, and taking this into account, a simple way to investigate where resiquimod may be having its action is to look at the induction of the NF-κB induced cytokines, such as TNFα, over a resiquimod dose range. If resiquimod is acting between the TLR7 receptor and the bifurcation of the signalling pathway, one would expect to observe a bell shaped dose response curve for the NF-κB induced cytokines as well as IFNα. Alternatively, if resiquimod is acting after the bifurcation and solely inhibiting the IFNα pathway, the NF-κB induced cytokines may continue to show an increase in serum concentrations with an increase in dose of resiquimod. The induction of other cytokines, such as TNFα over a dose/concentration range of resiquimod, has been investigated in both *in vivo* studies in mice and *in vitro* studies in human PBMC. These studies suggest that the resiquimod dose response for the induction of TNFα is not characterised by a bell shaped curve over the dose range administered, although it should be noted that the response appears to plateau in the human PBMCs and doesn't appear to be linear *in vivo.* Further evidence that resiquimod may be acting on the later stage of the signalling pathway comes from *in vitro* studies using human pDC investigating the inhibition of TLR9 mediated induction of IFNα with resiquimod. In these studies, resiquimod demonstrated a dose dependent inhibition of IRF7 and IFN mRNA induction by a TLR9 agonist although the NF-κB pathway was activated at similar levels by the TLR9 agonist in the presence and absence of resiquimod (Marshall et al, 2007), The authors concluded that the action of resiquimod action may be confined to the later stages of the pathway or the translocation of IRF7 into the nucleus.

As well as the components of the MyD88 pathway discussed above, other adaptors have been found to be essential for the control of the production of IFNα from pDC. Examples include a precursor of osteopontin (OPN), which is required for IRF7 activation, and the PI3K/mechanistic target of rapamycin (mTOR) pathway, which is required for the nuclear translocation of IRF7 (Kwaii and Akira, 2010). *In vitro* studies in human and mouse pDCs have demonstrated that the highly specific mTOR inhibitor rapamycin inhibited the TLR7 induced IFNα production by inhibiting the phosphorylation of IRF7. This was confirmed *in vivo* where pretreatment of mice with rapamycin inhibited the induction of IFNα by a TLR7 agonist (Cao et al, 2008). PI3K activation has been demonstrated to be an important step in the pathway leading to IRF7 nuclear translocation following both TLR7 and TLR9 activation (Guiducci et al, 2008) and has been proposed as a drugable target for drug investigation. In human pDCs, PI3K inhibition only resulted in impaired IFNα production, and IL6 and TNFα production were unaffected. As discussed previously, it may be possible to elucidate if resiquimod is having its effect by inhibiting PI3K by investigating the dose response curve for IL6 and TNFα although this would only narrow it down to the point of bifurcation of the two pathways and not to a specific component. A number of different subunits of PI3K are expressed in human pDCs and *in vitro* studies have demonstrated that following TLR activation, a PI3K δ specific inhibitor inhibited IFNα production in a dose dependent manner whereas a PI3K γ specific inhibitor only inhibited IFNα production at very high concentrations (>20μM). In *in vitro* studies in human PBMC, the PI3K δ specific inhibitor demonstrated approximately 40% inhibition of IFNα concentrations at 0.3 μM and a reduction in systemic serum IFNα concentrations was observed with a resiquimod C_{max} of approximately 0.2 μM (65 ng/mL). Although it is difficult to compare the two studies, it may be that resiquimod is inhibiting PI3K δ. However, it is also worth noting that in the reported study the PI3K δ showed concentration dependent inhibition of IFNα up to a concentration of 25 μM, where the IFNα concentrations appear close to baseline, whereas in the *in vivo* mouse study, the inhibition of serum IFNα concentrations appears to plateau. This may represent a difference between mouse and human, *in vivo* and *in vitro* systems, TLR agonist used or maybe simply that sufficient concentrations of resiquimod were not achieved in this study.

An alternative hypothesis could be that it is the system that is controlling the response via a feedback loop. It may be that the TLR signalling is tightly regulated to avoid aberrant production of IFNα and thus the development of autoimmune disease. Support for this

theory comes from the observation that other TLR agonists including both small molecules (imidazolquinolines) and synthetic single-stranded oligoribonucleotides (ORNs) have demonstrated bell shaped IFNα response curves *in vitro* in mouse splenocytes (Reiter et al, 1993; Isobe et al, 2006) in human PBMC (Marshall, et al, 2007; Forsback et al, 2012) and *in vivo* in the mouse (Reiter et al, 1993). Many negative regulators that suppress TLR signalling pathways have been identified and although these can regulate the immune responses at multiple levels, most appear to target the MyD88-dependent pathway (Liew et al, 2005).

A family of proteins that may regulate the IFNα response are the suppressors of cytokine signalling (SOCS) which are SH2-domin containing proteins which can be induced in various tissues and cell lines. Out of the SOCS family SOCS-1 and SOCS-3 have been recognized as the most important for regulating immune cells (Dalpke et al, 2001), and the thought is that induction of SOCS-1 and SOCS-3 prevents the overshooting of immune activation (Posselt et al, 2011). *In vitro* studies (Dalpke et al, 2001) using macrophages have demonstrated that TLR9 activation using CpG-ODN (CpG-oligodexoynucleotide) resulted in an induction in both SOCS 1 and 3 mRNA which is inhibited by chloroquine, with the mechanism of action attributed to inhibition of TLR9 signalling. Further *in vitro* studies (Posselt et al, 2011) using human monocyte derived dendritic cells have demonstrated that TLR activation by LPS results in the induction of SOCS1, 2 and 3 mRNA, and is a direct downstream effect of TLR activation. Following activation SOCS1 and 3 were induced within 1 h whereas SOCS2 was induced 8 h after activation peaking at 24 h post activation. The researchers also investigated the induction of SOCS2 following activation with different TLR agonists and demonstrated that resiquimod induces SOCS2 although SOCS1 and 3 were not investigated.

Other potential negative regulators of the TLR pathway include the two of the main targets for mTOR, 4E-BP1 and 4E-BP2, which are translational repressors, the regulatory protein Zc3h12a and the tyrosine phosphate SHP-1. The phosphorlyation of 4E-BP1 and 4E-BP2 by mTOR abrogates their ability to inhibit protein synthesis, and a study has shown that inhibiting expression of 4E-BP1 and 4E-BP2 enhances IRF7 translocation and increases virus-stimulated IFN release (Cao et al, 2008). The regulatory protein Zc3h12a is rapidly induced following TLR stimulation, and targets IL6 mRNA and IL12p40 mRNA for degradation via its RNase activity. Finally *in vivo* investigations in mice suggests that the tyrosine phosphate SHP-1 negatively regulates the MyD88-dependent pathway in response to TLR signalling and suppresses the action of both IRAK1 and IRAK2 (Kawai and Akira, 2010).

For many of these negative regulators it has been demonstrated that 1) they are induced by TLR ligands and 2) disruption of their function can lead to persistent inflammation. Taking this into account these negative regulators appear to act as a cellular self control system to avoid aberrant IFNα production. It may well be that excessive resiquimod concentrations would elicit a threshold response that initiates the production of one or more negative regulators to keep the response in check. The assumption could be made that there would be a time delay in the induction of the negative regulators following TLR stimulation, and this may explain why there appears to be a plateau in the inhibition of serum IFNα concentrations despite increasing concentrations of resiquimod. If this was the case an amount of IFNα would be produced following TLR activation prior to negative regulation which would inhibit further IFNα production, and higher concentrations of resiquimod would not speed up the production of the negative regulars so the observed IFNα response could feasibly be the same with increasing resiquimod doses and corresponding concentrations. It would be interesting to investigate if the initial rate of production of IFNα differs between the different dose groups, which the blood sampling regime was not designed to investigate in this study. If there is a delay in the induction of the negative regulators then the initial rate of production of IFNα should be comparable between all doses. However once the negative regulators have been induced then one would anticipate that the rate of production of the IFNα would change. It may be possible to investigate this with a more exhaustive sampling regime but would probably require the building of a composite profile using a larger population of mice.

In summary, both the resiquimod C_{max} and AUC broadly increase in a linear fashion with the increase in resiquimod dose. The IFNα response defined as serum IFNα AUC was characterised by a bell shaped dose-response curve, which is similar to previously reported studies, with the greatest IFNα response was observed at a dose of 0.09 mg/kg, however the IFNα response at these doses was associated with the highest variability. A dose of 0.4 mg/kg gave the lowest variability associated with the IFNα response therefore this dose is recommended for future *in vivo* studies.

4.4.3. Reproducibility of the response between study days

4.4.3.1. Resiquimod Pharmacokinetics

The reproducibility of the systemic exposure of resiquimod and the observed IFNα response was investigated following iv bolus administration of resiquimod 0.4 mg/kg over three separate study days. The mean CL_b and V_{ss} estimates with 0.4 mg/kg although slightly lower than the values determined following iv infusion of 0.25 mg/kg were comparable across all three groups/days. The terminal half-life was comparable between all mice given an iv bolus of 0.4 mg/kg (Groups 2, 3 and 4) and following iv infusion administration at 0.25 mg/kg (Group 1).

The variability observed for the CL_b and V_{ss} determined for group 3 was considerably higher than compared to that observed for the same parameters for group 4. Although CL_b and V_{ss} for group 3 were comparable between three of the mice, the values for one mouse, which demonstrated 7 fold greater systemic exposure of resiquimod compared to other similarly treated mice, were very different. Similar situations, whereby some mice demonstrated greater systemic exposure compared to the others were also observed in other dose groups within the dose response studies. The reason for these findings is not clear but it may have been due to an error in the administration of the compound to the mice. As both the syringe and dose concentration were measured in these studies, it is unlikely that the mice received a higher dose of resiquimod than expected; therefore the error may come from the actual administration of the dose itself. The dose in these studies was administered via the tail vein and the blood samples were taken from the tail vein on the opposite side to that which the dose was administered. As the mouse tail is very small, it may be that there was some contamination of the sampling site by dosing in such close proximity to the sampling site. Some of the administered iv dose may have been accidently administered subcutaneously to the area around the dose site and therefore when the blood sample was taken via venepuncture of the other tail vein any residual dose may have contaminated the blood sample giving artificially higher concentrations than those in the systemic circulation. This highlights a practical limitation of this model and raises questions as to its value and utility in providing consistent reproducible decision making data suitable to guide the selection of the most appropriate compounds.

4.4.3.2. Resiquimod induction of serum IFNα concentrations

Following iv bolus administration of resiquimod at 0.4 mg/kg to three separate groups comparable serum IFNα C_{max} and AUC were observed for each group with comparable intra group variability (determined as CV %). Interestingly in group 4 greater concentrations of resiquimod were observed for one mouse compared to the other three mice, however this did not translate to a higher serum IFNα response in this mouse. Furthermore the highest serum IFNα AUC was observed for a mouse in group 3, yet this mouse had comparable concentrations of resiquimod to other mice. In general, greater variability is observed for the serum IFNα response compared to the resiquimod systemic blood concentrations.

The variability in the IFNα response following resiquimod administration observed *in vivo* is not confined to the mouse. In preclinical studies in primates, a high degree of animal to animal variability was observed in the cytokine responses following oral administration of 0.01 0.1 or 1 mg/kg resiquimod (Wagner et al, 1997). Variability associated with the peak serum IFNα concentrations ranged from 184-200%, although it should be noted that at the 0.01 mg/kg dose only one of four monkeys produced any detectable increase above background IFN concentrations. The variability in IFNα response is not confined to preclinical species as other researchers have demonstrated that the response to TLR7 agonists results in widely varying induction of IFNα in humans (Basith et al, 2011). This variability led the authors to question the utility of preclinical studies and conclude that it is unlikely that cytokine induction in animal models will reveal the true range of the human response (Basith et al, 2011).

An explanation for the variability observed in the IFNα response between mice administered with the same dose has not been elucidated in this study. It may be that similar to the bell shaped curve, many factors are involved in contributing to the variability in the IFNα response. These may include the number of circulating pDCs, expression of TLR7 and/or components of the signalling cascade, and environmental factors. Within the clinic, researchers have concluded that the response to the TLR7 agonist imiquimod in patients can be predicted based on the pre-treatment levels of innate immune system molecules. Prior to imiquimod treatment complete responders had higher constitutive mRNA expression of STAT1 and IRF1 while incomplete responders had higher expression of STAT3 and IRF2 (Wang et al, 2005). It may therefore be that the IFNα response may be dependent

on the differential expression of IRF7 or other components of the signalling cascade between individual mice.

Statistical analysis of the data across three study days in mice treated with 0.4 mg/kg resiquimod suggested there was no discernible difference in the mean C_{max} and AUC determined on each study day. There are caveats conducting statistical analysis on such a small data set however the assessment of the reproducibility of the response across study days should be considered an ongoing investigation. On each study day the control treated animals which receive resiquimod treatment at a dose of 0.4 mg/kg to determine the baseline response should be included into a dataset that can be continually analysed as more studies are conducted.

Understanding how reproducible the response is between study days may be important in the drug discovery environment as it will allow more confidence in the comparison of efficacy observed for compounds between study days. For example if the model was being used for screening TLR7 inhibitor compounds the user may wish to compare the inhibition of the resiquimod induced response between compounds tested on one day to another day to select the best molecules for further profiling. If the response observed between treatment groups both on the same study day and alternative study days are comparable, this will gives confidence in the ranking of compounds to ensure that the best compounds are selected.

To understand how the model may be used practically within a drug discovery environment, taking into account the variability in the IFNα response expressed as either serum IFNα C_{max} or AUC, power analysis was conducted. The pharmaceutical industry is committed to the 3Rs (reduction, refinement and replacement) of animal studies and the design and conduct of *in vivo* studies comes under extensive scrutiny. A model that requires group sizes of 20 animals per treatment to reliably detect an effect would have little utility within drug discovery. If a maximum number of animals that may be feasibly included on a study day was 40 it would be difficult to see the model as a tool with sufficient throughput to be used to select the most appropriate compounds as part of a lead optimisation programme where there may be 20-30 compound of interest. The goal of the power analysis was to predict the group size that would be required to detect a specified level of inhibition in both the serum IFNα C_{max} or AUC in mice dosed with resiquimod at 0.4 mg/kg. This analysis demonstrates that feasibly up to 50% inhibition in both the serum IFNα C_{max} or

AUC could be detected with a group size of approximately 6-7 mice, but detecting less than 50% inhibition may be impractical as the group size increases and it is unlikely that due to the numbers the model would be utilised to detect 10% inhibition. This has a number of implications. If for example the goal is to select and rank a number of compounds for the most suitable for progression then it may be that the group size is set to 4 which should enable detection of greater than 60% inhibition. If the maximum number of mice that may be used on each study day is 40 this will allow investigation of 9 compounds per study day assuming one group is a non treatment challenge only group. On the other hand the power analysis gives confidence that for a given compound of interest, a truncated dose response curve could be investigated. If efficacy is determined as inhibition of IFNα AUC then with a total of 40 mice a dose response curve investigating from 40% to 100% inhibition could be investigated assuming 4 mice per group for vehicle and treatments targeting 100%, 90%, 80%, and 70% inhibition, and 5, 7 and 11 mice per group for doses targeting 60% 50% and 40% inhibition. This would allow an increased understanding of the concentration effect relationship, and will allow further definition of an *in vivo* IC_{50} which may ultimately be incorporated into the human dose predictions. The efficacious human dose prediction and corresponding systemic exposure will be integrated with toxicity data to assess the suitability of the compound for progression into the clinic.

In summary this study has demonstrated that following iv bolus administration of resiquimod at a dose 0.4 mg/kg a reproducible IFNα response can be achieved both between individual mice on a study day and across multiple study days. The overall goal was to deliver an acute inflammatory challenge model to investigate the inhibition of the response, and statistical and power analysis indicate that this model will have utility as both a screening tool to rank compounds and also enable characterisation of a dose response curve for selected compounds of interest.

4.5. Conclusion

This chapter describes the investigation of a mouse mechanistic challenge model investigated using the TLR7 agonist resiquimod as the challenge agent based on *in vitro* and *in vivo* studies that demonstrated that resiquimod treatment induces large amounts of the IFNα. The pharmacokinetics of resiquimod were successfully determined in the mouse following both iv infusion and iv bolus administration of resiquimod. This is the first time the PK parameters for resiquimod in the mouse have been reported and resiquimod was

found to have a moderate blood clearance, a moderate volume of distribution and a short half-life in the mouse. In addition the pharmacokinetics demonstrated low inter-mouse variability and increased in proportion to increasing dose. Following administration of resiquimod, an increase in serum IFNα concentrations were observed in all treated mice. The investigation of the dose response relationship delivered comparable data to that previously reported in the literature whereby the greatest response was observed at low doses of resiquimod and further increase in dose results in an apparent reduction in the IFNα response to a plateau. A number of hypothesis have been proposed to account for this profile ranging from a potential inhibitory action of resiquimod at another target to the potential cytotoxicity of resiquimod, however the exact mechanism has not been elucidated. The investigation did however provide the most appropriate dose, based on delivery of a measurable IFNα response with acceptable variability that will be used for subsequent *in vivo* studies. In addition these studies have demonstrated that a reproducible IFNα response can be achieved between mice receiving the same resiquimod treatment across multiple study days.

Chapter 5: Development of a population PK/PD model to describe the induction of serum IFNα concentrations in mice by the TLR7 agonist resiquimod.

5.1. Introduction

Chapter 4 described the investigation of the PK of resiquimod in mice using NCA and the associated IFNα response. There was an obvious lag between the resiquimod blood concentrations and the induction of serum IFNα concentrations and consequently counter clockwise hysteresis was observed. This is demonstrated in Figure 5.1 where the observed serum IFNα concentrations are plotted against the observed resiquimod blood concentrations in mice receiving iv infusion of resiquimod. This indicates that either an effect compartment model or indirect response model would be required to characterise the concentration effect relationship. Authors reviewing the use of these PK/PD models conclude that the decision of which model to use should be based on knowledge behind the mechanism or pathway of response (Upton and Mould, 2014). As IFNα production is known to involve a cascade following resiquimod stimulation of TLR7, an indirect response model appears to be the best model to describe the concentration effect relationship for resiquimod induced IFNα production.

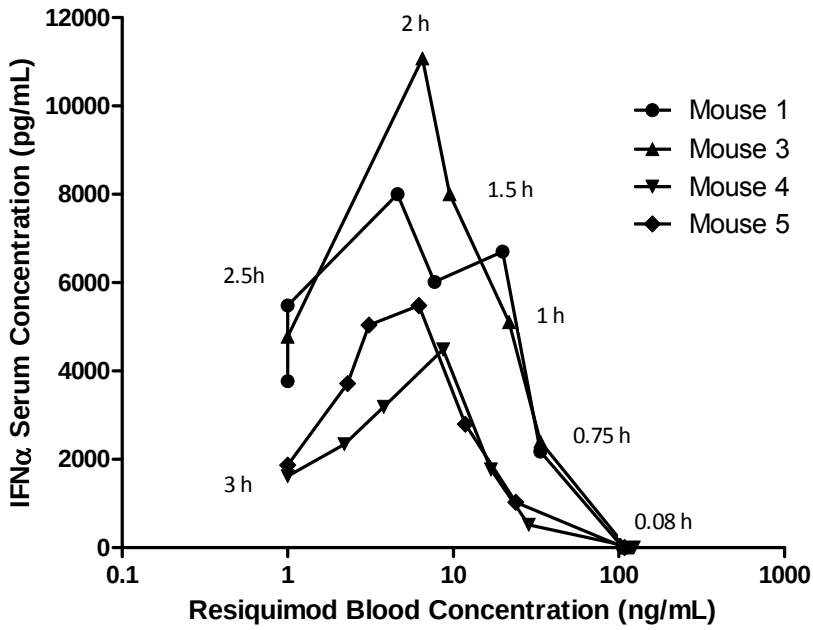

Figure 5.1 **Resiquimod induced serum IFNα concentrations plotted against resiquimod blood concentrations in time sequence in 5 conscious male CD1 mice following a 0.08 h constant rate iv infusion of resiquimod hydrochloride salt at a target dose of 0.25 mg/kg.**

A PK/PD model that describes the induction of serum IFNα concentrations by the TLR7 agonist 9-Benzyl-8-hydroxy-2-(2methoxyethoxy) adenine (BHMA) *in vivo* in the mouse has been described by Benson et al (2010). The authors found that an indirect response model provided an adequate description of the data, although they suggest that a more complex PK/PD model may be more appropriate to better describe the TLR7 agonist induction of IFNα.

Initial PK/PD modelling explorations to characterise the induction of serum IFNα concentrations in mice by resiquimod were conducted using an indirect response model within WinNonlin (not reported). The PK/PD relationship was modelled both in individual mice and using a naive pooled approach, however neither model adequately characterised the rate of production and release of IFNα into the system.

Another point for consideration is that, after an initial increase, the IFNα response fell as the dose of resiquimod was increased further. A review of the literature indicates that similar bell shaped dose response curves are observed for other TLR7 agonist compounds from various different chemotypes in both *in vitro* and *in vivo* studies. However, Benson et al (2010) observed a continuously increasing response over a dose range of 0.3 to 10 mg/kg. It is difficult to make a clear conclusion as to the dose-IFNα contcentration relationship in that study, but it appears that the highest response was observed at 5 mg/kg, a lower response was observed at 10 mg/kg and further increases in dose/concentration of the TLR7 agonist may result in a reduction in the IFNα concentrations.

This bell shaped dose response effect of resiquimod on IFNα response would not be described by a standard indirect response model, which assumes that the response will increase with dose until a plateau is reached. The mechanism that inhibits the response is unknown at this time but may be described using a negative feedback loop within the model that accounts for an endogenous modulator. There are examples in the literature where modulation pathways have been successfully incorporated with indirect response models to describe the PK/PD relationship for a drug induced biological response (Bundgaard et al, 2007; Luu et al, 2009) both of which are adapted from the empirical approach to model tolerance using a negative feedback loop (Gabrielsson and Weiner, 2000). The model presented by Luu et al (2009) describes a positive feedback whereby any perturbation of the response results in a change in the endogenous modulator i.e. when

the response increases then the modulator function increases which then further increases the response.

These findings suggest that the induction of serum IFNα concentrations following iv administration of resiquimod may be best described by a PK/PD model incorporating 1) a PK model to describe the time course of resiquimod concentrations in the blood, 2) a component to describe the observed lag time between the resiquimod concentrations and effect on serum IFNα concentrations such as an effect compartment and/or an indirect response model and 3) an inhibitory modulator component that accounts for the apparent inhibition of serum IFNα concentrations once the dose or concentrations of resiquimod exceed a certain threshold.

In Chapter 4, it was hypothesised that the bell shaped dose response curve could be a result of over stimulation of the TLR7 pathway driving a negative regulation of the response as a protective mechanism to avoid excessive IFNα production. In addition, it was concluded that a dose of resiquimod of 0.4 mg/kg gave a reproducible response (serum IFNα concentrations) in both magnitude and variability across studies and could be used as the dose of resiquimod for future challenge studies. This dose is higher than the dose resulting in the maximal response, and therefore gives a response that is less than the maximal response and, based on the hypothesis discussed above, the response would have been inhibited by the modulator pathway. Co-administration of a TLR7 antagonist with a dose of resiquimod at 0.4 mg/kg may result in less stimulation of the TLR7 pathway, therefore reducing the negative regulation and resulting in an increase in IFNα rather than the expected decrease. Simulations with a PK/PD model describing the effect of resiquimod on IFNα may help to understand the impact of a hypothetical inhibitor on the IFNα response with a fixed dose of resiquimod.

This chapter will describe the investigation of a population PK/PD model to describe the resiquimod induction of serum IFNα concentrations in the mouse over a resiquimod dose range. The model incorporates a PK model to describe the time course of resiquimod concentrations in the blood, an effect compartment to account for the lag and induction of serum IFNα concentrations by resiquimod and an inhibitory modulator component that accounts for the apparent inhibition of serum IFNα concentrations once concentrations of resiquimod exceed a certain threshold. The model parameters were then used to simulate the effect of a hypothetical TLR7 inhibitor on the observed resiquimod induction of serum

IFNα concentrations. This allows an investigation of the potential impact of co-administration of both the challenge and inhibitor with various PK and PD properties *in vivo.* This analysis is key to the validation of the mouse model and enables assessment of the potential for the model as a tool for selecting the most appropriate compounds to progress to the clinic.

5.2. Methods

5.2.1. Data

Resiquimod blood (PK) and IFNα serum (PD) concentration-time data derived following iv bolus administration of resiquimod to groups 2, 3 and 4 was used. The study designs and doses administered to each group are summarised in Table 5.1. For the purpose of modelling, mice in group 2 were numbered 5 to 32 as per Chapter 4 and mice in groups 3 and 4 were numbered 33 to 40. Following NCA of the resiquimod concentration time profiles in Chapter 4, the following samples were excluded from the data set; mouse 6 dose 0.04 mg/kg 2 h, mouse 7 dose 0.04 mg/kg 1 h, mouse 9 0.09 mg/kg 3 h, mouse 10 0.09 mg/kg 1 h and mouse 36 dose 0.4 mg/kg all samples.

Table 5.1 Study details including number of mice, and dose of resiquimod from which data incorporated in PK/PD modelling was derived

Group Number	Purpose of study	Number of mice	Dose of resiquimod administered
2	Investigate resiquimod dose response	28	0.04, 0.09, 0.16, 0.4, 1.1, 1.5, 4.8 mg/kg (n=4 mice per dose)
3	Investigate study day variability in PK/PD	4	0.4 mg/kg
4	Investigate study day variability in PK/PD	4	0.4 mg/kg

5.2.2. Modelling Strategy

The modelling to describe the PK/PD relationship was conducted sequentially. Initially a PK model was fitted to the resiquimod blood concentration-time profiles. Secondly, the population PK estimates (THETAS) and IIV (OMEGAS) were fixed and the PD parameters for the IFNα response following administration of resiquimod were estimated. All data were analysed with a population approach using nonlinear mixed effects modelling. A structural

model provided estimates of typical values of the model parameters, such as CL_b and V. The variance models are built using random variables, and describe the inter-individual variability (IIV) in the structural parameters within the study population, and the residual error or "noise", which includes variability associated with the assay and time measurements. All modelling was conducted using NONMEM version 7.2 (Beal et al, ICON Development Solutions).

The first-order conditional estimation method with interaction between the two levels of stochastic effects (FOCE interaction) was used (Benson et al, 2010).

Inter-individual variability (IIV) was described by an exponential model (equation 5.1) (Benson et al, 2010). For both PK and PK/PD modelling initially only the structural model parameters were derived using the model, following which it was investigated if introducing IIV in different parameters improved the model's ability to describe the observed data.

Equation 5.1

$$P_i = \theta * \exp(\eta_i)$$

Where θ is the typical value of the parameter, P_i is the individual prediction, and η_i is the random deviation of P_i from θ. The values of η_i were assumed to be log-normally distributed, with mean a mean of zero and a variance of ω^2.

The variance was converted to a coefficient of variation (CV) using equation 5.2

Equation 5.2

$$CV(\%) = \left(\sqrt{\exp(\omega^2) - 1}\right) * 100\%$$

The residual variability for all models was derived using the proportional error model (equation 5.3)

Equation 5.3

$$Y_{ij} = F_{ij} * (1 + \varepsilon_{ij})$$

Where Y_{ij} denotes the observation for the i^{th} individual at time t_j, F_{ij} denotes the corresponding predicted value based on the model and ε_{ij} denotes the residual random

error (Benson et al, 2010). The values of ε_{ij} are assumed to be normally distributed with a mean of zero and a variance of σ^2.

The objective function was determined for each model, and is defined as -2 times the log likelihood (Sherwin et al, 2012). The difference in the minimum value of the objective function (MVOF) for two nested models differing by 1 parameter can be considered statistically significant if it is greater than 3.84 points ($p < 0.05$) (Fisher and Shafer, 2007).

A covariance step was included which provides a covariance matrix, from which standard errors of the estimates of the model parameters are calculated. Goodness of fit plots were created using R Studio software (R version 2.13.1) and the Xpose4 package (Version 4.3.2).

For both PK and PK/PD models selection of the best model was based on

- Visual inspection of goodness of fit plots. The observed concentrations vs. individual or population predicted concentrations should be randomly distributed around the line of unity. The condition weighted residuals (CWRES) vs. time and/or population predictions should be evenly distributed around zero, without systematic bias, with most values within -2 to +2 SDs (Mould and Upton, 2013).
- Comparison of the minimum values of the objective function (MVOF). A model would be considered superior if a reduction in the MVOF is observed compared to the previous model i.e. 1 vs. 2 compartment model.
- Successful minimisation

5.2.3. Population Pharmacokinetic modelling of resiquimod blood concentration-time data

The blood concentration-time profiles for resiquimod were analysed using both 1 compartment and 2 compartment models described using the ADVAN1 TRANS2 (1 compartmental) and ADVAN3 TRANS4 (2 compartmental) sub-routines within the NONMEM (ICON Development solutions) library. A 1 compartment PK model is presented in Figure 5.2 and described by equation 5.4 and a schematic representation of a 2 compartment PK model is presented in Figure 5.3 and described by equation 5.5 and 5.6 respectively.

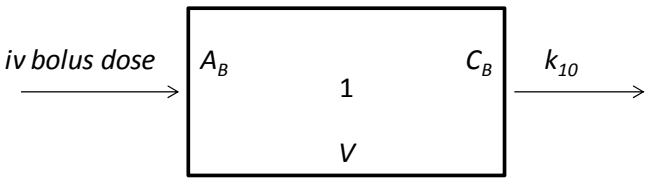

Figure 5.2 **Schematic representation of a 1 compartment pharmacokinetic model for resiquimod with iv bolus administration and first order elimination**

Equation 5.4

$$\frac{dA_B}{dt} = -k_{10} * A_B$$

$$A_B(0) = D$$

$$C_B = \frac{A_B}{V}$$

$$k_{10} = \frac{Cl}{V}$$

Where D is the iv bolus dose, A_B is the amount of resiquimod in the central or blood compartment (Compartment 1) (ng), $A_B(0)$ is the amount of resiquimod in the central or blood compartment at time 0 (ng), C_B is the concentration of resiquimod in the blood, V is the volume of the central compartment (Compartment 1) and k_{10} is the elimination rate from the body (h^{-1}).

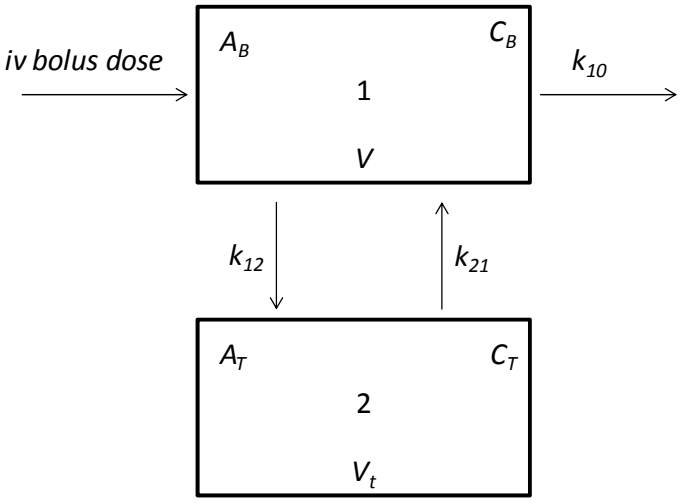

Figure 5.3 **Schematic representation of a 2 compartment pharmacokinetic model for resiquimod with iv bolus administration and first order elimination**

Equation 5.5

$$\frac{dA_B}{dt} = A_T * k_{21} - A_B * k_{10} - A_B * k_{12}$$

$$A_B(0) = D$$

$$C_B = \frac{A_B}{V}$$

$$k_{10} = \frac{Cl}{V}$$

$$k_{12} = \frac{Q}{V}$$

$$k_{21} = \frac{Q}{Vt}$$

Equation 5.6

$$\frac{dA_T}{dt} = A_B * k_{12} - A_T * k_{21}$$

$$A_T(0) = 0$$

Where D is the iv bolus dose, A_B is the amount of resiquimod in the central or blood compartment (Compartment 1) (ng), $A_B(0)$ is the amount of resiquimod in the central or blood compartment at time 0 (ng), A_T is the amount of resiquimod in the peripheral or tissue compartment (Compartment 2) (ng), $A_T(0)$ is the amount of resiquimod in the tissue compartment at time 0, k_{12} and k_{21} are the inter-compartmental rate constants which determine the rate of drug movement from the central to the peripheral compartment and back (h^{-1}), k_{10} is the elimination rate from the body (h^{-1}), Q represents the clearance from the second compartment, C_B is the concentration of resiquimod in the blood (ng/mL), V is the volume of the central compartment (mL) and V_T is the volume of the peripheral or tissue compartment (mL).

5.2.4. Population Pharmacokinetic/Pharmacodynamic modelling to describe the induction of serum IFNα concentrations following administration of a resiquimod challenge.

Modelling of the PK/PD relationship of the induction of IFNα serum concentration-time profiles following an iv bolus administration of resiquimod was conducted using the ADVAN 6 sub-routine within the NONMEM (Beal et al, ICON Development solutions) library. A schematic representation of the PK/PD model is presented in Figure 5.4 and described by equations 5.4, 5.7, 5.8 and 5.9. The PK parameters (CL and V) were fixed to the population values including IIV on CL determined from the previous PK modelling.

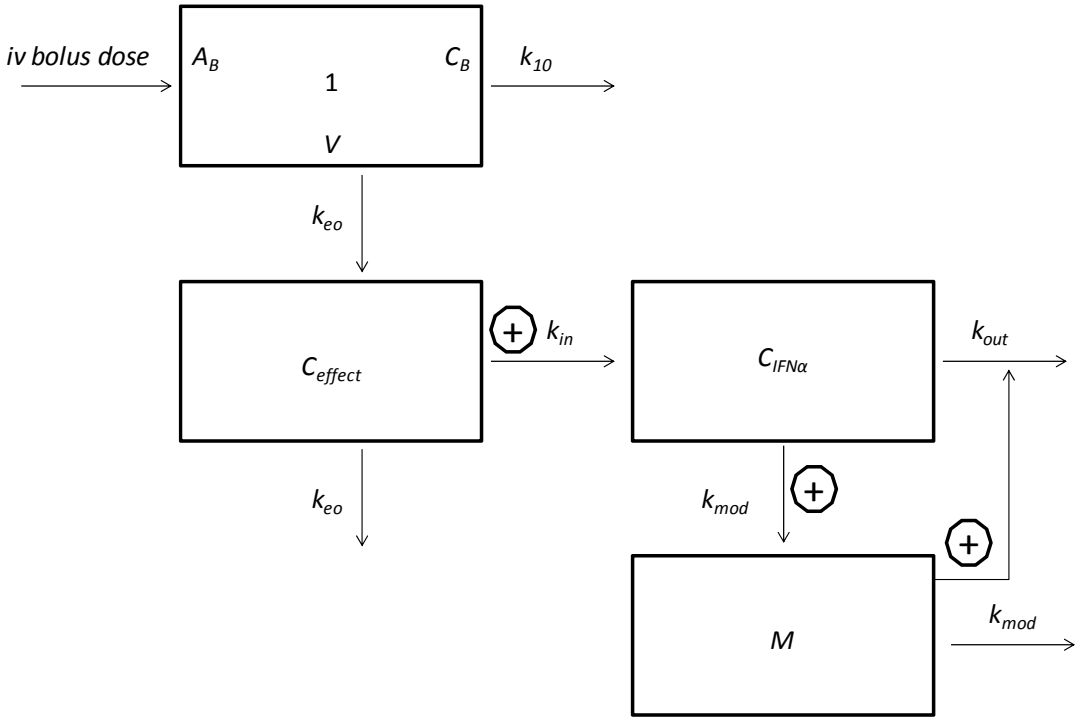

Figure 5.4 **Schematic representation of the PK/PD model to describe the resiquimod induction of serum IFNα concentrations. The model incorporates a pharmacokinetic model with iv bolus administration and first order elimination, an effect compartment, an indirect response model with stimulation of IFNα production and an endogenous modulator (M) function which positively regulates K_{out}.**

Equation 5.7

$$\frac{dC_{eff}}{dt} = (C_B - C_{eff}) * k_{eo}$$

$$C_B = \frac{A_B}{V}$$

Equation 5.7 describes the concentrations of resiquimod in the theoretical effect compartment; where A_B is the amount of resiquimod in the blood (ng/mL), C_B is the concentration of resiquimod in the blood (ng/mL), C_{eff} is the concentration of resiquimod in the effect compartment (ng/mL) and k_{eo} is the rate constant which determines the rate of drug movement into the effect compartment (h^{-1}).

Equation 5.8

$$\frac{dC_{IFN}}{dt} = k_{intot} - k_{out}\left(1 + \frac{M}{M_{50}}\right) * C_{IFN}$$

$$k_{intot} = k_{in0}\left(1 + \frac{E_{max} * C_{eff}^{\gamma}}{EC_{50}^{\gamma} + C_{eff}^{\gamma}}\right)$$

Equation 5.9

$$\frac{dM}{dt} = k_{mod} * C_{IFN} - k_{mod} * M$$

Equations 5.8 and 5.9 describe the induction of serum IFNα concentrations by resiquimod and also the formation of the endogenous modulator by serum IFNα and its subsequent inhibitory regulation on serum IFNα concentrations. An indirect response model with stimulation of input has been selected; the model assumes that a measured response to a drug may be produced by indirect mechanisms controlling the input or production (k_{in}) of the response. In this model k_{in} (ng/mL/h) represents the zero-order constant for production of the response, k_{out} (h^{-1}) defines the first-order rate constant for loss of the response, C_{IFN} is the response (IFNα serum concentration) (ng/mL), C_{eff} is concentration of drug in the effect compartment (resiquimod, ng/mL), EC_{50} is the drug concentration (ng/mL) which produces 50% of the maximum stimulation and E_{max} describes the maximum effect of the drug on k_{in}, γ is the sigmoidicity constant of the steady-state concentration-response relationship, M is the endogenous modulator which provides a positive feedback to k_{out}, M_{50} is the value of M that doubles k_{out}, and k_{mod} (h^{-1}) represents the first order constant for the turnover of M

which determines the onset and offset of modulator feedback. (Bundgaard et al, 2007). As the concentrations of IFNα were below the assay LLQ (200 pg/mL) in all predose samples the starting concentrations of IFNα ($C_{IFN}0$) prior to drug administration were set to 0.001 pg/mL. The baseline response of M (M_0) was also set to 0.001.

Prior to modelling of the data in NONMEM, simulations were conducted using the package deSolve in R to derive initial starting values for k_{in0}, k_{out}, E_{max}, EC_{50}, γ and k_{eo}. The parameters were selected as those that gave the best visual fit to the PK/PD relationship observed in mice dosed at 0.04 mg/kg and 0.09 mg/kg where no modulation of the response is observed.

A visual predictive check was conducted using the package deSolve in R incorporating the PK/PD model parameters and including inter-individual variability from the final PK/PD model. The resiquimod and IFNα concentration-time profiles were simulated for a 1000 individuals at resiquimod dose of 0.4 mg/kg and compared to the observed data.

5.2.5. Population Pharmacokinetic/Pharmacodynamic simulations to investigate the impact on the resiquimod induced serum IFNα concentrations by a hypothetical TLR7 inhibitor compound

Simulations were conducted using the package deSolve in R incorporating the PK/PD model parameters, including inter-individual variability, from the final PK/PD model. A schematic representation of a PK/PD model used for the simulations is presented in Figure 5.5 and is described by equations 5.4, 5.7 and 5.9 with the pharmacokinetics of the inhibitor defined by equations 5.10 and 5.11 and equation 5.8 replaced with equation 5.12 presented below.

Equation 5.10

$$\frac{dAI_B}{dt} = -inhibitor\ k_{10} * AI_B$$

$$AI_B(0) = DI$$

$$Ik_{10} = \frac{ICL}{VI}$$

Equation 5.11

$$\frac{dCI_{eff}}{dt} = \left(CI_B - CI_{eff}\right) * Ik_{eo}$$

$$CI_B = \frac{AI_B}{VI}$$

Equations 5.10 and 5.11 describe the concentrations of the inhibitor in the central (blood) compartment and the theoretical effect compartment; the terms are as described for equations 5.4 and 5.7 for resiquimod.

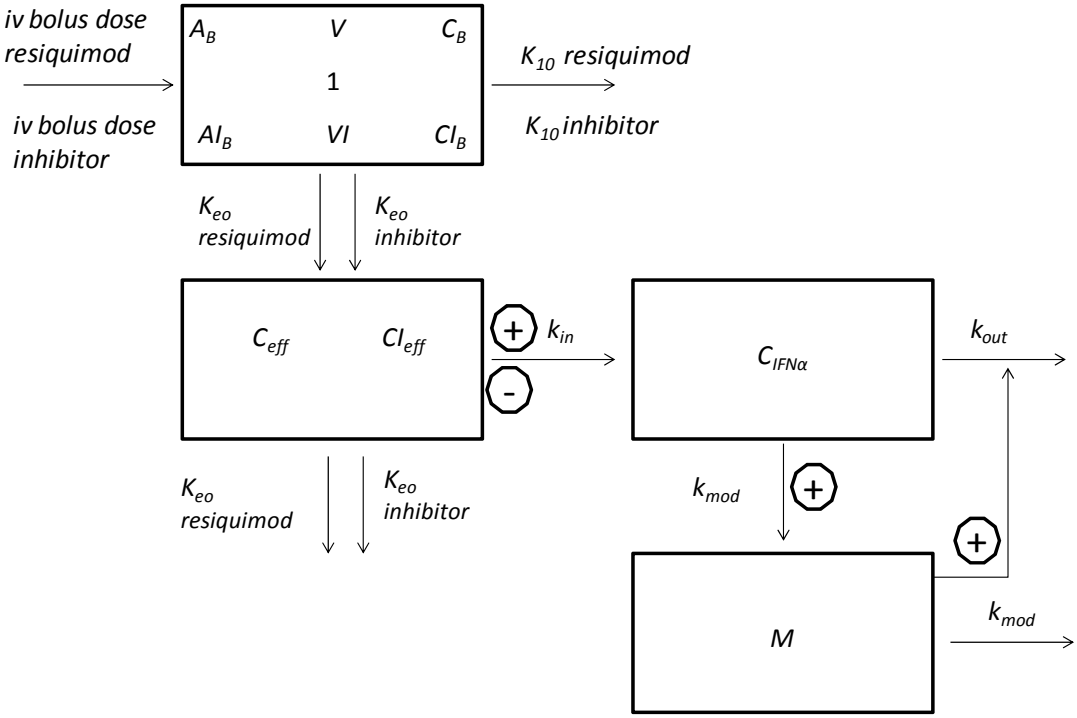

Figure 5.5 **Schematic representation of the PK/PD model to simulate the resiquimod induction of serum IFNα concentrations in the presence of a hypothetical TLR7 receptor inhibitor. The model incorporates a pharmacokinetic model with iv bolus administration and first order elimination for both resiquimod and the inhibitor compound, an effect compartment, an indirect response with model with both stimulation and inhibition of IFNα concentrations and an endogenous modulator (M) function which positively regulates K_{out}**

Equation 5.12

$$\frac{dC_{IFN}}{dt} = k_{intot} - k_{out}\left(1 + \frac{M}{M_{50}}\right) * C_{IFN}$$

$$k_{intot} = k_{in0}\left(1 + \frac{E_{max} * C_{eff}^{\gamma}}{EC_{50}^{\gamma} + C_{eff}^{\gamma}}\right) * \left(1 - \frac{I_{max} * CI_{eff}^{Hill}}{IC_{50}^{hill} + CI_{eff}^{Hill}}\right)$$

Equation 5.12 describes the induction of serum IFNα concentrations by resiquimod the inhibition of serum IFNα concentrations by the hypothetical inhibitor and also the induction of K_{out} by the endogenous modulator and its subsequent inhibitory regulation on serum IFNα concentrations. The model is as described previously (equation 5.8) with the addition of the following parameters; CI_{eff} is concentration of inhibitor in the effect compartment (ng/mL), IC_{50} is the inhibitor concentration (ng/mL) which produces 50% of the maximum stimulation and I_{max} describes the maximum effect of the inhibitor on k_{in}, *Hill* is the sigmoidicity constant of the steady-state concentration-response relationship.

For simulations, the final parameters determined from the PK/PD modelling of the entire data set were fixed to the estimated values including the predicted IIV for parameters, where determined, and a resiquimod dose of 0.4 mg/kg. The hypothetical inhibitor was assumed to be administered as an iv bolus, and have the same value for K_{eo} for the transfer of the compound to the effect compartment as resiquimod. The pharmacokinetics of the hypothetical inhibitor were set to target properties for drug discovery programme teams investigating small molecules of interest with a low CL_b of 1500 mL/h/kg (~20% LBF in the mouse) and a moderate V of 3000 mL/kg. Scaling these for a 40g mouse gives values of 60 mL/h and 120 mL for CL_b and V respectively. For the indirect response model the Hill slope was set to 1 for all simulations and the sensitivity of IC_{50}, dose and I_{max} on the observed IFNα response was investigated in the scenarios described below. For each simulation the profiles in 1000 individuals were simulated, and subsequently summarised in terms of median and & prediction interval.

1. Initially IC_{50} was set to a value of 0.03 µM, which is the typical value that drug discovery programme teams would target for a candidate compound, and gives an IC_{50} of 3.15 ng/mL assuming a MW of 350. The I_{max} was fixed at 1 in line with that observed for resiquimod, and with the fixed IC_{50} and I_{max} values a dose response of

inhibitor was investigated with doses over a range of 10 mg/kg, 3 mg/kg, 1 mg/kg, 0.3 mg/kg, 0.1 mg/kg 0.03 mg/kg and 0.01 mg/kg.

2. A predicted clinical dose of 100 mg is targeted by first intent at candidate selection, and assuming a 70 kg human this equates to a dose of 1.4 mg/kg. The dose was therefore set to 1.4 mg/kg (0.056 mg for a 40 g mouse) and once again the I_{max} was set to 1. The impact of IC_{50} was investigated by adjusting the value over a range of 0.05-100 ng/mL.
3. The dose was set to 1.4 mg/kg and the IC50 was set to 3.15 ng/mL. The impact of Imax was investigated by adjusting the value over a range of 0.001-1.

5.3. Results

5.3.1. Population Pharmacokinetic modelling of resiquimod blood concentration-time data

A summary of the models investigated to determine the population pharmacokinetic parameters for resiquimod in the mouse are presented in Table 5.2. The reference model relates to the model that subsequent models are compared.

Table 5.2 Population PK modelling summary

Model Number	Model Description	Reference model	MVOF	Difference in MVOF	COV step completed
1	1CMT	-	1386.326	-	Yes
2	1CMT with IIV on CL_B	1	1228.223	-158.103	Yes
3	1CMT with IIV on V	1	1337.691	-48.635	Yes
4	2CMT	1	1386.326	0	No
5	2CMT iiv on CL_b	4	1116.247	-270.079	No
6	2CMT iiv on V1	4	1333.576	-52.75	No

CMT = Compartment COV = Covariance

All the population PK models investigated gave a good visual description of the resiquimod blood concentration time profile. However, the one compartment model with IIV on CL was

deemed to best describe the resiquimod blood concentration-time profile. This model provided a difference in the MVOF of -158 compared to model 1. Although a 2 compartment model with IIV on CL (model 5) resulted in the smallest value of MVOF, a covariance step was not successfully completed for this model and so it was not deemed suitable. Additionally, visual inspection of the goodness of fit plots and individual fits showed that this model did not significantly improve the fit compared to model 2.

The observed concentrations vs. population (PRED) and individual predicted (IPRED) concentrations are presented in Figure 5.6 A and B. In both plots the data points appear randomly distributed around the line of unity at concentrations less than 500 ng/mL, although the model over predicts the concentrations between 500 and 1000 ng/mL. The CWRES plots vs. PRED and time (5.6 C and D) reveal that data are randomly distributed with no obvious patterns or bias and centred around zero. The majority of points fall with a value of +/- 2 SD.

The model PRED and IPRED concentration-time profiles and observed concentration-time profiles in individual animals are presented in Figure 5.7. For the majority of animals there is little difference between the population and individual concentration-time profiles, although the addition of IIV on CL did allow a better prediction of the lower concentrations which is noticeable for mouse 19, mouse 30 and mouse 31. The model gave poor predictions for mouse 11 and mouse 20 and the initial concentration (0.08 h) for mouse 8.

The final pharmacokinetic parameters derived using model 2 are presented in Table 5.3 where the IIV, residual error are presented as % and the precision of the parameter estimates are presented as Relative Standard Error (RSE). The pharmacokinetic parameters were well described with the highest CV observed for IIV on CL. The IIV on CL was 18% and the residual error was 40%.

Table 5.3 PK parameters of resiquimod in male CD1 mice following iv administration over a dose range of 0.04 to 4.8 mg/kg

Parameter	Estimate	RSE (%)
CL (mL/h)	123	11
V (mL)	70	13
IIV of CL (%)	18	53
Residual Error (%)	40	29

Key: CL = Clearance, V = Volume, IIV = Intra Individual Variability, RSE = Relative Standard Error

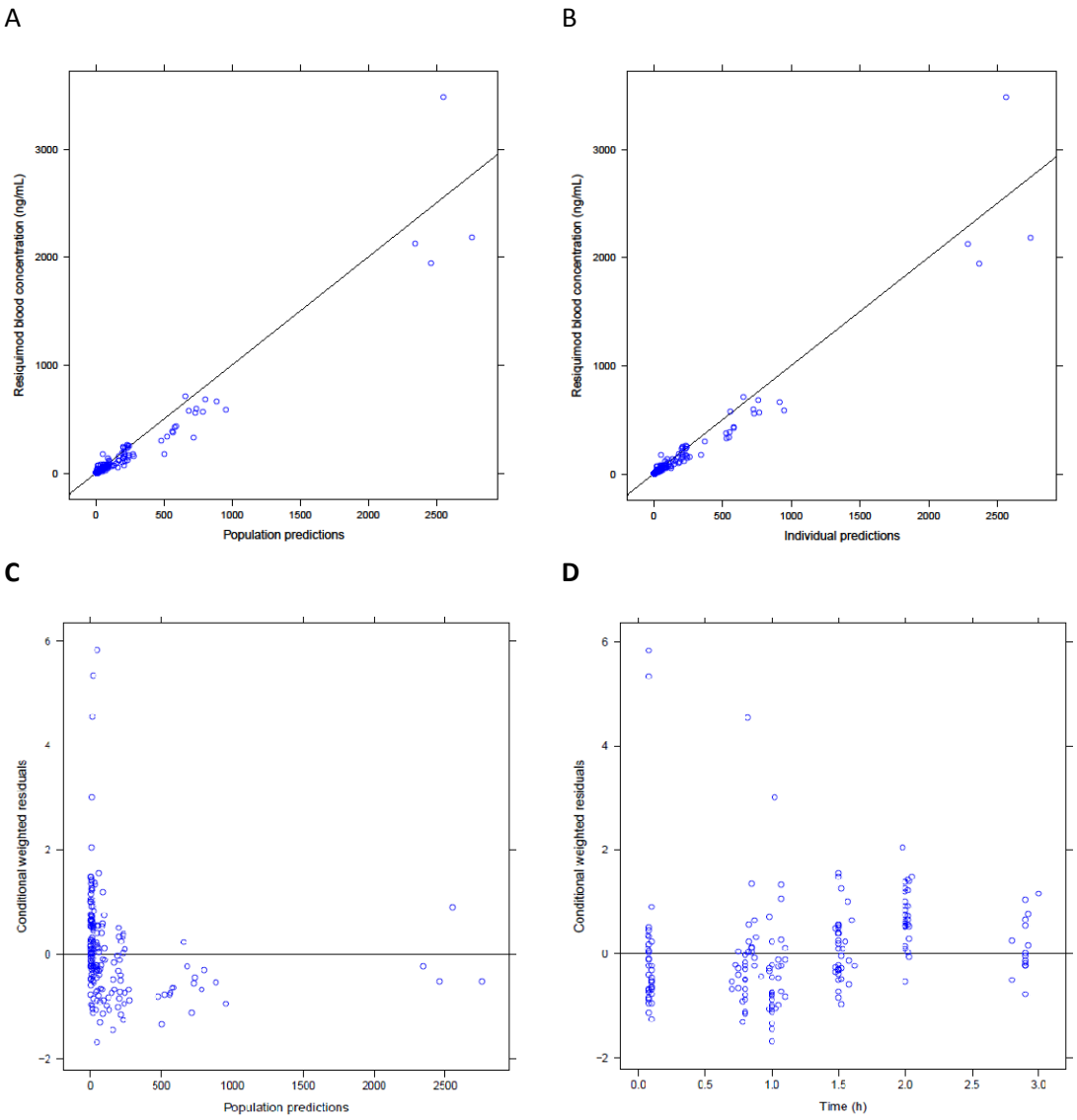

Figure 5.6 **Observed vs. population predicted concentrations (A), observed vs. individual predicted concentrations (B), conditional weighted residuals vs. population predicted concentrations (C) and conditional weighted residuals vs. time for (D)**

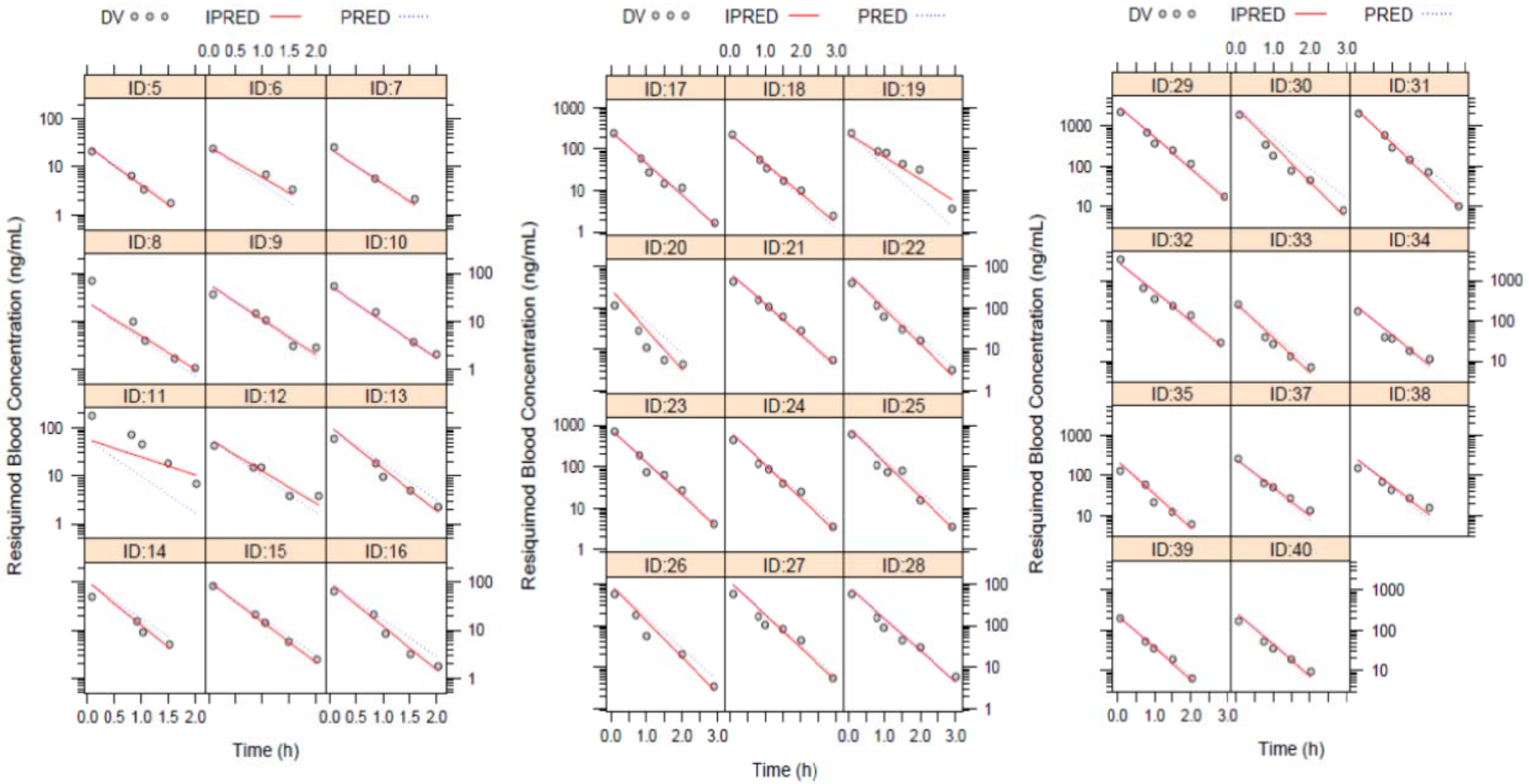

Figure 5.7 **Observed vs predicted blood concentrations time profiles for resiquimod at doses of 0.04 mg/kg (ID 5-8), 0.09 mg/kg (ID 9-12), 0.16 mg/kg (ID 13-16), 0.4 mg/kg (ID 17-20 and 33-40), 1.1 mg/kg (ID 21-24), 1.5 mg/kg (ID 25-28) and 4.8 mg/kg (ID 29-32). Black circles (DV) represent observed data, Red Line (IPRED) represents individual predictions and Blue dotted line (PRED) represents population predictions.**

5.3.2. Population Pharmacokinetic/Pharmacodynamic modelling to describe the induction of serum IFNα concentrations following administration of a resiquimod challenge.

A summary of the models investigated to determine the population PK/PD parameters of the resiquimod induction of serum IFNα concentrations in mice treated with resiquimod over a dose range of with 0.04 mg/kg to 4.8 mg/kg with a PKPD model incorporating a modulator function are presented in Table 5.4.

Minimisation was successful for the majority of models, however the covariance step only successfully completed once the values for K_{eo}, γ and M_{50} were fixed. The final model included IIV on K_{eo}, EC_{50} and E_{max} and the final model parameters are presented in Table 5.5. The model parameters were estimated with adequate precision except for IIV.

The value for K_{eo} was fixed to 0.32 h^{-1} and values of 7.5 for γ and 0.1 for M50 gave the best apparent reduction in MVOF and precision of the parameter estimates

Generally throughout the model optimisation the addition of parameters did not give a significant reduction in the MVOF once a threshold had been reached, therefore the focus was on the successful completion of a covariance step and precision of the parameter estimates.

Although high RSE values were observed for IIV in the final model, it was decided to keep IIV on K_{eo}, EC_{50} and E_{max} since that significantly improved the fit, and the imprecision of the parameter estimates is likely due to the rather large variability between animals (IIV in E_{max} is estimated to be greater than 100%), in combination with the limited amount of data available

Table 5.4 Population PK/PD modelling summary

Model Iteration	Data set used for modelling	Outcome
1	• Full data set • Model with modulator function	• Model failed to minimize on most occasions • Robust parameter estimates not defined • Covariance step did not complete • Inclusion of IIV did not improve model
2	• Mice dosed with 0.04 mg/kg and 0.09 mg/kg • Model without modulator function	• Model successfully minimized • IIV on K_{in} (41%) improved model • Estimate for γ very high 106 • Covariance step only completed for 1 model
3	• Mice dosed with 0.04 mg/kg and 0.09 mg/kg • Model without modulator function • γ not included	• Model successfully minimized in 70% of models • Robust parameter estimates not defined • Covariance step did not complete • Inclusion of IIV did not improve model
4	• Mice dosed with 0.04 mg/kg and 0.09 mg/kg • Model without modulator function • γ not included • Investigate different initial estimates for K_{in0}, K_{out} and E_{max}	• Model successfully minimized in only 33% of models • Robust parameter estimates not defined • Covariance step did not complete • Inclusion of IIV did not improve model
5	• Full data set • Model with modulator function • γ included	• Model successfully minimized in only 18% of models • Robust parameter estimates not defined • Covariance step did not complete • Inclusion of IIV did not improve model
6	• Full data set • Model with modulator function • Initial estimate for γ set 10 fold lower (7.9) • Different values of γ explored using likelihood method	• Model successfully minimized in 80% of models • Covariance step completed in 50% of models • Inclusion of IIV on K_{eo}, EC_{50} and E_{max} improved model • Value for γ of 7.5 gave best results
7	• Full data set • Model with modulator function • γ fixed to 7.5 derived from iteration 6 • k_{eo} fixed to 0.32h^{-1} derived from iteration 2 • Different values of M_{50} explored using likelihood method	• Model successfully minimized in 80% of models • Covariance step completed in 50% of models • Inclusion of IIV on K_{eo}, EC_{50} and E_{max} improved model • Value for M_{50} of 0.1 ng/mL gave results

Table 5.5 PK and PD parameters of resiquimod induced serum IFNα concentrations in male CD1 mice following iv administration of resiquimod over a dose range of 0.04 to 4.8 mg/kg

Parameter	Estimate	RSE (%)
CL (mL/h)	123	Fixed
V (mL)	70	Fixed
K_{eo} (h^{-1})	0.32	Fixed
K_{in0} (h^{-1})	1.03	8
γ	7.5	Fixed
K_{out} (h^{-1})	0.12	12
EC_{50} (ng/mL)	5.2	18
E_{max} (ng/mL)	2.2	24
M_{50} (ng/mL)	0.1	Fixed
K_{mod} (h^{-1})	0.12	14
IIV of CL (%)	18	Fixed
IIV of K_{eo} (%)	34	106
IIV of EC_{50} (%)	40	99
IIV of E_{max} (%)	127	47
Residual Error (%)	36	10

The goodness of fit plots are presented in Figure 5.9. Both the observed concentrations vs. PRED (5.9 A) and IPRED (5.9 B) appear randomly distributed around the line of unity. For the CWRES vs. PRED (5.9 C) the data are randomly distributed with no obvious patterns or bias and centred around zero. The CWRES vs. time (5.9 D) plots demonstrated bias with positive residuals at the time points associated with the greatest serum IFNα concentrations, and negative residuals at the remaining time points.

The model predicted population and individual concentration-time profiles and observed concentration-time profiles in individual animals are presented in Figure 5.10. The model broadly captured the bell shaped dose response curve, with increasing serum IFNα concentrations at doses up to 0.09 mg/kg and the inhibition of serum IFNα concentrations by the endogenous modulator at doses greater than 0.09 mg/kg. However, the general shape of the serum concentration-time profile for an individual animal or dose level was not described very well by the model. The model under predicted the rate of induction of serum IFNα, the maximum serum IFNα concentrations and the rate of elimination, resulting in a flatter predicted profile than the observed profile.

A

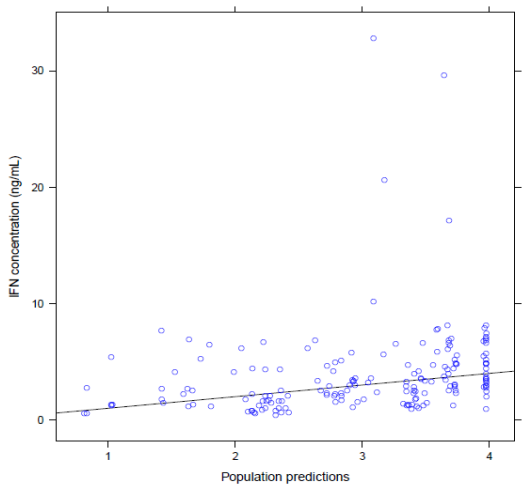

B

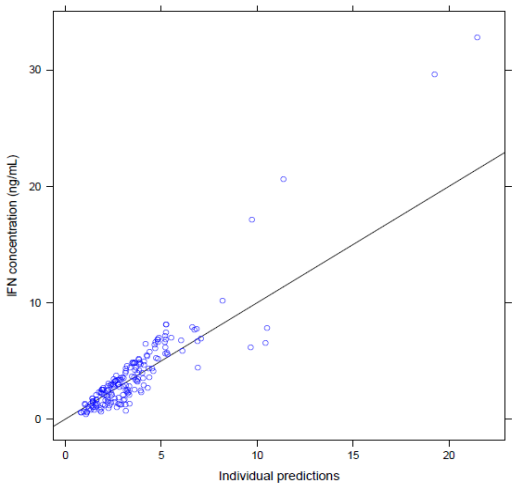

C

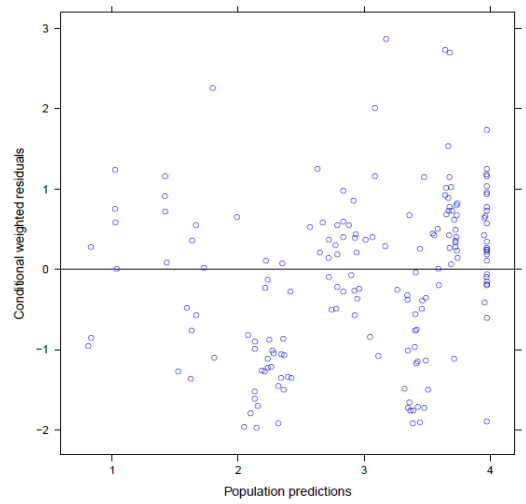

D

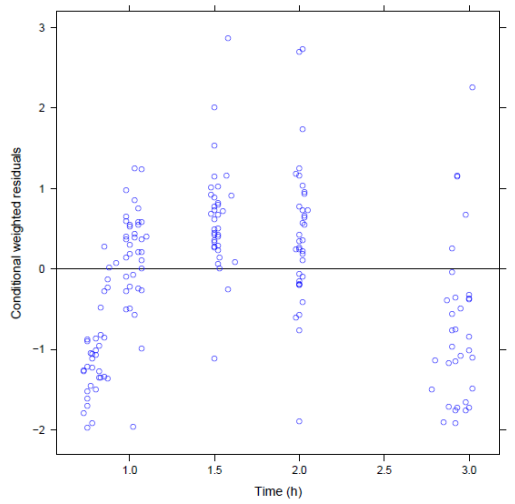

Figure 5.9 **Observed vs. population predicted concentrations (A), observed vs. individual predicted concentrations (B), conditional weighted residuals vs. population predicted concentrations (C) and conditional weighted residuals vs. time (D)**

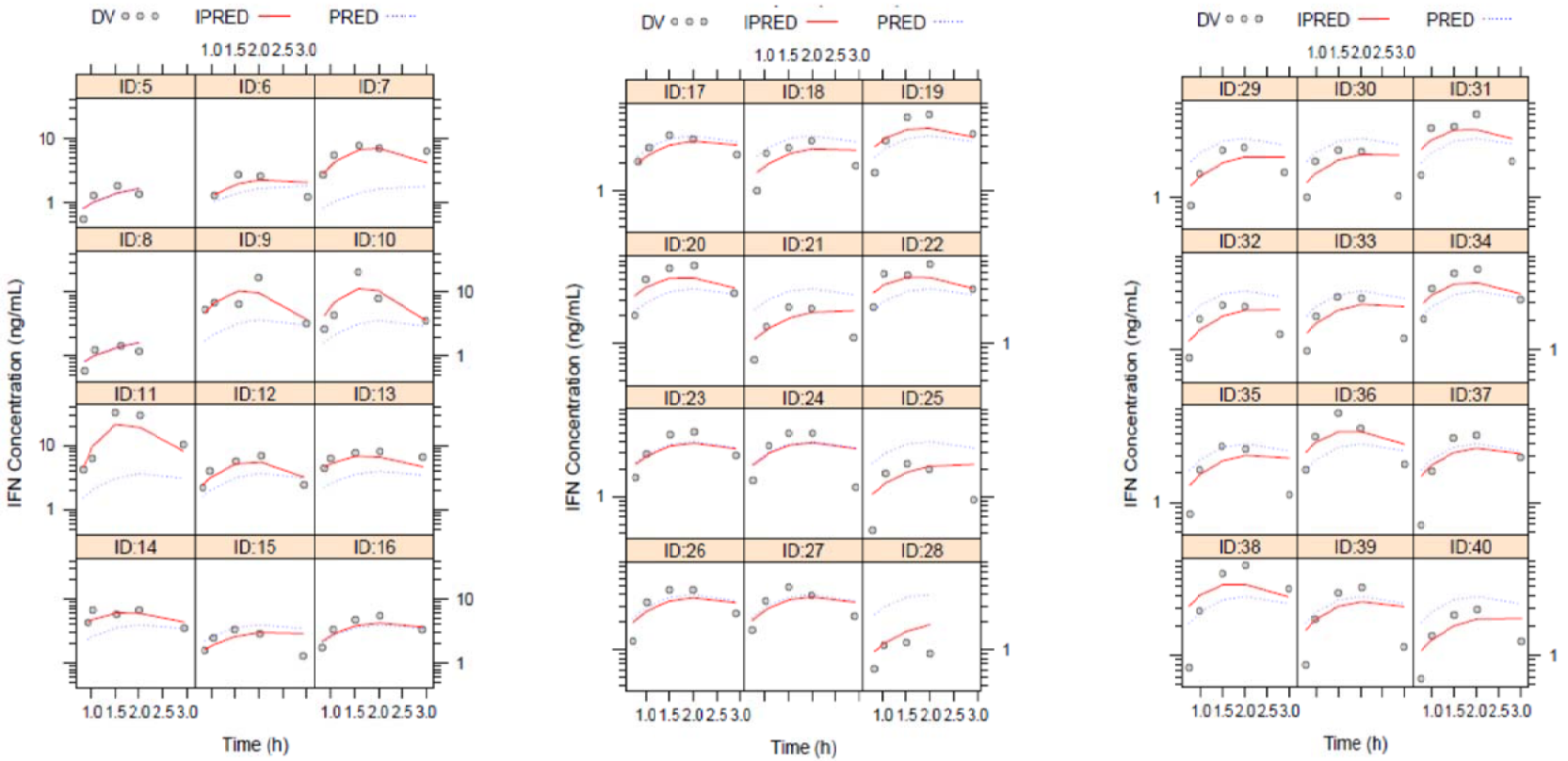

Figure 5.10 **Observed vs predicted serum concentrations time profiles for IFNα at doses 0.04 mg/kg (ID 5-8), 0.09 mg/kg (ID 9-12), 0.16 mg/kg (ID 13-16), 0.4 mg/kg (ID 17-20 and 33-40), 1.1 mg/kg (ID 21-24), 1.5 mg/kg (ID 25-28) and 4.8 mg/kg (ID 29-32). Black circles (DV) represent observed data, Red Line (IPRED) represents individual predictions and Blue dotted line (PRED) represents population predictions.**

The median and 95% prediction interval of the resiquimod and IFNα concentrations time profile obtained following 1000 simulations with the final PK/PD model at a resiquimod dose of 0.4 mg/kg are presented in Figure 5.11 A and B respectively and overlaid with the data at a resiquimod dose of 0.4 mg/kg to a 40 g mouse.

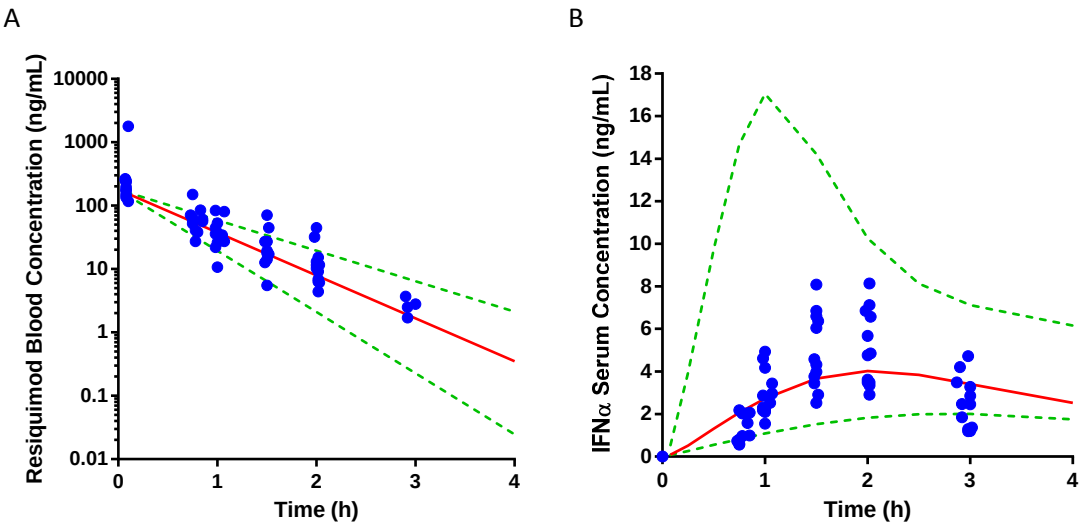

Figure 5.11 **Observed and simulated concentration vs. time profiles for resiquimod (A) and IFNα (B) following iv bolus administration of resiquimod at a dose of 0.4 mg/kg. Blue circles represent observed data, the red line represents the simulated population median, and the green dashed lines represent the 95% prediction interval.**

The simulated population median resiquimod concentration-time profile was consistent with the observed resiquimod concentration-time data (Figure 5.11 A), while the simulated population median IFNα concentration-time profile (Figure 5.11 B) is towards the lower range of the observed concentrations. For the resiquimod blood concentration data the prediction interval is close to the median and the majority of the observed data fall within the prediction interval. The majority of the concentrations at 0.08 h, the first time point, fall outside the prediction interval and at least two observations per time point fall outside the prediction interval. For the IFNα serum concentration data the prediction interval is much wider than that observed for resiquimod, although the interval does capture the majority of the data.

5.3.3. Population Pharmacokinetic/Pharmacodynamic simulations to investigate the impact on the resiquimod induced serum IFNα concentrations by a hypothetical TLR7 inhibitor compound.

The results of the simulations investigating the sensitivity of 1) the dose of the inhibitor, 2) the value for IC_{50} of the inhibitor and 3) the value for I_{max} for the inhibitor are presented in Figures 5.12, 5.13 and 5.14 respectively.

Simulation of the dose response of a hypothetical inhibitor (Figure 5.12) demonstrated that at a resiquimod dose of 0.4 mg/kg, increasing doses of inhibitor, or decreasing IC_{50} of the inhibitor, or increasing I_{max} of the inhibitor all reduced the IFNα induction by resiquimod. At the higher doses, the lower IC_{50} values and the higher I_{max} values the profile altered becoming flatter, IFNα T_{max} is later and there seems to be little to no elimination of IFNα.

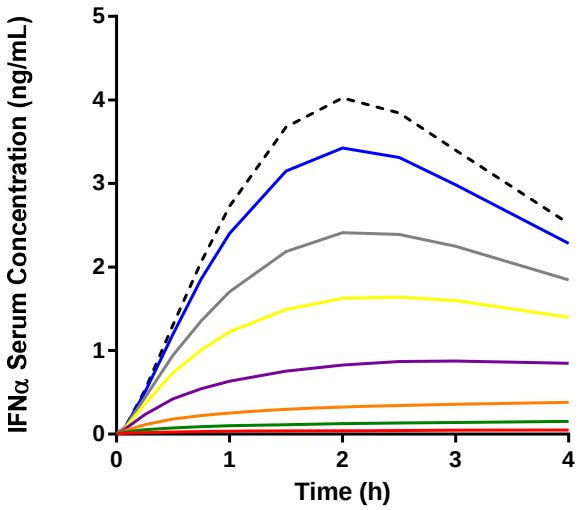

Figure 5.12 **Simulated resiquimod (0.4 mg/kg) induced serum concentration-time profiles for IFNα with co-administration of a hypothetical inhibitor at 10 mg/kg (red), 3 mg/kg (green), 1 mg/kg (orange), 0.3 mg/kg (purple), 0.1 mg/kg (yellow), 0.03 mg/kg (grey), 0.01 mg/kg (blue) no inhibitor (black dashed)**

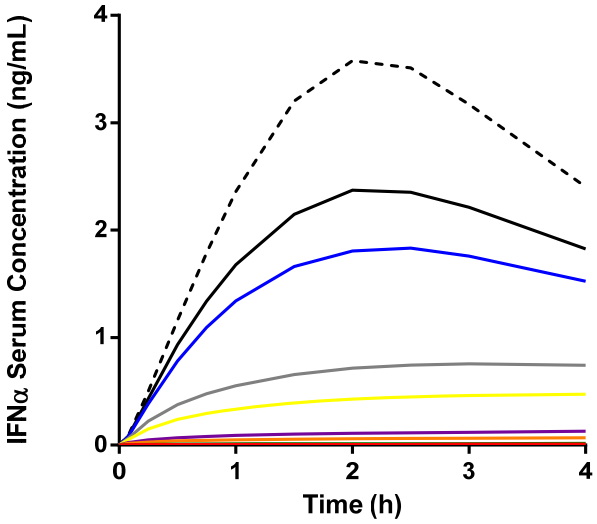

Figure 5.13 **Simulated resiquimod (0.4 mg/kg) induced serum concentration-time profiles for IFNα with co-administration of a hypothetical inhibitor at 1 mg/kg with the value for IC_{50} set at 0.05 ng/mL (red), 0.1 ng/mL (green), 0.5 ng/mL (orange), 1 ng/mL (purple), 5 ng/mL (yellow), 10 ng/mL (grey), 50 ng/mL (blue), 100 ng/mL (black) and no inhibitor (black dashed)**

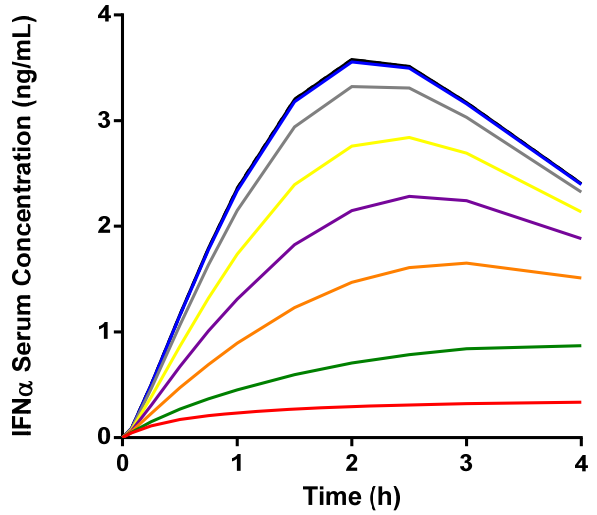

Figure 5.14 **Simulated resiquimod (0.4 mg/kg) induced serum concentration-time profiles for IFNα with co-administration of a hypothetical inhibitor at 1 mg/kg with the value for I_{max} set at 1 ng/mL (red), 0.9 ng/mL (green), 0.7 ng/mL (orange), 0.5 ng/mL (purple), 0.3 ng/mL (yellow), 0.1 ng/mL (grey), 0.01 ng/mL (blue), 0.001 ng/mL (black) and no inhibitor (black dashed)**

5.4. Discussion

Population PK/PD modelling to describe the resiquimod induction of serum IFNα concentrations in the male CD1 mouse was conducted in a sequential manner. Initially the pharmacokinetics of resiquimod were described using a population PK model, with a 1 compartmental iv bolus model with IIV on CL_b giving the best description of the observed resiquimod blood concentration time profile across the dose range. In general the model described the data well for the majority of the mice, and the structural model parameters were estimated with adequate precision. However, data from mouse 11 and the early concentrations in mouse 8 were poorly described. The blood concentrations in these mice were higher than observed in the other mice receiving the same dose and it might be justified to remove these animals or data points from the analysis as outliers. The final model parameters were considered suitable for the purpose of PK/PD modelling; however in the future it could be worth investigating the impact of removing these mice on the PK parameters which would give an indication as to the stability of the PK model. On review of the CWRES versus time plots derived from the final model, it could be argued that the profiles may be better characterised with a two-compartmental PK model. This model provided a large reduction in the MVOF value compared to the 1 compartment model, although visually it is subjective if the model give a better description of the observed vs. predicted concentration time profiles and a covariance step was not successfully completed, suggesting that the 2 compartmental model was over parameterised for the available data. It may have been possible to justify biphasic kinetics if concentrations had been measured over a longer time frame, however in this study due to the limit of the analytical assay it was not possible to determine the concentrations below 1 ng/mL. Furthermore since it is unlikely that concentrations below 1 ng/mL are pharmacologically relevant, for the purpose of PK/PD modelling the parameters derived using a 1 compartment model can be considered appropriate.

The addition of IIV to CL_b to the model resulted in a statistically significant improvement in the description of the observed-concentration time profile. IIV on V also improved the fit compared to the model with no IIV but to a lesser degree than IIV on CL_b did. The IIV determined on CL_b was low at 18%, which is unsurprising since the same strain, sex and approximately the same weight of mice, which were all sourced from the same supplier, were used across the studies.

The population PK parameter estimates derived from the modelling of the resiquimod blood concentration time profiles were fixed to enable sequential population PKPD analysis of the serum IFNα concentration time profiles. The PK/PD analysis was conducted using an indirect response model with stimulation of input, incorporating an effect compartment, and an inhibitory modulator function. Incorporating both a link model and indirect response model is feasible as other authors have concluded that both the link model processes and indirect response model processes can be concurrent *in vivo*, although they acknowledge that few data sets have enough information to support combined models (Upton and Mould, 2014).

Population PK/PD modelling of the serum IFNα concentration-time profile over a dose range of 0.04 mg/kg to 4.8 mg/kg using a model incorporating an endogenous inhibitory modulator function successfully described the dose response profile of resiquimod in mice including the reduction in the serum IFNα concentrations observed with doses greater than 0.09 mg/kg. Where estimated, the parameters were determined with adequate precision with the highest RSE (%) observed for the IIV on K_{eo}. Studies in house have demonstrated that measurable concentrations of IFNα do not occur until approximately 0.75 h post resiquimod challenge, and it became apparent that a simple indirect response model could not describe the observed time lag in production of IFNα. A hypothetical effect compartment was therefore included in the model on the premise that resiquimod distributes from the blood into the effect compartment which are the pDCs residing in both the blood and/or tissues such as the skin. The value for K_{eo} determines the rate at which equilibrium with the hypothetical effect compartment is reached. The K_{eo} estimate of 0.32 h^{-1} was relatively small suggesting that the distribution half-life to this effect compartment is about 2 h. This would fit with the observation that IFNα concentrations are not observed until approximately 0.75 h after the resiquimod C_{max}. It was necessary to fix the value of K_{eo} to 0.32 h^{-1} in the final model to enable to successful minimisation and complete the CV step, although IIV on this parameter was included in the final model. The IIV for K_{eo} was 35% indicating a degree of variability between animals, however the RSE% for IIV was >100% suggesting poor precision in the parameter estimate. If increased number of samples could be obtained between dosing and the 0.75 h time point, this may better capture the appearance of measurable concentrations of IFNα across the individual mice and allow a more robust estimation of K_{eo} and the associated IIV.

The model appeared to be very sensitive to the value of γ as it was only possible estimate model parameters when γ was fixed at 7.5. This value was determined from likelihood profiling and gave the best overall precision of the parameter estimates and so was selected as the final model. This is still quite a large value for a Hill co-efficient and suggests that the dose response relationship for the resiquimod induction of serum IFNα is very steep. This can be observed with the response observed at 0.04 mg/kg and 0.09 mg/kg as a small increase in blood concentrations (approximately 2 fold increase in resiquimod C_{max}) with increasing dose delivered a large increase in the serum IFNα concentrations. The parameters EC_{50}, K_{in} and γ were correlated with one another. If these parameters were optimised by the model and if IIV was included on these parameters the minimization often terminated and the covariance step would not complete. Fixing γ allowed the estimation of EC_{50} and K_{in},however IIV could still not be estimated for K_{in} and the estimation of the IIV for EC_{50} had a RSE >100% suggesting poor precision. Correlation amongst the parameters may mean that not all the parameters can be optimised simultaneously and may suggest uncertainty in the parameter estimates (Liefaard et al, 2005). The sensitivity of the model parameters and the model performance may suggest that the model may have found a local minimum rather than the global minimum. Local minima can arise for certain combinations of models and data when there are two sets of parameters that although different can provide similar fits to the data (Mould and Upton, 2012). Ordinarily this can be overcome by changing the initial input parameters by an order of magnitude however in this case changing individual parameters by up to 100 fold did not improve model performance.

The final model predicted a much longer terminal elimination phase of IFNα than observed. A value of 0.12 h^{-1} was determined for K_{out} giving a predicted half-life of IFNα of 5.6 h. In studies investigating an alternative TLR7 agonist a value of K_{out} of 0.96 h^{-1} was determined (Benson et al, 2010) and a value of 0.83 h^{-1} has also been reported in the literature. These values for K_{out} give a value for the terminal half-life of IFNα in mice of 0.7-0.83 h which is considerably shorter than that observed in this study. One of the reasons that the model may have struggled to give a good description of the terminal phase is the lack of data points in this phase. For many mice there was only the last measurable concentration at 3 h post dose following the IFNα C_{max} to define this phase of the profile and at best there was one additional data point between the C_{max} and the last measurable concentration. To derive more robust parameter estimates, this phase of the profile may require a greater

number of samples to be taken potentially using an optimal sampling design and/or composite study design.

The estimate of EC_{50} determined from the final model was 4.3 ng/mL or 0.012 µM using the MW of resiquimod (350.84). The efficacy of resiquimod has been determined in house in a number of *in vitro* human assays (The human biological samples were sourced ethically and their research use was in accord with the terms of the informed consents) with reported EC_{50} values of 292 to 694 ng/mL (0.83 to 1.79 µM). This suggests that resiquimod is almost 40 fold more potent *in vivo* than *in vitro* and/or 40 fold more potent at inducing IFNα in the mouse than in human. The EC_{50} reported for the TLR7 agonist BHMA was 135 ng/mL (Benson et al, 2010). This value in more in line with the value determined for resiquimod in the *in vitro* human assays compared to the value determined *in vivo* in the mouse in this study. On the face of it resiquimod appears to be a more potent inducer of IFNα than BHMA *in vivo,* however, the comparison between the two EC_{50} values should be interpreted with caution due to a number of differences between the studies. These include a different strain of mice, a different route of administration and a different PK/PD model. Also even though the EC_{50} was estimated with adequate precession, the estimate may not be believable as discussed later.

Inclusion of the endogenous modulator function enabled prediction of the reduced IFNα concentrations observed at doses >0.09 mg/kg. This is the first time an attempt has been made to describe the full dose response, including both the increase in response with dose and subsequent decrease in response after the dose reaches a threshold, for a TLR7 agonist using a PK/PD model. To enable the model to successfully converge and meet the required acceptance criteria it was necessary to fix the value for M_{50} to 0.1 ng/mL selected by likelihood profiling. The predicted value for k_{mod} was small at 0.11 h^{-1} and was estimated with a good degree of precision. As this represents the first order constant for the turnover of M and subsequently determines the onset and offset of modulator feedback, it suggests that modulator function is turned on and off slowly. As such the initial rate of induction of IFNα between mice may be comparable regardless of the dose of resiquimod administered before the modulator function has an inhibitor effect on the IFNα concentrations.

When reviewing the validation of population PK and PK/PD models, Sherwin et al (2012) summarised that as models can be used in the clinic to guide the optimal dosing strategy,

determine the first dose in humans, guide the optimal dosing strategy and may be used for dose scaling into special populations such as paediatrics, the model that is developed needs to be considered not only appropriate but also believable in terms of estimates. There are arguably some questions around the final model, on one hand the model does not appear to give a good prediction of the shape of the IFNα concentration-time profile but on the other hand does predict the dose response relationship with the apparent inhibition of the IFNα response once the dose exceeds a certain threshold. The model appears to be sensitive to the starting value for baseline which was set to 20 fold lower than the IFNα assay LLQ. The response at baseline, or R_0 can be determined by K_{in0}/K_{out} which, using the final model parameters gives a value of baseline of 8.5 ng/mL, which is approximately the maximum response observed in the majority of mice. This gives the first indication that the final model estimates are not believable. Sharma and Jusko, (1998) present that the baseline response and maximum response can be used to predict S_{max} which together with γ can subsequently be used to predict K_{in0} which in turn can be used to predict K_{out}. Using these equations the predicted S_{max} is almost 1000 fold higher than the value for S_{max} estimated from the final model, the value for K_{in0}, using the model estimated value for γ, is 250 fold lower than estimated from the final model and K_{out} is 4 fold higher than that predicted from the final model and more in line with that observed by Benson et al, (2010). Collectively this suggests that the estimated parameters should be interpreted with caution, and as S_{max} (or E_{max}) is derived from the experimental data this may be the most appropriate parameter to start with. The individual ETA estimates vs. dose plots for K_{eo}, EC_{50} and E_{max} demonstrated that while the ETAs for K_{eo} and EC_{50} are centred around zero for all groups the ETAs for E_{max} presented in Figure 5.15, show a bias. This demonstrates that the model is accounting for the reduction in the observed response at higher doses of resiquimod with IIV on E_{max} rather than using the modulator function. This suggests that the model is not working in the correct manner and the parameter estimates from the final model should therefore be interpreted with caution.

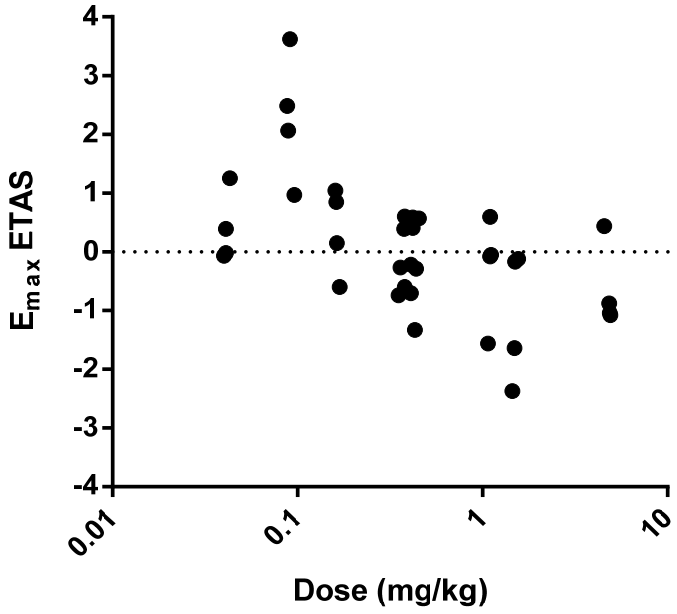

Figure 5.15 E_{max} ETAs vs. resiquimod dose in indivdiual mice derived using the final PK/PD model to describe the induction of serum IFNα concentrations by the TLR7 agonist resiquimod

The statement that "all models are wrong but some are useful" is quite important in this situation as one could question the utility of this model and the value it may have in our understanding of the application of this model. One of the key questions following to observation that increasing doses of resiquimod inhibit the IFNα response was whether the co-administration of a TLR7 receptor inhibitor with a higher dose of resiquimod would actually deliver a comparable response to that observed with a lower dose of resiquimod and result in propagation rather than inhibition of IFNα concentrations. In an effort to investigate this, simulations were conducted to investigate the impact of a hypothetical TLR7 inhibitor acting on K_{in} on the predicted IFNα concentrations. A sensitivity analysis was conducted to investigate the impact that the dose, and values of IC_{50} and I_{max} for the inhibitor had on the predicted IFNα concentrations. The simulations indicated that with a dose of resiquimod of 0.4 mg/kg the hypothetical TLR7 receptor inhibitor generally inhibited the predicted IFNα concentrations and did not deliver propagation of the response. Given what has been discussed above that the model is not actually using the modulator function to account for the reduction in the observed response it is unsurprising that the TLR7 agonist is predicted to deliver an inhibition of the response. The results of the

simulation should be interpreted with extreme caution until the concept can either be tested *in vivo* or a more robust PK/PD model is delivered. One point to consider if this model was to be used to deign future experiments is that the IFNα concentrations predicted for doses ≥ 1 mg/kg and IC_{50} values ≤ 5 ng/mL were all below the assay LLQ (200 pg/mL) used to measure the observed IFNα concentrations in this study. As the parameters for the inhibitor were selected based on desired target parameters in drug discovery for new small molecule inhibitors, it may highlight a limitation in the utility of the *in vivo* model moving forward i.e. will it simply be a model to demonstrate that a test inhibitor inhibits the IFNα concentrations to below the assay LLQ.

Reviewing the model output suggests that the data set may be limiting the performance of the model to derive reliable parameters to describe the PK/PD relationship of resiquimod induction of serum IFNα concentrations. There may be insufficient data on the terminal phase to confidently estimate the elimination phase of the profile and this is likely applicable to the other areas of the concentration-time profile such as the induction of IFNα and the C_{max} of IFNα, particularly with the large degree of inter-animal variability observed in the response with comparable resiquimod exposure. The visual predictive check demonstrated that the predicted IIV for IFNα is too large as the simulations predicted significantly higher IFNα concentrations than the observed data.

Expanding the data set by increasing the data points within the concentration-time curve may allow better estimation of the parameters; this could be achieved using a composite study design enabling sampling an increased number of times across the study duration. In addition, a better characterisation of the response at lower doses, where the IFNα concentrations increase with dose, and particularly around the dose delivering the maximum IFNα concentration (~0.09 mg/kg), may help to improve the model performance.

This study began with a simple indirect response model which was then tailored based on an understanding of the pharmacology to describe the target response. This highlights that the indirect response models can be viewed as starting points for PK/PD modelling, but the user should not be constrained to the simple model. In fact in many scenarios it can be expected that models will evolve depending on the pharmacodynamic response, and a similar view has been put forward by other researchers investigating the indirect response model to evaluate pharmacodynamic data (Krzyzanski and Jusko, 2001). It is acknowledged that the simulations incorporating a hypothetical inhibitor are simplistic and essentially

ignore receptor binding with the assumption that the inhibitor binds to the same receptor as resiquimod at the same affinity. The model may in the future be adjusted to account for competitive, non-competitive, reverse and partial antagonism if this information around a compound of interest is available. It may offer an interesting expansion of the modelling work conducted in this project where the action of the inhibitor on the resiquimod induction of serum IFNα concentrations are affected whether the inhibitor is a competitive or non competitive antagonist. When two drugs are administered at the same time that affect the same PD mechanism or pathway the concentration-effect relationship is a three dimensional surface, and defining the shape of this surface is reportedly a complex task (Upton and Mould, 2014). However, modelling and understanding this surface can quantify additive or synergistic effects (Upton and Mould, 2014) and equally in the case of resiquimod both inhibitor and stimulatory effects.

5.5. Conclusion

A population PK/PD model that can be used to simulate the resiquimod concentrations and corresponding IFNα concentrations was investigated. The incorporation of an endogenous modulator was attempted to enable the model to describe the bell shaped dose response curve observed for resiquimod and other TLR7 agonists, however it appears that in the final model IIV on E_{max} is the parameter that is delivering the predicted reduction in response at higher doses of resiquimod. Despite 15 years of interest in the development of TLR7 agonist compounds, this is the first time that a PK/PD model has been used to describe the dose response curve. This is far from a finished model, however, the PK/PD modelling investigations have highlighted the gaps in the data set and improved the understanding of the model that may require further investigation to deliver a robust population PK/PD model.

Chapter 6: Investigation of a in vivo PK/PD primate model using IFNα2b as a challenge agent

6.1. Introduction

As discussed in Chapter 2 translatable PK/PD models describing the IFNβ1a and IFNα2a induction neopterin concentrations in monkeys and humans have been demonstrated (Mager and Jusko, 2002, Mager et al, 2003, Kagan et al, 2011). A preclinical PK/PD model of IFNα2b challenge is not currently available therefore the objective of this chapter is to develop and validate a preclinical PK/PD model in the primate.

A phase I proof of mechanism (POM) study investigating a molecule inhibitor of Janus-Activated Kinase 1 (JAK1) in healthy volunteers was designed to provide early clinical pharmacodynamic data following an interferon-α (IFNα) challenge (Kahl et al, 2016). Subjects received the inhibitor as an oral capsule at various doses for 13 days, and on day 11 subjects were administered with an IFNα2b challenge as a single subcutaneous dose. The objective was to investigate the ability of the molecule to inhibit JAK1 mediated induction of neopterin and β2-microglobulin plasma concentrations and mRNA expression of IFNα and JAK pathway genes following IFNα challenge. The selected dose of the JAK 1 inhibitor inhibited neopterin and β2-microglobulin release and in general the expression of target genes was reduced by 10 days treatment with the molecule. It is anticipated that the PK/PD model for IFNβ1a can describe the PK/PD relationship observed following subcutaneous administration of recombinant IFNα2b. Therefore to enable the investigation of the translatability of the PK/PD relationship from monkey to human, PK and PD data following administration of an IFNα2b challenge in the cynomolgus monkey is required.

This chapter will describe the non compartmental pharmacokinetic analysis of IFNα2b serum concentration data to determine the pharmacokinetic parameters of IFNα2b in the primate following subcutaneous administration of recombinant human IFNα2b at two different doses. In addition the IFNα2b induction of a range of clinically relevant biomarkers including body temperature, cytokines/chemokines and neopterin as well as the noncompartmental analysis of the pharmacodynamic data, where applicable, will be described. Finally, the pharmacokinetic and pharmacodynamic relationship between IFNα2b and selected biomarkers will be investigated.

6.2. Methods

The in life and analytical protocols are presented in Chapter 3

6.2.1. NCA analysis

To enable pharmacokinetic analysis the dose of IFNα2b was converted from IU/kg to pg/kg using a specific activity for INTRON A of 2.6x 10^8 IU/mg of protein reported in the product information.

Pharmacokinetic (PK) analysis of the IFNα2b serum concentration data was performed to determine the maximum serum concentration (C_{max}), the area under the serum concentration-time curve (AUC), the terminal half-life ($t_{1/2}$), the apparent serum clearance (CL/F) and the apparent volume of distribution (V_z/F) where F is bioavailability. The pharmacokinetic parameters were determined using non-compartmental analysis (NCA) in the WinNonlin Phoenix software (Pharsight, version 6.2).

For NCA of the serum-concentration time profile for all cytokines, including IFNα2b determined following subcutaneous administration of IFNα2b, a blood/plasma extra vascular model (Model 200) was selected within WinNonlin. The data inputs for this model included the dose (only used for IFNα2b NCA), time for each sample and serum concentrations for each cytokine in each monkey at each dose. For IFNα2b at least the last three quantifiable blood samples were included in the estimation of the rate constant associated with the terminal elimination phase, which enabled PK parameters to be extrapolated to infinity. This rate constant was not estimated for other cytokines induced by IFNα2b.

The elimination rate constant was estimated by performing a regression of the natural logarithm of the concentration values in the selected range against sampling time. The AUC from the time of dosing to the last measurable blood concentration (AUC_{last}) was defined using the linear trapezoidal rule with uniform weighting, as follows:

$$AUC_{t_1}^{t_2} = \delta t * \frac{C_1 + C_2}{2}$$

where δt is (t_2- t_1), t_1 and t_2 represent the first and last times of the time interval, C is the concentration.

The AUC_{last} was extrapolated to give an AUC to infinity (AUC_∞) as follows:

$$AUC_{\infty} = AUC_{last} + \frac{C_{last}}{\lambda_z}$$

Where C_{last} is the last measurable blood concentration and λz is the elimination rate constant.

For the pharmacokinetic analysis, concentrations reported as below the assay LLQ will be set to zero up to, and including the time point before the first quantifiable concentration. If a sample at a particular time-point was below the assay LLQ for that particular cytokine but measurable concentrations were determined in the samples following that sample results for samples below the assay LLQ were set to half the LLQ. When three consecutive concentrations were reported as below the assay LLQ, the pharmacokinetic profile was considered to have ended and any measurable concentrations in later time-points were not included in the pharmacokinetic analysis. If IFNα2b concentrations were above the assay HLQ samples were diluted and re-analysed.

6.3. Results

6.3.1. Dose of IFNα2b administered to monkeys

The actual doses of IFNα2b administered to each mouse are presented in Table 6.1.

6.3.2. Cytokine analysis

Samples and cytokines that were below LLQ despite being preceded and followed by measurable values and were therefore set to half LLQ to enable PK analysis are presented in Appendix 2.1. Samples that were diluted and reanalysed and subsequently included in the pharmacokinetic analysis are presented in Appendix 2.2. Samples from monkeys 1 and 2 (10 MIU/kg) that were above the HLQ were not re-analysed and the data from these monkeys were not been included in the pharmacokinetic analysis. For MCP1 the following samples were above the HLQ but were not diluted and reanalysed and so an extrapolated value has been used to enable the plotting of a complete profile although these values would be excluded for any subsequent PK/PD analysis; 3 MIU/kg Monkey 1 (4 h), Monkey 3 (4, 6 h), Monkey 4 (6 h), Monkey 5 (4, 6, 8, 10 h), Monkey 6 (4, 6 h) and Monkey 7 (6, 8, 10 h); 10 MIU/kg Monkey 3 (2, 4, 6, 8 h), Monkey 4 (4, 6, 8 h), Monkey 5 (2, 4, 6, 8, 10 h), Monkey 8 (4, 6, 8, 10 h) and Monkey 9 (4, 6, 8 h).

Table 6.1 Individual monkey body weights and actual doses of IFNα2b administered to each monkey

Monkey Number	Monkey ID	Dose (MIU/kg)	Monkey Weight (kg)	Amount of IFNα administered (IU/kg)	Amount of IFNα administered (pg/kg)
1	129-184	3 MIU/kg	7.8	3000000	11538462
		10MIU/kg	6.8	10000000	38461538
2	129-208	3 MIU/kg	6.0	3000000	11538462
		10MIU/kg	6.6	10000000	38461538
3	M05814	3 MIU/kg	9.3	3000000	11538462
		10MIU/kg	9.3	10000000	38461538
4	129-204	3 MIU/kg	9.0	3000000	11538462
		10MIU/kg	9.2	10000000	38461538
5	70-207	3 MIU/kg	6.3	2380952	9157509
		10MIU/kg	6.2	10000000	38461538
6	M05212	3 MIU/kg	8.5	3000000	11538462
		10 MIU/kg		Monkey not dosed	
7	129-116	3 MIU/kg	9.1	3021978	11622992
		10MIU/kg	8.4	10000000	38461538
8	129-81	3 MIU/kg	7.0	3000000	11538462
		10MIU/kg	6.9	10000000	38461538
9	M05848	3 MIU/kg	9.0	3000000	11538462
		10MIU/kg	9.0	10000000	38461538

6.3.3. IFNα2b Pharmacokinetics

Following IFNα2b treatment at 3 MIU/kg and 10 MIU/kg, serum concentrations of IFNα2b were observed in all monkeys. Serum concentrations of IFNα2b in all monkeys following vehicle treatment were below the assay LLQ.

The individual serum concentration time profiles of IFNα2b are presented in Figure 6.1 A and B following IFNα2b administration at 3 MIU/kg and 10 MIU/kg respectively. The maximum IFNα2b serum concentration (C_{max}) was observed at a comparable time (T_{max}) between monkeys receiving the same dose and between doses, which was relatively early (2-8 h) in the sampling region. Following the C_{max} the serum concentrations declined with the last quantifiable concentration observed between 27 and 48 h post dose for the majority of monkeys across both doses. In general the serum concentration time profile followed a mono-exponential decline, however, the profile for monkey 3 appeared to follow a bi-exponential decline with an extended terminal phase and measurable serum

concentrations out to 96 and 120 h following 3 MIU/kg and 10 MIU/kg respectively. Following 3 MIU/kg, the terminal phase of the profile observed for Monkey 2 is very different from that observed in other monkeys. Initially, there is a decline in the serum concentrations following the C_{max} with concentrations below the assay LLQ at 48 h post dose. However, measurable concentrations were then observed at 72 and 96 h post dose before dropping again to below the assay LLQ at 120 h after which measurable concentrations were then determined at 168 and 240 h post dose.

The pharmacokinetic parameters determined for IFNα2b are presented in Table 5.2. The mean CL/F estimates were almost identical following administration of 3 MIU/kg and 10 MIU/kg. The CL/F determined in the monkeys dosed at 3 MIU/kg was more variable with a 4 fold range compared to that observed in monkeys dosed at 10 MIU/kg where a 1.7 fold range was observed.

The $t_{1/2}$ and V/F estimates were similar between monkeys both within and across dose groups although the variability was higher for these two parameters compared to CL/F. Following administration of 3 MIU/kg, $t_{1/2}$ and V/F for monkey 2 were approximately 6-37 fold higher than the values observed for the other monkeys. Higher values for both parameters were also observed for monkey 3 although these were only 2-6 fold higher than the values observed for the other monkeys. Following administration of 10 MIU/kg the $t_{1/2}$ and V/F for monkey 3 were approximately 4-15 fold higher than the values observed for the other monkeys although lower than those observed following administration of 3 MIU/kg to monkey 2.

The serum C_{max} increased in proportion to the increase in dose with a 4 fold increase in the mean serum C_{max} observed with a 3.3 fold increase in dose. Following administration of 3 MIU/kg, C_{max} values were similar in 8 of the 9 monkeys, but were 1.6 and 2.8 fold higher in monkey 4. Following administration of 10 MIU/kg, C_{max} values were similar in 5 of the 6 monkeys, but were 1.7 and 2.2 fold higher in monkey 3.

The serum AUC_{∞} roughly increased in proportion to the increase in dose as reflected in the dose normalised AUC (AUCD) which was generally within a 1.5 fold difference between doses. Following 3 MIU/kg a higher AUC and AUC/D was observed for monkey 4 compared to the other animals, and the AUC/D was approximately 2.6 fold higher than that determined at 10 MIU/kg. As mentioned earlier the C_{max} observed in this animal following 3

MIU/kg was higher than observed in other animals receiving the same dose and comparable to the C_{max} observed following 10 MIU/kg.

A

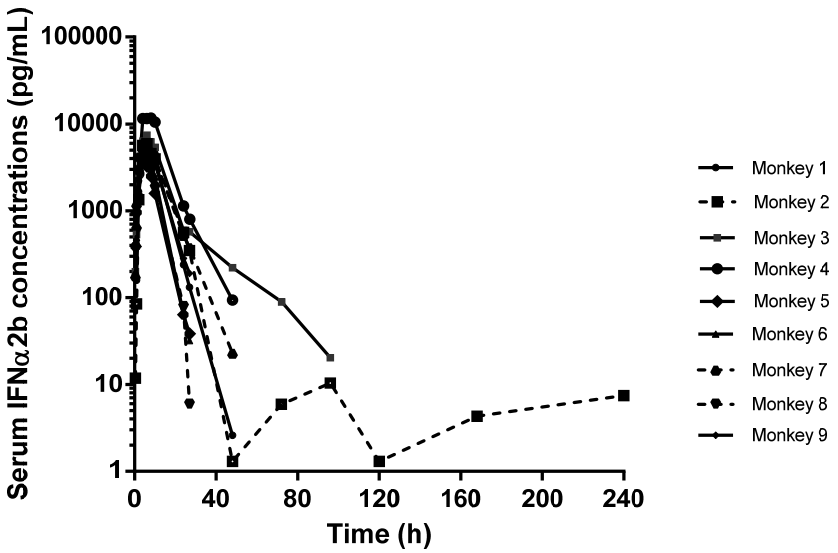

B

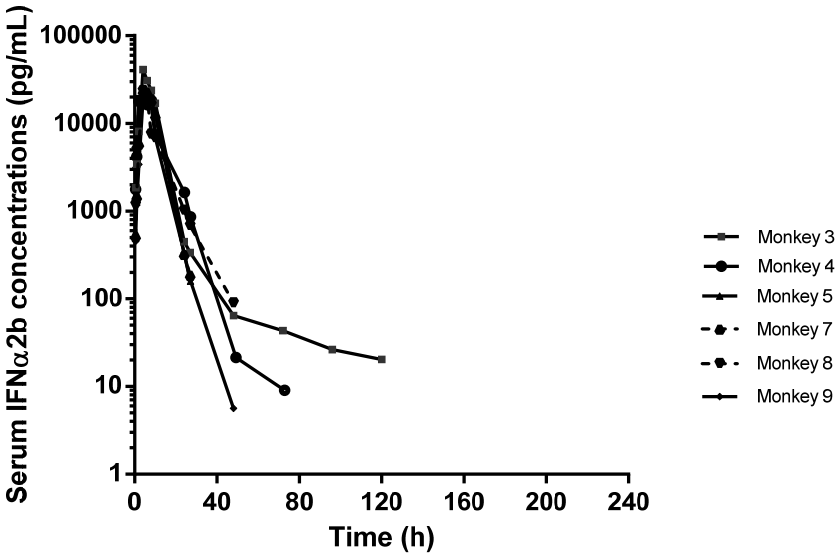

Figure 6.1 **Individual serum concentration time profiles for IFNα2b in male cynomolgus monkeys following a subcutaneous administration at target doses of (A) 3 MIU/kg and (B) 10 MIU/kg**

Table 6.2 **Individual and mean (SD and CV) pharmacokinetic parameters of IFNα2b in the male cynomolgus monkey following subcutaneous administration of IFNα2b at 3 MIU/kg and 10 MIU/kg**

Monkey	T_{max} (h)	C_{max} (pg/mL)	AUC_{0-t} (pg*h/mL)	$AUC_{0-\infty}$ (pg*h/mL)	$AUC_{0-\infty}/D$ (min/kg/L)	$t_{1/2}$ (h)	CL/F (mL/min/kg)	Vz/F (L/kg)
				3 MIU/kg				
1	8.1	4390	60614	60628	315	3.7	3.2	1.0
2	6.0	5927	75921	76261	397	88.6	2.5	19.3
3	6.0	7400	106347	106840	556	14.7	1.8	2.3
4	8.0	11678	177909	178819	930	6.7	1.1	0.6
5	2.1	4120	39742	39901	261	3.1	3.8	1.0
6	6.0	4101	45478	45599	237	2.7	4.2	1.0
7	4.0	5223	76348	76514	395	5.2	2.5	1.1
8	4.0	5083	45197	45241	235	2.4	4.3	0.9
9	6.0	5722	65867	66904	348	4.0	2.9	1.0
Mean		**5960**	**77047**	**77412**	**409**	**14.6**	**2.9**	**3.1**
Std		**2384**	**43057**	**43298**	**220**	**28.0**	**1.1**	**6.1**
CV (%)		**40**	**56**	**56**	**54**	**193**	**37**	**194**
				10 MIU/kg				
3	4.1	41104	350375	351554	548	42.2	1.8	6.7
4	4.2	18271	223466	223512	349	6.3	2.9	1.6
5	4	22162	259375	259978	406	2.7	2.5	0.6
7	4	23347	238113	238801	373	2.8	2.7	0.7
8	4.1	23613	206959	207651	324	6.2	3.1	1.6
9	6	20515	175583	175608	274	3.8	3.7	1.2
Mean		**24835**	**242312**	**242851**	**379**	**10.7**	**2.8**	**2.0**
Std		**8213**	**60074**	**60433**	**94**	**15.5**	**0.6**	**2.3**
CV (%)		**33**	**25**	**25**	**25**	**146**	**22**	**113**

6.3.4. Neopterin Concentrations

Serum concentrations of neopterin were observed in all monkeys following both vehicle and IFNα2b treatment at both 3 and 10 MIU/kg and are presented in Figure 6.3 A, B and C. The individual and mean pharmacokinetic parameters determined for neopterin are presented in Table 6.3.

Measurable concentrations were observed in the pre-dose samples from all monkeys prior to either vehicle or IFNα2b treatment. Following vehicle administration the serum neopterin concentrations were observed across the 240 h sampling region and remained broadly consistent to that observed in the pre-dose samples with a range of 944 – 3377 pg/mL giving a flat concentration-time profile.

Following subcutaneous administration of IFNα2b, serum concentrations of neopterin began to rise from the baseline around 8 h post dose with the maximum concentrations (C_{max}) observed at comparable times (T_{max}) between monkeys receiving the same dose of IFNα2b and between dose groups at approximately 24-27 h post dose. Following the C_{max} the serum concentrations of neopterin declined with concentrations returning to baseline by 240 h post dose. The shape of the serum concentration-time profile was generally consistent following administration of 3 MIU/kg and 10 MIU/kg, although there was more variability following 3 MIU/kg compared to 10 MIU/kg.

Higher serum neopterin C_{max} and AUC_{0-t} estimates were observed following both 3 MIU/kg and 10 MIU/kg IFNα2b compared to vehicle. The inter animal variability in C_{max} and AUC_{0-t} observed following each treatment was generally comparable with ranges of 2 to 3 fold for all three treatments. C_{max} and AUC_{0-t} generally increased with dose within individual animals except for monkey 8 and monkey 9 where higher C_{max} and AUC_{0-t} values were observed following 3 MIU/kg compared to 10 MIU/kg. Following a 3.3 fold increase in dose, a 1.3 and 1.2 fold increase was observed for mean neopterin C_{max} and AUC_{0-t}, respectively.

A

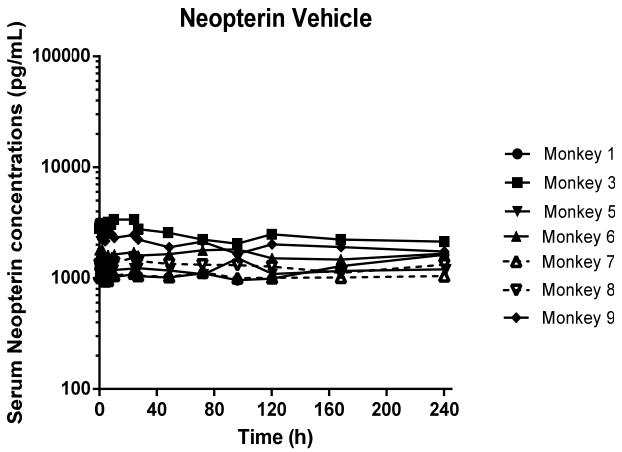

B

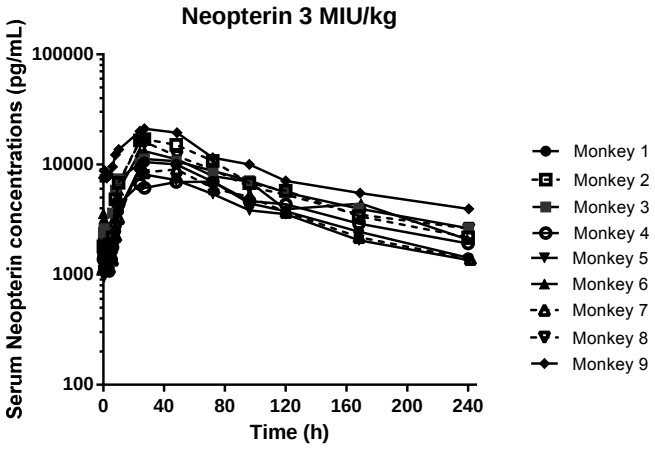

C

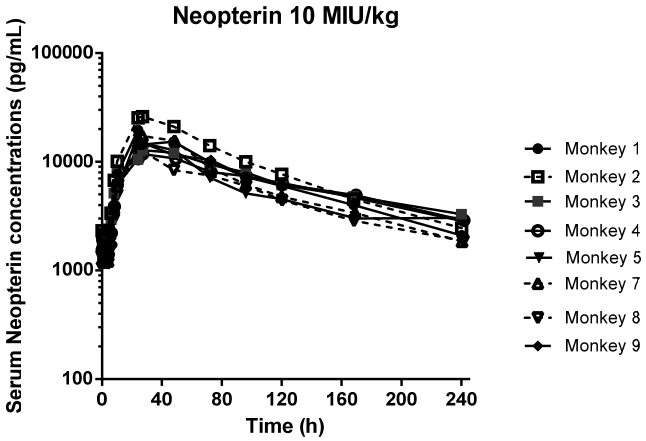

Figure 6.2 **Individual serum concentration-time profiles for neopterin in male cynomolgus monkeys following subcutaneous administration of (A) vehicle and IFNα2b at target doses of (B) 3MIU/kg and (C) 10 MIU/kg**

Table 6.3 Individual and mean (SD and CV) pharmacokinetic parameters of Neopterin in the male cynomolgus monkey following subcutaneous administration of vehicle and IFNα2b at 3 MIU/kg and 10 MIU/kg

Dose Group	Monkey	T_{max} (h)	C_{max} (pg/mL)	AUC_{0-t} (pg*h/mL)
Vehicle	1	240.2	1624	283132
	3	10.2	3377	577722
	5	96.5	1509	287984
	6	2.0	1823	387885
	7	8.7	1151	248974
	8	24.0	1533	306622
	9	0	3226	471829
	Mean		**2035**	**366307**
	Std		**889**	**120194**
	CV (%)		**44**	**33**
3 MIU/kg	1	27.0	10506	1081854
	2	27.0	17009	1671451
	3	27.0	11237	1466616
	4	72.1	6971	1016757
	5	24.0	8820	897995
	6	27.0	13206	1426322
	7	24.1	9842	1012348
	8	24.0	16302	1542397
	9	27.0	21097	2303462
	Mean		**12777**	**1379911**
	Std		**4545**	**441882**
	CV (%)		**36**	**32**
10 MIU/kg	1	24.0	19642	1712499
	2	27.0	26076	2329996
	3	27.0	12835	1651913
	4	27.1	11808	1547300
	5	27.1	14903	1392678
	7	27.0	17258	1558516
	8	24.0	13843	1240249
	9	24.0	17579	1700350
	Mean		**16743**	**1641688**
	Std		**4597**	**321006**
	CV (%)		**27**	**20**

6.3.5. Body Temperature

The individual body temperature-time profiles are presented in Figure 6.3 A, B and C following vehicle and IFNα2b administration at 3 MIU/kg and 10 MIU/kg, respectively. The individual and mean pharmacokinetic parameters determined for body temperature are presented in Table 5.4.

Following vehicle administration, the body temperature remained consistent with that observed in the pre-dose samples with a range of approximately 37-39°C. Following subcutaneous administration of IFNα2b at 3 and 10 MIU/kg the body temperature remained broadly similar to that observed following vehicle treatment although there was potentially an increase between 2-8 h. This was reflected by an earlier T_{max} following 10 MIU/kg IFNα2b (2-8 h) compared to vehicle (1.5-33 h), however, C_{max} and AUC_{0-t} were comparable between individuals and between treatments suggesting no treatment related response in body temperature.

A

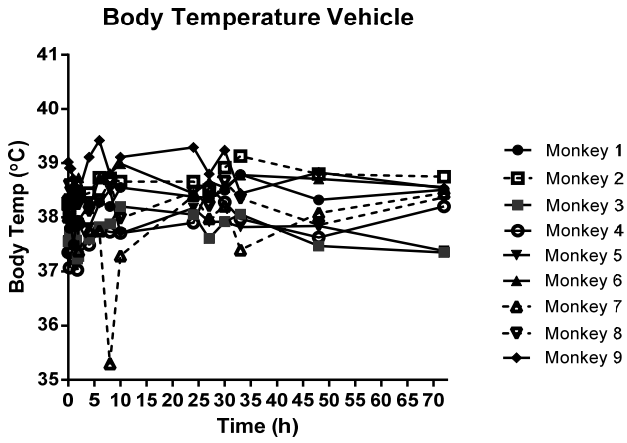

B

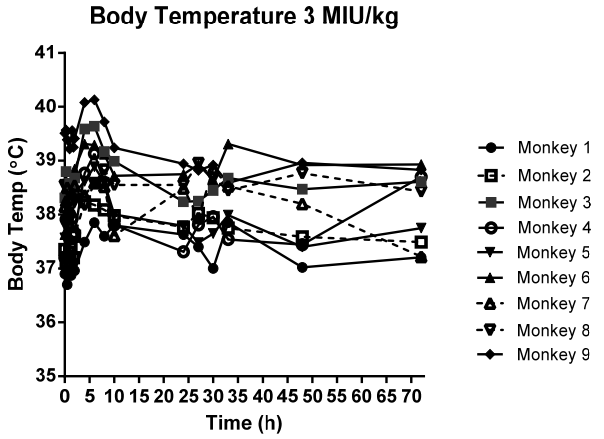

C

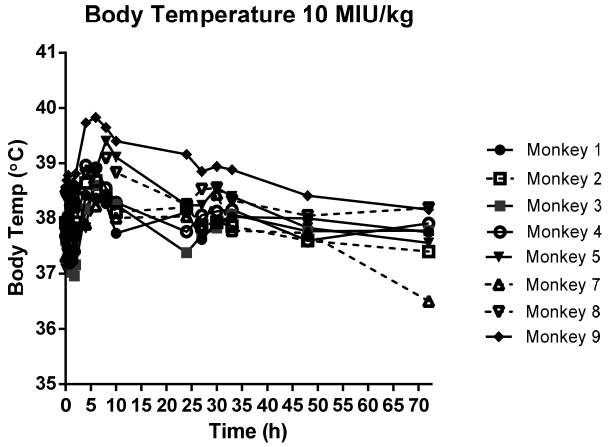

Figure 6.3 **Individual body temperature-time profiles for in male cynomolgus monkeys following subcutaneous administration of (A) vehicle and IFNα2b at target doses of (B) 3MIU/kg and (C) 10 MIU/kg**

Table 6.4 **Individual and mean (SD and CV) pharmacokinetic parameters of Body Temperature in the male cynomolgus monkey following subcutaneous administration of vehicle and IFNα2b at 3 MIU/kg and 10 MIU/kg**

Dose Group	Monkey	T_{max} (h)	Max Temp (°C)	AUC_{0-t} (°C*h)
Vehicle	1	33	38.79	2767
	2	33	39.13	2791
	3	10	38.20	2716
	4	27	38.56	2727
	5	8	38.50	2723
	6	10	38.99	2784
	7	1.5	38.51	2729
	8	8	38.66	2751
	9	33	38.79	2767
	Mean		**39**	**2754**
	Std		**0.4**	**32**
	CV (%)		**1**	**1**
3 MIU/kg	1	6	37.85	2691
	2	4	38.24	2717
	3	6	39.64	2781
	4	6	39.13	2726
	5	6	38.89	2721
	6	4	39.31	2802
	7	30	38.86	2743
	8	27	38.95	2778
	9	6	40.13	2809
	Mean		**39**	**2752**
	Std		**0.7**	**42**
	CV (%)		**2**	**2**
10 MIU/kg	1	4	38.42	2731
	2	6	38.68	2725
	3	6	38.60	2725
	4	4	38.96	2735
	5	8	39.40	2747
	7	2	38.55	2714
	8	8	39.09	2761
	9	6	39.83	2793
	Mean		**39**	**2741**
	Std		**0.5**	**25**
	CV (%)		**1**	**1**

6.3.6. Pharmacokinetics of other cytokines / chemokines

6.3.6.1. IL15

Serum concentrations of IL15 were observed in all monkeys, except for monkey 6 where all serum concentrations following vehicle treatment were below the assay LLQ. The individual serum concentration time profiles of IL15 are presented in Figure 6.4 A, B and C following vehicle and IFNα2b administration at 3 MIU/kg and 10 MIU/kg respectively. The individual and mean pharmacokinetic parameters are presented in Table 6.5.

Concentrations between 3 and 35 pg/mL were observed in the majority of the pre-dose samples. Serum concentrations of IL15 observed in the vehicle treated monkeys remained within this range with measurable concentrations observed over the entire sampling region in 4 of 7 the monkeys. Following IFNα2b, serum concentrations of IL15 begin to rise from the baseline between 2-6 h post dose with the C_{max} observed at a comparable T_{max} between monkeys receiving the same dose of IFNα2b and between dose groups at approximately 6-10 h post dose. The serum concentrations of IL15 then declined with concentrations returning to baseline between 27 and 240 h post dose. Measurable concentrations were observed across the entire sampling region in 7 monkeys following 3 MIU/kg IFNα2b and 4 monkeys following 10 MIU/kg IFNα2b. The shape of the serum concentration-time profile was similar following 3 MIU/kg and 10 MIU/kg, although there was more variability following at 10 MIU/kg compared to 3 MIU/kg.

Following administration of IFNα2b, serum IL15 C_{max} and AUC_{0-t} were higher following both 3 MIU/kg and 10 MIU/kg IFNα2b compared to vehicle. The serum C_{max} increased with dose in 7 of the 8 monkeys dosed with both 3 MIU/kg and 10 MIU/kg. The inter animal variability in serum C_{max} in each treatment group was comparable ranging from 2-3 fold. The serum AUC_{0-t} increased with dose in 6 of the 8 monkeys dosed with both 3 MIU/kg and 10 MIU/kg. The serum AUC_{0-t} observed in vehicle treated monkeys was highly variable with a 50 fold range, with lower variability in IFNα2b treated monkeys with ranges of 3 and 4 fold. Only a 1.4 fold increase in both C_{max} and AUC_{0-t} was observed with a 3.3 fold increase in the dose.

A

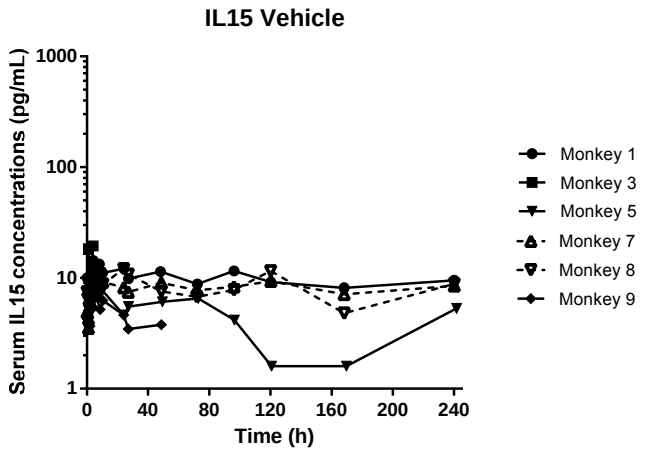

B

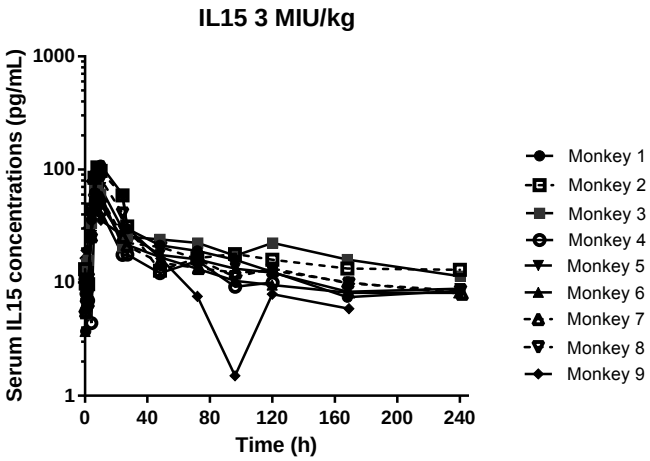

C

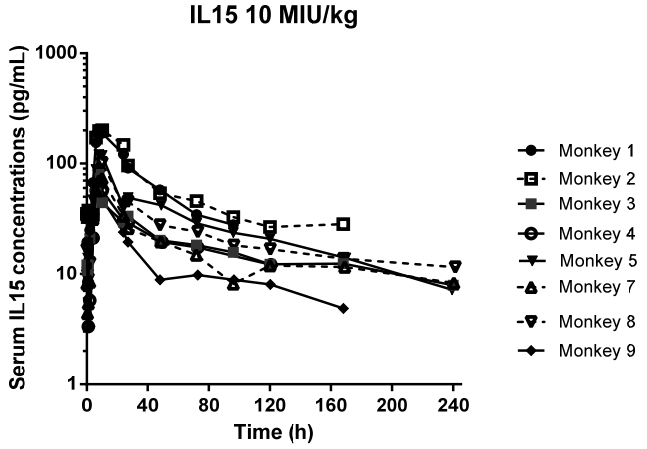

Figure 6.4 **Individual serum concentration-time profiles for IL15 in male cynomolgus monkeys following subcutaneous administration of (A) vehicle and IFNα2b at target doses of (B) 3MIU/kg and (C) 10 MIU/kg**

Table 6.5 **Individual and mean (SD and CV) pharmacokinetic parameters of IL15 in the male cynomolgus monkey following subcutaneous administration of vehicle and IFNα2b at 3 MIU/kg and 10 MIU/kg**

Dose Group	Monkey	T_{max} (h)	C_{max} (pg/mL)	AUC_{0-t} (pg*h/mL)
Vehicle	1	4.2	14.4	2317
	3	4.0	19.5	46
	5	4.2	8.1	970
	7	120.2	9.4	1952
	8	6.0	12.3	1940
	9	6.0	6.8	216
	Mean		**11.7**	**1240**
	Std		**4.7**	**970**
	CV (%)		**40**	**78**
3 MIU/kg	1	10.0	109.1	4659
	2	8.0	104.8	5106
	3	8.0	69.5	5020
	4	8.0	49.8	1903
	5	8.0	72.8	3843
	6	6.0	64.2	3252
	7	8.1	60.1	3534
	8	10.0	82.9	4098
	9	6.0	86.4	2407
	Mean		**77.7**	**3758**
	Std		**19.9**	**1113**
	CV (%)		**26**	**30**
10 MIU/kg	1	10.1	188.7	6976
	2	10.1	200.8	9667
	3	8.0	79.4	4136
	4	8.2	64.6	2733
	5	8.0	121.0	6505
	7	10.0	73.3	3947
	8	10.0	101.4	5595
	9	8.0	65.6	2160
	Mean		**111.9**	**5215**
	Std		**54.7**	**2478**
	CV (%)		**49**	**48**

6.3.6.2. IL1Ra

The individual serum concentration time profiles of IL1Ra in male cynomolgus monkeys are presented in Figure 6.5 A, B and C following vehicle and IFNα2b administration at 3 MIU/kg and 10 MIU/kg respectively. The individual and mean pharmacokinetic parameters determined for IL1Ra are presented in Table 6.6.

Measurable concentrations of IL1Ra were observed in all monkeys following vehicle treatment with concentrations ranging from 4-1338 pg/mL Measurable concentrations were generally observed over the entire sampling region including predose.

Following administration of IFNα2b serum concentrations of IL1Ra begin to rise from the baseline between 1-2 h post dose with C_{max} observed at comparable times (T_{max}) between monkeys receiving the same dose of IFNα2b and between dose groups at approximately 4-6 h post dose. Following the C_{max} the serum concentrations of IL1Ra decline with concentrations returning to baseline anywhere between 24 and 48 h post dose. Measurable concentrations were observed across the entire sampling region in 6 monkeys following 3 MIU/kg IFNα2b and 4 monkeys following 10 MIU/kg IFNα2b. The shape of the serum concentration-time profile is generally consistent following administration of 3 MIU/kg and 10 MIU/kg.

Following administration of IFNα2b a greater serum IL1Ra C_{max} and AUC_{0-t} was observed following both 3 MIU/kg and 10 MIU/kg IFNα2b compared to vehicle. The T_{max} was comparable between the treatment groups, although the greatest range was observed following vehicle treatment, suggesting that administration procedure may affect IL1Ra concentrations. The serum C_{max} and AUC_{0-t} observed in vehicle treated monkeys was more variable with a 22 fold and 290 fold range respectively however following IFNα2b treatment both the C_{max} and AUC_{0-t} were generally comparable between monkeys. Monkey 4 demonstrated a considerably greater C_{max} approximately 2-10 fold greater than the C_{max} observed in other monkeys at both 3 MIU/kg and 10 MIU/kg. Based on the mean C_{max} and AUC_{0-t} for each dose group only a 1.8 and 1.4 fold increase in C_{max} and AUC_{0-t} respectively was observed with a 3.3 fold increase in the dose.

A

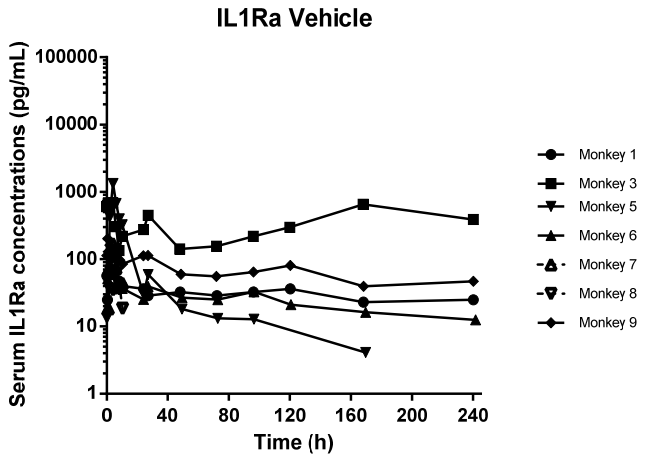

B

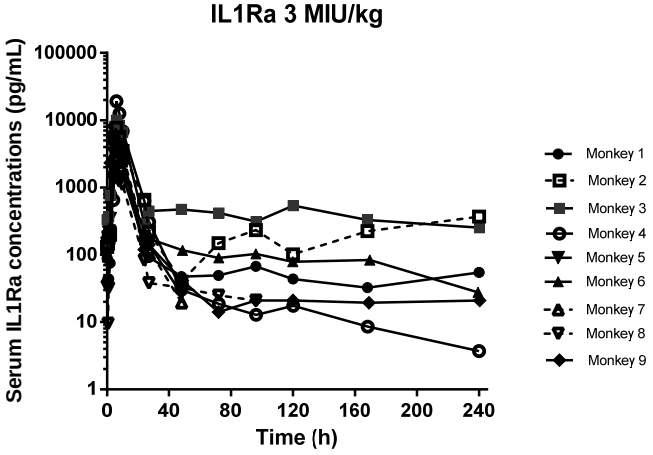

C

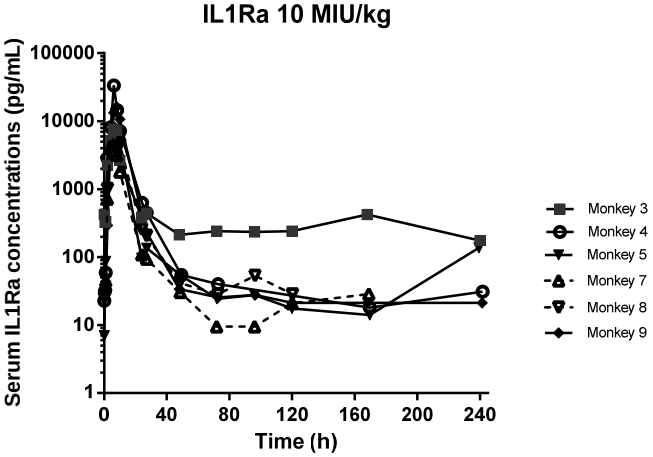

Figure 6.5 **Individual serum concentration-time profiles for IL1Ra in male cynomolgus monkeys following subcutaneous administration of (A) vehicle and IFNα2b at target doses of (B) 3MIU/kg and (C) 10 MIU/kg**

Table 6.6 **Individual and mean (SD and CV) pharmacokinetic parameters of IL1Ra in the male cynomolgus monkey following subcutaneous administration of vehicle and IFNα2b at 3 MIU/kg and 10 MIU/kg**

Dose Group	Monkey	T_{max} (h)	C_{max} (pg/mL)	AUC_{0-t} (pg*h/mL)
Vehicle	1	2.0	65.7	7213
	3	4.0	686.2	89840
	5	4.2	1337.9	10752
	6	6.2	115.3	5936
	7	4.2	169.6	758
	8	6.0	61.7	307
	9	0.6	201.0	6160
	Mean		**377**	**17281**
	Std		**476**	**32203**
	CV (%)		**126**	**186**
3 MIU/kg	1	6.0	2158	34499
	2	6.0	7673	114753
	3	6.0	9979	184020
	4	6.0	19140	133158
	5	6.0	4308	46105
	6	6.0	4321	61349
	7	4.0	5456	58587
	8	6.0	1953	20960
	9	4.0	8174	73017
	Mean		**7018**	**80716**
	Std		**5289**	**52926**
	CV (%)		**75**	**66**
10 MIU/kg	3	6.0	7644	130038
	4	6.2	33585	191976
	5	4.0	6673	85797
	7	6.0	4530	44157
	8	6.0	5921	77549
	9	8.0	16198	166080
	Mean		**12425**	**115933**
	Std		**11158**	**56621**
	CV (%)		**90**	**49**

6.3.6.3. Eotaxin

Following vehicle treatment, measurable serum concentrations of eotaxin were only observed in Monkey 1, Monkey 3, Monkey 7 (24 and 27 h) and Monkey 9. Monkey 1 and 3 had measurable eotaxin concentrations over the 240 h sampling time, with the highest concentrations observed in monkey 3 (30-64 pg/mL).

The individual serum concentration time profiles of eotaxin are presented in Figure 6.6 A, B and C following vehicle and IFNα2b administration at 3 MIU/kg and 10 MIU/kg respectively. The individual and mean pharmacokinetic parameters are presented in Table 6.7.

Measurable concentrations of eotaxin between 18 and 53 pg/mL were observed in the predose samples prior to administration of IFNα2b in 5 of the 9 monkeys (3 MIU/kg) and in 4 of the 8 monkeys (10 MIU/kg) prior to each dose. Following IFNα2b serum concentrations of exotaxin begin to rise from the baseline at around 6 h reaching C_{max} between 6-10 h post dose, following which the concentrations then declined returning to baseline between 24 and 48 h post dose. Measurable concentrations were observed across the entire sampling region in 5 monkeys following 3 MIU/kg IFNα2b and 4 monkeys following 10 MIU/kg IFNα2b.

Following administration of IFNα2b a greater serum eotaxin C_{max} was higher following both 3 MIU/kg and 10 MIU/kg IFNα2b compared to vehicle at a comparable T_{max} between the two IFNα2b dose groups. C_{max} generally increased with increasing dose indicating that there may be a potential dose response for eotaxin although this increase was of different orders of magnitude between monkeys. The serum AUC_{0-t} increased with dose in 5 of the 8 monkeys. However, only a 1.6 fold increase in AUC was observed with a 3.3 fold increase in the dose. The serum AUC_{0-t} observed in vehicle treated monkeys was variable with the third highest AUC value across all three treatment groups determined for Monkey 3 yet the lowest overall AUC was also observed in this treatment group (monkey 7). The mean AUC following vehicle was comparable to the AUC following 3 MIU/kg IFNα2b and only 1.6 fold lower than the AUC following 10 MIU/kg IFNα2b.

A

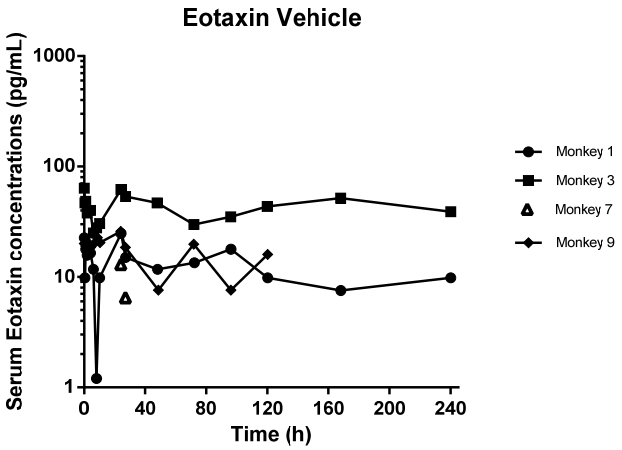

B

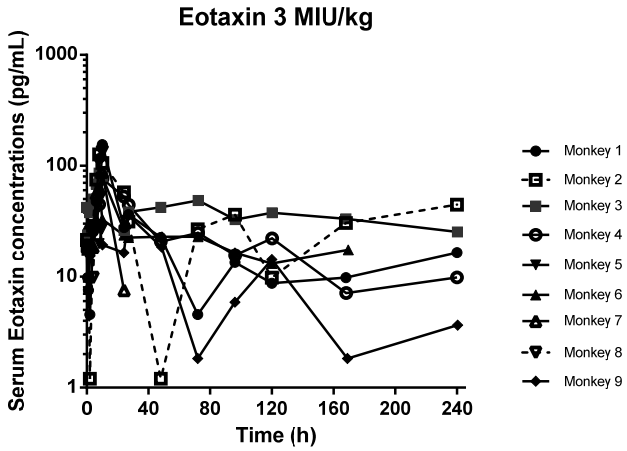

C

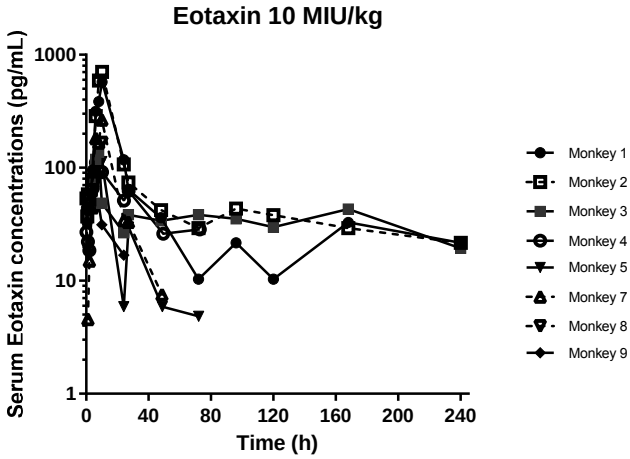

Figure 6.6 **Individual serum concentration-time profiles for Eotaxin in male cynomolgus monkeys following subcutaneous administration of (A) vehicle and IFNα2b at target doses of (B) 3MIU/kg and (C) 10 MIU/kg**

Table 6.7 **Individual and mean (SD and CV) pharmacokinetic parameters of Eotaxin in the male cynomolgus monkey following subcutaneous administration of vehicle and IFNα2b at 3 MIU/kg and 10 MIU/kg**

Dose Group	Monkey	T_{max} (h)	C_{max} (pg/mL)	AUC_{0-t} (pg*h/mL)
Vehicle	1	24.1	24.8	2751
	3	0	63.7	10415
	7	24	13.0	120
	9	24	25.9	1811
	Mean		**31.8**	**3774**
	Std		**22.0**	**4559**
	CV (%)		**69**	**121**
3 MIU/kg	1	10	155	4745
	2	8	127	7533
	3	8	85.9	9021
	4	10.1	76.3	4810
	5	10	27.0	66.8
	6	8	65.7	3480
	7	10	87.5	1027
	8	10	136	355
	9	6	40.2	2325
	Mean		**88.8**	**3701**
	Std		**43.1**	**3136**
	CV (%)		**49**	**85**
10 MIU/kg	1	10.1	572	12781
	2	10.1	705	16107
	3	8	137	8760
	4	6.2	111	3494
	5	10	114	1997
	7	10	265	3805
	8	10	167	466
	9	8	47.6	464
	Mean		**265**	**5984**
	Std		**241**	**5906**
	CV (%)		**91**	**99**

6.3.6.4. MCP1

The individual serum concentration time profiles of MCP1 in male cynomolgus monkeys are presented in Figure 6.7 A, B and C following vehicle and IFNα2b administration at 3 MIU/kg and 10 MIU/kg respectively. The individual and mean pharmacokinetic parameters determined for MCP1 are presented in Table 6.8.

Measurable concentrations of MCP1 were observed in the pre-dose samples from all monkeys prior to either vehicle or IFNα2b treatment. Following vehicle administration, serum MCP1 concentrations across the 240 h sampling region remained similar to the pre-dose samples with a range of 360-9000 pg/mL. The highest concentrations were observed around 24 h post dose.

Following IFNα2b serum concentrations of MCP1 begin to rise from the baseline around 2 h post dose reaching C_{max} at approximately 4-8 h post dose, following which concentrations declined returning to baseline by 72 h post dose. The shape of the serum concentration-time profile was similar following administration of 3 MIU/kg and 10 MIU/kg.

Following administration of IFNα2b greater serum MCP1 C_{max} and AUC_{0-t} were observed following both 3 MIU/kg and 10 MIU/kg IFNα2b compared to vehicle. The inter animal variability in C_{max} was 5 fold and 9 fold following administration at 3 MIU/kg and 10 MIU/kg respectively. The inter animal variability in AUC_{0-t} was lower than observed for C_{max} with ranges of 2 fold and 3 fold following administration at 3 MIU/kg and 10 MIU/kg respectively. The serum C_{max} and AUC_{0-t} generally increased with dose within individual animals except for monkey 7 where a greater C_{max} and AUC_{0-t} was observed following administration of 3 MIU/kg compared to 10 MIU/kg. Based on mean C_{max} and AUC_{0-t} a 1.7 and 1.6 fold increase was observed for C_{max} and AUC_{0-t} with a 3.3 fold increase in dose.

A

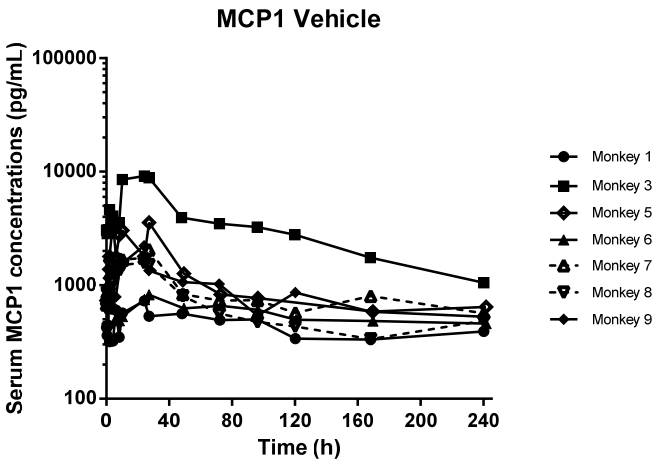

B

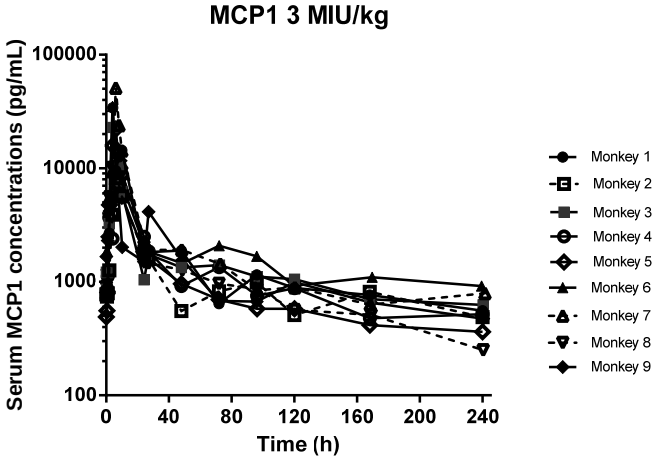

C

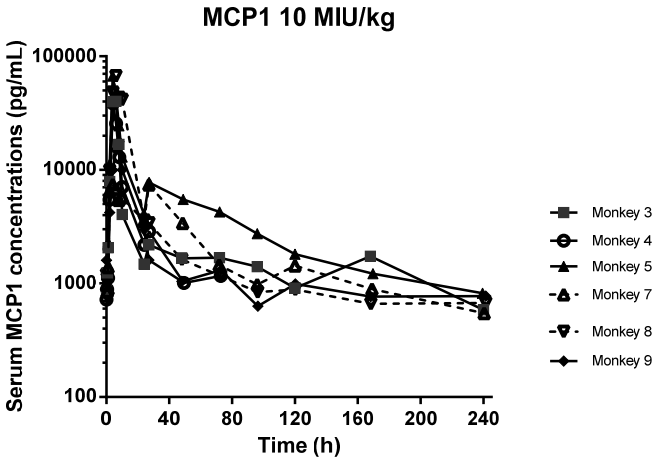

Figure 6.7 Individual serum concentration-time profiles for MCP1 in male cynomolgus monkeys following subcutaneous administration of (A) vehicle and IFNα2b at target doses of (B) 3MIU/kg and (C) 10 MIU/kg

Table 6.8 **Individual and mean (SD and CV) pharmacokinetic parameters of MCP1 in the male cynomolgus monkey following subcutaneous administration of vehicle and IFNα2b at 3 MIU/kg and 10 MIU/kg**

Dose Group	Monkey	T_{max} (h)	C_{max} (pg/mL)	AUC_{0-t} (pg*h/mL)
Vehicle	1	24.1	727	103532
	3	24.1	9157	777851
	5	27.1	3562	256134
	6	1.1	998	135394
	7	27.0	2063	209671
	8	24.0	1578	149464
	9	24.0	2227	203423
	Mean		**2902**	**262210**
	Std		**2911**	**233135**
	CV (%)		**100**	**89**
3 MIU/kg	1	4.1	34180	453741
	2	6.0	8221	262461
	3	4.2	22906	361490
	4	8.0	9693	313990
	5	6.0	22083	297701
	6	4.0	35053	478758
	7	6.0	50996	534876
	8	4.0	10100	299428
	9	6.0	10924	303196
	Mean		**22694**	**367293**
	Std		**14840**	**97085**
	CV (%)		**65**	**26**
10 MIU/kg	3	6.0	40182	544936
	4	4.2	38447	315286
	5	4.0	67143	983186
	7	4.0	7435	477090
	8	6.0	66923	912577
	9	8.0	17722	398715
	Mean		**39642**	**605298**
	Std		**24577**	**277159**
	CV (%)		**62**	**46**

6.3.6.5. IL6

The individual serum concentration time profiles of IL6 in male cynomolgus monkeys are presented in Figure 6.8 A, B and C following vehicle and IFNα2b administration at 3 MIU/kg and 10 MIU/kg respectively. The individual and mean pharmacokinetic parameters determined for IL6 are presented in Table 6.9.

Following vehicle treatment, measurable serum concentrations of IL6 were observed in all monkeys with a range of 3.4-456 pg/mL. The IL6 T_{max} was observed between 2 and 24 h, with no measurable serum IL6 concentrations observed post 27 h post vehicle treatment in any monkey.

Measurable concentrations of IL6 between 4 and 53 pg/mL were observed in the predose samples prior to administration of IFNα2b in 1 of the 7 monkeys (vehicle) 2 of the 9 monkeys (3 MIU/kg) and in 2 of the 8 monkeys (10 MIU/kg) prior to each dose. Following subcutaneous administration of IFNα2b serum concentrations of IL6 begin to rise from the baseline reaching T_{max} at approximately 2-6 h post dose following which concentrations of declined returning to baseline anywhere between 10 and 240 h post dose.

A comparable mean serum IL6 C_{max} was observed following both vehicle and 3 MIU/kg IFNα2b treatment while a 2.6 fold greater mean C_{max} was observed following 10 MIU/kg IFNα2b compared to 3 MIU/kg. The C_{max} determined within each treatment group was variable with the lowest range observed for 3 MIU/kg and the highest range observed for the vehicle. The C_{max} did not always increase with increasing dose of IFNα2b, for example, for monkey 3 the lowest C_{max} was observed following administration of 3 MIU/kg, then vehicle, with the highest C_{max} observed for 10 MIU/kg. For monkey 9 the lowest C_{max} was observed following administration of 10 MIU/kg, which was comparable to vehicle, with the highest C_{max} observed following 3 MIU/kg.

Following administration of IFNα2b a greater mean serum IL6 AUC_{0-t} was determined following both 3 MIU/kg and 10 MIU/kg IFNα2b compared to vehicle treatment. A 3 fold greater mean AUC_{0-t} was determined following 10 MIU/kg IFNα2b compared to 3 MIU/kg. As with C_{max} the AUC_{0-t} determined within each treatment group was variable with the lowest range observed following 3 MIU/kg and the highest range observed following vehicle treatment. Once again the AUC_{0-t} observed for individual animals did not always increase with increasing dose of IFNα2b following a similar pattern to the C_{max}.

A

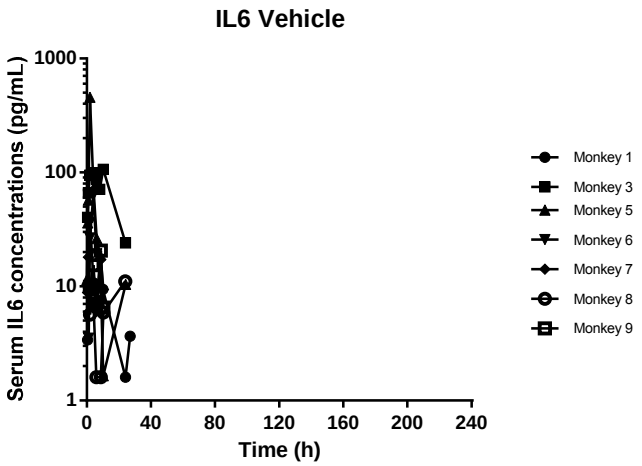

B

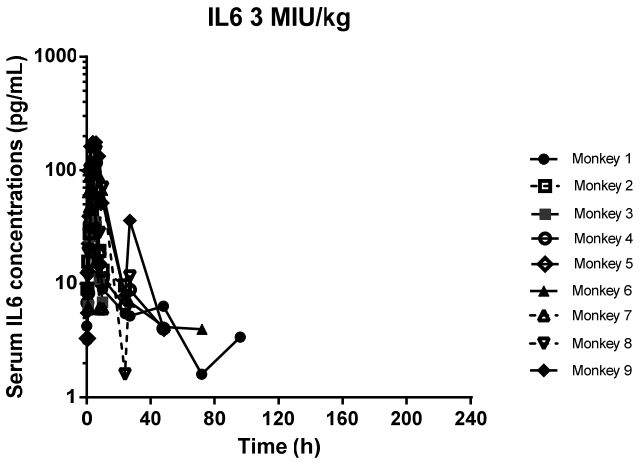

C

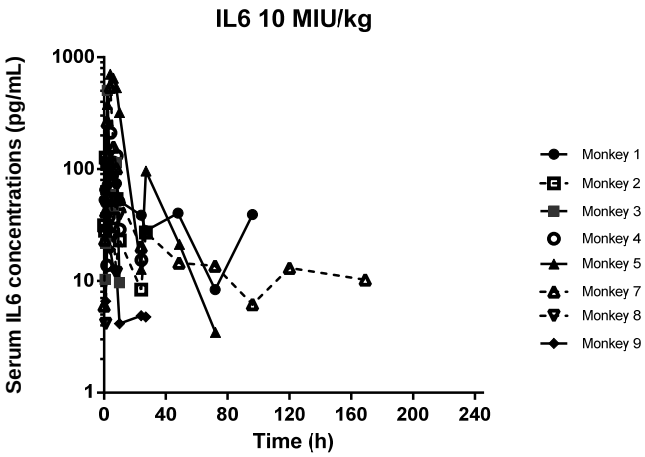

Figure 6.8 **Individual serum concentration-time profiles for IL6 in male cynomolgus monkeys following subcutaneous administration of (A) vehicle and IFNα2b at target doses of (B) 3MIU/kg and (C) 10 MIU/kg**

Table 6.9 **Individual and mean (SD and CV) pharmacokinetic parameters of IL6 in the male cynomolgus monkey following subcutaneous administration of vehicle and IFNα2b at 3 MIU/kg and 10 MIU/kg**

Dose Group	Monkey	T_{max} (h)	C_{max} (pg/mL)	AUC_{0-t} (pg*h/mL)
Vehicle	1	4.2	10.8	170
	3	10.2	106	1756
	5	2.0	456	1457
	6	4.1	63.3	196
	7	2.0	38.8	161
	8	24.0	11.1	152
	9	8.7	20.6	113
	Mean		**101**	**572**
	Std		**160**	**712**
	CV (%)		**159**	**125**
3 MIU/kg	1	4.1	90.4	734
	2	4.0	96.1	570
	3	4.2	35.2	206
	4	6.0	117	852
	5	2.1	99.0	490
	6	6.0	170	1947
	7	2.0	46.6	106
	8	6.0	149	1348
	9	4.0	178	2224
	Mean		**109**	**942**
	Std		**50.2**	**746**
	CV (%)		**46**	**79**
10 MIU/kg	1	4.0	89.8	3350
	2	2.0	126	1641
	3	2.1	506	1237
	4	2.0	211	922
	5	4.0	705	8796
	7	4.0	541	4498
	8	2.1	48.0	258
	9	2.1	24.8	212
	Mean		**281**	**2614**
	Std		**263**	**2911**
	CV (%)		**93**	**111**

6.3.7. IP10, GMCSF, IL7, IL12p70, IFNγ, IL17

The individual serum concentration-time profiles of GMCSF, IP10, IFNγ, IL7, IL17 and IL12p70 in male cynomolgus monkeys following vehicle and IFNα2b administration at 3 MIU/kg and 10 MIU/kg are presented in Appendix 2.3 to 2.8 and the data for each cytokine is briefly summarised below. Where concentrations of these cytokines were observed there was generally little difference between the three treatments.

6.3.7.1. IP10

Following vehicle treatment, measurable serum concentrations of IP10 were only observed in Monkey 3 and Monkey 6, but were observed across the entire sampling region in these animals. Following IFNα2b treatment at 3 MIU/kg and 10 MIU/kg measurable serum concentrations of IP10 were observed in 6 and 7 of the Monkeys respectively generally up to 240 h post dose. The C_{max} for IP10 was observed between 0-6 h post IFNα2b treatment following which serum concentrations declined towards baseline in some animals, but remained relatively consistent others giving a flat concentration-time profile.

6.3.7.2. GMCSF

Following vehicle, measurable serum concentrations of GMCSF were only observed in Monkey 1 and Monkey 3. Measurable serum concentrations of GMCSF were observed in 6 following IFNα2b treatment at 3 MIU/kg and 5 following treatment at 10MIU/kg. Only 3 measurable concentrations at GMCSF were observed for Monkey 4 across both IFNα2b treatments and these were close to the assay LLQ. For Monkey 6, Monkey 7 and Monkey 8 no measurable GCSMF concentrations were observed following IFNα2b treatment at 10MIU/kg despite measurable concentrations being observed at 3 MIU/kg for these animals.

6.3.7.3. IL7

Following vehicle, measurable serum concentrations of IL7 were observed in all monkeys generally over the entire 240 h sampling region. The serum concentrations were comparable across the monkeys with a range of 3-85 pg/mL. Following IFNα2b treatment measurable serum concentrations of IL7 were observed in all monkeys including predose samples. Measurable serum concentrations were determined up to between 4-240 h and serum concentrations were comparable within the dose groups and between dose groups.

Following both vehicle and IFNα2b treatment the C_{max} for IL7 was observed relatively early in the profile for the majority of monkeys, following which the serum concentrations in all monkeys remained relatively consistent across the sampling region giving a flat concentration-time profile, although at 10 MIU/kg there is a suggestion that following the C_{max} the concentrations decline to approximately 48 h before rising again to give a plateau for the remainder of the profile.

6.3.7.4. IL12p70

Following vehicle, measurable serum concentrations of IL12p70 were observed in Monkeys 1 and 3 and a single measurable serum concentrations was observed for Monkey 9 pre-dose and was close to the assay LLQ. Following IFNα2b at 3 MIU/kg measurable serum concentrations of IL12p70 were observed for monkeys 1, 2, 3, 6 and 9 although were close to the assay LLQ in Monkey 1 and 9. The serum concentrations of IL12p70 determined in Monkeys 2, 3 and 6 were broadly consistent between the three animals and consistent across the sampling region giving a relatively flat shaped profile in these animals. Following IFNα2b at 10 MIU/kg measurable serum concentrations of IL12p70 were observed in all monkeys except for Monkey 9. Only a single concentration close to the LLQ was observed for Monkey 7, and in Monkey 5 all concentrations were close to the assay LLQ.

6.3.7.5. IL17A

Following vehicle treatment, measurable serum concentrations of IL17A were only observed in monkey 1, monkey 3 and monkey 9, but were observed across the entire sampling region in these animals and in the predose samples. Following IFNα2b treatment at 3 MIU/kg monkeys can be grouped into three groups depending on the observed serum concentrations. No measurable serum concentrations of IL17A were observed in monkey 5 and monkey 7, while monkeys 4, 6 and 8 demonstrated comparable serum concentrations of IL17A with a range of 3-23 pg/mL and monkeys 1, 2 and 9 demonstrated comparable but higher serum concentrations with a range of 56-201 pg/mL including the pre-dose samples. Following IFNα2b treatment at 10 MIU/kg monkeys can be grouped together in a similar manner as following 3 MIU/kg. Monkeys 1, 2, and 3 demonstrated the highest serum IL17A concentrations with a range of 28-204 pg/mL, monkeys 7 and 9 demonstrated comparable serum IL17A concentrations with a slightly lower range of 21-54 pg/mL and monkeys 4 and 5 demonstrated the lowest serum concentrations with a range of 3-25 pg/mL although the

majority the serum concentrations in these monkeys were close to the assay LLQ. Following IFNα2b treatment the C_{max} for IL17A was observed relatively early in the profile for the majority of monkeys and on 6 occasions the C_{max} was observed in the predose sample. The serum concentrations in all monkeys remained relatively consistent across the sampling region giving a flat concentration-time profile.

6.3.7.6. IFNγ

Following vehicle treatment, measurable serum concentrations of IFNγ were only observed in monkey 1, monkey 3 and monkey 6, but were observed across the entire sampling region in these animals and in the predose samples. Following IFNα2b treatment at 3 MIU/kg measurable serum concentrations of IFNγ were observed for monkeys 1, 2, 3, 6, 8 and 9. The serum concentrations were determined across the sampling region including the pre-dose samples and ranged from 3.6-224 pg/mL. Following IFNα2b treatment at 10 MIU/kg measurable serum concentrations of IFNγ were observed for monkeys 1, 2, 3, 5 and 7. The serum concentrations were determined across the sampling region including the pre-dose samples and ranged from 11-326 pg/mL. Following all three treatments the concentrations of IFNγ were determined were broadly consistent across the sampling region giving a relatively flat shaped serum concentration-time profile in all animals at all treatments.

6.3.7.7. Other cytokines

The serum concentration-time profiles for the remaining 17 cytokines that were triaged out of the final analysis are presented in Appendix 2.7 and briefly summarised below. In general either insufficient data or a lack of response compared to the vehicle dose group was observed for all cytokines/chemokines and it was decided that the data were not suitable for pharmacokinetic analysis. Generally monkey 3 demonstrated the highest measurable concentrations of each cytokine and also demonstrated measurable concentrations across the entire sampling region.

The serum concentrations of IL3, IL4 and IL5 were below the assay LLQ for all monkeys following all three treatments. Measurable serum concentrations of IL10 were observed in Monkey 3 across the entire sampling region following IFNα2b treatment 10 MIU/kg and in Monkey 2 at a single time point following IFNα2b treatment 3 MIU/kg. Measurable serum concentrations of IL8, VEGF and EGF were determined in all monkeys following all treatments. Concentrations of IL8 were determined across the entire sampling region in all

monkeys, whilst concentrations of VEGF and EGF were observed across the entire sampling region for the majority of animals. In general, the concentration-time profiles of all three cytokines demonstrated variability between similar treated animals making it difficult to determine any dose response relationship.

Measurable serum concentrations of GSCF were determined in all monkeys following all treatments, although only at a single time point for Monkey 1 (Vehicle and 3 MIU/kg) and Monkey 8 (3 MIU/kg), while only two measurable concentrations were determined for Monkey 9 (3 MIU/kg). Measurable serum concentrations of IL2, IL13, IL1α and IL1β were observed in Monkey 3 across the entire sampling region following all three treatments. Measurable concentrations of TNFα were observed in Monkey 3 across the entire sampling region following IFNα2b treatment at 3 and 10 MIU/kg and up to 6h post dose following vehicle treatment. A small number of measurable concentrations of IL2, IL13 IL1β and TNFα were observed for Monkey 2 following treatment at 3 MIU/kg however these were close to the assay LLQ. Measurable concentrations of IL1α were observed for Monkey 2 following treatment at 3 MIU/kg and 10 MIU/kg.

Serum concentrations of MIP1α were observed in all monkeys except Monkeys 7, 8 and 9, although only a single measurable concentration was observed in Monkey 1 (Vehicle) and Monkey 5 (10 MIU/kg). Serum concentrations of MIP1β were observed in all monkeys except Monkey 8, although only a single measurable concentration was observed in Monkey 2 (10 MIU/kg) and Monkey 5 (10 MIU/kg).

Measurable serum concentrations of IL12p40 were determined in 4 monkeys following treatment at 3 MIU/kg and 2 monkeys following treatment at 10 MIU/kg although all concentrations were close to the assay LLQ. Measurable serum concentrations of TNFβ were determined in 3 monkeys following treatment at 3 MIU/kg and 2 monkeys following treatment at 10 MIU/kg although a number of concentrations were close to the assay LLQ, and only one measurable concentration was determined for Monkey 5 (10 MIU/kg). No measurable concentrations of either IL12p40 or TNFβ were observed following vehicle treatment.

6.4. Discussion

6.4.1. Pharmacokinetics of IFNα2b

In this study, the pharmacokinetic parameters of recombinant human IFNα2b were successfully determined following subcutaneous administration at 3 and 10 MIU/kg to the male cynomologus monkey. The systemic exposure increased in proportion to the increase in dose as demonstrated by a comparable dose normalised AUC and apparent clearance and volume of distribution were consistent between dose groups. It has been reported that the major route of elimination of the IFNs is renal filtration followed by renal catabolism during proximal tubular re-absorption (Wills, 1990) which results in negligible amounts of intact IFN in the urine. This route of elimination is supported by tissue distribution studies in preclinical species which have demonstrated high concentrations of IFN in the kidney following administration of recombinant IFN (Palleroni and Bohoslawec, 1984; Bohoslawec, Trown and Wills, 1986; Trown, Wills and Kamm, 1986; Bannai et al, 1987). The extent of clearance by renal filtration alone is dependent on both the unbound fraction of the drug and the glomerular filtration rate. In monkeys the glomerular filtration rate (GFR) is around 2.1 mL/min/kg (Mahmood, 1998). As the clearance determined in this study is greater than the clearance determined by filtration alone there may be another process involved in the elimination of IFNα2b in the monkey. This could be active secretion in the kidney or a non renal clearance mechanism or a combination of the two. Supporting this is evidence that IFNα can undergo a small amount of catabolism in the liver (Gloff and Wills, 1992).

The apparent volume of distribution (V/F) was comparable between the two dose groups and was generally comparable between individuals. One monkey in each dose group had a higher V/F than the other monkeys within each dose group. Excluding these outliers and assuming complete bioavailability, the apparent volume of distribution of IFNα2b following sc administration to the primate was 2-3.1 L/kg, which is higher than total body water (0.7 L/kg, Kerns and Di, 2008) indicating some distribution into the tissues. This is higher than reported in the literature where the V_{ss} for recombinant IFNα is generally about the same as extracellular fluid (Collins et al, 1985). The volume of distribution of recombinant IFNα is generally limited by the size of the molecule. It has a large molecular weight of approximately 19,000 and is too large to penetrate intracellular spaces.

Although the pharmacokinetics of recombinant IFNα2b in both the cynomolgus monkey and human have previously been reported in the literature the data are often only briefly summarised, or different routes of administration, strains of monkeys, dosing regimens and sampling regimes were used, making it difficult to compare the results with the present study. A number of studies have investigated the pharmacokinetics of modulated IFN in primates, such as pegylated IFNs, which are more slowly cleared and allow for prolonged systemic exposure. In these studies un-modified IFN is often administered as a comparison to understand if the modulation improves the pharmacokinetics, which provides a pool of PK and in some cases PD information in the monkey. In one study the subcutaneous administration of INTRON A at a dose of 40 µg/kg (equivalent to 10 MIU/kg) was investigated (Osborn et al, 2002). An apparent clearance (CL/F) of 3.6 mL/min/kg was determined which is similar to that observed in this study. The half life at approximately 5 h is lower than observed in this study (11 h), although the mean was biased by data from 3 monkeys. Excluding these monkeys gives a $t_{1/2}$ value of 4 h, which is comparable to that reported in the literature. Pharmacokinetic data following administration of INTRON A to primates is reported in two FDA documents, the pharmacologist review for Rebetol and INTRON A and the toxicologist review for polyethylene glycol (PEG)-INTRON. Following subcutaneous administration to rhesus monkeys INTRON A was rapidly absorbed with peak concentrations observed approximately 4 hours post dose, with a terminal half life of approximately 3.5 h. The clearance was reported to be 0.7-0.9 mL/min/kg and although it was not specified whether CL_b was determined following iv or sc administration, the reported bioavailability of INTRON A following subcutaneous administration is reported 83-104 % indicating that the CL and CL/F are essentially the same. In the toxicologist review for PEG-INTRON, INTRON A was also investigated to provide a comparison. Following subcutaneous administration at a dose of 1345 µg/m^2 peak serum concentrations were achieved by 2 h post dose with no IFN detectable after 24 h post dose and a reported terminal elimination half-life of 3.6 h. The primary route of elimination was identified as catabolism and excretion by the kidneys in rhesus monkeys, and following radiolabelled studies no free IFN was detected in the urine.

The pharmacokinetics of type I IFNs have been investigated in other studies including other versions of IFNα such as IFNα2a (Trown, Wills and Kamm et al, 1986), and IFNβ (Mager et al, 2003) and recombinant IFNαa (Bannai et al, 1985). In general, following iv administration concentrations of IFN decline in a biphasic manner, characterised by an initial rapid

distribution phase followed by a slower elimination phase (Wills et al, 1984; Collins et al, 1985; Bannai et al, 1985; Bannai, 1986; Mager et al, 2003). Following either im or sc administration, a prolonged absorption phase masks the rapid distribution phase of IFN and the concentrations demonstrate a mono-phasic decline (Wills et al, 1984; Collins et al, 1985; Mager et al, 2003; Cai et al, 2012). Following 1 h iv infusion administration of 3 MIU/kg a CL_b of 2.75 mL/min/kg, an Vss of 0.2 L/kg and a terminal half life of 2.9 h were observed. Assuming complete bioavailability following subcutaneous administration, the CL determined following iv infusion is comparable to that observed in this study (Wills, Spiegel and Soike, 1984). Following iv bolus and sc administration of recombinant human IFNβ1a a supra proportional increase in systemic exposure (C_{max} and AUC) with increasing dose was observed with both routes of administration, which was due to an apparent reduction in CL/ CL/F and V_{ss} (Mager et al, 2003). The authors hypothesised that the primary route of elimination of IFNβ1a was due to target (or receptor) mediated drug disposition with liver and kidney catabolism and proteolytic degradation also proposed as potential elimination pathways which do not become significant until the dose and corresponding concentrations are high enough to saturate the receptor mediated clearance. This concept is presented graphically in Figure 6.9. The renal clearance/catabolism is present at a constant rate regardless of the concentrations of IFN. As the concentrations of IFN increase and the contribution of the saturable clearance component to the total clearance decreases then so the renal clearance becomes a more significant component of the total clearance. What is worth noting is that following administration of IFN the contribution of clearance will change over time; at low concentrations receptor mediated clearance will dominate whereas at higher concentrations renal clearance will be the main driver of clearance. As the concentrations decline over time, the mechanism of clearance will change back to receptor mediated clearance and therefore increase.

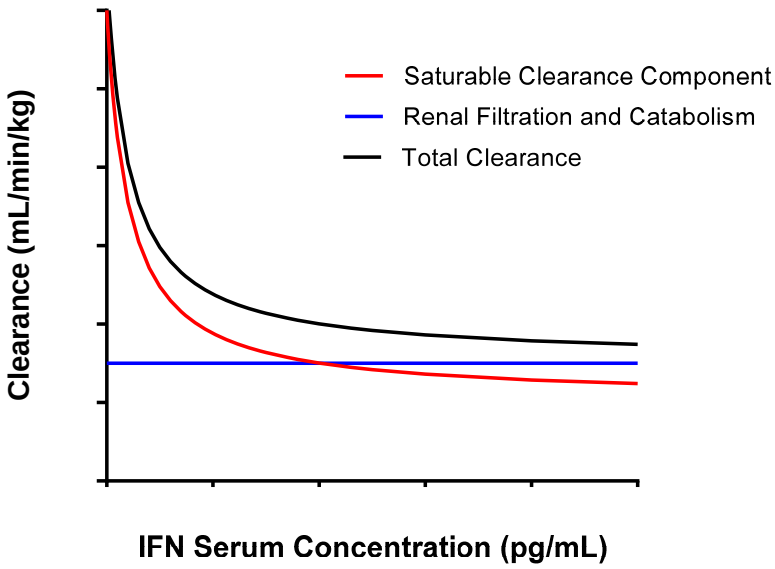

Figure 6.9 **Hypothetical IFN clearance-concentration profiles for a saturable clearance component (Red), renal filtration and catabolism mediated clearance (blue) and corresponding total clearance (black)**

The CL/F for IFNβ1a determined by Mager et al, (2003) is approximately 6 and 2.5 fold higher than that observed at equivalent doses of IFNα2b in this study. The clearance attributed to filtration is likely to be consistent between the two proteins and it has been hypothesised that the variation in clearance across the family of IFNs reflects differences in the natural internal digestion and turnover of these proteins (Wills 1990). For example, it has been suggested that liver catabolism is the predominant pathway of elimination for IFNβ (Gloff and Wills, 1992) and renal elimination for IFNα.

The different elimination pathways suggest that there is the potential for a right shift in the IFNα concentration-receptor mediated clearance curve for IFNα2b to IFNβ1a. This is presented hypothetically in Figure 6.10, at the doses of IFNα2b administered the receptor mediated elimination for IFNα2b is completely saturated, and whereas at the equivalent doses of IFNβ1a the receptor mediated elimination is still on the downward slope of the concentration-clearance curve. As both IFNα2b and IFNβ1a bind to the same receptor, the apparently different concentration response curves for the saturation of receptor mediated clearance could be explained by different affinities of each cytokine to the receptor, which could certainly be feasible as IFNβ and IFNα only share about 30% homology with each

other (Buchwalder et al, 2000). This may explain why in preclinical pharmacokinetic studies of INTON A the primary route of elimination was determined as catabolism in the kidney. The receptor mediated clearance is likely to be saturated at the doses (and corresponding concentrations) investigated in these studies skewing the clearance to renal catabolism as a major route of elimination.

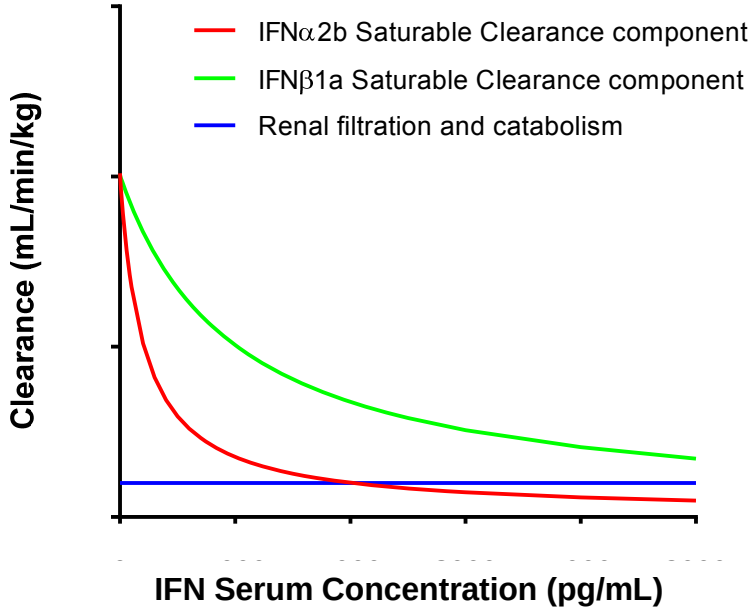

Figure 6.10 **Hypothetical IFN clearance-concentration profiles for IFNα2b (Red) and IFNβ1a (Green) saturable clearance components, and clearance mediated by non saturable renal filtration and catabolism (blue)**

One of the key goals of developing a preclinical PK/PD model is to deliver a model that is translatable to the clinical situation. It is therefore important to understand the pharmacokinetics of the challenge in humans and how it compares to preclinical species. Many researchers have concluded that monkey is the preferred animal to investigate the PK characteristics of IFNs to relate to human (Cai et al, 2012) and the pharmacokinetics appear to be comparable between the two species. In one investigation in healthy volunteers following a 30 min iv infusion, concentrations of IFNα2b declined in a biphasic manner with an initial rapid distribution phase followed by a longer elimination phase with a $t_{1/2}$ of approximately 1.7 h (Radwanski et al, 1987). Also, as observed in the monkey following sc and im administration, a prolonged absorption phase masks the distribution giving a mono-exponential decline with a half life of 2.2-2.9 h (Radwanski et al, 1987). In

another study the pharmacokinetics of INTRON A in healthy volunteers following im administration at 10 MIU (0.14 MIU/kg) were reported. INTRON A had a C_{max} of 6 pg/mL , a T_{max} of 5.2 h, a CL/F of 4.2 mL/min/kg, a V/F 2.6 L/kg and a $t_{1/2}$ of 7.8 h (Rodriguez et al, 2000) all of which are broadly comparable to the pharmacokinetic parameter estimates observed in the monkey in this study. There is evidence to suggest that renal elimination is also the predominant clearance mechanism in humans since the apparent clearance of IFNα in patients undergoing haemodialysis was reduced by 64% and 78% respectively compared with patients with normal renal function (Glue et al, 2000). One important factor that needs to be considered is that recombinant IFNα2b readily induces the formation of neutralising antibodies in animals upon repeated dosing because of species specificity. This would have implications if longer repeat challenge studies were required but should not have an impact with an acute single challenge study such as in this study.

Similar shaped concentration-time profiles to IFNα2b have been observed in healthy volunteers following iv or extravascular administration of the subtypes IFNαA (Wills et al, 1983) and IFNβ1a (Buchwalder et al, 2000). As definitive PK information for these two subtypes has been reported it is possible to draw some conclusions around the translatability between the two species. For IFNβ1a the systemic concentrations were much higher in the monkey, but at the highest dose in human and lowest dose in monkey the clearance was broadly comparable with values of 0.3 and 0.48 L/h/kg despite a 5 fold difference in systemic concentrations. The volume was much lower in the monkey ranging from 0.06 to 0.3 L/kg compared to approximately 1 L/kg in man (Buchwalder et al, 2000, Mager et al, 2003) but was consistent across the doses. Interestingly the bioavailability of IFNβ1a following sc administration in man was 28% which is lower than that reported for IFNα although comparable to that reported in the monkey (33%). A longer T_{max} of 10 h was reported for IFNβ1a in man compared the 3-4 h in the monkey.

For recombinant human IFNαA the clearance determined in the African green monkey following iv 1 h infusion administration at 3 MIU/kg was comparable that determined in man following 0.67 h infusion at 0.5 MIU/kg (Wills et al, 1983; Wills Spiegel and Soike, 1984). However despite comparable clearance there is some evidence that the pharmacokinetics of recombinant IFNαa are different between monkeys and humans. The elimination $t_{1/2}$ was shorter in monkeys (2.9 h) compared to humans (5.1 h) and the V_{ss} was approximately half that observed in humans (0.19 L/kg compared with 0.40 L/kg) (Wills et

al, 1984), as with the studies investigating IFNβ1a it is difficult to make a true comparison between the two species due to the different doses administered.

6.4.2. IFNα2b mediated induction of relevant biomarkers

In this study the effects of IFNα2b treatment was investigated on a large number of biomarkers. A key goal is to deliver a translatable PK/PD model so where possible the biomarkers that were selected have been reported to have relevance to SLE and/or demonstrated effects following IFNα2b treatment in the clinic, such as the IFN gene signature panel. As well as the biomarkers that have a well established link to elevated systemic levels of IFN in the clinic, such as neopterin, the cytokine/chemokine multiplex system allowed the speculative analysis of a large number of cytokines to investigate if there are some potential cytokines of interest that have not previously been considered.

6.4.2.1. Body temperature

Following administration of interferon treatment in the clinic, patients can often develop flulike symptoms, including a fever with an increase in body temperature that generally coincides with peak serum concentrations of IFN (Reddy, 2004). Following iv, sc and im administration of IFNα2b to healthy volunteers a 1°F increase in body temperature, was observed in 100% of subjects for each dose route (Radwanski et al, 1987). In another study following subcutaneous administration of IFNα2b to HCV patients at a dose of 0.05 MIU/kg, a mean peak body temperature of 1 °C over baseline was observed which had returned to baseline between 24 to 36 h post dose in all subjects (Glue et al, 2000). Consequently it was considered that body temperature may offer a simple translatable pharmacodynamic marker of systemic IFNα2b treatment and so was investigated in this study. An increase in rectal body temperature was not apparent in monkeys in this study, and a similar finding has been observed in toxicology studies. No change in body temperature was observed in monkeys following subcutaneous administration of INTRON A at a dose of 3105 $\mu g/m^2$ which is approximately 4 MIU/kg for 1 month and intramuscular administration of INTRON A at doses of 4, 20 and 100 MIU/kg/day for 3 months. Further evidence for a lack of response with regard to body temperature in monkeys following IFN treatment comes from an acute toxicity study investigating IFNα2a in the rhesus monkey where no increase in rectal body temperature was observed following a single im and iv administration at 260

MIU/kg for 8 h post dose despite maximum serum IFN concentrations of approximately 3500000 pg/mL (Toxicologist review – Pegylated ineterferon-α2b, 19 December 2000).

Together this information suggests that with regard to body temperature monkeys may tolerate IFN better than humans thus making it unsuitable as a translatable biomarker of a response to IFN. Within GSK, a dose dependent increase in body temperature has been observed in studies investigating the intranasal administration of TLR7 agonists to cynomolgus monkeys and healthy volunteers. The increase in body temperature in monkeys was observed from 5 h post dose and had returned to baseline by the 20 h post dose (Tsitoura et al, 2015) which generally mirrored the cytokine profile alterations seen over the same time period. What this suggests is that endogenous monkey IFNα has the ability to induce body temperature in the monkeys, but human recombinant IFNα does not. The IFN induced increase in body temperature has been hypothesised to not be related to binding of IFN to the common type I IFN receptor but rather related to the interaction of IFNα to hypothalaimic μ opioid receptors (Garcia-Garcia et al, 2010). It may be that human recombinant IFNα2b does not bind to the monkey μ opioid receptors with the same affinity as the human receptors thus requiring larger systemic concentrations to elicit the same IFNα2b response. Alternatively the monkey and human μ opioid receptors may not share sufficient homology for recombinant IFNα2b to bind to and elicit a change in body temperature.

6.4.2.2. Cytokines/Chemokines

The 29 cytokines/chemokines that were investigated can be categorised as follows; 1) those that show a clear response to IFNα 2) those that potentially show a response to IFNα 3) those where measurable concentrations were observed but showed no response to IFNα and 4) those where no measurable serum concentrations were determined. For a number of cytokines, such as IP10 and IL7, it was difficult to make an assessment whether a dose response has been observed. In these cases more monkeys had measurable serum concentrations following IFNα2b compared to vehicle suggesting there may be some response. However the concentrations of cytokines observed following IFNα2b treatment at 3 MIU/kg and 10 MIU/kg were broadly comparable, and often in the case of Monkey 3 comparable to those observed following vehicle treatment. Also the variability observed in the serum concentrations of many of the cytokines between individual monkeys at each dose also makes it difficult to determine if there was a true response to IFNα2b treatment.

Measurable concentrations of the majority of the cytokines were observed in monkey 3 even when little to no measurable concentrations were observed in other monkeys. Also, monkey 3 often demonstrated higher concentrations than other monkeys when measurable cytokine concentrations were observed and therefore this monkey was considered a high responder. One question that arises is whether monkey 3 is truly a high responder or may have had an underlying infection or illness that could have resulted in elevated cytokine/chemokine response as often elevated levels were observed following vehicle treatment. All monkeys underwent a health screen prior to the start of the study which included complete blood count as well as blood chemistry analysis which included markers such as aspartate aminotransferase and alanine transaminase amongst others. Although all levels were within the normal range and did not preclude any animal being included on the study it does not rule out there could potentially be underlying factors that may have had an impact on the observed cytokine levels.

The cytokines/chemokines IL15, IL1Ra, eotaxin, MCP1 and IL6 were induced following IFNα2b treatment, although generally a less than proportional increase in both C_{max} and AUC were observed with the increase in IFNa2b dose from 3 MIU/kg to 10 MIU/kg. The closest to a dose proportional increase in systemic exposure was observed for IL6 for both C_{max} and AUC and eotxain for C_{max}. All five cytokines/chemokines have relevance to SLE; elevated circulating levels of IL15, IL6 and IL1Ra have been observed in patients with active disease and SLE patients who flared generally had higher baseline plasma levels of Eotaxin and MCP1. Each of these cytokines/chemokines has the potential to be of value to investigate the efficacy of treatments of SLE and has the potential to be a translatable biomarker. Each of these cytokines/chemokines will be expanded on briefly below

IL15 is expressed in a wide variety of cell types including activated monocytes, differentiated antigen-presenting cells and phagocytes such as dendritic cells and macrophages (Ruckert et al, 2009). Studies have demonstrated that following viral infection, as well as an increase in IFNα concentrations, an increase in IL15 receptor α (IL15Rα) on dendritic cells was observed suggesting that these cells play an important role in the production of IL15 (Richer et al, 2015). Although it should be noted modest increases in IL15Rα were also observed on monocytes/macrophages and B cells. IL15 has been demonstrated to be an essential cytokine in the development and survival of NK cells and NKT cells (Ohteki et al, 2001), and basal levels of IL15 have been reported to have a role in

the homeostatic maintenance of memory $CD8^+$ T cells (Richer et al, 2015). Elevated levels of IL15 have been found *in vivo* during chronic inflammatory disorders and autoimmune disorders (Lauw et al, 1999) and it is considered likely that IL15 contributes to T cell mediated immunopathology (Ruckert et al, 2008). IL15 serum levels are elevated in patients with RA and this increased concentration correlates with disease activity, and also the blockade of IL15 prevents collagen induced arthritis in the mouse. More importantly, serum levels of IL15 are elevated in approximately 40% of patients with SLE and levels correlated consistently with lymphocyte Bcl-2 (an antiapoptotic protein elevated in SLE patients) (Aringer et al, 2001). Despite this, researchers have concluded that IL15 is not directly associated with disease activity, but may be involved in tuning the immune system towards autoimmunity. Its actions may impact on the exacerbation and the perpetuation of the disease activity of SLE, and due to this it could offer another translatable biomarker for SLE that can be investigated in the primate model.

IL1Ra is a member of the IL-1 family and is secreted by many cells of monocyte and macrophage lineage (Suzuki, Takemura and Kashiwagi, 1995). Its role is to regulate IL1 activity in inflammatory and immunologic disorders. It is stimulated by immune complexes which are known to be elevated in SLE, and researchers have observed elevated concentrations of circulating IL1Ra in patients with active disease and strong correlation between IL1Ra concentration and clinical activity of SLE.

MCP1 (monocyte chemoattractant protein-1), also known as CCL2, is a potent chemotactic factor for monocytes that is produced by a variety of cells types either constitutively after induction by oxidative stress, cytokines or growth factors. Monocytes and macrophages are considered to be the main producers of MCP1 which regulates the migration and infiltration of monocytes, macrophages T cells and NK cells (Deshmane et al, 2009). An increase in serum MCP1 has been reported to occur with the progression of disease activity in SLE patients compared to healthy controls, and elevated plasma levels are observed in SLE patients even in the absence of symptoms. It can be easily measured in the urine so offers the potential as an attractive biomarker as levels of MCP1 in the urine of patients with SLE correlated directly with the SLEDAI score, and was elevated in patients with severe disease compared to mild disease (Barbado et al, 2012). Interestingly IL15 has been demonstrated to induce the production of MCP1 by monocytes (Budagian et al, 2006) and so it could be that in this model it is IL15 rather than IFNα that is inducing the systemic

concentrations of MCP1. However, contradictory to this hypothesis the T_{max} for both cytokines is comparable around 4 to 6 h and arguably the T_{max} for MCP1 earlier than observed for IL15 suggesting that it is more likely that IFNα is driving the MCP1 response than IL15. Although MCP1 has the potential to be a useful biomarker a number of caveats have been highlighted during *in vivo* studies within GSK which temper the interest as MCP1 as a biomarker to predict efficacy of drugs in disease models. Elevated levels have been observed in vehicle animals which are believed to be due to *in vivo* procedure related damage to certain cells. Delivery of a challenge results in exacerbation of this effect and significantly higher systemic concentrations than would be expected. This makes the relevance of systemic concentrations of MCP1 in these models to the clinic questionable. In addition, serum concentrations of MCP1 are highly sensitive to the assay used. This would not be an issue if a standard approach could be used within the preclinical environment and clinical environment; however this is not always possible and so may confound the understanding of any response.

Eotaxin also known as CCL11 is a chemokine that plays an important role in eosinophilic infiltration and is involved in both chemotaxis of eosinophils to the inflammatory site and induction of eosinophil degranulation and super oxide anion generation (Sato et al, 2003). The induction of eotaxin secretion by the cytokines IL4, IL13, IL1, TNFα is well established as well as the role IFNγ plays in the modulation of this induction. Little to no measurable concentrations of these cytokines were observed in this study suggesting that another pathway or cell type (previous investigations utilised mouse embryonic fibroblasts) may be involved in the production of eotaxin in this model.

IL6 is a cytokine expressed by a wide variety of cells including mononuclear phagocytes, T cells, B cells, fibroblasts, endothelial cells, kerationcytes, hepatocytes and bone marrow cells (Turner et al, 2014). It has a wide range of functions and is involved in T cell activation, differentiation and regulation of Th2 and Treg phenotypes, maturation of B cells into antibody producing plasma cells and the secretion of acute phase proteins from the liver. Higher levels of IL6 have been observed in the sera from SLE patients with active and inactive disease compared to healthy controls, with higher levels observed in the patients with active disease compared to inactive disease (Linker-Israeli et al, 1991; Ripley et al, 2005). Further *in vitro* studies using the sera from SLE patients demonstrated that IL6 has an important pathogenic role in the B cell hyperactivity observed in SLE. The IL6 receptor

signalling involves the activation of JAK1 so in the context of this model to investigate JAK1 inhibitors as potential therapies for SLE it may offer an option to investigate the inhibition of further biomarkers downstream of IL6 receptor activation. This could allow a complex systems biology type model to be developed with multiple cytokines and inhibition sites and potential adverse events incorporated which may be powerful in the selection of certain therapies and dosing regimes in the clinic depending on what pathway to target.

As well as the disease relevance of these cytokines they have been shown to be induced by IFNα in a number of *in vitro* and i*n vivo* studies reinforcing the apparent relationship observed in this study. In *in vitro* studies using human DCs, stimulation with IFNα induced concentrations of both IL15 and IL6 in the supernatant (Jinushi et al, 2003). The concentrations of both IL15 and IL6 determined *in vitro* were comparable to those observed *in vivo* in this study at ~70 pg/mL and ~170 pg/mL respectively. Despite comparable concentrations it is difficult to draw comparison as the IFNα challenge used in the *in vitro* study was ~360000 pg/mL for 24 h which is approximately 20 fold higher than the mean C_{max} for IFNα observed in this study. Interestingly IL15 stimulation (50 ng/mL) of DCs in vitro for 24 h resulted in large induction of IFNα approximately 200-250 pg/mL which was significantly reduced the presence of an IFN receptor antibody (Jinushi et al, 2003). This may indicate that the interplay between the cytokines in this model may be more complex than simply the induction of certain cytokines by IFNα. Conversely to this studies using human pDCs stimulated *in vitro* with TLR7 and TLR7/8 agonists for 4 h did not produce increased levels of MCP1 protein compared to vehicle or demonstrate induction of MCP1, Eotaxin or IL1Ra genes despite increase in IFNα production (Birmachu et al, 2007). Although in support of the data generated in this study IL6 was induced. It may be that with the exception of IL6 the other cytokines and chemokines are upregulated later than 4 h which is supported by the work in this study where for IL1Ra, eotxain and MCP1 the T_{max} were generally observed between 4-8 h post challenge and for IL6 the T_{max} was earlier at 2-6 h post challenge.

6.4.2.3. Neopterin

In this study following IFNα2b treatment the induction of systemic neopterin concentrations compared to vehicle treatment was observed at both doses, although only a small increase in systemic neopterin concentrations was observed with an increase in the

dose from 3MIU/kg to 10 MIU/kg. A similar response to IFNα2b treatment to primates has been reported in the literature (Zhang et al, 2008) where following im administration of IFNα2b at a dose of 3 MIU/kg, serum neopterin concentrations began to increase 6h after injection and reached a peak of approximately 10000 pg/mL around 24 h post dose and returned to baseline approximately 288 h post dose. Peak concentrations of IFNα2b and neopterin were positively correlated i.e. concentration response, and a change in neopterin concentrations is in fact a reflection of a change in the IFN concentration. A neopterin response was observed in the clinic following administration of IFNα2b at 3MIU/kg with maximum concentrations of approximately 22000 pg/mL (Glue et al, 2000), although the neopterin concentration-time profile was not presented so it is not possible to comment on the kinetics of the response in humans. It has however been reported in the clinic that neopterin levels in urine reach a plateau following administration of approximately 1 MIU of IFNα2b and further increase in dose does not increase neopterin levels (Fuchs et al, 1992). In the clinical trial investigating the JAK inhibitor compound following IFNα2b challenge (Kahl et al, 2016) elevated levels of neopterin were observed which were successfully inhibited with the JAK1 inhibitor. The induction of serum neopterin concentrations has been investigated following iv and sc IFNβ1a challenge in monkeys (Mager et al, 2003) and following iv, im and sc IFNβ1a challenge in humans (Buchwalder et al, 2000). Following iv and sc administration in monkeys at doses of 1, 3 and 10 MIU/kg serum neopterin concentrations increased in a less than proportional manner with increasing dose. The C_{max} observed following each dose was comparable between the route of administration (10000 pg/mL, 13000 pg/mL and 20000 pg/mL) although an earlier T_{max} was observed following iv administration compared to sc administration (30 vs 50 h post dose) which reflects the earlier IFN1βa T_{max} observed following iv administration compared to sc administration. In general the plasma neopterin concentrations had not returned to baseline by the T_{last} which was 100 h post dose. In human following iv administration of IFNβ1a at 6, 12 and 18 MIU comparable systemic neopterin concentrations were observed with all three doses with a C_{max} of around 30000 pg/mL observed at a T_{max} of 24 h post dose. Following sc administration at 18 MIU (equivalent to 0.25 MIU/kg assume a body weight of 70 kg) comparable maximum serum concentrations were observed at a comparable T_{max} to iv administration at the equivalent dose. This suggests that humans are more sensitive to IFN1βa with regard to neopterin induction as greater systemic neopterin concentrations are observed with a lower dose and consequently lower systemic concentrations of IFN1βa. It

also appears the neopterin response is faster in humans compared to monkeys with the T_{max} following sc administration almost 30 h later in monkeys compared to humans. Despite differences in the apparent PK/PD relationship of IFN1βa induction of neopterin concentrations between monkey and human translatable in silico PK/PD models have been developed that successfully characterise the induction of neopterin in monkey and man with only minor scaling of certain species specific parameters (Mager and Jusko, 2002; Mager et al, 2003; Kagan et al, 2010)

The reported success in PK/PD modelling of the IFN1βa induction of neopterin concentrations in monkeys and humans suggests that neopterin has potential as a translatable biomarker that may be used to predict clinical efficacy in preclinical models. In addition neopterin has been shown to be a biomarker of disease activity in SLE in a number of studies. In one such study authors investigated 52 SLE patients using the The index of European Consensus Lupus activity measurement (ECLAM) index and demonstrated that most markers including neopterin correlated with disease and is a useful independent marker for disease activity in SLE (Samsonov et al, 1995). In another study neopterin concentrations in SLE patients ranged from approximately 1000 pg/mL to 18000 pg/mL (median of 3000 pg/mL) with 45% of SLE patients presenting neopterin concentrations higher than the 95th percentile of healthy subjects (Widner et al, 2000). Finally neopterin levels have been shown to decrease in patients in whom corticosteroid therapy has demonstrated clinical improvement, suggesting it may be a useful marker for monitoring efficacy of medication (Fuchs et al, 1992). Neopterin is a marker of immune cell activation and as all the immune cells have been implicated in SLE disease progression in one way or another it is unsurprising that elevated levels are observed in patients with the disease making it a biomarker for predicting disease in the clinic. This does however not necessarily make it a suitable biomarker for acute challenge models predicting clinical efficacy from preclincal models. One concern with using neopterin as a biomarker is that it is only observed in monkey and humans and is not measurable in other preclinical species such as mouse and rat (Duch et al, 1984) which means that it will not have utility as a biomarker from early screening studies through to the clinic.

Although neopterin was a primary biomarker investigated in this study it was necessary to review the cytokine induction profile prior to reviewing the neopterin response in an effort to understand what may be driving the induction of neopterin. Neopterin is primarily

produced by macrophages upon stimulation by IFNγ, however in this study following IFNα2b treatment systemic concentrations of IFNγ were broadly comparable between treatment groups, suggesting little to no response to IFNα2b treatment. It should be noted that despite concentrations being comparable, more monkeys demonstrated measurable serum concentrations if IFNγ following IFN treatment at each dose than vehicle treatment. In the absence of measurable concentrations of IFNγ in treated monkeys three questions arise. Firstly what is stimulating the production of neopterin if it is not IFNγ? And secondly what cells are releasing the neopterin? A similar situation has been observed in the clinic where hepatitis C patients treated with high doses of IFNα2b demonstrated elevated levels of neopterin without an elevation in IFNγ (Murr et al, 2002). As a large number of cytokines were screened it was hoped that this may provide an indication around the pathways behind the IFNα2b induction of neopterin. In an ideal scenario this may allow a systems biology type approach incorporating several cytokines/chemokines and or pathways in one model to describe the induction of neopterin, by which, it may give a better indication of how a NCE under investigation in the model is eliciting any observed inhibition of neopterin.

Monocytes/macrophages stimulated with IFNγ produce 180% neopterin compared to immature or stimulated DCs (Wirleitner et al, 2002). Despite the evidence indicating IFNγ as the major inducer of neopterin production, high levels of neopterin have been observed in patients with an impairment of the IFNγ pathway (Sghiri et al, 2005). In clinical studies, it was observed that neopterin levels are increased in patients with the following receptor deficiencies IFNγ R1D, IFNγ R2D, IL12p40d and IL12Rb1D, which demonstrates that the levels of serum neopterin are increased *in vivo*, in patients where no effect of IFNγ is possible due to complete absence of expression of its receptor (Sghiri et al, 2005). IFNα certainly has pleiotropic effects on various cell types in the immune systems such as macrophages, NK cells, and T cells (Kadowaki et al, 2000) and the IFNAR is found on most cell types (De weerd and Nguyen, 2012). In this model it may therefore be that IFNα is having a direct effect on macrophage, supporting this hypothesis, the induction of neopterin release in response to IFNα has been described in monocytes and macrophages *in vitro* (Wirleitner et al, 2002). Despite this evidence, the contribution of IFNα to the induction in neopterin from macrophages *in vivo* is questionable. *In vitro* studies investigating the ability of various IFNs to stimulate macrophages concluded that IFNγ is the

most potent inducer of neopterin release, and approximately 1000 fold higher IFNα concentrations are required to deliver a comparable neopterin response (Huber et al, 1984). Based on this other researchers have speculated that as the high levels of IFNα required to obtain neopterin release from macrophages are unlikely to be reached under *in vivo* conditions.

Although macrophages have been identified as the major type of human cell that produces neopterin when they are stimulated *in vitro* with IFNγ (Sghiri et al, 2005) a large number of immune cells also produce neopterin. In this model the increase in neopterin concentrations may be due to secretion by dendritic cells stimulated by IFNα (Sghiri et al, 2005). In support of this *in vitro* studies have demonstrated that cultured monocyte derived DC are a rich source of neopterin, and neopterin production induced by IFNα was 150% in immature DC and 200% in stimulated DC compared with monocytes/macrophages (Wirleitner et al, 2002). It can therefore be concluded that at least a portion of the neopterin observed in the primate is coming from IFNα induced DCs.

One further potential factor that is worth considering is whether one of the cytokines induced by IFNα may drive at least some of the induction of serum neopterin concentrations. A delay is observed between IFNα administration, systemic IL15 concentrations and subsequent neopterin concentrations. It may therefore be questioned if IL15 is part of the pathway that results in the induction of neopterin concentrations following IFNα challenge. It has been reported that IL15 is not essential for macrophage differentiation but strongly induces macrophage activation in vivo (Ruckert et al, 2008). As neopterin is a marker for immune cell activation it may be that activation of macrophages by IL15 results in the production of neopterin from these cells.

6.5. Conclusion

In this study the pharmacokinetics of IFNα2b in the monkey were successfully determined following subcutaneous administration at two different dose levels. The pharmacokinetics were broadly comparable to those reported in the literature, and both the apparent clearance and volume increased in proportion to the increase in dose. As IFNα2b demonstrated linear pharmacokinetics over the investigated dose range it can be concluded that the receptor mediated clearance had become saturated and the clearance was driven by renal elimination and catabolism. The induction of serum neopterin

concentrations, a marker of immune cell activation, compared to vehicle controls was observed following IFNα2b treatment, although a less than proportional increase in serum neopterin concentrations were observed with the increase in dose. With the absence of measurable concentrations of IFNγ it is hypothesised that neopterin is being produced by dendritic cells following direct stimulation by IFNα2b. As well as neopterin, elevated levels of the cytokines/chemokines IL15, IL6, MCP1, eoxtaxin and IL1Ra which have all been implicated in the pathogenesis of SLE, were also observed in the challenged primates. This has therefore provided a number of clinically relevant biomarkers to enable further PK/PD modelling.

Chapter 7: Development of a population PK/PD model to describe the induction of serum concentrations of 6 biomarkers in monkeys following an IFNα2b challenge.

7.1. Introduction

Population modelling of the PK/PD relationship for the induction of various cytokines following treatment with recombinant IFNα to the male cynomolgus monkey can be approached in two different ways. Firstly, Mager et al, (2003) and Kagan et al, (2010) successfully used a target mediated drug disposition model (TMDD) to describe the pharmacokinetics of Type I IFNs over a dose range in both the monkey and man (as described in Chapter 2). However when systemic concentrations of IFNα are high, the pharmacokinetics become linear and therefore can be described using standard compartmental PK models. Both the TMDD model and the compartmental PK model can be coupled with the same PD model to describe the response. As hysteresis is observed between IFNα concentrations and the subsequent concentrations of various biomarkers of interest such as neopterin (Jusko and Mager, 2003) then, as with the PK/PD modelling of the mouse data (Chapter 5), an indirect response model would appear to be the most suitable choice to describe the PK/PD relationship.

This chapter will describe the investigation of a population PK/PD model to describe the IFNα2b induction of a number of biomarkers in the cynomologus monkey. NCA of the IFNα2b serum concentration-time data in the monkey presented in Chapter 6 indicates that the pharmacokinetics of recombinant IFNα2b are linear over the dose range of 3 MIU/kg and 10 MIU/kg. Since lower doses that enabled the observation of the non-linear kinetics were not administered in this study, there is potentially insufficient information to estimate the parameters of the TMDD model. Consequently, this study will first use a traditional population compartmental PK model. Following this, the IFNα2b induction of serum concentrations of the biomarkers neopterin, IL15, IL6, MCP1 and eotaxin will be described using the fixed population PK parameters with an indirect response model with stimulation of input. The derived model parameters were then used to simulate the effect of hypothetical inhibitor acting downstream of the IFNAR, such as a JAK inhibitor on the observed IFNα2b induction of various biomarkers. This allows an investigation of the predicted inhibition of the cytokines with an inhibitor with typical target properties from a drug discovery program.

Parameter estimates are available from the PK/PD modelling of the induction of neopterin by Type I IFNs in the monkey using a TMDD model incorporating an indirect response model (Mager et al 2003; Kagan et al 2010). As an addition to the PK/PD modelling

described above these parameters will be used with the model described in the literature to conduct simulations of the IFNα2b and neopterin serum concentration time profiles following subcutaneous administration at 3 MIU/kg and 10 MIU/kg. These can then be compared to the data derived in this study. The Mager et al (2003) and Kagan et al (2010) models are applicable to describe the IFNα2b induction of neopterin observed in this study as a number of the parameters are system specific so will be applicable across the Type I IFN subtype investigated. However there are a number of parameters that are drug specific and these may require some optimisation to give the best fit of the data derived in this study.

7.2. Methods

7.2.1. Modelling Strategy

The modelling strategy to describe the PK/PD relationship of the induction of selected biomarkers by IFNα2b was conducted as described for the mouse PK/PD modelling in Chapter 5. Briefly, the modelling was conducted in two stages, with the serum concentration time profiles for IFNα2b following sc administration described with a PK model to determine the PK parameters following which the PK parameters were fixed and the PD parameters for the biomarker response following administration of IFNα2b were estimated. All data were analysed with a population approach using nonlinear mixed effects modelling.

7.2.2. Population Pharmacokinetic modelling of IFNα2b serum concentration-time data

The serum concentration-time profiles for IFNα2b following subcutaneous administration at 3 and 10 MIU/kg to monkeys were analysed using both 1 compartment and 2 compartment models described using the ADVAN 2 (1 compartment) TRANS2 parameterisation and ADVAN 4 (2 compartment) TRANS4 parameterisation sub-routines with the NONMEM (Beal et al, ICON Development Solutions) library. Equations 7.1 and 7.2 describe a 1 compartment PK model with first order input and Equations 7.3, 7.4 and 7.5 describe a 2 compartment PK model with first order input.

Equation 7.1

$$\frac{dA_D}{dt} = -A_D * k_a$$

$$A_D(0) = D_{SC}$$

Equation 7.2

$$\frac{dA_S}{dt} = k_a * A_D - A_S * k_{10}$$

$$A_S(0) = 0$$

$$C_S = \frac{A_S}{V}$$

$$k_{10} = \frac{Cl}{V}$$

Where D_{sc} is the subcutaneous dose, k_a is the absorption rate constant, A_D is the amount in the dosing compartment, $A_D(0)$ is the administered dose, A_S is the amount in the serum, $A_S(0)$ is the amount in the serum at time 0, C_S is the concentration of IFNα2b in the serum, V is the volume of the central compartment (Compartment 1), CL is the clearance and k_{10} is the elimination rate from the body (h^{-1}).

Equation 7.3

$$\frac{dA_D}{dt} = -A_D * k_a$$

$$A_D(0) = Dsc$$

Equation 7.4

$$\frac{dA_S}{dt} = k_a * A_D + A_T * k_{21} - A_S * k_{10} - A_S * k_{12}$$

$$A_S(0) = 0$$

$$C_S = \frac{A_S}{V}$$

$$k_{10} = \frac{Cl}{V}$$

$$k_{12} = \frac{Q}{V}$$

$$k_{21} = \frac{Q}{V_T}$$

Equation 7.5

$$\frac{dA_T}{dt} = A_S * k_{12} - A_T * k_{21}$$

$$A_T(0) = 0$$

Where D_{sc} is the subcutaneous dose, k_a is the absorption rate constant, A_D is the amount in the dosing compartment, $A_D(0)$ is the administered dose, A_S is the amount of IFNα2b in the central or serum compartment (Compartment 1) (ng), $A_S(0)$ is the amount in the serum at time 0, A_T is the amount of IFNα2b in the peripheral or tissue compartment (Compartment 2)(ng), $A_T(0)$ is the amount in the tissue at time 0, k_{12} and k_{21} are the inter-compartmental rate constants which determine the rate of drug movement from the central to the peripheral compartment and back (h^{-1}), k_{10} is the elimination rate from the serum (h^{-1}), C_S is the concentration of IFNα2b in the serum (ng/mL), V is the volume of the central compartment (mL) and V_T is the volume of the peripheral or tissue compartment (mL).

The inclusion of inter-occasion variability (IOV) greater than 0 in different parameters improved the model's ability to describe the observed data. IOV was described by an exponential model (Equation 7.6) (Karlsson and Sheiner, 1993)

Equation 7.6

$$P_i = \theta * \exp(\eta_i)$$

$$P_{ij} = P_i * \exp(\kappa_j)$$

Where θ is the typical population value for the parameter, P_i is parameter value of the *i*th inidviudal, η_i is the random derivative of P_i from θ, $P_{i\,j}$ is the parameter value of the *i*th inidviudal at the *j*th occasion and κ_j is the random deviation of P_{ij} from $P_{i.}$ The values of η_i and κ_j were assumed to be log-normally distributed, with mean a mean of zero and a variance of ω^2 and π^2 respectively. The η model represents the between individual differences and the κ model represents the between occasion differences within an individual. The determined variance was converted to a coefficient of variation (CV).

7.2.3. Population Pharmacokinetic/Pharmacodynamic modelling to describe the induction of serum neopterin and IL15, IL6, MCP1, IL1Ra and Eotaxin concentrations following administration of an IFNα2b challenge.

The PK/PD relationship of an induction of serum concentrations of neopterin, IL15, IL6, MCP1, IL1Ra and eotaxin following sc administration of IFNα2b were described using an indirect response model (stimulation of input) (Dayneka et al, 1993). The modelling was conducted using the ADVAN 6 TRANS 1 sub-routine within the NONMEM (Beal et al, ICON Development Solutions) library and was described by equation 7.7. The PK parameters (CL/F, V/F, Q/F, V_T/F and K_a) for each individual were fixed to the population parameter estimates including IIV on CL/F and IOV on V/F determined from the previous PK modelling.

Equation 7.7

$$\frac{dC_{biomarker}}{dt} = k_{in} * \left(1 + \frac{E_{max} * C}{EC_{50} + C}\right) - k_{out} * C_{biomarker}$$

$$k_{in} = Baseline\ C_{biomarker} * k_{out}$$

Equation 7.7 describes the induction of serum biomarker concentrations by IFNα2b, where k_{in} (ng/mL/h) represents the zero-order constant for production of the response, k_{out} (h^{-1}) defines the first-order rate constant for loss of the response, $C_{biomarker}$ is the response (induction of biomarker serum concentration) (ng/mL), C is concentration of drug (IFNα2b, ng/mL), EC_{50} is the drug concentration in the serum/central compartment (ng/mL) which produces 50% of the maximum stimulation and E_{max} describes the effect of the drug on k_{in}. Models were tested with and without IIV.

A visual predictive check was conducted using the package deSolve in R incorporating the PK/PD model parameters and both inter-individual and inter-occasion variability from the final PK/PD model. The IFNα2b, neopterin and IL15 concentration-time profiles were simulated for 1000 individuals at IFNα2b doses of 3MIU/kg and 10 MIU/kg and compared to the observed data.

7.2.4. Population Pharmacokinetic/Pharmacodynamic simulations to investigate the impact on the IFNα2b induction of the serum concentrations of neopterin, IL15 and IL1Ra by the pan JAK inhibitor Xeljaz™ (tofacitinib)

Simulations were conducted using the package deSolve in R incorporating the PK/PD model parameters, and both inter-individual and inter-occasion variability derived from PK/PD

modelling described above. The PK/PD model is described by equations 7.8, with the pharmacokinetics of IFNα2b described by equations 7.3 to 7.5 and the pharmacokinetics of the inhibitor defined by equations 7.9 and 7.10.

Equation 7.8

$$\frac{dC_{biomarker}}{dt} = k_{in}\left(1 + \frac{E_{max} * C}{EC_{50} + C}\right) * \left(1 - \frac{I_{max} * CI^{Hill}}{IC_{50}^{Hill} + CI^{Hill}}\right) - k_{out} * C_{biomarker}$$

Equation 7.8 describes the induction of serum biomarker concentrations by IFNα2b and the predicted inhibition of serum biomarker concentrations by the pan JAK inhibitor toficitinib. The model is as described previously (equation 7.7) with the addition of the following parameters; *CI* is concentration of inhibitor in the central compartment (ng/mL), IC_{50} is the inhibitor concentration in serum/central compartment (ng/mL) which produces 50% of the maximum stimulation, I_{max} describes the effect of the inhibitor on k_{in}, and *Hill* is the sigmoidicity constant of the steady-state concentration-response relationship.

Equation 7.9

$$\frac{dAI_D}{dt} = -AI_D * Ik_a$$

$$AI_D(0) = IDpo$$

Equation 7.10

$$\frac{dAI_S}{dt} = Ik_a * AI_D - AI_S * Ik_{10}$$

$$AI_S(0) = 0$$

$$Ik_{10} = \frac{ICl}{IV}$$

$$CI_S = \frac{AI_S}{IV}$$

Equations 7.9 and 7.10 describe the concentrations of the inhibitor (toficitinib) in the central compartment, where ID_{po} is the oral dose, Ik_a is the absorption rate constant, AI_D is the amount in the dosing compartment, $AI_D(0)$ is the administered dose, AI_s is the amount of inhibitor in the serum, $AI_S(0)$ is the amount if inhibitor in the serum at time 0, CI_S is the

concentration of inhibitor in the serum, *IV* is the volume of the central compartment (Compartment 1), *ICL* is the inhibitor clearance, and Ik_{10} is the elimination rate from the body (h^{-1}).

Simulations were conducted using the final parameter estimates including IIV determined from the PK/PD modelling for neopterin IL15 and IL1Ra. The pharmacokinetics of tofacitinib in the monkey have been reported following iv and oral administration at 3 and 5 mg/kg respectively (Flannigan et al 2010) and were as follows CL_b 18 mL/min/kg, V_{ss} 1.7 L/kg, bioavailability (F) 48%. Flannigan et al (2010) did not report whether tofacitinib displayed mono or bi-phasic kinetics in the monkey so for all simulations a 1 compartmental PK model with first order input was used. In addition the PK and PD parameters for IFNα2b and the various biomarkers were derived from serum-concentration time data whereas the reported PK parameters for tofacitinib were derived from blood. As the blood:serum ratio for tofacitinib is unknown it was assumed to be 1 in the simulation.

For the indirect response model the Hill slope was set to 1 for all simulations. The IC_{50} was set to 44 nM or 13772 pg/mL (assuming a MW of 313 for toficitinib, Paniagua et al, 2005) derived in an *in vitro* human whole blood study investigating the inhibition of IFNα signalling in $CD3^+$ T cells by toficitinib (Meyer et al, 2010). For simulations the dose response of toficitinib was investigated with doses over a range of 0.01 to 10 mg/kg.

7.2.5. Pharmacokinetic/Pharmacodynamic simulations using published TMDD models to predict the serum IFNβ1a and serum neopterin concentration-time profiles.

Simulations were conducted using the package deSolve in R. The differential equations and derived model parameters for the TMDD model presented by Kagan et al (2010), were used to simulate the induction of serum neopterin concentrations by IFNβ1a. The simulated IFN and neopterin concentration-time profiles were compared to those presented by Kagan et al (2010) which were digitised (with permission) using Plot digitizer software (version 2.6.2), to validate the ability of the model and parameters with a different software and user to replicate the presented IFN and neopterin concentration-time profiles.

Following validation the TMDD model presented by Kagan was adjusted to simulate IFNα2b following sc administration. The value for K_a determined from the population PK modelling for IFNa2b in the monkey (described above) was incorporated into the model. The

simulated IFNα2b and neopterin profiles following 3 MIU/kg were adjusted to pg/mL using the MW and compared to the observed data.

7.3. Results

7.3.1. Population Pharmacokinetic modelling of IFNα2b concentration-time data

A summary of the various models investigated to determine the population pharmacokinetic parameters of IFNα2b in the monkey is presented in Table 7.1. The reference model relates to the model that subsequent models were compared to.

The 2 compartmental model gave a better description of the observed data compared to a 1 compartmental model, which was reflected both in the difference in the MVOF between models 1 and 5 and also visual inspection of the diagnostic plots. Overall a two compartment model with IIV on CL (model 6) best described the IFNα2b serum concentration-time profile. This model provided a significant difference in the MVOF of -18 ($p<0.001$) compared to model 5. Inclusion of IOV on CL gave a statistically significant reduction in the MVOF compared to model 6 with only IIV on CL, however the value for IIV was $<3x10^{-5}$ when IOV was included. The addition of IOV on V together with IIV on CL (model 11) gave a significant reduction in MVOF compared to model 6 and values for both omegas could be estimated therefore model 11 was deemed to best describe the IFNα2b serum concentration-time profile.

The goodness of fit plots and the observed, PRED and IPRED vs. time profiles are presented in Figures 7.1 and 7.2. In all goodness of fit plots the data points appear randomly distributed around the line of unity. The model tended to under predict high concentrations particularly >7000 pg/mL, but gave a good prediction of the concentrations <5000 pg/mL. For the CWRES vs. population predicted concentrations and time, data are randomly distributed with no obvious patterns or bias, centred around zero and with majority of points falling within a value of +/- 2.

Table 7.1 PK modelling summary

Model Number	Model Description	Reference model	MVOF	diffMVOF	CV step completed
1	1CMT	-	2320	-	Y
2	1CMT with IIV on CL	1	2234	-85	Y
3	1CMT with IIV on V	1	2278	-41	Y
4	1CMT with IIV on k_a	1	2278	-41	Y
5	2CMT	1	2236	-84	Y
6	2CMT IIV on CL	5	2217	-18	Y
7	2CMT with IIV on V	5	2235	-1	Y
8	2CMT with IIV on k_a	5	2235	-1	Y
9	2CMT IIV on CL and V	5	2216	-19	Y
10	2CMT IIV on CL and IOV on CL	6	2181	-36	N
11	2CMT IIV on CL and IOV on V	6	2187	-30	Y

CMT= Compartment

The model gave a good description of the overall shape of the observed concentration time profile in all animals, including monkeys 3 and 4 that demonstrated an extended terminal phase following administration of 10 MIU/kg IFNα2b. The model tended to under predict the C_{max}, particularly for monkey 3 with 3MIU/kg and monkey 8 with 10 MIU/kg, but gave a good description of the terminal phase in all monkeys. For the majority of animals there was little difference between the population and individual concentration-time profiles, although the addition of IIV on CL and IOV on V did allow a better prediction of the terminal phase in some monkeys, particularly monkey 3 following of 3MIU/kg IFNα2b.

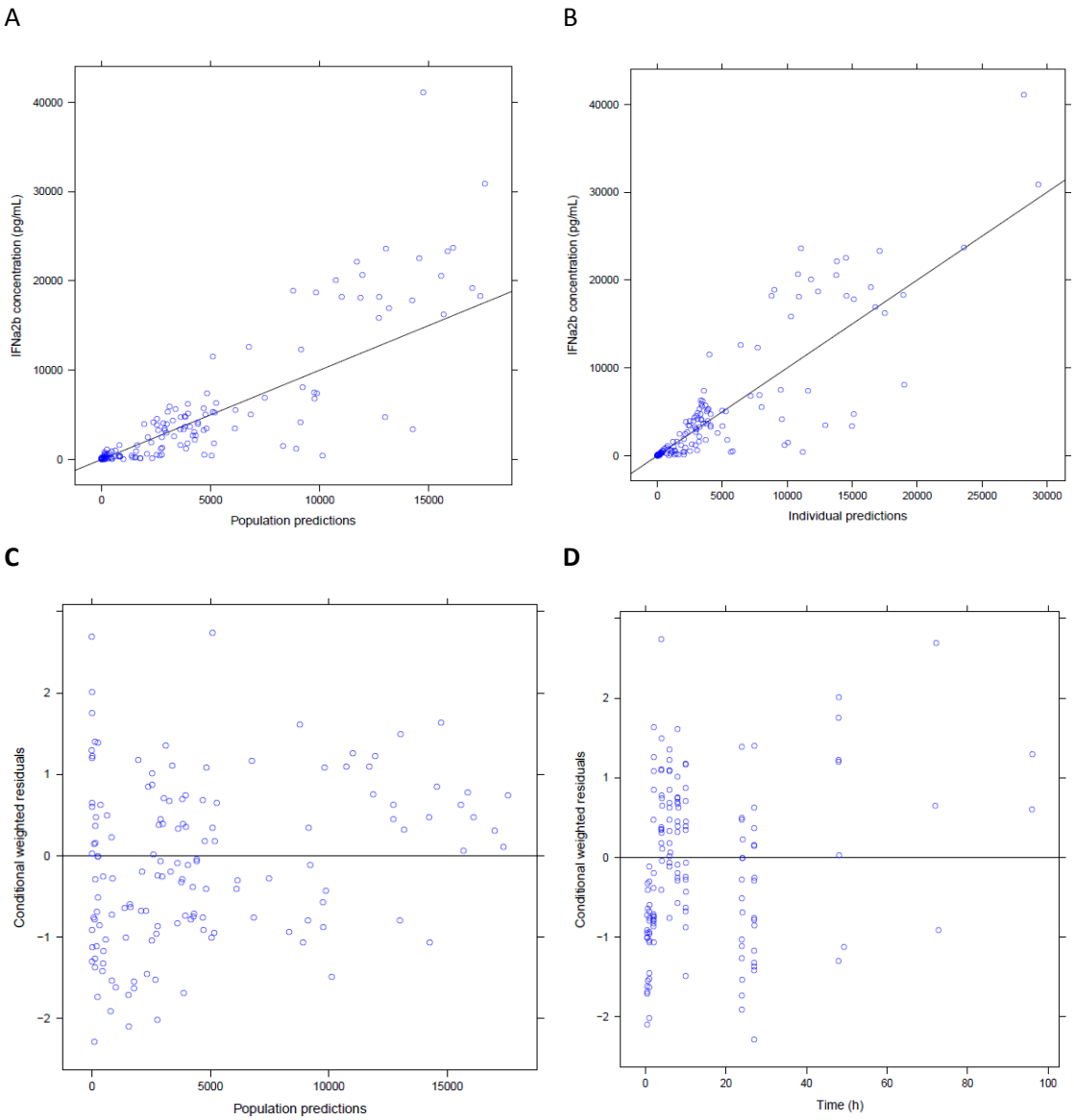

Figure 7.1 **Observed vs. population predicted concentrations (A), observed vs. individual predicted concentrations (B), conditional weighted residuals vs. population predicted concentrations (C) and conditional weighted residuals vs. time (D)**

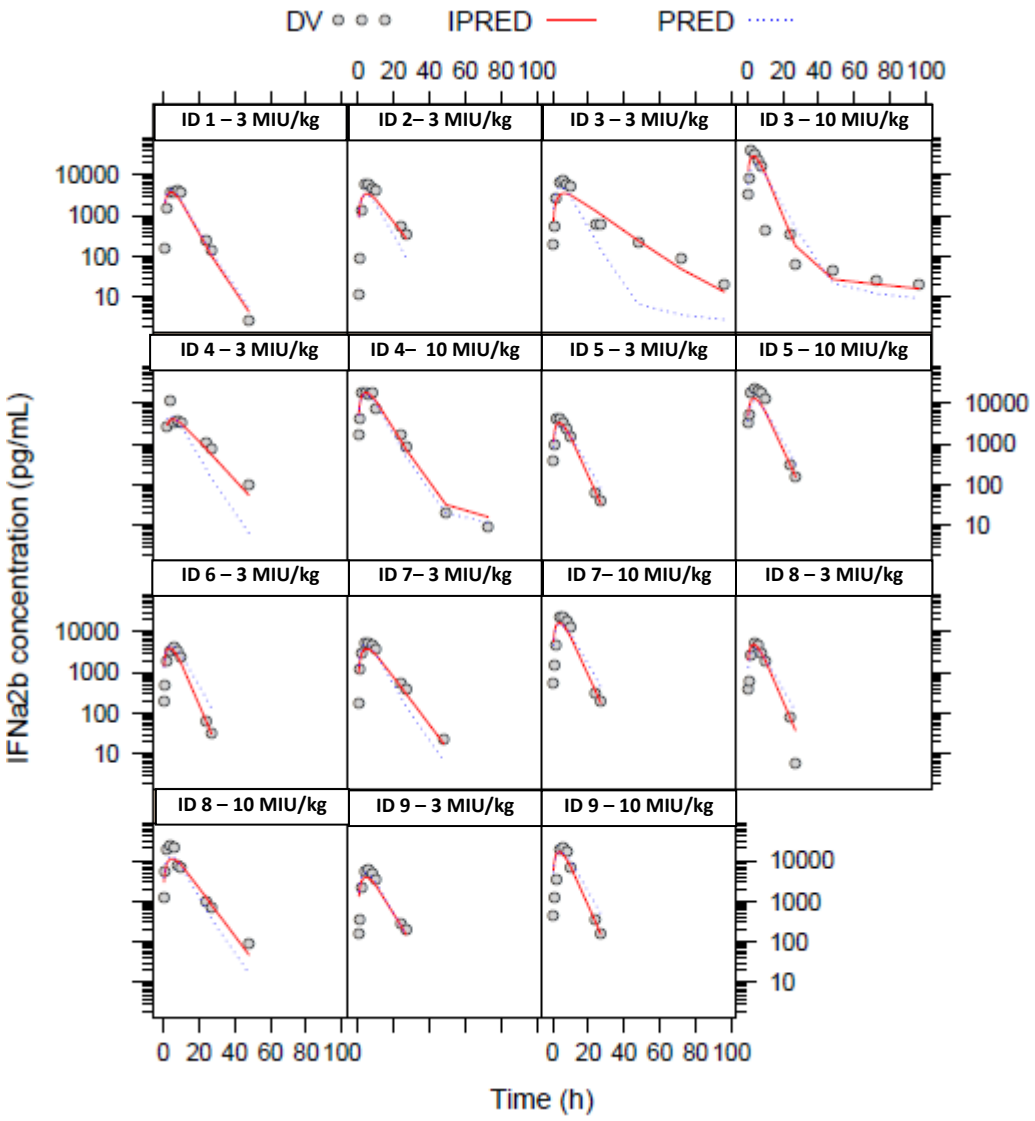

Figure 7.2 **Observed (Circles, DV), population predicted (dotted blue line, PRED) and individual predicted (red line, IPRED) concentration-time profiles for IFNα2b following sc administration at 3 MIU/kg and 10 MIU/kg to the male cynomolgus monkey.**

The final pharmacokinetic parameters derived using model 11 are presented in Table 7.2 where the IIV, IOV and residual errors are presented as CV% and the precisions of the parameter estimates are presented as RSE. The pharmacokinetic parameters were well described with the highest CV observed for IIV on CL (58%). The residual error was 57%.

Table 7.2 PK parameters of IFNα2b in male cynomolgus monkeys following subcutaneous administration at 3 MIU/kg and 10 MIU/kg

Parameter	Estimate	RSE (%)
CL (mL/h)	1798	9
V (mL)	8801	9
k_a (h^{-1})	0.29	7
Q (mL/h)	19.6	23
V2 (mL)	1827	44
IIV of CL (%)	22	58
IOV of V (%)	42	49
Residual Error (%)	57	8

The relationship between individual estimates of CL and V and body weight are presented in Figure 7.3 A and B respectively. There was no obvious relationship between body weight and either parameter.

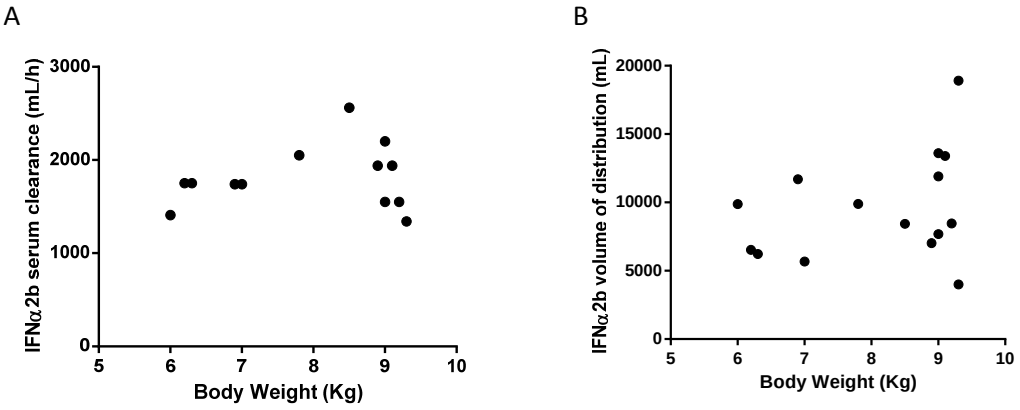

Figure 7.3 Individual estimates of IFNα2b CL (A) and V (B) vs body weight following sc administration at 3 MIU/kg and 10 MIU/kg to the male cynomolgus monkey

7.3.2. Population Pharmacokinetic/Pharmacodynamic modelling to describe the induction of serum neopterin, IL15, IL6, MCP1, IL1Ra and eotaxin concentrations following administration of an IFNα2b challenge.

The results of the population PK/PD modelling of the IFNα2b induction of serum biomarker concentrations in monkeys treated with IFNα2b at 3 MIU/kg and 10 MIU/kg with fixed population PK parameters are presented in Table 7.3.

Table 7.3 PK/PD modelling summary

	Neopterin	IL15	IL6	MCP1	IL1Ra	Eotaxin
Model Description	IIV included on Baseline and E_{max}	IIV included on Baseline, K_{out}, and E_{max}	IIV included on Baseline and E_{max}	IIV included on Baseline and E_{max}	IIV included on Baseline and EC_{50}	IIV included on Baseline and EC_{50}
diffMVOF	-345	-111	-216	-304	-389	-118
p value	<0.001	<0.001	<0.001	<0.001	<0.001	<0.001
CV step completed	Y	Y	Y	Y	Y	Y

Note - diffMVOF calculated by comparing the MVOF of the final model to the MVOF of the model with no IIV included. For eotaxin the model with no IIV failed to minimise so the reference model had IIV included on K_{out}

The CWRES vs. time plots are presented in Figure 7.4, and other goodness of fit plots are presented in Appendices 3.1 to 3.7. For the CWRES vs. time plots the majority of the data points fell within a range of +/- 2, however a small number of data points had residuals of >4 in some of the biomarkers e.g. neopterin. For neopterin, IL6, IL1Ra and eotaxin, the data were randomly distributed with no obvious patterns or bias and centred around zero. However, for IL15 negative residuals were observed between 24 to 56 h post dose while at later time points the residuals were generally positive. For MCP1, the residuals at the earlier time points were positive but as the serum concentrations declined over time, the pattern of the residuals becomes increasingly more negative. The observed vs. individual predicted concentrations (Appendix 3.1-3.7) appeared randomly distributed around the line of unity for all the biomarkers. The plots indicate that in all cases the model tended to under predict the serum biomarker concentrations, however at higher concentrations the data were closer to the line of unity for neopterin, IL15 and eotaxin suggesting a better overall description of the observed data for these biomarkers by the model compared to the other cytokines, which were more variable.

A) Neopterin

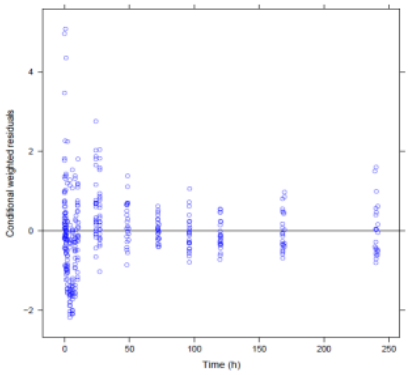

B) IL15

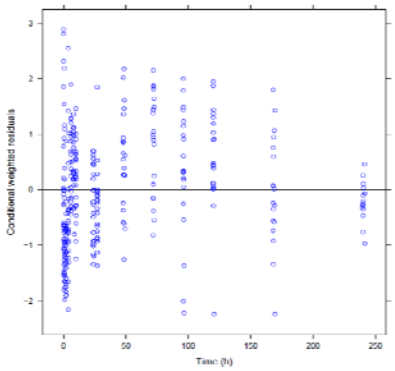

C) IL6

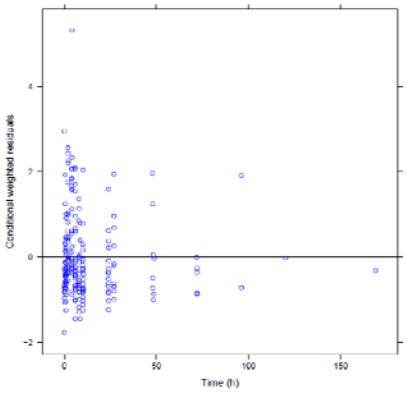

D) MCP1

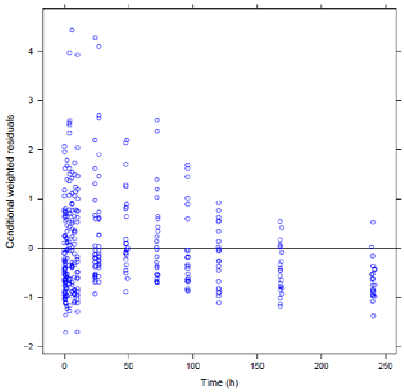

E) IL1Ra

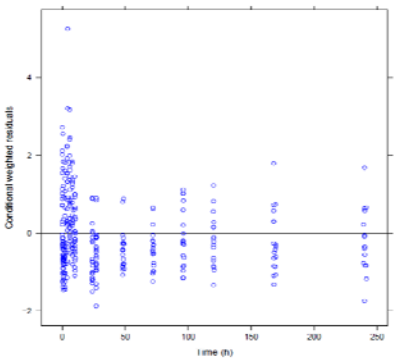

F) eotaxin

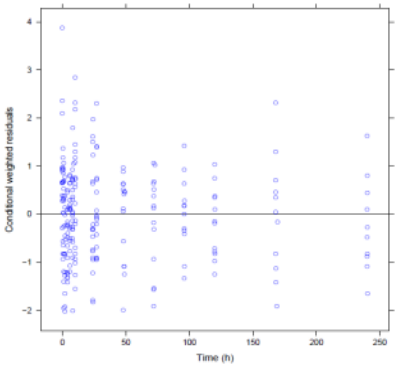

Figure 7.4 Conditional weighted residuals vs. time for neopterin (A), IL15 (B), IL6 (C), MCP1 (D), IL1Ra (E) and eotaxin (F)

The observed, population predicted and individual predicted concentration vs time profiles are presented in Figures 7.5, 7.6, 7.7, 7.8, 7.9 and 7.10 for neopterin, IL15, IL6, MCP1, IL1Ra and eotaxin, respectively.

The models gave a good description of the serum concentrations of neopterin, IL15, IL1Ra and eotaxin in all vehicle treated animals except for monkey 9 neopterin and monkey 5

IL1Ra where the model over predicted the serum neopterin levels over the rest of the sampling regime. The serum concentration of IL6 and MCP1 in vehicle treated animals appeared to vary over time following administration. In addition, the serum concentration-time profiles of MCP1 in vehicle treated animals suggested a vehicle response as there was a distinct induction phase of MCP1 with a defined T_{max} around 24 h post dose followed by an elimination phase where the serum concentrations return to baseline. In the IFNα2b treated animals the models gave a good description of the overall shape of the concentration-time profile including the induction of response, but tended to under predict the maximum concentrations for neopterin, IL15, IL1Ra and IL6 and MCP1. Limited measurable serum concentrations of eotaxin were observed in monkeys 7 and 8 following both doses and monkey 9 following 10 MIU/kg; however the model appears to describe the concentration-time profiles in these animals. The models predicted a bi-phasic elimination profile with an initial faster elimination followed by a longer terminal half-life for IL15, MCP1, IL1Ra and eotaxin. The models did give a good description of the terminal phase in the majority of the monkeys across both doses for neopterin, IL15, IL1Ra and eotaxin. The model over predicted eotaxin concentrations in the terminal phase in 2 monkeys following 3 MIU/kg and 4 monkeys following administration of IFNα2b at 10 MIU/kg. The model gave a poor prediction of the rate of disappearance of IL6 from the system in monkey 1 (3MIU/kg), monkey 5 (10MIU/kg) and 6 (10MIU/kg) resulting in over prediction of serum concentrations in the terminal phase and a bi-phasic profile when the observed data indicates a mono-phasic decline. The model generally predicted the shape of the profile and the disappearance of IL6 from the system quite well in the other monkeys although the variability in IL6 serum concentrations made visual assessment difficult. For MCP1, the model did not give a good prediction of the terminal phase observed on approximately 50% of occasions and particularly over predicted the concentrations from approximately 48 h post dose in monkey 3 following both doses and monkey 5 following 3 MIU/kg compared to the observed concentrations in these animals.

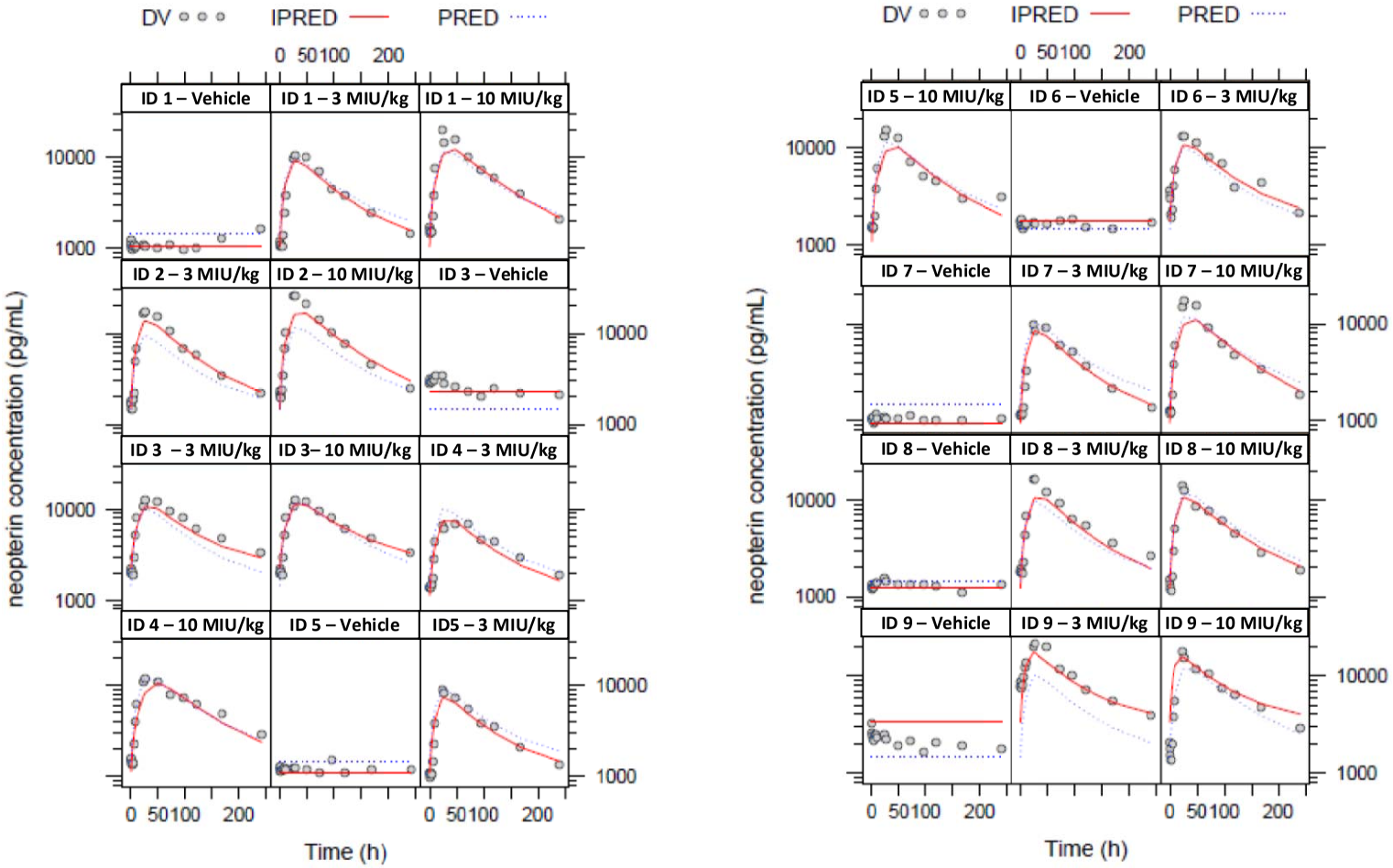

Figure 7.5 **Observed (Circles, DV), population predicted (dotted blue line, PRED) and individual predicted (red line, IPRED) concentration-time profiles for neopterin following sc administration of vehicle or IFNα2b at 3 MIU/kg and 10 MIU/kg to the male cynomolgus monkey.**

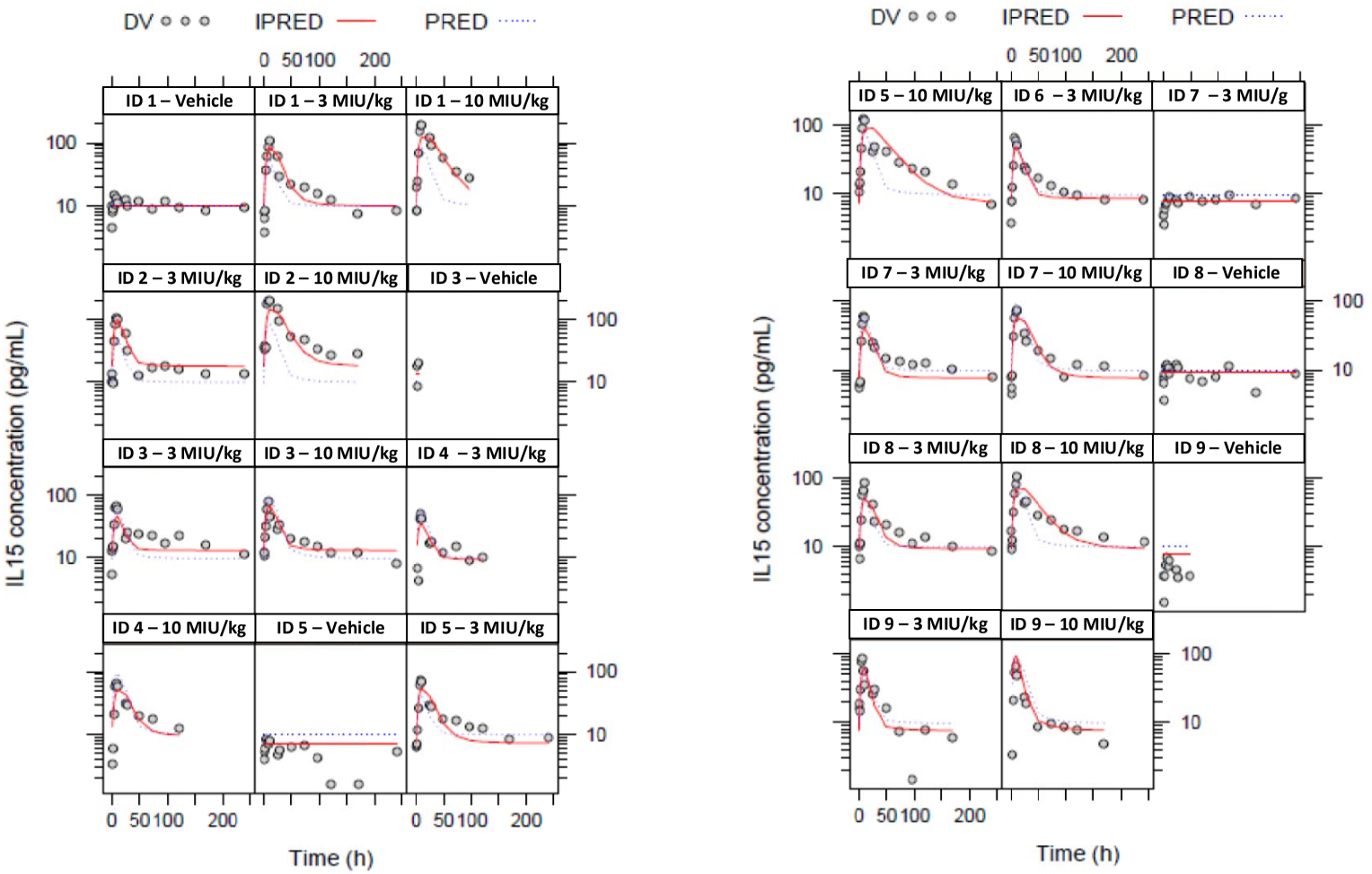

Figure 7.6 **Observed (Circles, DV), population predicted (dotted blue line, PRED) and individual predicted (red line, IPRED) concentration-time profiles for IL15 following sc administration of vehicle or IFNα2b at 3 MIU/kg and 10 MIU/kg to the male cynomolgus monkey.**

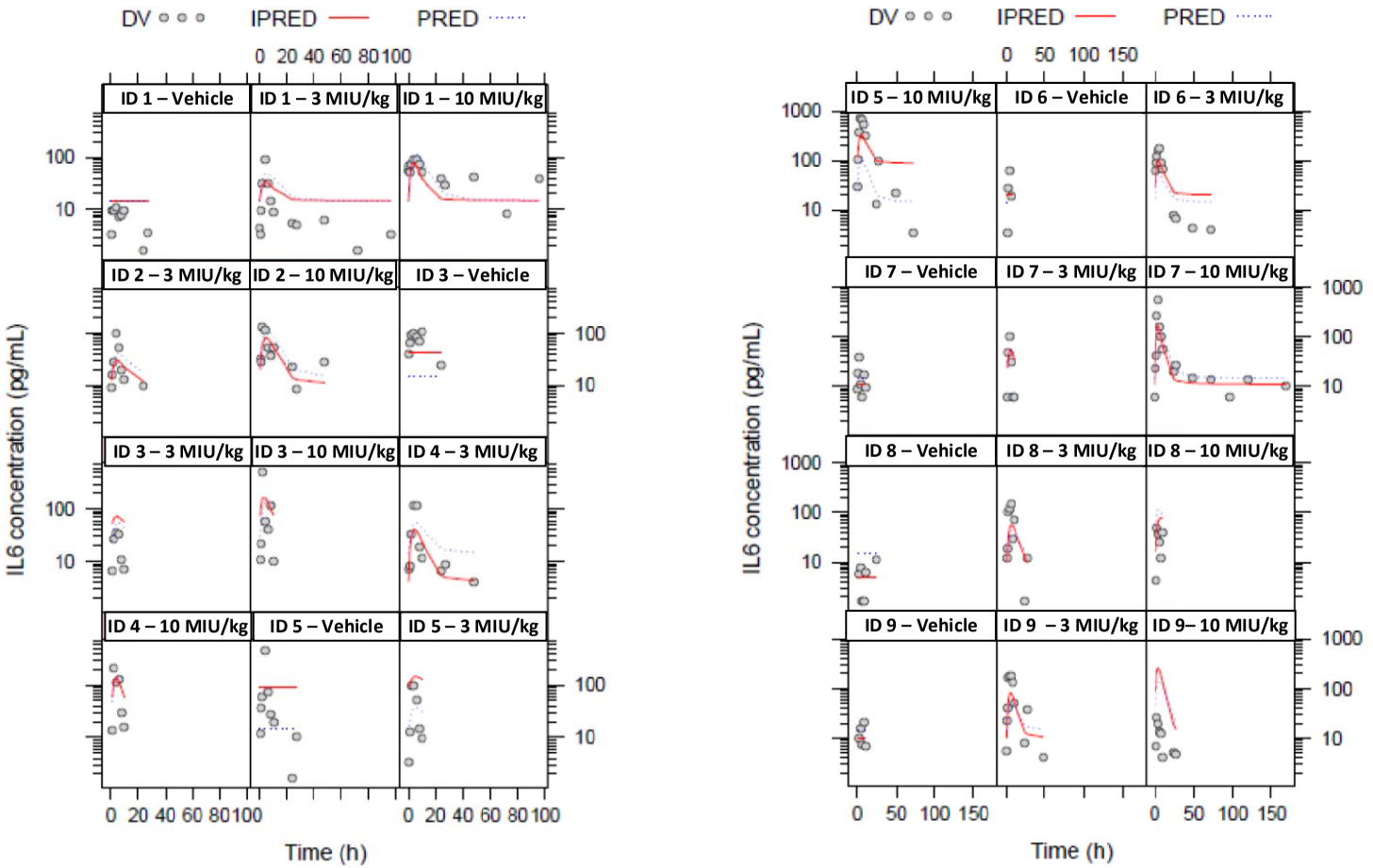

Figure 7.7 **Observed (Circles, DV), population predicted (dotted blue line, PRED) and individual predicted (red line, IPRED) concentration-time profiles for IL6 following sc administration of vehicle or IFNα2b at 3 MIU/kg and 10 MIU/kg to the male cynomolgus monkey. Monkey number and 0 = vehicle, 1= 3 MIU/kg and 2 =10 MIU/kg**

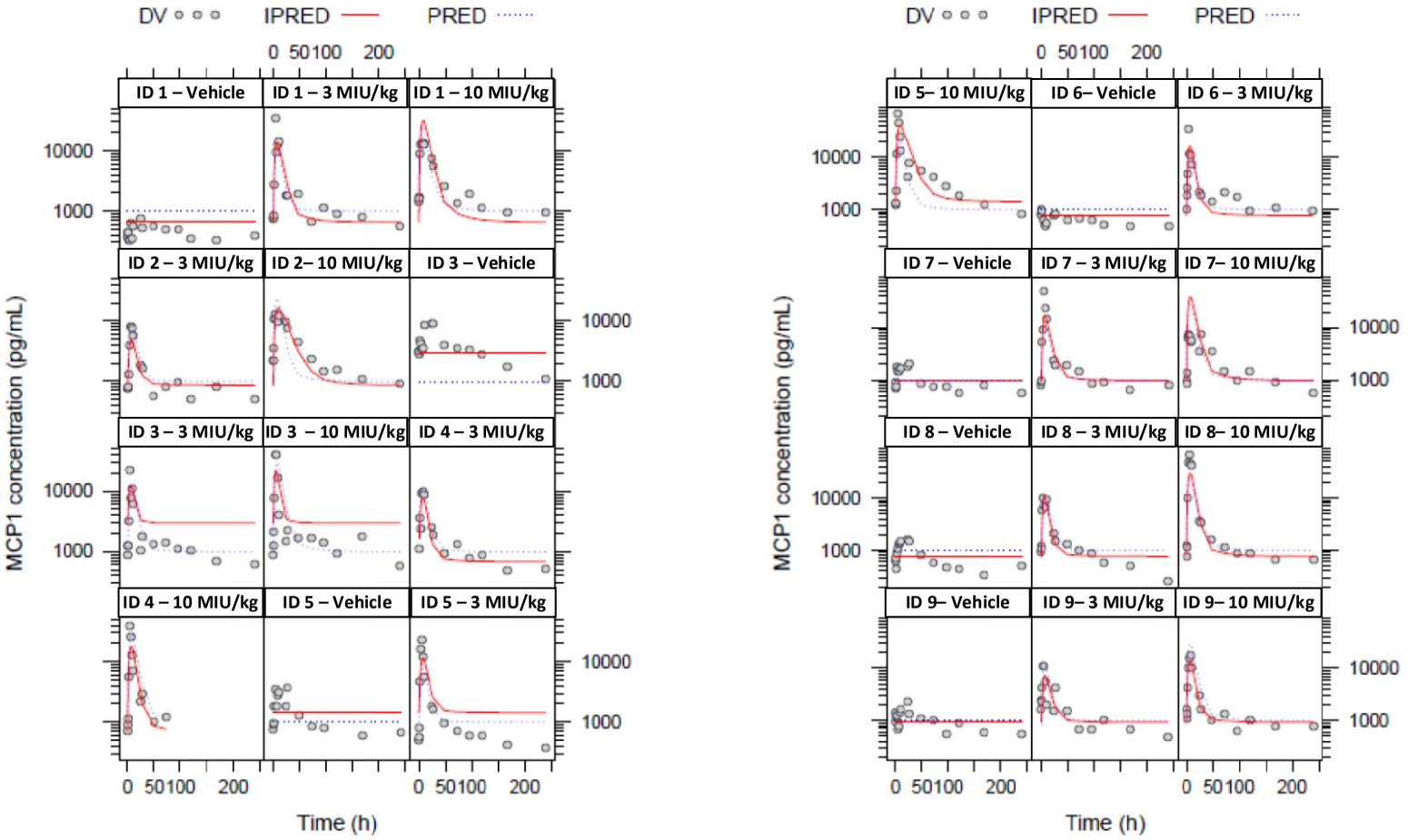

Figure 7.8 **Observed (Circles, DV), population predicted (dotted blue line, PRED) and individual predicted (red line, IPRED) concentration- ime profiles for MCP1 following sc administration of vehicle or IFNα2b at 3 MIU/kg and 10 MIU/kg to the male cynomolgus monkey.**

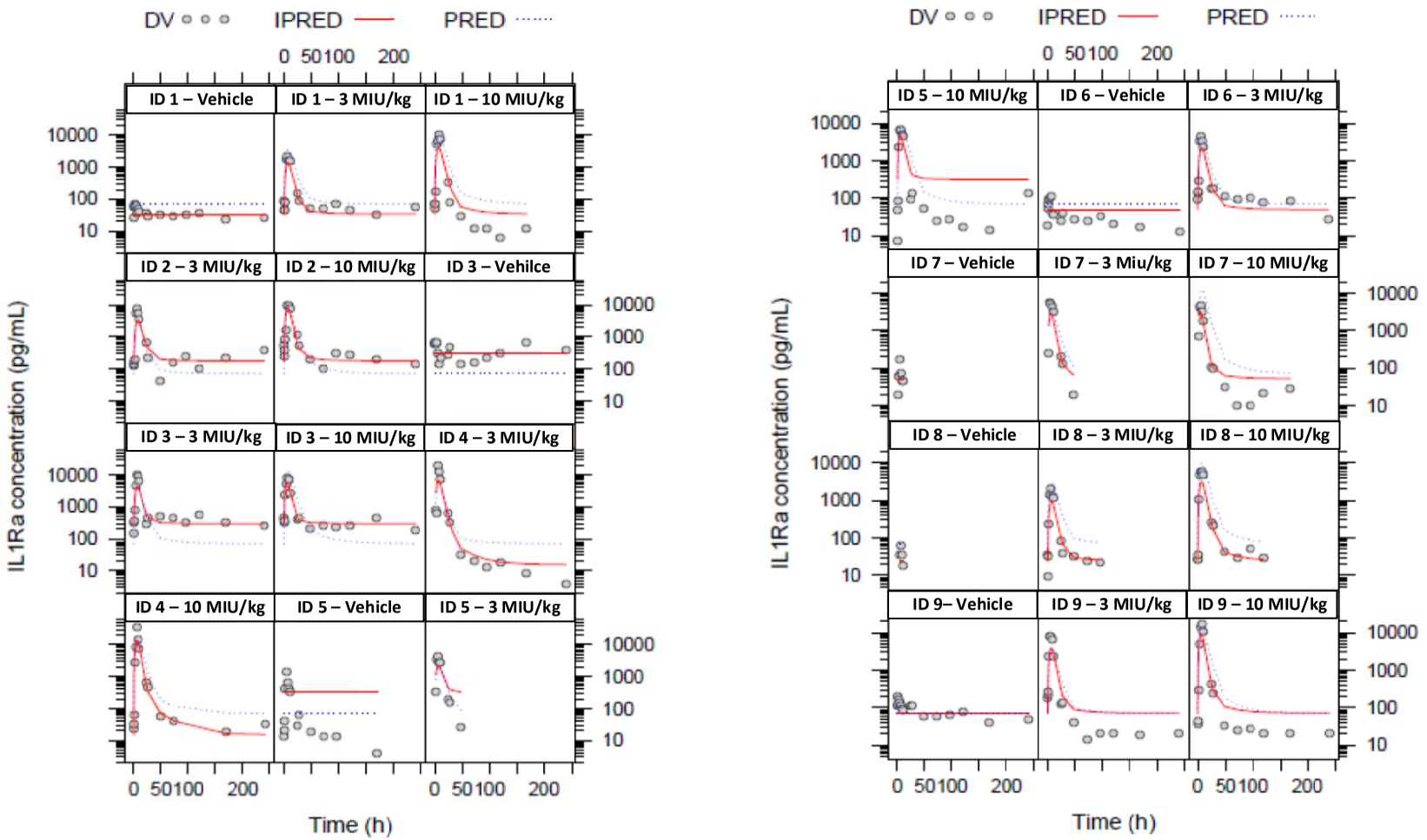

Figure 7.9 **Observed (Circles, DV), population predicted (dotted blue line, PRED) and individual predicted (red line, IPRED) concentration time profiles for IL1Ra following sc administration of vehicle or IFNα2b at 3 MIU/kg and 10 MIU/kg to the male cynomolgus monkey.**

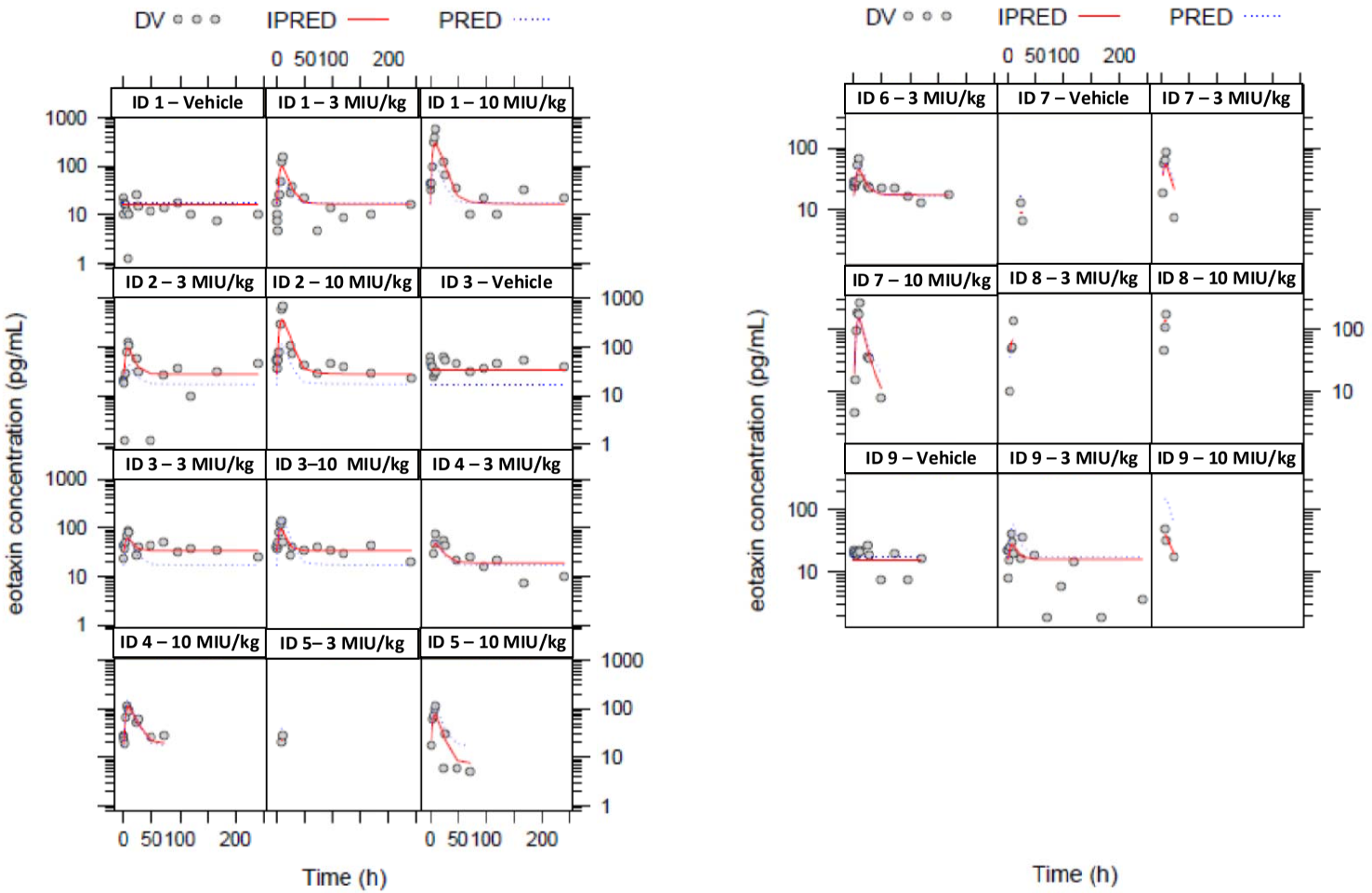

Figure 7.10 **Observed (Circles, DV), population predicted (dotted blue line, PRED) and individual predicted (red line, IPRED) concentration time profiles for eotaxin following sc administration of vehicle or IFNα2b at 3 MIU/kg and 10 MIU/kg to the male cynomolgus monkey.**

The final model parameter estimates for all 6 biomarkers are presented in Table 7.4. Baseline and K_{out} were well described with the highest CV observed for the IL1Ra baseline. The estimated values for EC_{50} demonstrated the greatest range across the 6 biomarkers and were high for IL6, MCP1, IL1Ra and eotaxin in relation to the IFNα serum concentrations. The highest RSEs for all the parameter estimates were observed for EC_{50} and E_{max} for IL6. IIV was included on at least 2 parameters for all 6 biomarkers. IIV was included on baseline for all biomarkers with values ranging from 32–83% and on EC_{50} for IL1Ra and Eotaxin, E_{max} for neopterin, IL15, IL6 and MCP1 and K_{out} for IL15. The highest value for IIV was observed on Baseline and EC_{50} for IL1Ra and E_{max} for IL6 with values of >100%. The residual error ranged from 31-83% but was estimated with a good degree of precision.

Table 7.4 PK/PD parameters of 6 biomarkers in male cynomolgus monkeys following subcutaneous administration of IFNα2b at 3 MIU/kg and 10 MIU/kg

Parameter	Estimate (RSE %)					
	Neopterin	IL15	IL6	MCP1	IL1Ra	Eotaxin
Baseline (pg/mL)	**1460** (8)	**9,78** (12)	**14.6** (30)	**999** (10)	**68.5** (37)	**16.9** (23)
K_{out} (h^{-1})	**0.015** (8)	**0.212** (13)	**1.42** (20)	**0.62** (20)	**0.41** (7)	**0.17** (12)
EC_{50} (pg/mL)	**309** (64)	**5189** (75)	**520274** (735)	**679691** (107)	**385861** (46)	**1750490** (58)
E_{max}	**23.9** (20)	**14.1** (49)	**321** (704)	**1729** (118)	**3756** (32)	**1273** (59)
IIV of Baseline (%)	**40** (48)	**31** (56)	**91** (45)	**46** (60)	**105** (32)	**48** (83)
IIV of K_{out} (%)	-	**13** (68)	-	-	-	-
IIV of EC_{50} (%)	-	-	-	-	**110** (63)	**92** (52)
IIV of E_{max} (%)	**33** (49)	**47** (48)	**103** (48)	**72** (62)	**-**	**-**
Residual Error (%)	**31** (24)	**40** (15)	**83** (16)	**58** (17)	**76** (19)	**44** (21)

The median and 95% prediction interval of the IFNα2b, neopterin, IL15 and IL1Ra concentration-time profiles obtained following 1000 simulations with the final PK/PD model at a IFNα2b dose of 3MIU/kg and 10MIU/kg are presented in Figure 7.11 and overlaid with the observed data.

The simulated population median IFNα2b, neopterin, IL15 and IL1Ra concentration-time profiles were consistent with the observed concentration-time data for both doses (Figure 7.11 – 1, 2, 3 and 4). For the IFNα2b concentration data, the prediction interval is close to the median although the majority of the observed data at and around the C_{max} fall outside the prediction interval. For neopterin, IL15 and IL1Ra concentration data, the prediction interval is much wider than that observed for IFNα2b. The prediction interval for neopterin and IL1Ra captures the majority of the data, however for IL15 some of the observed data between 40 and 120 h following 10 MIU/kg fell outside the prediction interval.

1A) IFNα2b 3 MIU/kg

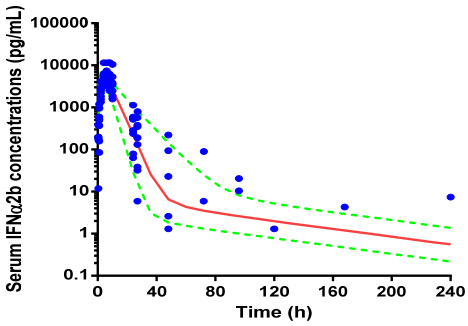

1B) IFNα2b 10 MIU/kg

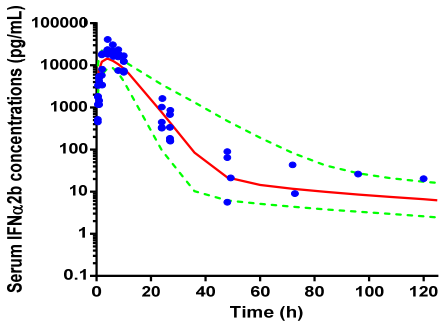

2A) Neopterin following IFNα2b 3 MIU/kg

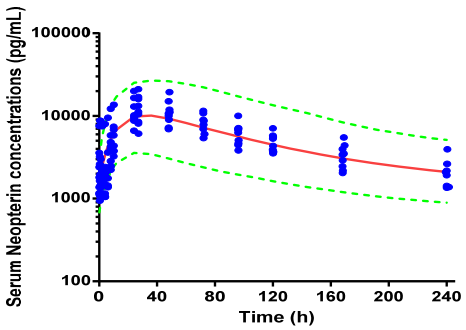

2B) Neopterin following IFNα2b 10 MIU/kg

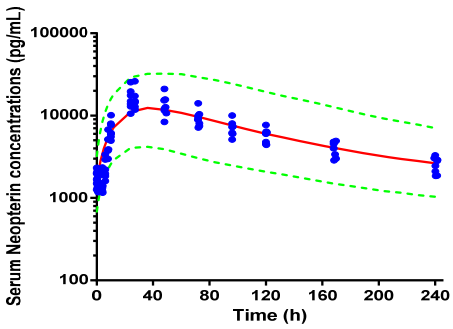

3A) IL15 following IFNα2b 3 MIU/kg

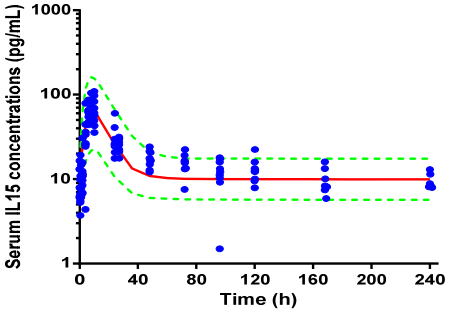

3B) IL15 following IFNα2b 10 MIU/kg

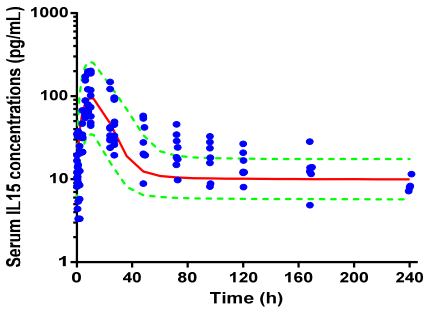

4A) IL1Ra following IFNα2b 3 MIU/kg

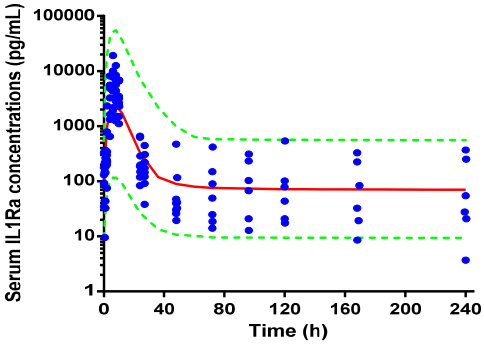

4B) IL1Ra following IFNα2b 10 MIU/kg

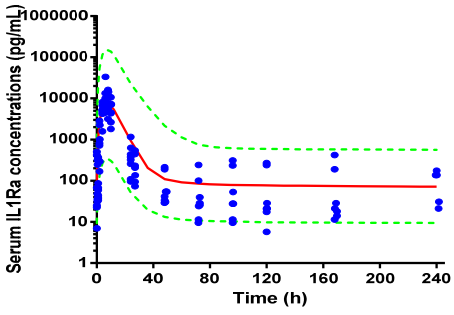

Figure 7.11 **Observed vs. simulated concentrations time profiles for IFNα2b (1), neopterin (2), IL15 (3) and IL1Ra (4) following sc administration of IFNα2b at doses of 3 MIU/KG (A) and 10 MIU/kg (B). Blue circles represent observed data, Red Line represents the simulated population median, and Green dashed lines represent the 95% prediction interval.**

7.3.3. Population Pharmacokinetic/Pharmacodynamic simulations to investigate the impact on the IFNα2b induction of the serum concentrations of neopterin, IL15 and IL1Ra by the pan JAK inhibitor Xeljaz™ (tofacitinib)

The results of the simulations investigating the sensitivity of the dose of toficitinib on neopterin, IL15 and IL1Ra concentration-time profiles are presented in Figures 5.12, 5.13 and 5.14 respectively.

The simulations demonstrated that at an IFNα2b dose of 3 MIU/kg, increasing doses of inhibitor delivered inhibition of neopterin, IL15 and IL1Ra induction by IFNα2b in a dose proportional manner. All doses delivered an initial reduction of all three biomarkers to levels below baseline following which an induction of neopterin, IL15 and IL1Ra concentrations greater than baseline was predicted to some degree at all doses.

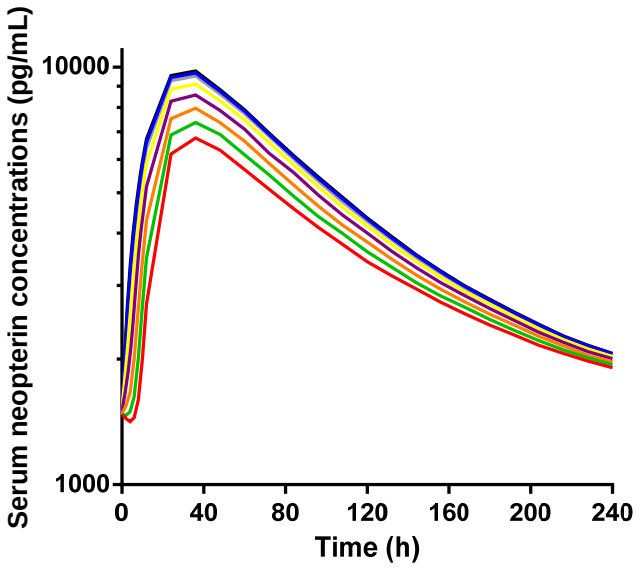

Figure 7.12 **Simulated IFNα2b (3 MIU/kg) induced serum concentration-time profiles for neopterin with co-administration of toficitinib at 10 mg/kg (red), 3 mg/kg (green), 1 mg/kg (orange), 0.3 mg/kg (purple), 0.1 mg/kg (yellow), 0.03 mg/kg (grey), 0.01 mg/kg (blue) no inhibitor (black)**

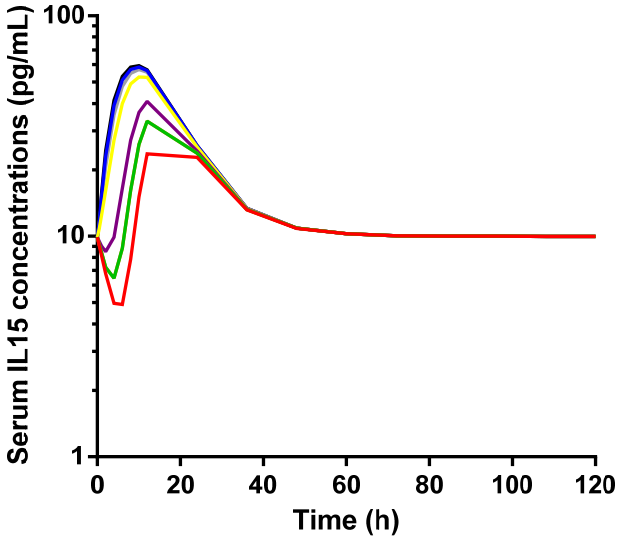

Figure 7.13 **Simulated IFNα2b (3 MIU/kg) induced serum concentration-time profiles for IL15 with co-administration of toficitinib at 10 mg/kg (red), 3 mg/kg (green), 1 mg/kg (orange), 0.3 mg/kg (purple), 0.1 mg/kg (yellow), 0.03 mg/kg (grey), 0.01 mg/kg (blue) no inhibitor (black)**

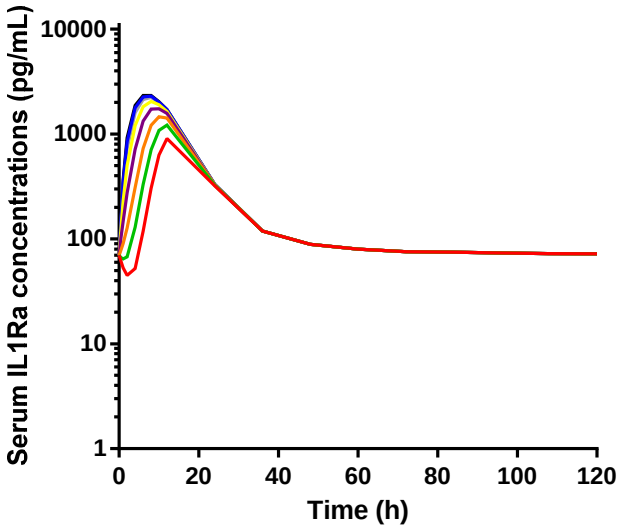

Figure 7.14 **Simulated IFNα2b (3 MIU/kg) induced serum concentration-time profiles for IL1Ra with co-administration of toficitinib at 10 mg/kg (red), 3 mg/kg (green), 1 mg/kg (orange), 0.3 mg/kg (purple), 0.1 mg/kg (yellow), 0.03 mg/kg (grey), 0.01 mg/kg (blue) no inhibitor (black)**

7.3.4. Pharmacokinetic/Pharmacodynamic simulations using the TMDD models presented in the literature to predict the serum IFNα2b and serum neopterin concentration-time profiles observed in this study.

The digitised vs. simulated IFNβ1a plasma concentration-time profiles and neopterin concentration-time profiles following iv bolus administration of IFNβ1a at doses of 1, 3 and 10 MIU/kg using the model equations and parameters detailed by Kagan et al (2010) are presented in Figure 7.15 A and B respectively. The simulated profiles were comparable to the digitized profiles at all 3 doses.

The observed vs. simulated IFNα2b and neopterin concentration time profiles in monkeys following IFNα2b at 3 MIU/kg using the TMDD incorporating the parameter estimates for IFNα2b where applicable are presented in Figure 7.16 A and B respectively. The model predicted a bi-phasic IFNα2b concentration time profile with quicker absorption compared to the observed concentration time profile. The predicted concentrations are broadly comparable although the model slightly over predicts the maximum concentrations and underpredicts the concentrations in the terminal phase. The rate of elimination in the terminal phase appears to be comparable between the predicted and observed concentration-time profiles The shape of the predicted and observed neopterin concentration time profiles were comparable, however the predicted concentrations were at the higher end of the observed concentrations.

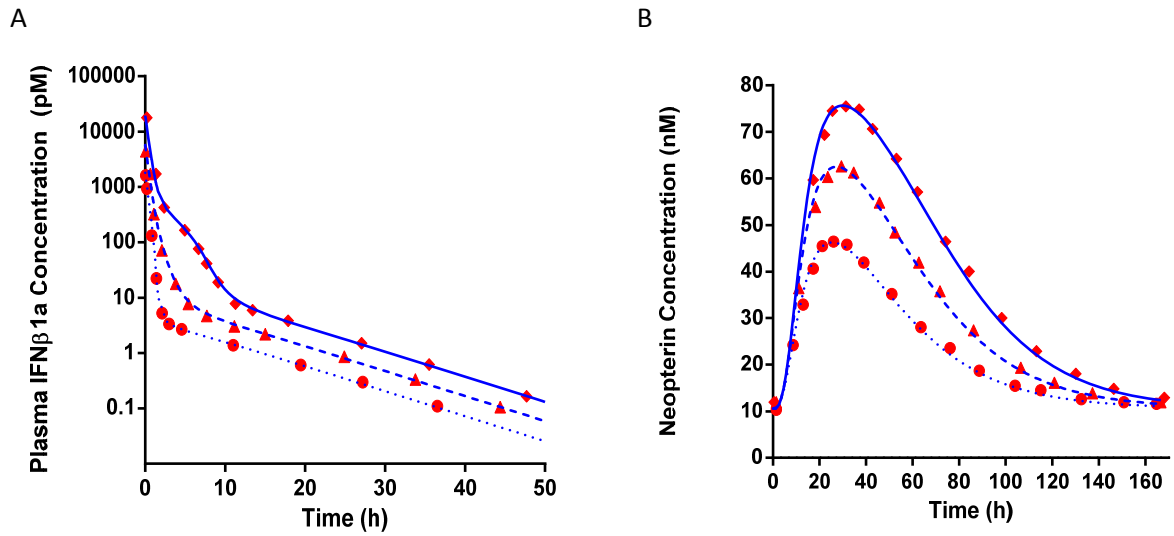

Figure 7.15 **Simulated vs. Digitized (with permission) IFNβ1a plasma concentration-time profile (A) and neopterin plasma concentration-time profile (B) (Blue lines simulated data, dots = 1 MIU/kg, dashed = 3 MIU/kg and solid = 10 MIU/kg. Red symbols digitised data, circles = 1 MIU/kg, trianlges= 3 MIU/kg and diamonds = 10 MIU/kg)**

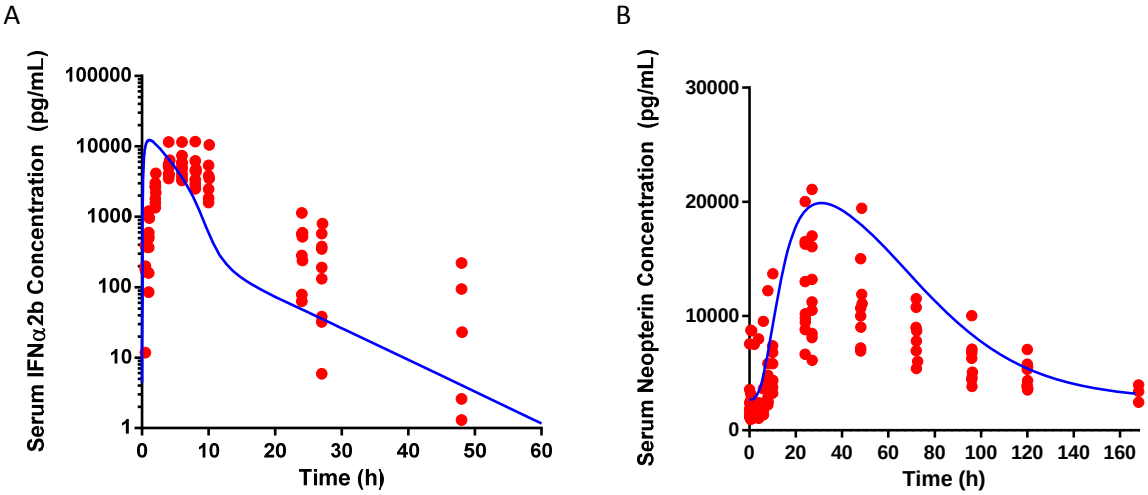

Figure 7.16 **Simulated vs. observed IFNα2b serum concentration-time profile (A) and neopterin plasma concentration-time profile (B) (Blue lines simulated data, red cricles observed data)**

7.4. Discussion

7.4.1. Population Pharmacokinetic modelling of IFNα2b concentration-time data

Population PK/PD modelling to describe the IFNα2b induction of serum concentrations of 6 biomarkers in the male cynomolgus monkey was conducted in a sequential manner. The pharmacokinetics of IFNα2b were described using a 2 compartmental population PK model with first order absorption. The incorporation of IIV on CL_b and IOV on V gave the best

description of the observed IFNα2b serum concentration-time profile across the two doses investigated in this study. The model generally gave a good prediction for the majority of the monkeys over both dosing occasions, and the structural model parameters were estimated with adequate precision.

The selection of the 2 compartmental structural models appeared to be driven by the profiles observed in monkey 3 and 4 with the remaining demonstrating monophasic profiles. As monkey 3 also demonstrated the greatest response to IFNα2b, it may be that this monkey had different underlying biology making it more sensitive to IFNα2b leading to an impact on the observed pharmacokinetics. It may be that if higher doses of IFNα2b had been administered to the other monkeys similar profiles to that observed for monkey 3 would have been observed.

The low IIV on CL is unsurprising considering inbred animals of approximately comparable age and weight were used. Individual pharmacokinetic parameters can change between study occasions (Mould and Upton 2013). As the monkeys received IFNα2b on two different occasions the inclusion of IOV on the model parameters was investigated. Inclusion of IOV together with IIV on CL, caused the estimated value for IIV to collapse to zero. Essentially there was not enough data for the model to estimate both IIV and IOV on CL and therefore the observed variability is assigned to one of the omegas in this case IOV. However, a comparison of IIV and IOV on CL suggested that the variability within an animal between two occasions for CL was greater than the variability in CL between animals. The inclusion of IIV on CL and IOV on V indicated that there is a moderate degree of variability in the determined value of V across dosing occasions within an individual. The inclusion of IOV on V generally resulted in a lower estimation of V/F following administration of 10 MIU/kg and consequently improved the prediction of IFNα2b C_{max} following the higher dose. Karlsson and Sheiner (1993) conclude that when IOV is ignored it either inflates IIV or residual error. In this study the inclusion of IOV in the model resulted in a reduction in the residual error of approximately 10%.

Investigations of covariates that are predictive of pharmacokinetic variability such as body weight, age, race, renal function or disease amongst others are important in population pharmacokinetic studies. As the monkeys used in this study were inbred animals from the same supplier the only covariate that was easily accessible for investigation was body weight on the study day. A simple covariate analysis was conducted whereby the individual

CL and V were plotted against body weight on the study day. From these plots no obvious relationship was observed between either parameter and body weight so no further covariate analysis was conducted.

The majority of the pharmacokinetic parameters for type I IFNs across the species are generally derived by non-compartmental analysis. This is one of the few studies where population PK modelling has been used to derive the pharmacokinetic parameters of type I IFNs particularly IFNα2b in the monkey. However, population pharmacokinetic modelling of IFNα in patients with chronic HCV receiving INTRON A (IFNα2b) subcutaneously at 3 MIU 3 times a week has been investigated (Chatelut et al, 1999). The pharmacokinetics of IFNα2b were determined after the first dose and a 1 compartment model with a combined zero-order and first-order absorption was selected as the most appropriate structural model to describe the observed concentration-time profile. The combination of zero-order followed by first order was included as there appeared to be a different rate of absorption up to 2.5 h post dose compared to the rate of absorption observed after this time, however, none of the proposed mechanisms of absorption in human could give an adequate explanation for this finding. Only first-order absorption was included in the population PK model in this study, however the individual plots suggest that the absorption phase not well described. For the purpose of developing a PK/PD model of the effect of IFNα2b, the PK model was considered adequate, but if in the future a better description of the absorption phase is required a model incorporating both zero-order followed by first-order absorption could be explored. Despite this, the rate of first-order absorption of IFNα2b was broadly comparable between monkey and man with 0.24 h^{-1} observed in this study for the monkey and 0.18 h^{-1} observed in HSV patients. In both species the absorption of IFNα following sc administration is protracted with maximum concentrations observed between 1-6 h for monkeys and 1-8 h for humans (Gloff and Wills, 1992)

IFN concentrations decline in a bi-phasic manner described by a rapid distribution phase ($t_{1/2}$ 0.1 h) followed by a longer elimination phase ($t_{1/2}$ 1.7 h) (Radwanski et al, 1987; Willis, 1990). Longer values for the terminal half-life of IFNα in man have been reported ranging from 4-16 h (Gloff and Wills, 1992), the lower end of which is comparable to the terminal half life determined from population PK modelling in the monkey in this study. It has been widely reported that absorption of the IFNs following sc and im administration is slow and that the terminal half-life is influenced by the absorption process (Chatelut et al, 1999).

In this situation the prolonged absorption masks the rapid distribution phase giving a mono-phasic profile (Wills, Spiegel and Soike, 1984) as observed in this study in a number of the monkeys across both doses. This process is known as flip-flop kinetics (Mould and Upton, 2013).

A CL/F of 1829 mL/h was determined for IFNα2b in the monkey, assuming a mean monkey weight of 8 kg for this study gives a CL/F of 228 mL/h/kg. In HCV patients the determined CL/F was about 2 fold higher at 486 mL/h/kg (assuming a mean weight of 74 kg). Although it appears that the CL of IFNα2b in man is higher than that observed in the monkey it is important to take into account the apparent bioavailability (F%) when comparing between species. If the F% following subcutaneous administration of IFNα2b is comparable to that for IFNβ1a in both monkey and man (Mager and Jusko 2002; Mager et al 2003) then the calculated CL for IFNα2b becomes comparable between the two species (164 mL/h/kg vs. 155 mL/h/kg in monkey and man respectively).

7.4.2. Population Pharmacokinetic/Pharmacodynamic modelling to describe the induction of serum neopterin and IL15, IL6, MCP1, IL1Ra and Eotaxin concentrations

PKPD analysis of the serum concentration-time profiles was conducted for 6 biomarkers. A delay was observed between the maximum concentrations of IFNα2b and the maximum concentrations of all 6 biomarkers. For example, the median T_{max} observed for IFNα2b was 4 h compared to a median T_{max} of 27 h observed for neopterin. Plotting the serum concentrations of each biomarker in individual monkeys against the serum concentrations of IFNα2b revealed counter clockwise hysteresis as presented for neopterin in Figure 7.17 below. As discussed in Chapter 2, this delay can be explained by the synthesis and release of the biomarker from cells following activation by IFNα2b, therefore an indirect response model with stimulation of the input rate was the most appropriate model to describe the PK/PD relationship of the IFNα2b induction of the selected biomarkers. Numerous efforts using PK/PD modelling and population PK/PD modelling to describe the induction of neopterin by type I IFNs in both monkey and man have been reported, however this is the first occasion that PK/PD modelling has been used to describe the induction of IL15, IL6, MCP1, IL1Ra and eotaxin by any type I IFNs in the monkey. One point to consider is that the induction of one of the biomarkers of interest may not be solely driven by IFNα2b but may be driven by one of the other cytokines that is also induced by IFNα2b. For example,

neopterin is undoubtedly induced by IFNα2b, however hysteresis is also observed when neopterin concentrations are plotted against the IL15 concentrations, suggesting a delay between the appearance if IL15 and the appearance of neopterin. IL15 has the capacity to activate immune cells, for example, stimulating monocytes into dendritic cells (Saikh et al, 2001) and the differentiation of NK cells (Fehniger and Caligiuri 2001) suggesting that it may induce the production of neopterin from these cells. It is not possible to tease out the relative contributions of the various cytokines to the production of neopterin in this study but may be of interest in the future if the goal was to build a more complex quantitative systems pharmacology model where multiple pathways and their actions on one another are modelled simultaneously.

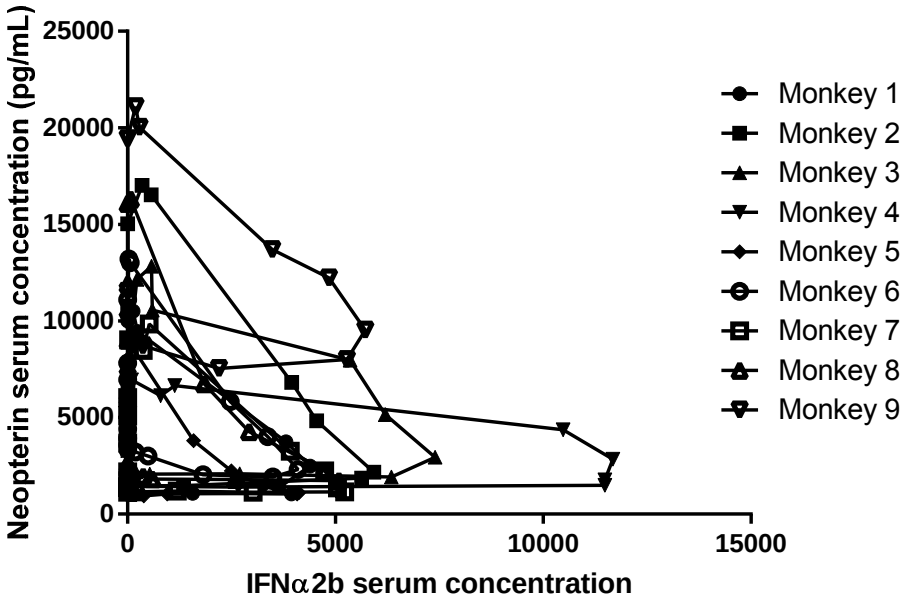

Figure 7.17 IFNα2b induced neopterin concentrations plotted against IFNα2b serum concentrations in time sequence in male cynomolgus monkeys following sc administration of IFNα2b at 3 MIU/kg

Following population PK/PD modelling estimates for baseline and K_{out} and the residual error were predicted with a good degree of precision for all 6 biomarkers. The parameters for neopterin were estimated with the greatest precision whereas the parameters for IL6 demonstrated some of the highest RSEs. EC_{50} and E_{max} had the highest RSE values across all 6 biomarkers. One point that raises concerns around the performance of the model is that although realistic parameter estimates for EC_{50} were obtained for neopterin and IL15 the parameter estimates for EC_{50} for IL6, MCP1, IL1Ra and eotaxin were higher than

concentrations of IFNα2b observed in this study even at 10 MIU/kg. For example the mean IFNα2b C_{max} following 10 MIU/kg was approximately 16 fold lower than the EC_{50} determined for IL1Ra and 70 fold lower than the EC_{50} determined for eotaxin. This would suggest that the model is predicting that the response for these biomarkers has the potential to be much greater than observed in this study despite appearing to saturate the response based on the exposure of the biomarkers observed at 3 MIU/kg and 10 MIU/kg (Chapter 4). If the model is having difficulty in determining the stimulatory effect (E_{max}) of IFNα2b on the relative biomarkers it is perhaps unsurprising that the precision associated with this parameter is also high for the majority of the biomarkers. Mager, Neuterboom and Jusko (2005) consider a value for S_{max} of 72 to be relatively large following PK/PD modelling of the PEGylated IFNβ1a induction of neopterin in the monkey. If this is the case then high values for E_{max} were observed for 4 of the 6 biomarkers in this study with those determined for MCP1, IL1Ra and eotaxin being extremely high. Mager, Neuterboom and Jusko (2005) suggest that in their model EC_{50} and E_{max} are correlated as the relatively large S_{max} is countered by a large SC_{50} value. This appears that this may be the case for the estimated parameters derived in this study. Taking this together indicates that the parameter estimates for EC_{50} and E_{max} derived using this data set and model particularly for IL6, MCP1, IL1Ra and eotaxin should be interpreted with caution. The limitation of the model to derive robust parameter estimates for EC_{50} and E_{max} may stem from the data set used for PK/PD modelling. When designing *in vivo* PK/PD studies with the end goal of PK/PD modelling to derive robust parameters estimates the desired number of doses to be investigated is 5 ideally spread across the dose response curve. As only two doses were investigated in this study, the data set may be too limited to derive reliable parameter estimates. For the majority of the biomarkers, little increase in the systemic concentrations was observed with the increasing dose of IFNα2b from 3 MIU/kg to 10 MIU/kg suggesting that the response is on the upper non linear portion of the concentration-response curve. If lower doses were to be investigated it may enable the model to deliver more reliable estimates of both EC_{50} and E_{max}. The high level of variability observed in this data set may suggest that an alternative model may deliver more robust parameter estimates. Upton and Mould (2014) suggest that for data that demonstrates a high intrinsic variability, such as cytokines, a log-linear concentration effect model may be more appropriate to model the response. This was not explored in this study but may be something to consider for future modelling efforts.

IIV was included for baseline for all 6 biomarkers indicating a degree of variability between the baseline levels in the animals. The model failed to predict the C_{max} in some animals and it appears that even with the inclusion of IIV the individual predicted baseline may have been different to the observed value. The inclusion of IOV on baseline taking into account that the values may vary between study days may have given a more robust estimate of this parameter and enabled a better fitting of the early part of the concentration-time profile.

The residual error ranged from 31 to 83 % with the highest residual error observed for IL6; however the residual error was estimated with an acceptable level of precision for all 6 biomarkers. A residual error can be attributed to assay variability, errors in sampling time collection and model misspecification (Mould and Upton, 2013). It has been discussed previously that an alternative model may be more appropriate, particularly for the cytokines which show increased variability, which may have reduce the higher residual variability observed for those biomarkers. Generally the samples were taken at the specified time or within an acceptable time frame making it unlikely that timing would have contributed significantly to the residual error. However there did appear to be some variability in the analytical assay between different days of analysis for some of the biomarkers, as presented by the different LLQ and HLQ values in Chapter 3. This may offer an alternative explanation as to why higher residual errors were observed for some of the biomarkers, although it should be noted that Mould and Upton (2013) summarise that assay error is often only a minor component of residual error so its contribution to the higher residual error values observed in this study may be questionable.

Generally all the parameters were estimated with good precision, which suggests that an appropriate model was selected, as models with poor parameter precision are often over parameterised (Mould and Upton 2013). This suggests that the model for at least IL6 and MCP1 may be over parametised and a more extensive data set may be required to deliver robust parameter estimates. For most PK models <30% RSE for fixed effects and <50% RSE for residual effects are usually achievable (Mould and Upton, 2013). The precision for the residual error and approximately 60% of the model parameters was <50% boundary suggesting that the data set may be adequate to determine parameter estimates of acceptable precision.

The PK/PD relationship describing the induction of neopterin by Type I IFNs has been investigated using a number of different PK/PD models. Generally the values for baseline and K_{out} for neopterin determined were in line with those previously reported for monkeys (Mager et al, 2003) and healthy volunteers (Jeon et al, 2013). This is perhaps unsurprising as once formed there is no metabolism of neopterin and its elimination is via renal filtration. Glomerular filtration rates (GFR) are comparable between monkeys and humans with values of 2.1 and 1.8 mL/min/kg respectively (Davis and Morris, 1993).

The induction of neopterin by type I IFNs has been demonstrated to be saturable in studies investigating IFNβ1a where a linear increase in neopterin concentrations was not observed with increasing dose of IFNβ1a in healthy volunteers. This was also the case in the primate in this study where NCA showed a less than proportional increase in neopterin C_{max} and AUC with increasing IFNα2b dose. To model the PK/PD relationship for neopterin an indirect response model was used. This model has also been successfully used in other studies investigating the PK/PD relationship of type I IFNs and neopterin in the monkey (Mager, Neuteboom and Jusko, 2005). However other authors have explored different PK/PD models in an effort to describe the apparent saturation of the neopterin response.

Following a single administration, the saturation of the neopterin response with increasing doses of type I IFNs have been described in healthy volunteers by Jeon et al (2013) using the concept of time-dependent attenuation of EC_{50}, and in monkeys by Hu et al (2011) using a model incorporating a negative feedback loop where concentrations of neopterin inhibit further production of neopterin. The second model was based on the understanding of down-regulation of the IFN receptor by sustained concentrations of IFN and/or negative feedback by prolonged elevation of neopetrin concentrations. It should be noted that Jeon et al (2013) attempted to describe the neopterin data observed in healthy volunteers with the model presented by Hu et al (2011) without success. Hu et al (2011) concluded that the saturation of the response following both single and repeat doses may be due to either saturation of the receptor or saturation of the biological response downstream of the receptor. An alternative PK/PD model is the precursor model presented by Sharma, Ebling and Jusko (1998) and subsequently used by Mager et al, (2003), which merges the properties of a nonlinear indirect responses with a precursor of limited capacity. This model predicted a theoretical saturation of the response with increasing dose following single administration. Although this model successfully described the saturation in the neopterin

response in monkeys following a single dose of IFNβ1a, the precursor was primarily used to describe both rebound and a reduction in the observed response; in this case induction of neopterin concentrations with repeat dosing. Both the precursor and negative feedback loop models are essentially concerned with tolerance of the response defined as "an attenuation of drug response at the same dose and concentration due to prior drug exposure" (Sharma, Ebling and Jusko, 1998). This does not seem applicable to this study as only single doses followed by a long wash out period would negate tolerance, and therefore these models were not considered to be of interest in this study.

The PD models presented by Mager, Neuteboom and Jusko, (2005) Hu et al, (2011) and Jeon et al, (2013) have one thing in common that they all incorporate transit compartments to describe the initial lag time for the neopterin response. The neopterin response observed in monkeys following treatment of IFNα2b at both 3 and 10 MIU/kg was similar to the values determined in the predose samples out to approximately 8 h post dose therefore there could be considered to be a lag in the appearance of the response. A transit compartment model was not included in the indirect response model in this study but it may be worth revisiting in the future to see if it improves the ability of the model to describe the PK/PD relationship, particularly for some of the other cytokines where no measurable concentrations were observed in the early samples indicating a delay or lag in the response.

7.4.3. Population Pharmacokinetic/Pharmacodynamic simulations to investigate the impact on the IFNα2b induction of the serum concentrations of neopterin, IL15 and IL1Ra by the pan JAK inhibitor Xeljaz™ (tofacitinib)

Simulations investigating the capability of tofacitinib to inhibit IFNα2b serum concentrations of neopterin, IL15 and IL1Ra demonstrated that all doses of tofacitinib would be predicted to deliver at least some inhibition of the observed response. The inhibition profiles differ among the cytokines which is reflected by the difference in the EC_{50} and E_{max} values for the three cytokines (fold difference between minimum and maximum of 266 and 1200 respectively). All doses of tofacitinib were predicted to inhibit concentrations of the biomarkers below the baseline for some duration.

The model suggests that a dose of 10 mg/kg would deliver 31% inhibition of neopterin concentrations, and 60% inhibition of IL15 and IL1Ra concentrations based on the C_{max} values with and without inhibitor. This suggests that if this was translatable for a 70kg

human tofacitinib could have a clinical dose of ≥700 mg depending on the mechanistic biomarker. These simulations should be interpreted with caution as the model does not give a robust prediction of EC_{50} or E_{max} for any biomarker, but serves as a theoretical example of how the model once updated with more data can be used.

7.4.4. Pharmacokinetic/Pharmacodynamic simulations using the TMDD models presented in the literature

It is well established that the pharmacokinetics of the Type I IFNs can be described using a TMDD model incorporating both linear and nonlinear elimination pathways in both the monkey and humans (Mager et al, 2003; Kagan et al, 2010). In addition these models have been incorporated with an indirect response model to describe the induction of neopterin by subtypes of IFNα and IFNβ in both the monkey and humans. These full PK/PD models are describe by a large number of parameters (up to 18 for a subcutaneous model) which are comprised of both system specific, such as the number of receptors, and drug specific such as the receptor binding affinity and EC_{50} and 8 compartments. Initial efforts to model the induction of neopterin by IFNα2b in the monkey were met with limited success as the model failed to complete the minimisation step on all occasions (data not shown). This may be due to the number of parameters to be estimated, the limited dose range administered in this study and/or that the pharmacokinetics of IFNα2b were broadly linear over the dose range administered potentially making it difficult for the model to provide a robust estimation of the parameters. Therefore simulations of IFNα2b and neopterin profiles using the models and parameter estimates presented in the literature were conducted with the objectives of eventually comparing them to the data observed in this study.

Using the same equations and parameters it was possible to simulate comparable profiles for IFNβ1a and neopterin in the monkey to those presented by Kagan et al (2010). This gave confidence to use the model to simulate the IFNα2b and neopterin in the monkeys following sc administration of IFNα2b at 3 MIU/kg using the estimates for K_a from the population PK modelling were incorporated into the model. The TMDD model predicted faster absorption than observed which is unsurprising considering this is the phase that the population PK model poorly predicted. The TMDD model predicted biphasic kinetics, with an initial distribution phase between 1-10 h followed by the terminal elimination phase. The terminal elimination phase was comparable between the predicted and observed profiles however the distribution phase predicted by the TMDD model was not evident in

the observed data. This may be as a result of the prolonged absorption masking this phase in the observed data as well as the absence of data collected at the appropriate time points to characterise this phase. In general though the model gave good prediction IFNα2b concentrations although tended to over predict the C_{max} and under predicted the terminal phase. Another consideration is that given previous work indicates that the receptor mediated clearance becomes saturated at lower concentrations for IFNα2b compared to IFNβ1a it may be that the KD is different for IFNα2b to that used in the model which was predicted for IFNβ1a. Adjusting the KD 10 fold gave a predicted concentration profile more comparable to the observed concentration time profile which may suggest that KD as well as K_a requires optimisation to predict the observed IFNα2b concentration time profile.

The TMDD model predicted neopterin concentrations towards the higher end of the observed neopterin concentrations. Kagan et al, (2010) assume that the induction of neopterin is driven by the activated receptor and SC_{50} and S_{max} are considered a system specific parameter and equivalent between IFN subtypes. The amounts of activated receptor are driven by the KD value therefore the different KD values between the different IFN subtypes deliver different amounts of activated receptor and therefore different amounts of neopterin. Adjusting the KD value predicted by Kagan et al (2010) for IFNβ1a by approximately 10 fold to gave a better prediction of the observed IFNα2b concentration time profile and also gave a better prediction of the neopterin concentration time profile providing confidence that a KD value for IFNα2b may be around 7. Although promising this has only investigated IFNα2b at a single dose and it may be more complicated than simply adjusting 1 parameter and expecting the model to fit both profiles and probably requires optimisation of a number of both the drug and system specific parameters to deliver comparable simulated profiles for both IFNα2b and neopterin to the observed data.

7.5. Conclusion

A population PK/PD model that describes the induction of 6 biomarkers that potentially have relevance to SLE following IFNα2b challenge in the monkey was developed. Due to the dose proportional increase in systemic exposure the PK of IFNα2b were described with a 2 compartment PK model and were comparable to that reported in the literature both in monkeys and humans. This is the first time that PK/PD modelling for the induction of IL15, IL6, MCP1, IL1Ra and exotaxin has been conducted. Once updated to obtain more reliable parameter estimates for EC_{50} and E_{max}, the model can be used for the simulation of the

impact of a pan JAK inhibitor, such as toficitinib, on the IFNα2b induction of the most promising clinical biomarkers for SLE that were investigated in this study, neopterin, IL15 and IL1Ra. Due to the translatability of the biology between primate and humans this project has therefore delivered a PK/PD model with disease relevant endpoints that can be used to screen compounds and potentially predict efficacious clinical doses.

Chapter 8: Conclusion and Future Perspectives

8.1. Conclusion

This project has explored two preclinical mechanistic *in vivo* challenge PK/PD models around a common pathway, as an alternative to traditional disease models in drug discovery. The latter models attempt to replicate the human disease in a preclinical species, and whilst they have undoubtedly increased our understanding of the pathways involved in a particular disease, they have not been particularly successful in delivering new medicines. As an alternative, mechanistic models look to replicate a single or small number of mechanisms, following administration of a challenge agent, that are believed to be involved in the pathogenesis of the disease and can be reliably translated from preclinical species to the human. This approach requires an in-depth understanding of the pathways involved in the pathogenesis of the disease to enable a hypothesis or clinical question to be formed around the role of the target mechanism in the disease and the tractability of targeting as a therapeutic option. For this project, the chronic autoimmune disease systemic lupus erthyematosus (SLE) was selected as a target disease. This is a complex disease involes almost all the immune cells, multiple organ systems, and multiple feedback loops that lead to exacerbation of the disease. Whilst the standard of care has improved in recent years, it has traditionally been difficult to identify new treatments with only one new approval in the last 60 years. Evidence suggests that the cytokine IFNα has a central role in both the initiation and exacerbation of the disease, and appears to be a suitable candidate to target. Importantly, evidence suggest that the IFN pathway can be readily investigated in preclinical species, has been linked to the observation of SLE like symptoms in preclinical disease models, and has a number of clinically relevant translatable biomarkers that can be measured in preclinical species. Taking this into account two *in vivo* models that use different challenge agents to induce components of the IFNα pathway in preclinical species were selected and their utility as models in the drug discovery environment was successfully determined.

A mouse TLR7 agonist challenge model using the TLR7 agonist resiquimod was investigated and is considered to be a higher throughput screening model. This model was hypothesised to allow the investigation of TLR7 antagonists following co-administration with a TLR7 agonist, however, could feasibly be used to investigate inhibitors that have their action at any point downstream of the TLR7 receptor. Resiquimod induce IFNα production from pDC both *in vitro* and *in vivo* in human and preclinical species and therefore potentially offers a

translatable challenge. In this project resiquimod was shown to induces IFNα production following iv administration in the CD1 mouse. In addition, the investigation of the dose response demonstrated a bell shaped dose response curve as presented in the literature for almost all TLR7 agonists investigated both *in vivo* and *in vitro*. A resiquimod dose of 0.4 mg/kg, despite inducing a sub maximal response, delivered the most reproducible response between mice and also delivered a comparable response between study days and was selected as the fixed challenge for future studies. This provided confidence that a robust response could be observed between studies enabling the comparison of the ability of compounds of interest to inhibit the IFNα response between study days. The characterisation of the variability of the response and subsequent analysis indicated that the model may be used to investigate up to 9 compounds per study at a single dose or a dose response curve investigating concentrations of an inhibitor that would be predicted to deliver inhibition between 40-90%. As well as the IFNα response, the pharmacokinetics of resiquimod were successfully determined in the mouse following iv bolus administration. This is the first time they have been reported despite considerable interest in this compound. Resiquimod was a moderate clearance compound, with a moderate volume of distribution and a short half life. The variability of the PK parameters between mice was low and demonstrated considerably less variability that the PD (response) parameters. This project has confirmed that resiquimod induces IFNα levels in mice. With a fixed resiquimod dose of 0.4 mg/kg the model meets the requirements of what would be expected of a preclinical challenge model to investigate inhibitors of the IFNα pathway downstream of the TLR7 receptor.

The mechanisms behind the bell shaped resiquimod dose response curve were explored which led to the hypothesis that an endogenous modulator function either driven by resiquimod or the system itself may be responsible. Although this has been observed in numerous *in vitro* and *in vivo* studies over the 15 years or so that TLR7 agonists have been investigated, no one has previously attempted to model the bell shaped dose response relationship with a population PK/PD model. The ability of a population PK/PD model with a one compartment PK model, an indirect response model with stimulation of input to describe the induction of IFNα and an endogenous modulator function to describe the resiquimod dose response curve were explored. Whilst the modelling was encouraging, this requires further work, particularly around the endogenous modulator function. The modelling did highlight phases of the profile where it would be beneficial to generate

further data and will guide the design of future studies to enable optimal data collection to ensure successful population PK/PD modelling.

The second model investigated was a primate recombinant IFNα2b challenge model that is considered to represent a lower throughput but more predictive or translatable model of clinical efficacy. This model was selected based on evidence that the PK/PD for the subtype IFNβ1a relationship observed in monkeys can be translated to human and that an IFNα2b challenge study had been successfully utilised in Phase I to demonstrate efficacy of a JAK inhibitor. The pharmacokinetics of IFNα2b in the monkey following sc administration were successfully determined. Linearity in the PK was observed over the dose range investigated indicating that receptor mediated clearance is saturated at these doses and renal elimination is likely to be the primary route of elimination. The induction of neopterin concentrations was observed and was a comparable response to that previously reported. In addition the induction of 6 cytokines/chemokines in the monkey, all of which have been demonstrated to be elevated in SLE, has been reported for the first time. These biomarkers offer potential as translatable biomarkers to predict efficacy of new drug for SLE. An increase in body temperature is observed in the clinic following administration of recombinant IFNα2b and was predicted to be a translatable measure of efficacy from monkey to man. Following administration of recombinant IFNα2b no increase in body temperature was observed in monkeys. Taking this finding with the information that following administration of TLR7 agonists an induction of both IFNα and body temperature was observed indicates that in monkeys it may only be endogenous IFNα that induces body temperature and not the human form. In summary this study has provided a PK/PD model in the monkey that can be used to investigate the inhibition of a wide range of clinically relevant biomarkers by inhibitor compounds that have their action downstream of the IFN receptor such as JAK1.

Population PK/PD modelling using a 2 compartment PK model and an indirect response model stimulation of input was successfully used to describe the PK/PD relationship of the IFNα2b induction of 6 biomarkers. There was little difference in the response of each biomarker observed at the lower and higher dose of IFNα2b, additional doses to expand the dose-response curve may be necessary to help define the PK and PD parameters. Simulations using the reported parameters for the pan JAK inhibitor toficitinib demonstrated that at least 30% inhibition of neopterin and 60% of IL15 and IL1Ra by

tofacitinib would be predicted although the predicted dose range is large depending on the biomarker.

This project has successfully designed and validated two preclinical *in vivo* mechanistic PK/PD challenge models based on the hypothesis that the cytokine IFNα is central to the pathogenesis in SLE and that the mechanisms behind the induced response are translatable between species. This project has demonstrated that both models have potential in drug discovery to be used as valuable tools in the selection of the most appropriate compounds for progression to the clinic and the prediction of efficacious doses.

8.2. Future Perspectives

The work reported in this thesis was designed and conducted to investigate the utility of mechanistic acute inflammatory challenge models in different species but focusing on a common disease mechanism in the drug discovery environment. It was possible to conclude that both models would be suitable tools to enable the investigation of the inhibition of challenge induced disease relevant biomarkers. Despite this positive conclusion, further work is required to validate, test, refine and ultimately increase the understanding of the models and their predictive value in both the selection of the most appropriate compounds for progression and efficacious clinical doses. Throughout the work a number of questions were raised which future studies should look to address to deliver more robust models and data sets to enable population PK/PD modelling. Some of the key questions that should be focused on are

- **Can the response be inhibited using a gold standard therapy for the target disease?**

As part of the validation of the model, it is important to test whether the target mechanism or pathway can be inhibited by either a therapy specific to the mechanism of interest, or a therapy that is utilised in the treatment or management of the target disease. Ideally, the models would be tested with a TLR7 antagonist for the mouse model and a JAK1/TYK2 specific inhibitor for the primate model; however at the time of writing small molecule inhibitors for either target were not commercially available. There are a number of pan JAK inhibitors such as Toficitinib and Baricitinib that are available to potentially test the primate model and there are realistic options for the future as there are a number of TLR7, 8 and 9 antagonists currently in clinical trials for SLE or other indications and a number of TYK2 compounds in early clinical development. In the absence of TLR7 or JAK1/TYK2 specific

inhibitor compounds the alternative option would be to investigate therapy that is utilised in the treatment or management of the target disease. Current treatments regimens include three major medication classes, corticosteroids, immunosuppressants and anti-malarials, however the mechanism of action of corticosteroids and anti-malarials make them unsuitable for the TLR7 mouse model and potentially their action is too early in the pathway for the primate model which potentially only leaves immunosuppressants.

- **Could a translatable/bridging biomarker across all species be indentified?**

A biomarker that can be used to demonstrate efficacy and that is translatable from preclinical PK/PD models to the clinic is highly desirable. When using a TLR7 agonist as the challenge agent IFNα is clearly a translatable biomarker, however at low doses of challenge agent the sensitivity of the assay may limit the utility of this cytokine as a biomarker. Body temperature may serve as a translatable biomarker in a TLR7 agonist challenge model as an increase in body temperature has been observed in monkeys and humans following administration of TLR7 agonists and this could be explored in rodents. A large number of biomarkers were investigated in the primate IFNα2b model and it is possible that some of these markers may be translatable across the species. It has been reported that IFNα2b is not active in rodents, which would therefore mean that as a model the challenge may not translatable from mouse to human, although this is presented by authors who have used neopterin as a biomarker which rodents are known not to have the capacity to produce. Equally evidence suggests that the translatability of cytokines between species is questionable. *In vitro* and *in vivo* studies have demonstrated that the pattern of cytokines and chemokines induced by TLR7 agonists are notably different between mouse and monkey while monkey is comparable to human. This raises some concerns around translatability of cytokine profiles from mouse to primate, particularly as when the same cytokine is induced in both species the levels can be very different between the two. It does however give confidence that the primate cytokine profile may be translatable to man.

A translatable biomarker would ideally be utilised in the clinic as part of the diagnosis of the disease or to determine the response to a particular treatment and therefore would be disease relevant. Such a biomarker may be incorporated into experimental strategies where by a challenge study using a similar challenge/study design to the preclinical challenge studies is conducted as part of the Phase I healthy volunteer study. An example of such a biomarker would be one or a panel of the IFN inducible genes that make up the IFN gene

signature such as OAS or Mx1. They have clinical significance with regard to SLE, have been measured in preclinical species, and have been demonstrated to be up regulated following administration of a TLR7 agonist in humans, monkeys and mice even at low doses where no systemic concentrations of IFNα were observed. This suggests that the IFN gene signature may represent a more sensitive biomarker to determine efficacy than systemic IFNα concentrations which may be a key consideration to investigate when further developing this model with the goal of delivering translatable predictions of efficacy from *in vivo* screening to the clinic. Unfortunately due to the lack of available technology and capability it was not possible to investigate the IFN gene signature in the mouse studies and whilst this was initially explored in the primate model logistical complications meant that it was never fully explored. This however remains a key area to explore in the future for both challenge models.

- **Would a more robust PD data set deliver a more robust population PK/PD model?**

In discussions of both Chapter 5 and 7 the potential impact that the limitations in the data set had on the delivery of a final PK/PD model were raised. If the objective is to deliver a population PK/PD model then the development of a more robust data set would be a key objective for future studies. The resiquimod mouse model may benefit from both investigations of further doses particularly at the low doses either side of the dose that delivered the maximum response and a more extensive concentration-time profile at each dose. The maximum number of samples that could be taken from an individual mouse were collected in this study however they were all collected at the same time point. It may be worth increasing the numbers of mice in the group at particular doses of interest and incorporating a composite sampling regime to deliver increased samples on the different phases of the IFNα concentration-time profile for example the elimination phase which was poorly characterised in this study. Investigating both the PK and PD at lower doses of IFNα2b in the primate IFN challenge model may allow a better characterisation of the dose/concentration-effect relationship of the biomarkers of interest and also potentially allow the PK to be described using the TMDD model. This may also be important to understanding the feasibility of using the model to screen and select compounds. The IFNα2b challenge is very expensive so if modelling and simulation can be used to demonstrate that the response is sufficient that the *in vivo* efficacy of a compound can be reliably predicted from a lower dose of challenge it is going to make the model more attractive in drug discovery where costs are always under consideration.

- **Can a more robust population PK/PD model be delivered to describe the dose response relationship for the resiquimod induction of IFNα in the mouse?**

The limitations of the population PK/PD model were discussed in Chapter 5 and were disappointing that a final optimal population PK/PD model was not delivered. PK A key focus of the future work will be to re-investigate this to describe the reduction of the response at higher doses with the endogenous modulator function rather than the addition of variability on E_{max}. This is the first time in TLR7 agonist development that population PK/PD modelling of the dose response relationship had been conducted and merits further investigation. This potentially goes hand in hand with the development of an increased concentration-time profile described above but may also be feasible with the current data set. The delivery of a model that is using the endogenous modulator function will enable the re-investigation of the hypothesis around co-administration of the challenge with a TLR7 antagonist.

The questions discussed above are just a selection, and potentially the first that would be focused on, of those that this project has raised. There are a great many other questions that this work has raised that may be considered for the future and highlights the complexity of the immune system such as; Is resiquimod the best challenge agent for the model? Would a different TLR agonist deliver a different serum IFNα response? Is it possible to distinguish the IFN subtype profile induced by resiquimod and other TLR agonists? What is responsible for the lag in the IFNα response following resiquimod administration? Which cells produces IFNα in the mouse, can we be sure it is the pDCs? Is it possible to distinguish endogenous IFNα subtypes from the IFNα2b challenge in the monkey? Is recombinant human IFNα2b truly inactive in rodents or does it induce cytokines and the IFN gene signature? Is it possible to link the induction and interplay of the different biomarkers /cell types following IFNα2b administration to begin to develop quantitative systems pharmacology (QSP) model?

References

Abud-Mendoza, C., de la Fuente, H., Cuevas-Orta, E., Baranda, L., Cruz-Rizo, J. and González-Amaro, R. (2003) Therapy with statins in patients with refractory rheumatic diseases: a preliminary study. *Lupus,* 12, pp. 607-611

Agoram B.M. and Van Der Graaf P.H. (2012) Biomarkers and biomeasures: Key enablers for pharmacokinetic- pharmacodynamic modeling in drug discovery and development. *Bioanalysis*,4, pp. 1143-1145

Akgul, E.O., Aydin, I., Cayci, T., Kurt, Y.G., Aydin, F.N., and Agilli, M. (2013) The indicator of Cellular Response in Body Fluids: Neopterin. Gulhane medical Journal, 55, pp.1-7

Akira, S. and Takeda, K. (2004) Toll-loke receptors signalling. *Nature Reviews: Immunology,* 4, pp. 499-511

Alarcon-Riquelme, M.E., (2006) Nucleic Acid by-products and chronic inflammation. *Nature Genetics,* 38(8), pp.866-867

Amuro, H., Ito, T., Miyamoto, R., Sugimoto, H., Torii, Y., Son, Y., Nakamichi, N., Yamazaki, C., Hoshino, K., Kaisho, T., Ozaki, Y., Inaba, M., Amakawa, R. and Fukuhara, S. (2010) Statins, Inhibitors of 3-Hydroxy-3-Methylglutaryl-Coenzyme A Reductase, Function as Inhibitors of Cellular and Molecular Components Involved in Type I Interferon Production. *Arthritis and* Rheumatism, 62, pp. 2073-2085

Aringer M., Stummvoll G.H., Steiner G., Köller M., Steiner C.W., Höfler E., Hiesberger H., Smolen J.S. and Graninger W.B. (20010 Serum interleukin-15 is elevated in systemic lupus erythematosus. *Rheumatology*, 40, pp. 876-881

Asselin-Paturel, C., Brizard, G., Pin, J.J., Brière, F. and Trinchieri, G. (2003) Mouse Strain Differences in Plasmacytoid Dendritic Cell Frequency and Function Revealed by a Novel Monoclonal Antibody. *Journal of Immunology.* 171, pp. 6466-6477

Asselin-Paturel, C., Brizard, G., Chemin, K., Boonstra, A., O'Garra, A., Vicari, A. and Trinchieri, G. (2005) Type I interferon dependence of plamacytoid dendritic cell activation and migration. *Journal of Experimental Medicine.* 201, pp. 1157-1167

Baccala R., Kono D.H. and Theofilopoulos A.N. (2005) Interferons as pathogenic effectors in autoimmunity. *Immunological Reviews,* 204, pp. 9-26

Baccala, R., Hoebe, K., Kono, D.H., Beutler, B. and Theofilopoulos, A.N. (2007) TLR-dependent and TLR-independent pathways of type I interferon induction in systemic autoimmunity. *Nature Medicine*, 13, pp. 543–551

Baechler E.C., Batliwalla F.M., Karypis G., Gaffney P.M., Ortmann W.A., Espe K.J., Shark K.B., Grande W.J., Hughes K.M., Kapur V., Gregersen P.K. and Behrens T.W. (2003) Interferon-inducible gene expression signature in peripheral blood cells of patients with severe lupus.

Proceedings of the National Academy of Sciences of the United States of America, 100, pp. 2610-2615

Bauer, J.W., Petri, M., Batliwalla, F.M., Koeuth, T., Wilson, J., Slattery, C., Panoskaltsis-Mortari, A., Gregersen, P.K., Behrens, T.W. and Baechler, E.C. (2009) Interferon-Reguated Chemokines as Biomarkers of Systemic Lupus Erythematosus Disease Activity: A Validation Study. *Arthritis & Rheumatology,* 60, pp. 3098-3107

Baig, E. and Fish, E.N. (2008) Distinct signature type I interferon responses are determined by the infecting virus and the target cell. *Antiviral Therapy,* 13, pp.409-422

Bannai, H., Tatsumi, M., Hohase, M., Onishi, E. and Yamazaki, S. (1985) Pharmacokinetic study of human recombinant ineterferon (Re-IFN-αA) in cynomolgus monkeys 2'-5' oligoadenylate synthetase assay. *Japan Journal of Medical Science and Biology,* 38, pp. 113-124

Bannai, H., (1986) Comparison of pharmacokinetic behaviours of two human interferons (Lb-IFN-α and Re-IFN-αA) in cynomolgus monkeys by 2'-5' Oligoadenylate synthetase assay. *Japanese Journal of Medicinal Science and Biology,* 38, pp.113-124

Barbado, J., Martin, D., Vega, L., Almansa, R., Gonçalves, L., Nocito, M., Jimeno, A., Ortiz de Lejarazu, R. and Bermejo-Martin, J.F. (2012) MCP-1 in urine as biomarker of disease acivity in Systemic Lupus Erythematosus. *Cytokine*, 60, pp. 583-586

Barbhaiya M.A and Costenbader K.H. (2014) Ultraviolet radiation and systemic lupus erythematosus. *Lupus*, 23, pp. 588-595

Barrat, F.J., Meekre, T., Gregorio, J., Chan, J.H., Uematsu, S., Akira, S., Chang, B., Duramad, O. and Coffman, R.L. (2005) Nucleic acids of mammalian origin can acts as endogenous ligands for Toll-like receptors and may promote systemic lupus erythematosus. *Journal of Experimental Medicine,* 202, 1131-1139

Barrat, F.J. and Coffman, R.L. (2008) Development of TLR inhibitors for the treatment of autoimmune diseases. *Immunological Reviews,* 223, pp. 271-283

Basith, S., Manavalan, B., Lee, G., Kim, G.S. and Choi, S. (2011) Toll-like receptor modulators: a patent review (2006-2010). *Expert Opinion on Therapeutic Patents*, 21, pp.927-944

Beal, S., Sheiner, L.B., Boeckmann, A., & Bauer, R.J., NONMEM User's Guides. (1989-2009), Icon Development Solutions, Ellicott City, MD, USA, 2009.

Bengtsson, A., Sturfelt, G., Truedsson, L., Blomberg, J., Alm, G., Vallin, H. and Rönnblom, L., (2000) Activation of type I interferon system in systemic lupus erythematosus correlates with disease activity but not antiviral antibodies. *Lupus*, 9, pp.664-671

Bertsias, G.K., Salmon, J.E. and Boumpas, D.T. (2010) Therapeutic opportunities in systemic lupus erythematosus: state of the art and prospects for the new decade. *Annals of Rheumatic Disease*, 69, pp. 1603-1611

Birmachu, W., Gleason, R.M., Bulbulian, B.J., Riter, C.L., Vasilakos, J.P., Lipon, K.E. and Nikolsky, Y. (2007) Transcriptional networks in plasmacytoid dendritic cells stimulated h synthetic TLR 7 agonists. *BMC Immunology,* 8, pp 1-19

Bohoslawec O., Trown P.W. and Wills R.J. (1986) Pharmacokinetics and tissue distribution of recombinant human alpha A, D, A/D(Bgl), and I interferons and mouse alpha-interferon in mice. *Journal of Interferon Research*, 6, pp.207-213

Bonjardim, C.A. (2005) Interferons (IFNs) are key cytokines in both innate and adaptive antiviral immune response-and viruses counteract IFN action. *Microbes and Infection,* 7, pp.569-578

Buchwalder, PA., Buclin, T., Trinchard, I., Munafo, A. and Biollaz, J. (2000) Pharamcokinetcis and Pharmacodynamics of IFN-β1a in Healthy Volunteers. *Journal of Interferon and Cytokine Research,* 20, pp. 857-866

Budagian V., Bulanova E., Paus R. and Bulfone-Paus S. (2006) IL-15/IL-15 receptor biology: A guided tour through an expanding universe. *Cytokine and Growth Factor Reviews*, 17, pp. 259-280

Bundgaard, C., Larsen, F., Jørgensen, M. and Mørk, A. (2007) Pharmacokinetic/Pharmacodynamic Feedback Modelling of the Functional Corticosterone Response in Rats after Acute Treatment with Escitalopram. *Basic & Clinical Pharmacology and Toxicology,* 100, pp. 182-189

Burdick L.M., Somani N. and Somani A.-K. (2009) Type I IFNs and their role in the development of autoimmune diseases. *Expert Opinion on Drug Safety*, 8, pp. 459-472

Cai, Y., Zhang, Z., Fan, K., Zhang, J., Shen, W., Li, M., Si, D., Luo, H., Zeng, Y., Fu, P. and Liu, C. (2012) Pharmacokinetics, tissue distribution, excretion and antiviral activity of pegylated recombinant human consensus interferon-α variant in monkeys, rats and guinea pigs. *Regulatory Peptides,* 173, pp.74-81

Caricchio, R. and Cohen, P.L. (1999) Spontaneous and induced apoptosis in systemic lupus erythematosus: multiple assays fail to reveal consistent abnormalities. *Cellular Immunology,* 25, pp. 54-60

Cao W., Manicassamy S., Tang H., Kasturi S.P., Pirani A., Murthy N. and Pulendran B. (2008) Toll-like receptor-mediated induction of type I interferon in plasmacytoid dendritic cells requires the rapamycin-sensitive PI(3)K-mTOR-p70S6K pathway. *Nature Immunology*, 9, pp. 1157-1164

Chan, K.L. and Mok, C.C. (2013) Development of systemic lupus erythematosus in a male-to-female transsexual: the role of sex hormones revisited. *Lupus,* 22, pp 1399-1402

Chatelut, E., Rostaing, L., Grégoire, N., Payen, JL., Pujol, A., Izopet, J., Housin, G., and Canal, P. (1999) A pharmacokinetic model for alpha interferon administered subcutaneously. *British Journal of Clinical Pharamcology,*47. Pp365-371

Chiche, L., Jourde, N., Bardin, N., Bornet, C., Darque, A., Mancini, J. (2012) New treatment options for lupus-a focus on belimumab. *Therapeutics and Clinical Risk Management,* 8, pp.33-43

Chun, H.Y., Chung, J.W., Kim, H.A., Yun, J.M., Jeon, J.Y., Ye, Y.M., Kim, S.H., Park, H.S. and Suh, C.H. (2007) Cytokine IL-6 and IL-10 as Biomarkers in Systemic Lupus Erythematosus. *Journal of Clinical Immunology,* 27, pp. 461-466

Clarke, S., Laxton, C., Horscroft, N., Richard, V., Thomas, A. and Parkinson, T. (2009) Comparison of Rat and Human Responses to Toll-like Receptor 7 Activation. *Journal of Interferon & Cytokine Research,*29, pp. 113-126

Collins J.M., Riccardi R., Trown P., O'Neil, D. and Poplack D.G. (1985) Plasma and cerebrospinal fluid pharmacokinetics of recombinant interferon alpha A in monkeys: Comparison of intravenous, intramuscular, and intraventricular delivery. *Cancer Drug Delivery*, 2, pp. 247-253

Comte D., Karampetsou M.P. and Tsokos G.C. (2015) T cells as a therapeutic target in SLE. *Lupus*, 24, pp. 351-363

Connolly, D.J. and O'Neill, L.A.J. (2012) New developments in Toll-like receptor targeted therapeutics. *Current Opinion in Pharmacology,* 12, pp.510-518

Cox, K.L., Devanarayan, V., Kriauciunas, A., Manetta, J., Montrose, C. and Sittampalam, S. (2012) Immunoassay Methods. *Assay Guidance Manual.* https://www.ncbi.nlm.nih.gov/books/NBK92434/pdf/Bookshelf_NBK92434.pdf

Czarniecki, M. (2008) Small Molecule Modulators of Toll-like Receptors. *Journal of Medicinal Chemistry,* 51, pp. 6621-6626

Danhof, M., de Lange, E.C.M., Della Pasqua, O.E., Ploeger, B.A. and Voskuyl, R.A. (2008) Mechanism-based pharmacokinetic-pharmacodynamic (PK/PD) modeling in translational drug research. *Trends in Pharmacological Sciences,* 29, pp. 186-191

Dayneka N.L., Garg V. and Jusko W.J. (1993) Comparison of four basic models of indirect pharmacodynamic responses. *Journal of Pharmacokinetics and Biopharmaceutics,* 21, pp. 457-478

Davis, B. and Morris, T. (1993) Physiological Parameters in Laboratory Animals and Humans. *Pharmaceutical Research*, 10, pp.1093-1095

Dale, R.C. and Brilot, F. (2010) Biomarkers of inflammatory and auto-immune central nervous system disorders. *Current Opinion in Paediatrics,* 22, pp.718-725

Dalpke A.H., Opper S., Zimmermann S. and Heeg K. (2001) Suppressors of cytokine signaling (SOCS)-1 and SOCS-3 are induced by CpG-DNA and modulate cytokine responses in APCs1. *Journal of Immunology*, 166, pp. 7082-7089

Deane, J.A., Pisitkun, P., Barrett, R.S., Feigenbaum, L., Town, T., Ward, J.M., Flavell, R.A. and Bolland, S. (2007) Control of Toll-like Receptor 7 Expression Is Essential to Restrict Autoimmunity and Dendritic Cell Proliferation. *Immunity,* 27, pp. 801-810

Delgado-Vega A.M., Alarcón-Riquelme M.E. and Kozyrev S.V. (2010) Genetic associations in type I interferon related pathways with autoimmunity. *Arthritis Research and Therapy*, 12:SUPPL. 1 Article Number S2

Derendorf, H. and Meibohm, B. (1999) Modeling of Pharmacokinetic/Pharmacodynamic (PK/PD) Relationships: Concepts and Perspectives. *Pharmaceutical Research,*16, pp.176-185

De Weerd N.A. and Nguyen T. (2012)The interferons and their receptors-distribution and regulation. *Immunology and Cell Biology*, 90, pp. 483-491

Deshmane S.L., Kremlev S., Amini S. and Sawaya B.E. (2009) Monocyte chemoattractant protein-1 (MCP-1): An overview. *Journal of Interferon and Cytokine Research,* 29, pp. 313-325

Dockrell, D.H. and Kinghorn, G.R. (2001) Imiquimod and resiquimod as novel immunomodulators. *Journal of Antimicrobial Chemotherapy,* 48, pp. 751-755

Du, X., Poltorak, A., Wei, Y. and Beutler, B. (2000) Three novel mammalian toll-like receptors; gene structure, expression and evolution. *European Cytokine Network,* 11, pp. 362-371

Duch, D.S., Woolf, J.H., Nichol, C.A., Davidson, J.R. and Garbutt, J.C. (1984) Urinary excretion of bioterin and neopterin in psychiatric disorders. *Psychiatry Research,* 11, pp. 83-89

Durcan L. and Petri M. (2016) Immunomodulators in SLE: Clinical evidence and immunologic actions. *Journal of Autoimmunity*, 74, pp. 73-84

Egner, W. (2013) The use of laboratory test in the diagnosis of SLE. *Journal of Clinical Pathology*, 53, pp. 424-432

Eloranta, ML. and Rönnblom, L. (2016) Cause and consequence of the activated type I interferon system in SLE. *Journal ofMolecular Medicine,* 94, pp.1103-1110

Elwy M.A., Galal Z.A. and Hasan H.E. (2010) Immunoinflammatory markers and disease activity in systemic lupus erythematosus: Something old, something new. *Eastern Mediterranean Health Journal,* 16, pp. 893-900

Engel, A.L., Holt, G.E. and Lu, H. (2011) The pharmacokinetics of Toll-lie receptor agonists and the impact on the immune system. *Expert Reviews in Clinical Pharmacology,* 4, pp.275-289

Eriksson, C. and Rantapää-Dahlqvist, S. (2014) Cytokines in relation to autoantibodies before onset of symptoms for systemic lupus erythematosus. *Lupus,* 23, pp. 691-696

European Medicines Agency (2013) Guideline on clinical investigation of medical products for the treatment of systemic lupus erythematosus and lupus nephritis. EMA/CHMP/51230/2013

Fehniger T.A. and Caligiuri M.A. (2001) Interleukin 15: Biology and relevance to human disease. *Blood*, 97, pp 14-32

Flanagan, M.E., Blumenkopf, T.A., Brissette, W.H., Brown, M.F., Casavant, J.M., Shang-Poa, C., Doty, J.L., Elliott, E., Fisher, M.B., Hines, M., Kent, C., Kudlacz, E.M., Lillie, B.M., Magnuson, K.S., McCurdy, S.P., Munchhof, M.J., Perry, B.D., Sawyer, P.S., Strelevitz, T.J., Subramanyam, C., Sun, J., Whipple, D.A. and Changelian, P.S. (2010) Discovery of CP-690,550: A Potent and Selective Janus Kinase (JAK) Inhibitor for the Treatment of Autoimmune Disease and Organ Transplant Rejection. *Journal of Medicinal Chemistry,* 53, pp. 8468-8484.

Fitzgerald-Bocarsly, P., Dai, J. and Singh, S. (2008) Plasmacytoid dendritic cells and type I IFN: 50 years of convergent history. *Cytokine & Growth Factor Reviews,* 19, pp. 3-19

Food and Drug Administration (2004) Innovation or stagnation: challenge and opportunity on the critical path to new medicinal products.

Food and Drug Administration (2010) Guidance for Industry: Systemic Lupus Erythematosus – Developing medical products for treatment

Forsbach A., Müller C., Montino C., Kritzler A., Nguyen T., Weeratna R., Jurk M. and Vollmer J. (2012) Negative regulation of the type i interferon signaling pathway by synthetic toll-like receptor 7 ligands. *Journal of Interferon and Cytokine Research*, 32, pp. 254-268

Frasen, J.H. van der Vlag, J., Ruben, J., Adema, G.J., Berden, J.H and Hillbrands, L.B.(2010) The role of dendritic cells in the pathogenesis of systemic lupus erythematosus. *Arthritis* Research and Therapy,12, pp. 207-215

Frieri M. (2013) Mechanisms of disease for the clinician: Systemic lupus erythematosus. *Annals of Allergy, Asthma and Immunology*, 110, pp. 228-232

Fuchs D., Weiss G., Reibnegger G. and Wachter H. (1992) The role of neopterin as a monitor of cellular immune activation in transplantation, inflammatory, infectious, and malignant diseases. *Critical Reviews in Clinical Laboratory Sciences*, 29, pp. 307-341

Fuchsberger, M., Hochrein, H., and O'Keeffe, M. (2005) Activation of plasmacytoid dendritic cells. *Immunology and Cell Biology,* 83, pp. 571-577

Fulmer, T (2010) Sparing Steroids in Lupus. *SciBX*, 3

Gabrielsson, J. and Weiner, D. (2000) *Pharmacokinetic & Pharamcodynamic data analysis-Concepts and Applications*, 3rd ed Stockholm, Sweden: Swedish Pharmaceutical Press

Garcia-Garcia, I., Gonzάlez-Delgardo, C.A., Valenzuela-Silva, C.M., Diaz-Machado, A., Marisol Cruz-Díaz, M., Nodarse-Cuní, H., Orlando Pérez-Pérez, O., Bermúdez-Badell, C.H., Ferrero-Bibilonia, J., Páez-Meireles, R., Bello-Rivero, I., Castro-Odio, F.R. and López-Saura, P.A. (2010) Pharmacokinetic and pharmacodynamic comparison of two "pegylated" interferon alpha-2 formulations in healthy male volunteers: a randomized, crossover, double-blind study. *BMC Pharmacology,* 10, pp.1-11

Gary-Gouy H., Lebon P. and Dalloul A.H. (2002) Type I interferon production by plasmacytoid dendritic cells and monocytes is triggered by viruses, but the level of production is controlled by distinct cytokines. *Journal of Interferon and Cytokine Research*, 22, pp. 653-659

Gibiansky L., Gibiansky E., Kakkar T. and Ma P. (2008) Approximations of the target-mediated drug disposition model and identifiability of model parameters. *Journal of Pharmacokinetics and Pharmacodynamics*, 35, pp. 573-591

Gibson, S.J., Lindh, J.M., Riter, T.R., Gleason, R.M., Rogers, L.M., Fuller, A.E., Oesterich, J.L., Gorden, K.B., Qiu, X., McKane, S.W., Noelle, R.J., Miller, R.L., Kedl, R.M., Fitzgerald-Bocarsly, P., Tomai, M.A. and Vasilakos, J.P. (2002) Plasmacytoid dendritic cells produce cytokines and mature in response to the TLR7 agoinsts, imiquimod and resiquimod. *Cellular Immunology,* 218, pp. 74-86

Gloff, C.A and Wills, R.J. (1992) Pharamcokinetics and Metabolism of Therapeutic Cytokines. *Protein Pharamacokinetics and Metabolism,* Chapter 5, pp.127-150

Glue, P., Fang, J.W., Rouzier-Panis, R., Raffanel, C., Sabo, R., Gupta, S.K., Salfi, M. and Jacobs, S. (2000) Pegylated interferon-alpha: pharmacokinetics, pharmacodynamics, safety, and preliminary data. Hepatitis C intervention Therapy Group. *Clinical Pharamcology and Therapeutics,* 68, pp.556-567

Goldblatt, F. and Isenberg, D.A. (2005) New therapies for systemic lupus erythematosus. *Clinical &Experimental Immunology,* 140, pp. 205-212

González-Navajas, J.M., Lee, J., David, M. and Raz, E. (2012) Immunomodulatory functions of type I interferons. *Nature Reviews: Immunology,* 12, pp. 125-135

Gorden, K.B., Gorski, K.S., Gibson, S.J., Kedl, R.M., Kieper, W.C., Qiu, X., Tomai, M.A., Alkan, S.S. and Vasilakos, J.P. (2005) Synthetic TLR agonists reveal functional differences between Human TLR7 and TLR8. *Journal of Immunology,* 174, pp. 1259-1268

Graul, A. and Castaner, J. (1999) S-28463. Treatment of Hepatitis C Interferon Inducer. *Drugs of the Future,* 24, pp. 622-627

Guggino, G., Giardina, A.R., Ciccia, F., Triolo, G., Dieli, F. and Sireci, G. (2012) Are Toll-like receptors and decoy receptors involved in the immunopathogenesis of Systemic Lupus Erythematosus and lupus-like sysndromes? *Clinical and Developmental Immunology,* pp.1-5

Guiducci, C., Coffman, R.L. and Barrat, F.J. (2009) Signalling pathways leading to IFN-α production in human plasmacytoid dendritic cell and the possible use of agonists or antagonists of TLR7 and TLR9 in clinical indications. *Journal of Internal Medicine,* 265, pp. 43-57

Guiducci C., Ghirelli C., Marloie-Provost M.-A., Matray T., Coffman R.L., Liu Y.-J., Barrat F.J. and Soumelis V. (2008) PI3K is critical for the nuclear translocation of IRF-7 and type I IFN production by human plasmacytoid predendritic cells in response to TLR activation. *Journal of Experimental Medicine,* 205, pp. 315-322

Hayashi, T. (2010) Therapeutic Strategies for SLE Involving Cytokines: Mechanism-Oriented Therapies Especially IFN-γ Targetting Gene Therapy. *Journal of Biomedicine and Biotechnology,* 1-19

Hemmi, H., Kaisho, T., Takeuchi, O., Sat, S., Sanjo, H., Hoshino, K., Horiuchi, T., Tomizawa, H., Takeda, K. and Akira, S. (2002) Small anti-viral compounds activate immune cells *via* the TLR7 MyD88-dependent signalling pathway. *Nature Immunology,* 3, pp.196-200

Herrmann, M., Voll, R.E., Zoller, O.M., Hagenhofer, M., Ponner, B.B. and Kalden, J.R. (1998) Impaired phagocytosis of apoptotic cell material by monocyte-derived macrophages from patients with systemic lupus erythematosus. *Arthritis and Rheumatism,* 41, pp.1241-1250

Horscroft, N.J., Pryde, D.C. and Bright, H. (2012) Antiviral applications of Toll-like receptor agonists. *Journal of Antimicrobial Chemotherapy,* 67, pp.789-801

Hu, X., Olivier, K., Polack, E., Crossman, M., Zokowski, K., Gronke, R.S., Parker, S., Li, Z., Nestorov, I., Baker, D.P., Clarke, J. and Subramanyam, M. (2011) In Vivo Pharmacology and Toxicology Evaluation of Polyethylene Glycol-Conjugated Interferon β-1a. *The Journal of Pharmacology and Experimental Therapeutics,* 338, pp. 984-996

Huber, C., Batchelor, J.R., Fuchs, D., Hausen, A., Lang, A., Niederwieser, D., Reibnegger, G., Swetly, P., Troppmair, J. and Wachter, H (1984) Immune response-associated production of neopterin. Release from macrophages primarily under control of interferon-gamma. *Transplantation Proceedings*, 17, pp. 582-585

Hui-Yuen J.S., Nguyen S.C. and Askanase A.D. (2016) Targeted B cell therapies in the treatment of adult and pediatric systemic lupus erythematosus. *Lupus*, 25, pp. 1086-1096

Illei, G.G, Tackey, E., Lapteva, L. and Lipsky, P.E. (2004) Biomarkers in Systemic Lupus Erythematosus II. Markers of Disease Activity. *Arthritis and Rheumatism,* 50, pp. 1709-1720

Illei, G.G, Tackey, E., Lapteva, L. and Lipsky, P.E. (2004) Biomarkers in Systemic Lupus Erythematosus I. General Overview of Biomarkers and Their Applicability. *Arthritis and Rheumatism,* 50, pp. 2048-2065

Imbertson, L.M., Beaurline, J.M., Couture, A.M., Gibson, S.J., Smith, R.M.A., Miller, R.L., Reiter, M.J., Wagner, T.L. and Tomai, M.A. (1998) Cytokine induction in hairless mouse and rat skin after topical application of the immune response modifiers imiquimod and S-28463. *The Journal of Investigative Dermatology,* 100, pp. 734-739

Ingartua, M. and Pedraz, J.L. (2010) Topical resiquimod: a promising adjuvant for vaccine development ? *Expert Reviews of Vaccines,* 9, pp. 23-27

Isobe Y., Kurimoto A., Tobe M., Hashimoto K., Nakamura T., Norimura K., Ogita H. and Takaku H. (2006) Synthesis and biological evaluation of novel 9-substituted-8-hydroxyadenine derivatives as potent interferon inducers. *Journal of Medicinal Chemistry*, 49, pp. 2088-2095

Ito T., Amakawa R., Kaisho T., Hemmi H., Tajima K., Uehira K., Ozaki Y., Tomizawa H., Akira S. and Fukuhara S (2002) Interferon-α and interleukin-12 are induced differentially by toll-like receptor 7 ligands in human blood dendritic cell subsets. *Journal of Experimental Medicine,* 195, pp. 1507-1512

Iyengar, R., Zhao, S., Chung, S-W., Mager, D.E. and Gallo, J.M. (2012) Merging Systems Biology with Pharmacodynamics. *Science Translational Medicine,* 4, pp. 1-12

Jacob, N. and Stohl, W. (2011) Cytokine disturbances in systemic lupus erthyematosus. *Arthritis Research and Therapy*, 13, pp. 228-239

Jeon, S., Juhn, JH., Han,S., Lee, J., Hong, T., Paek, J. and Yim, DS. (2013) Saturable human neopterin response to interferon-α assessed by a pharmacokinetic pharamcodynamic model. *Journal of Translatable Medicine,* 11, pp.240-249

Jin, O., Sun, L., Zhou, KX., Zhang, XS., Feng, XB., Mok, MY., and Lau, CS. (2005) Lymphocyte apoptosis and macrophage function: Correlation with disease activity in systemic lupus erythematosus*. Clinical Rehumatology, 24 pp. 107-110*

Jin, O., Kavikondala, S., Sun, L., Fu, R., Mok, MY., Chan, A., Yeung, J. And Lau, CS. (2008) Systemic lupus erythematosus patients have increased number of circulating plasmacytoid dendritic cells, but decreased myeloid dendritic cells with deficient CD83 expression. *Lupus,* 17, pp. 654-662

Jin, O., Kavikondala, S., Mok, MY., Sun, L., Gu, J., Fu, R., Chan, A., Yeung, J., Nie, Y. and Lau, CS. (2010) Anromalities in circulating plasmacytoide dendritic cells in patients with systemic lupus erythematosus. *Arthritis Research and Therapy*,12, R137

Jinushi M., Takehara T., Kanto T., Tatsumi T., Groh V., Spies T., Miyagi T., Suzuki T., Sasaki Y. and Hayashi. N. (2003) Critical role of MHC class I-related chain A and B expression on IFN-α-stimulated dendritic cells in NK cell activation: Impairment in chronic hepatitis C virus infection. *Journal of Immunology*, 170, pp. 1249-1256

Jones, H.M., Dickens, M., Youdim, K., Gosset, J.R., Attkins, N.J., Hay, T.L., Gurrell, I.K., Logan, Y.R., Bungay, P.J., Jones, B.C., and Gardner, I.B. (2012) Application of PBPK modelling in drug discovery and development at Pfizer. *Xenobiotica,* 42, pp.94-106

Jurk, M., Heil, F., Vollmer, J., Schetter, C., Krieg, A.M., Wagner, H., Lipford, G. and Bauer, S. (2002) Human TLR7 or TLR8 independently confer responsiveness to the antiviral compound R-848. *Nature immunology,* 3, pp. 499

Jusko, W.J. (2013) Moving from Basic Toward Systems Pharmacodynamic Models. *Journal of Pharmaceutical Sciences,* 102, pp. 2930-2940

Kadowaki N., Antonenko S., Lau J.Y.-N. and Liu Y.-J. (2000) Natural interferon α/β-producing cells link innate and adaptive immunity. *Journal of Experimental Medicine*,192, pp. 219-225

Kagan, L.K., Abraham, A.K., Harrold, J.M. and Mager, D.E. (2010) Interspecies scaling of Receptor-Mediated Pharmacokinetics and Pharmacodynamics of Type I Interferons. *Pharmaceutical Research,* 27, pp. 920-932

Kahl, L., Patel, J., Layton, M., Binks, M., Hicks, K., Leon, G., Hachulla, E., Machado, D., Staumont-Sallé, D., Dickson, M., Condreay, L., Schifano, L., Zamuner, S. and van Vollenhoven, R.F. (2016) Saftey, tolerability, efficacy and pharmacodynamics of the selective JAK1 inhibitor GSK2586184 in patients with systemic lupus erythematosus. *Rheumatology,* 25, pp. 1420-1430

Kalliolias, G.D. and Ivashkiv, L.B. (2010) Overview of the biology of type I interferons. *Arthritis Research & Therapy,* 12, Suppl 1, pp. 1-9

Kalunian, K.C. (2016) Interferon-targeted therapy in systemic lupus erythematosus: Is this an alternative to targeting B and T cells? *Lupus,* 25, pp. 1097-1101

Kandimalla, E.R., Bhagat, L., Wang, D., Yu, D., Sullivam, T., La Monica, N. and Agrawal, S.(2013) Design, synthesis and biological evaluation of novel antagonist compounds of Toll-like receptors 7, 8 and 9. *Nucleic Acids Research*, 41, pp.3947-3961

Karlsson, M.O. and Sheiner, L.B. (1993) The Importance of Modelling Interoccasion Variability in Population Pharmacokinetic Analyses. *Journal of Pharmacokinetics and Biopharmaceutics,* 21, pp. 735-749

Kawai, T. and Akira, S. (2007) Antiviral signaling through pattern recognition receptor. *Journal of biochemistry,* 141, pp. 137-145

Kawai, T. and Akira, S. (2010) The role of pattern-recognition receptors in innate immunity: Update on toll-like receptors. *Nature Immunology,* 11, pp. 373-384

Kazemipour N., Qazizadeh H., Sepehrimanesh M. and Salimi S. (2015) Biomarkers identified from serum proteomic analysis for the differential diagnosis of systemic lupus erythematosus. *Lupus*, 24, pp. 582-587

Kerns, E.H. and Li, D. (2008) *Drug-like properties: concepts, structure design and method: from ADME to toxicology optimization*. 3rd ed. Oxford: Academic Press, Elsevier

Khoo, JJ., Foster, S. and Mansell, A. (2011) Toll-Like Receptors as Interferon-Regulated Genes and Their Role in Disease. *Journal of Interferon & Cytokine Research,* 31, pp.13-25

Kiang T.K.L., Sherwin C.M.T., Spigarelli M.G. and Ensom M.H.H. (2012) Fundamentals of population pharmacokinetic modelling: Modelling and software. *Clinical Pharmacokinetics*, 51, pp. 515-525

Kim, JM., Park, SH., Kim, HY. and Kwok, SK. (2015) A Plasmacytoid Dendritic Cells-Type I Interferon Axis Is Critically Implicated in the Pathogenesis of Systemic Lupus Erythematosus. *International Journal of Molecular Sciences,* 16, pp.14158-14170

Kirou, K.A. and Gkrouzman, E. (2013) Anti-interferon alpha treatment in SLE. *Clinical Immunology,* 148, pp. 303-312

Krzyzanski W. and Jusko W.J. (2001) Indirect pharmacodynamic models for responses with multicompartmental distribution or polyexponential disposition. Journal *of Pharmacokinetics and Pharmacodynamics*, 28, pp.57-78

Kumar, V., Cotran, R.S. and Robbins, S.l. (2003) *Robbins Basic Pathology.* 7th ed. Philadelphia: Saunders

Kuznik, A., Bencina, M., Svajger, U., Jeras, Matjaz, Rozman, B. and Jerala R. (2011) Mechanism of Endosomal TLR inhibition by Antimalarial Drugs and Imidazoquionlines. *The Journal of Immunology*, 186

Lalonde R.L., Kowalski K.G., Hutmacher M.M., Ewy W., Nichols D.J., Milligan P.A., Corrigan B.W., Lockwood P.A., Marshall S.A., Benincosa L.J., Tensfeldt T.G., Parivar K., Amantea M., Glue P., Koide H. and Miller R. (2007) Model-based drug development. *Clinical Pharmacology and Therapeutics*, 82, pp. 21-32

Lauw F.N., Dekkers P.E.P., Te Velde A.A., Speelman P., Levi M., Kurimoto M., Hack C.E., Van Deventer S.J.H. and Van Der Poll T. (1999) Interleukin-12 induces sustained activation of multiple host inflammatory mediator systems in chimpanzees. *Journal of Infectious Diseases*, 179, pp. 646-652

Lee, P.Y., Kumangi, Y., Li, Y., Takeuchi, O., Yoshida, H., Weinstein, J., Kellner, E.S., Nacionales, D., Barker, T., Kelly-Scumpia, K., van Rooijen, N., Kumar, H., Kawai, T., Satoh,

M., Akira, S. and Reeves, W.H. (2008) TLR7-dependent and FcγR-independent production of type I Interferon in experimental mouse lupus. *Journal or Experimental Medicine,* 205, pp. 2995-3006

Leng, S.X., McElhaney, Walston, J.D, Xie, D., Fedarko, N.S. and Kuchel, G.A. (2008) Elisa and Multplex technologies for cytokine measurement in inflammation and aging research. *Journal Gerontology A: Biological Sciences and Medical Sciences,* 63, pp.879-884

Liefaard L.C., Ploeger B.A., Molthoff C.F.M., Boellaard R., Lammertsma A.A., Danhof M. and Voskuyl R.A. (2005) Population pharmacokinetic analysis for simultaneous determination of Bmax and KD In Vivo by positron emission tomography. *Molecular Imaging and Biology*, 7, pp.411-421

Liew, F.Y., Xu, D., Brint, E.K. and O'Neil, L.A.J. (2005) Negative Regulation of Toll-Like Receptor-Mediated Immune Responses. *Nature Reviews:Immunology,* 5, pp.446-458

Linker-Israeli, M., Deans, R.J., Wallace, D.J., Prehn, J., Ozeri-Chen, T. and Klinenberg, J.R. (1991) Elevated levels of endogenous IL-6 in systemic lupus erythemastosus. A putative role in pathogenesis. *The Journal of Immunology,* 147, pp.117-123

Liu, CC. (2005) IPC: Professional Type I Interferon-Producing Cells and Plasmacytoid Dendritic Cell Precursors. *Annual Reviews. Immunology,* 23, pp. 275-306

Liu, CC. and Ahearn, J.M. (2009) The search for lupus biomarkers. *Best Practice & Research Clincial Rheumatology,* 23, pp. 507-523.

Luu, K.T., Zhang, E.Y., Prasanna, G., Xiang, C., Anderson, S., Fortner, J. and Vicini, P. (2009) Pharmacokintic-Pharmacodynamic and Response Sensitization Modelling of the Intraocular Pressure-Lowering Effect of the EP4 Agonist 5-{3-[(2*S*)-2-{(3*R*)-3-hydroxy-4-[3-(trifluoromethyl)phenyl]butyl}-5-oxopyrrolidin-1-yl]propyl}thiophene-2-carboxylate (PF-04475270). *The Journal of Pharmacology and Experimental Therapeutics,* 331, pp. 627-635

Mager, D.E. and Jusko, W.J. (2002) Receptor-Mediated Pharmacokinetic/Pharmacodynamic Model of Interferon-β 1a in Humans. *Pharamceutical Research,* 19, pp.1537-1543

Mager, D.E. and Jusko, W.J. (2008) Development of Translational Pharmacokinetic-Pharmacodynamic Models. *Clinical Pharmacology & Therapeutics,* 83, pp.909-912

Mager, D.E. and Krzyzanski, W. (2005) Quasi-equilibrium pharmacokinetic model for drugs exhibiting target-mediated drug disposition *Pharmaceutical Research*, 22, pp.1589-1596

Mager, D.E, Neuteboom, B., Efthymiopoulos, C., Munafo, A. and Jusko, W.J. (2003) Receptor-Mediated Pharmacokinetics and Pharamcodynamics of Interferon-β1a in Monkeys. *The Journal of Pharamcology and Experitmental Therapeutics,* 306, pp.262-270

Mager, D.E, Neuteboom, B. and Jusko, W.J. (2005) Pharmacokinetics and Pharamcodynamics of PEGylated IFN-β 1a Following Subcutaneous Administration in Monkeys. *Pharamceutical Research,* 22, pp.58-61

Mager, D.E, Wyska, E. and Jusko, W.J. (2003) Diversity of mechanism-based pharmacodynamic models. *Drug Metabolism and Disposition ,* 31, pp.510-519

Majno, G. and Joris, I. (2004) *Cell, Tissues and Disease*. 3rd ed. New York: Oxford University Press

Mahmood, I. (1998) Interspecies scaling of renally secreted drugs. *Life Sciences,* 63, pp. 2365-2371

Marshak-Rothstein, A. (2006) Toll-like receptors in systemic autoimmune disease. *Nature Reviews Immunology*, 6, pp. 823-835

Marshall, J.D., Heeke, D.S., Gesner, M.L., Livingston, B. and Van Nest, G. (2007) Negative regulation of TLR9-mediated IFN-α induction by a small-molecule, synthetic TLR7 ligand. *Journal of Leukocyte Biology*, 82, pp. 497-508

McKenna, K., Beignon, AS. and Bhardwaj, N. (2005) Plasmacytoid Dendritic Cells: Linking Innate and Adaptive Immunity. *Journal of Virology,* 79, pp.1-24

Medzhitov, R. (2001) Toll-like receptors and innate immunity. *Nature reviews. Immunology,* 1, pp. 135-145

Medzhitov, R. (2008) Origin and physiological roles of inflammation. *Nature,* 454, pp. 428-435

Meyer, O. (2009) Interferons and autoimmune disorders. *Joint Bone Spine*,76, pp.464-473

Miller, R.L., Gerster, J.F., Owens, M.L., Slade, H.B. and Tomai, M.A. (1999) Imiquimod applied topically: a novel immune response modifier and new class of drug. *International Journal of Immunopharmacology*, 21, pp.1-14

Mittleman, B.B. (2004) Biomarkers for systemic lupus erythematosus: Has the right time finally arrived? *Arthritis Research and Therapy*, 6, pp. 223-224

Mok, C.C and Lau, C.S (2003) Pathogenesis of Systemic Lupus Erythematosus. *Journal of Clinical Pathology,* 56, pp. 481-490

Mosak, J. and Furie, R. (2013) Breaking the ice in systemic lupus erythematosus: belimumab, a promising new therapy. *Lupus,* 22, pp. 361-370

Mould, D.R. and Upton, R.N. (2012) Basic Concepts in Population Modelling, Simulation, ad Model-Based Drug Development. *CPT Pharmacometrics & Systems Pharmacology,* 1,

Mould, D.R. and Upton, R.N. (2013) Basic concepts in population modeling, simulation, and model-based drug development - Part 2: Introduction to pharmacokinetic modeling methods. *CPT: Pharmacometrics and Systems Pharmacology*, 2,

Munoz, L.E., van Bavel, C., Franz, S., Berden, J., Herrmann, M. and van der Vlag, J. (2008) Apoptosis in the pathogenesis of systemic lupus erythematosus. *Lupus,* 17, pp. 371-375

Murr, C., Widner, B., Wirleitner, B. and Fuchs, D. (2002) Neopterin as a marker for immune system activation. *Current Drug Metabolism,* 3, pp. 175-187

Nandkumar, P. and Furie, R. (2016) T-cell-directed therapies in systemic lupus erythematosus. *Lupus,* 25, pp. 1080-1085

Nials, A.T. and Uddin, S. (2008) Mouse models of allergic asthma: acute and chronic allergen challenge. *Disease Models & Mechanisms,* 1, pp.213-220

Nieforth, K.A., Nadeau, R., Patel, I. and Mould, D. (1996) Use of an indirect pharmacodynamic stimulation model of MX protein induction to compare in vivo activity of interferon alfa-2a and a polyethylene glycol-modified derivative in healthy subjects. *Clinical Pharmacology and Therapeutics,* 59, pp.636-646

Niewold, T.B. (2008) Interferon alpha-induced lupus: Proof of principle. *Journal of Clinical Rheumatology*, 14, pp. 131-132

Ohl, K. and Tenbrock, K. (2011) Inflammatory Cytokines in Systemic Lupus Erythematosus. *Journal of Biomedicine and Biotechnology,* 1-14

Ohteki, T., Suzue, K., Maki, C., Ota, T. and Koyasu, S. (2001) Critical role of IL15-IL15R for antigen-presenting cell functions in the innate immune response. *Nature Immunology,* 2, pp. 1138-1143

O'Neill, L.A.J., Golenbock, D. and Bowie, A.G. (2013) The history of Toll-like receptors-redefining innate immunity. *Nature Reviews: Immunology,* 13, pp.453-460

Osborn, B.L., Olsen, H.S., Nardelli, B., Murray, J.H., Zhou, J.X.H., Garcia, A., Moody, G., Zaritskaya, L.S. and Sung, C. (2002) Pharmacokinetics and pharmacodynamic studies of a human serum, albumin-interferon-α fusion protein in cynomolgus monkeys. *The Journal of Pharmacology and Experimental Therapeutics,* 303, pp.540-548

O'Shea, J.J., Kontzias, A., Yamaoka, K., Tanaka, Y. and Laurence, A. (2013) Janus kinase inhibitors in autoimmune disease. *Annals of Rheumatic Disease,* 72, pp.111-115

Palleroni, A.V. and Bohoslawec, O. (1984) Use of 125I-interferons in pharmacokinetic and tissue distribution studies. *Journal of Interferon Research*, 4, pp.493-498

Parodis, I., Axelsson, M. and Gunnarsson, I. (2013) Belimumab for systemic lupus erythematosus: a practice-based view. *Lupus,* 22, pp. 372-380

Pascual, V., Chaussabel, D. and Banchereau, J. (2010) A Genomic Approach to Human Autoimmune Diseases. *Annual Review of Immunology*, 28, pp.535-71

Pascual, V., Farkas, L. and Banchereau, J. (2006) Systemic lupus erythematosus: all roads lead to type I interferons. *Current Opinion in Immunology*, 18, pp. 676-682

Paterson, H.M., Murphy, T.J., Purcell, E.J., Shelley, O., Kriynovich, S.J., Lien, E., Mannick, J.A. and Lederer, J.A. (2003) Injury Primes the Innate Immune System for Enhanced Toll-Like Receptor Reactivity. *Journal of Immunology*, 171,pp. 1473-1483

Pathak, S. and Mohan, C. (2011) Cellular and molecular pathogenesis of systemic lupus erythematosus: lessons from animal models. *Arthritis research &therapy,* 13, pp.241-249

Patrignani, C., Lafont, D.T., Muzio, V., Gréco, B., Hooft van Huijsduijen, R., and Zaratin, P. (2010) Characterization of protein tyrosine phosphate H1 knockout mice in animal models of local and systemic inflammation. *Journal of Inflammation,* 7, pp.1-14

Perera, G. (2009) Clinical models and their use in translation. *Online presentation, Accessed April 2012* http://www.immunology.org/document.doc?id=288

Perry, D., Sang, A., Yin, Y., Zheng, Y-Y, and Morel, L. (2011) Murine models of systemic lupus erythematosus. *Journal of Biomedicine and Biotechnology.* Article ID 271694,

Pestka, S., Langer, J.A., Zoon, K.C., Samuel, C.E. (1987) Interferons and their actions. *Annual Review of Biochemistry*, 56, pp. 727-777

Petri, M. (2008) Sex hormones and systemic lupus erythematosus. *Lupus,* 17, pp 412-415

Pockros, P.J., Guyader, D., Patton, H., Tong, M.J., Wright, T., McHutchison, J.G. and Meng, T-C. (2007) Oral resiquimod in chronic HCV infection: Safety and efficacy in 2 placebo-controlled, double-blind phase IIa studies. *Journal of Hepatology,* 47, pp.174-182.

Posselt, G., Schwarz, H., Duschl, A. and Horejs-Hoeck, J. (2011) Suppressor of cytokine signaling 2 is a feedback inhibitor of TLR-induced activation in human monocyte-derived dendritic cells. *Journal of Immunology*, 187, pp. 2875-2884

Prasad, K.V. and Prabhakar, B.S. (2003) Apoptosis and autoimmune disorders. *Autoimmunity,*36, pp. 323-330

Radwanski, E., Perentesis, G., Jacobs, S., Oden, E., Affrime, M., Symchowicz, S. and Zampagoline, N. (1987) Pharmacokinetics of Interferon α2b in Healthy Volunteers. *Journal of Clinical Pharmacology,* 27, pp. 432-435

Rahman, A. and Isenberg, D.A. (2008) Systemic Lupus Erythematosus. *The New Engalnd Journal of Medicine,* 358, pp. 929-937

Rao, V. and Gordon, C. (2014) Advances in the assessment of lupus disease activity and damage. *Current Opinion in Rheumatolog,* 26, pp. 510-519

Reddy, K.R. (2004) Development and Pharmacokinetics and Pharmacodynamics of Pegylated Interferon Alfa-2a (40 kD). *Seminars in Liver Disease,* 24, Supplement 2, pp. 33-38

Reizis, B., Colonna, M., Trinchieri, G., Barrat, F. and Gilliet, M. (2011) Plasmacytoid dendritic cells: one-trick ponies or workhorses of the immune system? *Nature Reviews: Immunology,* 11, pp. 558-565.

Rho, Y.H., Solus, J., Raggi, P., Oeser, A., Gebretsadik, T., Shintani, A. and Stein, C.M. (2011) Macrophage activation and coronary atherosclerosis in systemic lupus erythematosus and rheumatoid arthritis. *Arthritis care & research*, 63, pp. 535-541

Richer, M.J., Pewe, L.L., Hancox, L.S., Hartwig, S.M., Varga, S.M. and Harty, J.T. (2015) Inflammatory IL-15 is required for optimal memory T cell responses. *Journal of Clinical Investigation*, 125, pp.3477-3490

Ripley, B.J.M., Goncalves, B., Isenberg, D., Latchman, D.S. and Rahman, A. (2005) Raised levels of interleukin 6 in systemic lupus erythematosus correlate with anaemia. *Annals of Rheumatic Disease*, 64, pp.849-853

Rodriguez, J.L., Valenzuela, C., Marin, N., Ferrero, J., Duconge, J., Castillo, R., Pontigas, V., Deas, M., Gonzalez-Suarez, R. and Lopez-Saura, P. (2000) Comparative pharmacokinetics and pharmacodynamics of two recombinant human interferon alpha-2b formulations administered intramuscularly in healthy male volunteers. *Biotecnologia Aplicada*, 17, pp. 166-170

Romange, F. (2006) Current and future drugs targeting one class of innate immunity receptors:the Toll-like receptors. *Drug Discovery Today*, 12, pp. 80-87

Rönnblom, L. and Pascual, V. (2008) The innate immune system in SLE: Type I interferons and dendritic cells. *Lupus*, 17, pp. 394-399

Rönnblom, L. (2010) Potential role for IFNα in adult lupus. *British Arthritis Research &Therapy*, 12 (Supplement 1).

Rönnblom, L., Eloranta, ML., (2013) The interferon signature in autoimmune disease. *British Current Opinion in Rheumatology*, 25 pp. 248-253

Rottman, J.B. and Willis, C.R. (2010) Mouse Models of Systemic Lupus Erythematosus Reveal a Complex Pathogenesis. *Veterinary Pathology,* 47, pp.664-676

Rückert R., Brandt K., Ernst M., Marienfeld K., Csernok E., Metzler C., Budagian V., Bulanova E., Paus R. and Bulfone-Paus S. (2009) Interleukin-15 stimulates macrophages to activate CD4+ T cells: A role in the pathogenesis of rheumatoid arthritis? *Immunology*, 126, pp.63-73

Sams-Dodd, F. (2006) Strategies to optimize the validity of disease models in the drug discovery process. *Drug Discovery Today,* 11, pp. 355-363

Samsonov, M.Y., Tilz, G.P., Egorova, O., Reibnegger, G., Balabanova, R.M., Nassonov, E.L., Nassonova, V.A., Wachter, H. and Fuchs, D. (1995) Serum soluble markers of immune activation and disease activity in systemic lupus erythematosus. *Lupu*s, 4, pp. 29-32

Sato, T., Saito, R., Jinushi, T., Tsuji, T., Matsuzaki, J., Koda, T., Nishimura, S.-I., Takeshima, H. and Nishimura, T. (2003) IFN-γ-induced SOCS-1 regulates STAT6-dependent eotaxin production triggered by IL-4 and TNF-α. *Biochemical and Biophysical Research Communications*, 314, pp. 468-475

Schiller, M., Metze, D., Luger, S.G. and Gunzer, M. (2006) Immune response modifiers-mode of action. *Experimental Dermatology,* 15, pp.331-341

Schmidt, K.N. and Ouyang, W. (2004) Targeting interferon-*α*: a promising approach for systemic lupus erythematosus therapy. *Lupus,*13,pp. 348-352

Seavey, M.M. and Dobrzanski, P. (2012) The many faces of Janus kinase. *Biochemical Pharmacology*, 83, pp. 1136-1145

Seavey, M.M., Lu, L.D. and Stump, K.L. (2011) Animal models of Systemic Lupus Erythematosus (SLE) and ex vivo assay design for drug discovery. *Current Protocols in Pharmacology,* Supplement 53, unit 5.60, pp.1-40

Sharma, A., Ebling, W. and Jusko, W.J. (1998) Precursor-Dependent Indirect Pharamcodynamic Response Model for Tolerance and Rebound Phenomena. *Journal of Pharmaceutical Sciences*, 87, pp. 1577-1584

Sharma, A., and Jusko, W.J. (1998) Characteristics of indirect pharmacodynamic models and applications to clinical drug responses. *British Journal of Clinical Pharmacology,* 45, pp. 229-239

Sheiner, L.B. and Grasela, T.H. Jr (1991) An introductionto mixed effect modeling:concepts, definitions, and justification. *Journal of Pharmacokinetics and Biopharmaceutics,* 19, pp. 11-23

Sherwin, C.M.T., Kiang, T.K.L., Spigarelli, M.G. and Ensom, M.H.H. (2012) Fundamentals of Population Pharmacokinetic Modelling: Validation Methods. *Clinical Pharmacokinetics,* 51, pp. 573-590

Shodell, M., Shah, K. and Siegal, F.P. (2003) Circulating human plasmacytoid dendritic cells are highly sensitive to corticosteroid administration. *Lupus*, 12, pp. 222-230

Sghiri, R., Feinberg, J., Thabet, F., Dellagi, K., Boukadida, J., Ben Abdelaziz, A., Casanova, J.L., Barbouche, M.R. (2005) Gamma interferon is dispensable for neopterin production in vivo. *Clinical and Diagnostic Laboratory Immunology*, 12, pp. 1437-1441

Smith, M.F.Jr, Hiepe, F., Dörner, T. and Burmester, G. (2009) Biomarkers as tools for improved diagnostic and therapeutic monitoring in Systemic Lupus Erythematosus. *Arthritis Research & Therapy,* 11, pp. 1-7

Stark, G.R., Kerr, I.M., Williams, B.R.G., Silverman, R.H. and Schreiber, R.D. (1998) How cells respond to interferons. *Annual Reviews of Biochemistry,* 67, pp.227-264

Stichweh, D., Pascual, V. and Banchereau, J. (2006) Recent advances in therapeutic strategies for SLE. *Drug Discovery Today: Therapeutic Strategies*, 3, pp. 5-10

Stypińska, B. and Paradowska-Gorycka, A. (2015) Cytokines and microRNAs as candidate biomarkers for systemic lupus erythematosus. *International Journal of Molecular Sciences,* 16, pp. 24194-24218

Suzuki, H., Takemura, H. and Kashiwagi, H. (1995) Interleukin-1 Receptor Antagoist in Patients with Active Systemic Lupus Erythematosus. *Arthritis and Rheumatism,* 38, pp.1055-1059

Theofilopoulos, A.N., Baccala, R., Beutler, B. and Kono, D.H. (2005) Type I interferons (α/β) in immunity and autoimmunity. *Annual Review of Immunology*, 23, pp. 307-336

Tektonidou, M.G. and Ward, M.M. (2010) Validity of clinical associations of biomarkers in translational research studies: the case of systemic autoimmune diseases. *Arthritis Research & Therapy,* 12, pp.1-10

Tektonidou, M.G. and Ward, M.M. (2011) Validation of new biomarkers in systemic autoimmune disease. *Nature Reviews: Immunology,* 7, pp.708-717

Thibault, D.L., Graham, K.L., Lee, L.Y., Balboni, I., Hertzog, P.J. and Utz, P.J. (2009) Type I interferon receptor controls B-cell expression of nucleic acid-sensing Toll-like receptors and autoantibody production in a murine model of lupus. *Arthritis Research and Therapy*, 11, Article Number R112

Tomai, M.A., Gibson, S.J., Imbertson, L.M., Miller, R.L., Myhre, P.E., Reiter, M.J., Wagner, T.L., Tamulinas, C.B., Beaurline, J.M., Gerster, J.F. and Horton, V.L. (1995) Immunomodualting and antiviral activities of the imidazoquinoline S-28463. *Antiviral Research,* 28, pp.253-264

Tomai, M.A, Miller, R.L., Lipson, K.E., Kieper, W.C., Zarraga, I.E. and Vasilakos, J.P. (2007) Resiquimod and other immune response modifiers as vaccine adjuvants. *Expert Reviews of Vaccines,* 6, pp. 835-847

Tomai, M.A and Vasilakos, J.P. (2011) TLR-7 and -8 agonists as vaccine adjuvants. *Expert Review of Vaccines,* 10, pp. 405-407

Tron, F. (1990) Contribution of murine models of spontaneous lupus to the analysis of genetic factors in human disease. *Annales de Médecine Interne*, 141, pp. 217-221

Trown, P.W., Wills, R.J. and Kamm, J.J. (1986) The preclinical development of Roferon®-A. *Cancer*, 57, pp. 1648-1656

Tsitoura, D., Ambery, C., Price. M., Powley, W., Garthside, S., Biggadike, K. and Quint, D. (2015) Early Clinical Evaluation of the Intranasal TLR7 Agonist GSK2245035: Use of Translational Biomarkers to Guide Dosing and Confirm Target Engagement. *Clinical Pharmacology & Therapeutics,* 98, pp. 369-380

Turner, M.D., Nedjai, B., Hurst, T. and Pennington, D.J. (2014) Cytokines and chemokines: At the crossroads of cell signalling and inflammatory disease. *Biochimica et Biophysica Acta - Molecular Cell Research*, 1843, pp. 2563-2582

Upton, R.N. and Mould, D.R. (2014) Basic Concepts in Population Modelling, Simulation, ad Model-Based Drug Development: Part 3-Introduction to Pharmacodynamic Modelling Methods*. CPT Pharmacometrics & Systems Pharmacology,* 3,

Utz, P.J. (2004) Multiplexed assays for identification of biomarkers and surrogate markers in systemic lupus erythematosus. *Lupus*, 13, pp. 304-311

Van der Graaf, P.H. and Gabrielsson, J. (2009) Pharmacokinetic-pharmacodynamic reasoning in drug discovery and early development. Future Medicinal Chemistry*,* 1, pp. 1371-1374

Van der Graaf, P.H. and Benson, N. (2011) Systems Pharmacology: Bridging Systems Biology and Pharmacokinetics-Pharmacodynamics (PK/PD) in Drug Discovery and Development. *Pharmaceutical Research,* 28, pp. 1460-1464

Via, C.S. (2010) Advances in lupus stemming from the parent-into-F1 model. *Trends in Immunology,* 31, pp.236-245

Villinger, F., Brar S.S., Mayne, A., Chikkala, N. and Ansar,i A.A. (1995) Comparative sequence analysis of cytokine genes from human and nonhuman primates. *Journal of Immunology*, 155, pp. 3946-3954

Vodovotz, Y., Chow, C.C., Bartels, J., Lagoa, C., Prince, J.M., Levy, R.M., Kumar, R., Day, J., Rubin, J., Constantine, G., Billiar, T.R., Fink, M.P. and Clermont, G. (2006) *In Silico* models of acute inflammation in animals. *Shock,* 26, pp.235-244

Wagner, T.L., Horton, V.L., Carlson, G.L., Myhre, P.E., Gibson, S.J., Imbertson, L.M. and Tomai, M.A. (1997) Induction of cytokines in cynomolgus monkeys by the immune response modifiers, imiquimod, S-27609 and S-28463, *Cytokin*e, 9, pp. 837-845

Wang, Y., Abel, K., Lantz, K., Krieg, A.M., McChesney, M.B. and Miller, C.J. (2005) The toll-like receptor 7 (TLR7) agonist, imiquimod, and the TLR9 agonist, CpG ODN, induce antiviral cytokines and chemokines but do not prevent vaginal transmission of simian immunodeficiency virus when applied intravaginally to rhesus macaques. *Journal of Virology,*79, pp.14355-14370

Widner, B., Sepp, N., Kowald,E., Ortner, U., Wirleitner, B., Fritsch, P., Baier-Bitterlich, G. and Fuchs, D. (2000) Enhanced tryptophan degradation in systemic lupus erythematosus. *Immunobiology*, 201, pp. 621-630

Willis, R., Seif, A.M., McGwin, Jr. G., Martinez-Martinez, L.A., González, E.B., Dang, N., Papalardo, E., Liu, J., Vilá, L.M., Reveille, J.D., Alarcón, G.S. and Pierangeli, S.S. (2012) Effect of hydroxychloroquine treatment on pro-inflammatory cytokines and disease activity in SLE patients: Data from LUMINA (LXXV), a multiethnic US cohort. *Lupus*, 21, pp. 830-835

Wills, R.J., Dennis, S., Speigel, H.E., Gibson, D.M. and Nadler, P.I. (1984) Interferon kinetics and adverse recation after intravenous, intramuscular and subcutaneous injection. *Clinical Pharmacokinetics,* 19, pp.390-399

Wills, R.J., Dennis, S., Speigel, H.E. and Soike, K.F. (1984) Pharamcokinetics of Recombinant Alpha A Interferon Following IV infusion and Bolus, IM and PO Administrations to African Green Monkeys. *Journal of Interferon Research,* 4, pp. 399-409

Wills, R.J. (1990) Clinical Pharmacokinetics of Interferons. *Clinical Pharmacology and Therapeutics,* 35, pp.722-727

Wirleitner, B., Reider, D., Ebner, S., Böck, G., Widner, B., Jaeger, M., Schennach, H., Romani, N. and Fuchs, D. (2002) Monocyte-derived dendritic cells release neopterin. *Journal of Leukocyte Biology*, 72, pp. 1148-1153

World Health Organisation (2006) Principles and methods for assessing autoimmunity associated with exposure to chemicals. *Environmental Health Criteria,* 236

Wu, J.J., Huang, D.B. and Tyring, S.K. (2004) Resiquimod: a new immune response modifier with potential as a vaccine adjuvant for Th1 immune responses. *Antiviral Research,* 64, pp. 79-83.

Xu, R.N. Fan, L., Rieser, M.J. and EL-Shourbagy, T.A. (2007) Recent advances in high-throughput quantitative bioanalysis by LC-MSMS. *Journal of Pharmaceutical and Biomedical Analysis,* 44, pp. 342-355

Yap, D.Y.H. and Lai, K.N. (2013) The role of cytokines in the pathogenesis of systemic lupus erythematosus - From bench to bedside. Nephrology, 18, pp. 243-255

Yildrim-Toruner, C. and Diamon, B. (2011) Current and novel therapeutics in the treatment of systemic lupus erythematosus. *Journal of Allergy and Clinical Immunology,* 127, pp. 303-312

Zhang, L., Pfister, M. and Meibohm, B. (2008) Concepts and Challenges in Quantitative Pharmacology and Model-Based Drug Development. *The AAPS Journal,* 10, pp. 552-559

Zhang, Y., Yang, F., Yang, Y., Song, F-I. and Xu, A. (2008) Recombinant interferon-alpha2b poly(lactic-co-glycolic acid) microspheres: pharmacokinetics-pharmacodynamics study in rhesus monkeys following intramuscular administration. *Acta Pharamcol Sin,*29, pp.1370-1375

Of mice and men – are mice relevant models for human disease? (21 May 2010)
Outcomes of the European Commission workshop, London, UK
http://ec.europa.eu/research/health/pdf/summary-report-25082010_en.pdf

Toxicologist review – Pegylated ineterferon-α2b (19 December 2000)
http://www.fda.gov/downloads/Drugs/DevelopmentApprovalProcess/HowDrugsareDevelopedandApproved/ApprovalApplications/TherapeuticBiologicApplications/ucm094485.pdf

Pharmacology review – IntronA/Rebetol (1998)

http://www.accessdata.fda.gov/drugsatfda_docs/nda/98/20903_INTRON%20A%20REBETOL_PHARMR_P1.PDF

Figure 2.1- Vodovotz, Y., Chow, C.C., Bartels, J., Lagoa, C., Prince, J.M., Levy, R.M., Kumar, R., Day, J., Rubin, J., Constantine, G., Billiar, T.R., Fink, M.P. and Clermont, G. (2006) *In Silico* models of acute inflammation in animals. *Shock,* 26, 3, pp.235-244. http://ovidsp.tx.ovid.com/sp-3.24.1b/ovidweb.cgi?QS2=434f4e1a73d37e8cf7fe2b149b8e4b50dfe1ae6af393c474eaf5834bcbfddc63b8768b99f28904415d04ce65a72ec53203fa9263abddaa96c6c30de6f598b69ffa0ddeb3c59cdd918c55d83c11b87d963b044124516ee017790d94ba7a75a0889ce8b479657aab3afa2e0ceb7518d0e6dbecf76d105f118e43ecdee8bcd041dd3044d2e591e9c47af9d54365e73ff3286929575665adbfa30428383003b81ef601b2c1f5f8ae96efc611006a88b415c6e81946aa666f3c63223fb5c019c3bc9a145a6489fe61a14ca85107974b696818ddb419eb8ea4b71d383c2d4f0f1b799d7d6266ebbe5d3f0ccd5137b6eb828200e4e13081cb47f1837b11237db59e49e48273438c560d65d7

Figure 2.6 – Reprinted from Drug Discovery Today, 11, 7-8, Sams-Dodd, F. Strategies to optimize the validity of disease models in the drug discovery process, pp. 355-363 (2006) with permission from Elsevier.

Figure 2.8 - Pharmaceutical Research*,* Modeling of Pharmacokinetic/Pharmacodynamic (PK/PD) Relationships: Concepts and Perspectives, 16, (1999) pp.176-185 Derendorf, H. and Meibohm, B. (© Plenum Publishing Corporation 1999) "With permission of Springer"

Figure 7.15 - Data Digitized from; Pharmaceutical Research, Interspecies scaling of Receptor-Mediated Pharmacokinetics and Pharmacodynamics of Type I Interferons. 27(2010) pp. 920-932, Kagan, L.K., Abraham, A.K., Harrold, J.M. and Mager, D.E. (© Springer Science+Business Media, LLC 2010) "With permission of Springer"

Appendicies

Appendix 1.1 Group 2 preparation of resiquimod dose solutions

Target Dose concentration (mg/mL)	Volume of 10 mg/mL DMSO sock solution added (mL)	Volume of DMSO added (mL)	Volume of Kleptose Saline added (mL)
0.006 mg/mL	0.0042	0.346	6.65
0.014 mg/mL	0.0098	0.252	6.65
0.02 mg/mL	0.0140	0.336	6.65
0.06 mg/mL	0.0420	0.308	6.65
0.14 mg/mL	0.0980	0.252	6.65
0.2 mg/mL	0.1400	0.210	6.65
0.6 mg/mL	n/a	0.660	12.54

Appendix 1.2 UPLC conditions

Strong Wash	methanol:water (90:10 v/v)
Weak Wash	methanol:water (10:90 v/v)
Injection Mode	Partial Loop
Injection Volume	10 µL
Flow Rate	1 mL/min
Analytical Column	Acquity BEH C18 1.7 µm, 50mm x 2.1 mm (Waters, Part no. 186002350)
Column Temperature	30°C
Run Time	1 min
Mobile Phase A	water containing 0.1% (v/v) formic acid.
Mobile Phase B	acetonitrile containing 0.1% (v/v) formic acid

Appendix 1.3 UPLC Gradient Profile

Time (mins)	Solvent A (%)	Solvent B (%)	Flow Rate (mL/min)
0.00	95	5	1
0.01	95	5	1
0.80	5	95	1
0.84	5	95	1
0.85	95	5	1
1.00	95	5	1

Appendix 1.4 Dilution steps for the preparation of resiquimod dose solutions from study day 3 for concentration analysis

Dose	Dose Concentration (mg/mL)	Required dilution to achieve 0.0002 mg/mL	First dilution	Second dilution
0.03 mg/kg Resiquimod	0.006	1:10	1:10 Dilution Dilute 50 µL of original dose solution with 450 µL of 1:1 (v/v) acetonitrile:water	NA
0.07 mg/kg Resiquimod	0.014	1:100	1:10 Dilution Dilute 50 µL of original dose solution with 450 µL of 1:1 (v/v) acetonitrile:water	1:10 Dilution Dilute 1.5 µL of 1:10 solution 13.5 µL of 1:1 (v/v) acetonitrile:water
0.1 mg/kg Resiquimod	0.02	1:100	1:10 Dilution Dilute 50 µL of original dose solution with 450 µL of 1:1 (v/v) acetonitrile:water	1:10 Dilution Dilute1.5 µL of original dose solution with 13.5 µL of 1:1 (v/v) acetonitrile:water
0.3 mg/kg Resiquimod	0.06	1:100	1:10 Dilution Dilute 50 µL of original dose solution with 450 µL of 1:1 (v/v) acetonitrile:water	1:10 Dilution Dilute 1.5 µL of original dose solution with 13.5 µL of 1:1 (v/v) acetonitrile:water
0.7 mg/kg Resiquimod	0.14	1:1000	1:10 Dilution Dilute 50 µL of original dose solution with 450 µL of 1:1 (v/v) acetonitrile:water	1:100 Dilution Dilute 5 µL of original dose solution with 495 µL of 1:1 (v/v) acetonitrile:water
1 mg/kg Resiquimod	0.2	1:1000	1:10 Dilution Dilute 50 µL of original dose solution with 450 µL of 1:1 (v/v) acetonitrile:water	1:100 Dilution Dilute 5 µL of original dose solution with 495 µL of 1:1 (v/v) acetonitrile:water
3 mg/kg Resiquimod	0.6	1:3000	1:10 Dilution Dilute 50 µL of original dose solution with 450 µL of 1:1 (v/v) acetonitrile:water	1:300 Dilution Dilute 3 µL of original dose solution with 897 µL of 1:1 (v/v) acetonitrile:water

Appendix 1.5 Dilution steps for the preparation of resiquimod stock solutions for blood sample concentration analysis

Stock ID	Required Resiquimod Concentration (mg/mL)	Stock Solution Preparation Scheme
A1	0.01	0.1 mL A0 made up to 1 mL with 1:1 (v/v) acetonitrile:water
A2	0.001	0.1 mL A1 + 0.9 mL 1:1 (v/v) acetonitrile:water
A3	0.0001	0.1 mL A2 + 0.9 mL 1:1 (v/v) acetonitrile:water
A4	0.00001	0.1 mL A3 + 0.9 mL 1:1 (v/v) acetonitrile:water

Appendix 1.6 LC conditions

Strong Wash	Methanol (Sigma-Aldrich, Cat no. 65542-2.5L):water (85:15 v/v) containing 0.02M ammonium acetate at 0.02M (Sigma-Aldrich, Cat no. 431311-250G) and 0.1% methylamine hydrochloride (Sigma-Aldrich, Cat no. M0505-500G)
Weak Wash	acetonitrile:water (20:80 v/v)
Injection Mode	Partial Loop
Injection Volume	2 µL
Flow Rate	1 mL/min
Analytical Column	Phenomenex Kinetex C18 2.6µm, 50mm x 2.1 mm (Phenomenex, Part no. 00B-4462-AN)
Column Temperature	40°C
Run Time	1.4 min
Mobile Phase A	Water containing 0.1% (v/v) formic acid (Fisher Scientific, Cat no. F/1900/PB15).
Mobile Phase B	Acetonitrile containing 0.1% (v/v) formic acid

Appendix 1.7 LC Gradient Profile

Time (mins)	Solvent A (%)	Solvent B (%)	Flow Rate (mL/min)
0.00	95	5	1
1.30	5	95	1
1.35	5	95	1
1.36	95	5	1
1.39	95	5	1

Appendix 1.8 Group 1. Mean, (SD and CV) peak area values for resiquimod standards A,B,C, pre and post filter dose aliquots and differences from the reference solution (B)

Sample Name	Mean Peak Area (n=9)	Standard Deviation (SD)	CV (%)	Difference in Mean Peak area to selected reference solution (%)
Standard A	34171	97	0.3	-4
Standard B	32829	213	0.7	Reference
Standard C	34120	585	1.7	+4
IV dose Pre filter	34253	104	0.3	+4
IV dose Post filter	33886	120	0.4	+3

Appendix 1.9 Group 3 and 4. Mean, (SD and CV) peak area values for resiquimod standards A,B,C, and pre and post filter dose aliquots and differences from the reference solution (B)

Sample Name	Mean Peak Area (n=9)	Standard Deviation (SD)	CV (%)	Difference in Mean Peak area to selected reference solution (%)
Standard A	41679	15531	37	-15.8
Standard B	49478	1617	3.3	Reference
Standard C	51672	893	1.7	+4
Study day 4 IV dose Pre filter	61842	1387	2.2	+25
Study day 4 IV dose Post filter	62194	1432	2.3	+26
Study day 5 IV dose Pre filter	62573	1002	1.6	+27
Study day 5 IV dose Post filter	64428	3751	5.8	+30

Appendix 1.10 Analytically measured dose concentration and percentage differences from the nominal dose concentrations for the dose solutions administered to Group 2 (0.03-3 mg/kg)

Treatment group	Aliquot	Measured concentration of diluted dose solution (mg/mL)	Mean Measured concentration of diluted dose solution (mg/mL)	Dilution Factor	Actual concentration dose solution (mg/mL)	Nominal dose concentration (mg/mL)	Percentage difference to nominal dose concentration (%)
0.03 mg/kg	Pre A	0.000593					
	Pre B	0.000721	0.000695	1:10	0.00695	0.006	16
	Pre C	0.000771					
	Post A	0.000744					
	Post B	0.000853	0.000777	1:10	0.00777	0.006	29
	Post C	0.000732					
0.07 mg/kg	Pre A	0.000193					
	Pre B	0.000173	0.000177	1:100	0.0177	0.014	27
	Pre C	0.000166					
	Post A	0.000169					
	Post B	0.000168	0.000167	1:100	0.0167	0.014	20
	Post C	0.000166					
0.1 mg/kg	Pre A	0.000264					
	Pre B	0.000252	0.000248	1:100	0.0248	0.02	24
	Pre C	0.000231					
	Post A	0.000296					
	Post B	0.000342	0.000305	1:100	0.0305	0.02	53
	Post C	0.000278					
0.3 mg/kg	Pre A	0.000847					
	Pre B	0.000715	0.000778	1:100	0.0778	0.06	30
	Pre C	0.000772					
	Post A	0.000825					
	Post B	0.000761	0.000819	1:100	0.0819	0.06	36
	Post C	0.000870					
0.7 mg/kg	Pre A	0.000204					
	Pre B	0.000205	0.000209	1:1000	0.209	0.14	49
	Pre C	0.000217					
	Post A	0.000208					
	Post B	0.000181	0.000206	1:1000	0.206	0.14	47
	Post C	0.000230					
1 mg/kg	Pre A	0.000273					
	Pre B	0.000301	0.000288	1:1000	0.288	0.2	44
	Pre C	0.000289					
	Post A	0.000292					
	Post B	0.000286	0.000282	1:1000	0.282	0.2	41
	Post C	0.000266					
3 mg/kg	Pre A	0.000870					
	Pre B	0.000816	0.000866	1:1000	0.866	0.6	44
	Pre C	0.000913					
	Post A	0.000874					
	Post B	0.000886	0.000908	1:1000	0.908	0.6	51
	Post C	0.000964					

Appendix 1.11 Time points in individual monkeys where body temperature was not recorded

	Sample time point (h)		
Monkey	Dosing Occasion 1	Dosing Occasion 2	Dosing Occasion 3
1			1.25, 1.75
2			1.25, 1.75
3			1.25, 1.75
4	1.25, 1.5	0.25, 1.25, 1.5, 1.75	1.25, 1.75
5	1.25, 1.5, 1.75	0.25, 1.25, 1.5, 1.75	1.25, 1.75
6	1.25, 1.75	0.25, 1.25, 1.5, 1.75	1.25, 1.75
7	1.25, 1.5	1.25, 1.75	1.25, 1.75
8	1.25, 1.5	1.25, 1.75	1.25, 1.75
9	1.25	1.25, 1.75	1.25, 1.75

Appendix 1.12 Lower limits of quantification (LLQ) for individual cytokines determined across separate plates and analytical occasions

	Assay LLQ (pg/mL)					
	First Analytical Occasion	Second Analytical Occasion		Third Analytical Occasion		
Analyte	Plate 1	Plate 1	Plate 2	Plate 1	Plate 2	Plate 3
IFNα2b	94.4	2.6	19.3	17.9	18.8	18.1
IL15	17.0	3.0	3.1	3.2	3.1	3.2
IFNγ	2.5	3.2	3.1	3.2	3.2	3.3
MCP1	20.6	17.2	17.4	3.1	2.7	3.0
IL6	16.7	3.2	3.3	3.1	3.2	3.3
TNFα	2.6	3.1	3.2			
TNFβ	20.0	2.5	2.7			
IL2	20.5	3.2	3.2			
IL3	2.9	3.2	3.2			
IL4	67.7	13.9	2.3			
IL5	3.0	3.1	3.2			
IL7	18.4	18.0	18.5	3.2	3.0	3.2
IL8	2.6	3.2	3.2			
IL10	20.2	3.0	3.4			
IL13	20.8	3.3	3.2			
IL17A	2.8	3.2	3.2	3.2	3.2	3.2
Eotaxin	20.7	2.3	3.7	3.8	3.7	15.2
VEGF	484.3	376.2	74.2			
GMCSF	2.2	2.7	3.2	3.1	3.2	3.1
IP-10	14.9	20.3	2.8	3.5	2.5	3.2
IL1Ra	11.4	19.0	3.3	2.9	18.2	19.6
IL1α	15.1	2.7	17.3			
IL1β	20.5	3.2	3.2			
IL12p40	77.4	3.0	2.6			
IL12p70	2.8	3.2	3.2	3.2	3.1	3.2
MIP1α	2.7	3.3	3.5			
MIP1β	79.6	19.6	18.5			
EGF	19.4	2.9	3.0			
GCSF	10000	9998	10031			

Appendix 1.13 Higher limits of quantification (HLQ) for individual cytokines determined across separate plates and analytical occasions

	Assay HLQ (pg/mL)					
	First Analytical Occasion	Second Analytical Occasion		Third Analytical Occasion		
Analyte	Plate 1	Plate 1	Plate 2	Plate 1	Plate 2	Plate 3
IFNα2b	10000	10000	10000	10000	10000	10000
IL15	10454	10030	10066	9984	10100	10013
IFNγ	10002	10004	10000	9988	10008	9963
MCP1	10140	10090	10090	1039	10219	10112
IL6	10128	10004	9984	9911	9979	9967
TNFα	10114	10071	10006			
TNFβ	10000	10000	10000			
IL2	10043	10041	10011			
IL3	10202	10178	10085			
IL4	10048	10239	10000			
IL5	10143	10041	10006			
IL7	1883	10034	10032	8368	1970	9276
IL8	10282	10081	9723			
IL10	10028	10027	9990			
IL13	10011	9996	9999			
IL17A	10018	10004	10002	10012	10021	9935
Eotaxin	10299	1999	2000	9667	9901	9473
VEGF	10214	9932	10000			
GMCSF	10000	10004	10000	10000	10000	10022
IP-10	10000	10118	10014	9986	10007	10002
IL1Ra	10000	10043	9998	10021	10033	10066
IL1α	10000	2004	10043			
IL1β	10060	10019	10002			
IL12p40	10012	10025	10014			
IL12p70	10061	10152	10088	9996	10093	10140
MIP1α	1627					
MIP1β	10006					
EGF	11814					
GCSF	10000	9998	10031			

Appendix 1.14 Samples where the concentrations of various analytes were not determined due to equipment failure

	Sample time point (h)		
	Monkey 4		Monkey 5
Analyte	3 MIU/kg	10 MIU/kg	Vehicle
IFNα2b	0, 0.5, 2, 4	96, 120, 240	120
IL15	0, 0.5, 1	96, 240	120
IFNγ	0, 0.5, 1, 4	96, 240	120
MCP1	0, 0.5	96, 120, 168, 240	120
IL6	0	96, 120, 168, 240	120
IL7	0, 0.5, 1	96, 120, 168, 240	120
IL17A	0, 0.5, 1, 4	96, 168, 240	120
Eotaxin	0, 0.5, 1, 2, 4	96, 120, 168, 240	120
GMCSF	0, 0.5, 1	96, 120, 240	120
IP-10	0, 1	96, 120, 168, 240	120
IL1Ra	0, 0.5, 1	96, 120	120
IL12p70	0, 0.5, 2	96, 120, 168, 240	

Appendix 2.1 Primate samples for different cytokines that were below LLQ and set to half LLQ to enable PK analysis

Analayte	Dose	Monkey	Time points (h)
IFNα2b	3 MIU/kg	4	2 and 4
IL15	Vehicle	3 5 9	2 120 and 168 1
	3 MIU/kg	9	96
	10 MIU/kg	1	0.5 and 1
Eotaxin	Vehicle	1	8
	3 MIU/kg	2	2 and 48
	10 MIU/kg	1 9	120 1, 2, 48 and 72
IL6	Vehicle	1 5 8	24 24 6 and 8
	3 MIU/kg	1 8	72 24
	10 MIU/kg	1	120 and 168
GMCSF	3 MIU/kg	2 8	48 48 and 96
	10 MIU/kg	5 7	24 0.5 and 96
IP10	Vehicle	1	8
	3 MIU/kg	2 4	48 and 120 4
	10 MIU/kg	1 4 5 8	0.5 48 24 and 27 0.5, 1, 48 and 96
IL7	Vehicle	1 6 8	27 96 1 and 10
	3 MIU/kg	2 4 5 9	48 4 72 10 and 24
	10 MIU/kg	3 7	10 48 and 96
IL17A	10 MIU/kg	5	24, 48 and 72
IL12p70	Vehicle	1	2 and 4
	10 MIU/kg	1 5	10 6
IFNγ	Vehicle	6	1, 48 and 96

Appendix 2.2 Primate samples that were diluted and reanalysed and subsequently included in the pharmacokinetic analysis

Analayte	Dose	Monkey	Time points (h)
IFNα2b	10 MIU/kg	3	2, 4, 6, 8 and 10
		4	2, 4, 6 and 8
		5	2, 4, 6, 8 and 10
		7	4, 6, 8 and 10
		8	2, 4, and 6
		9	6 , 6 and 8
IL1Ra	3 MIU/kg	4	6 and 8
	10 MIU/kg	4	6 and 8
		9	6, 8 and 10
MCP1	3 MIU/kg	8	4
		9	4 and 6

Appendix 2.3 **Individual serum concentration time profiles for IP10 in male cynomolgus monkeys following subcutaneous administration of vehicle (A) and IFNα2b at target doses of (B) 3 and (C) 10 MIU/kg.**

A

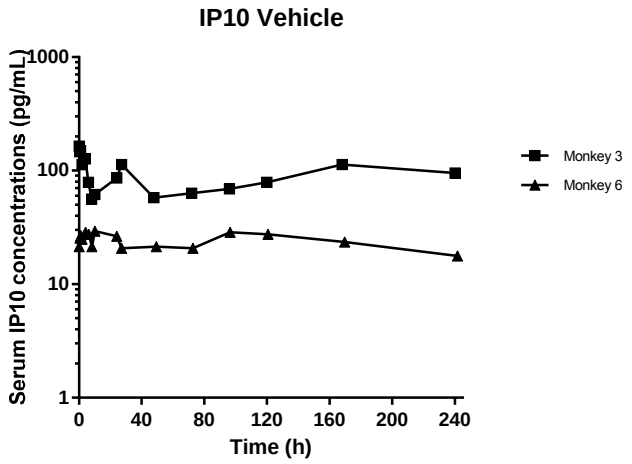

B

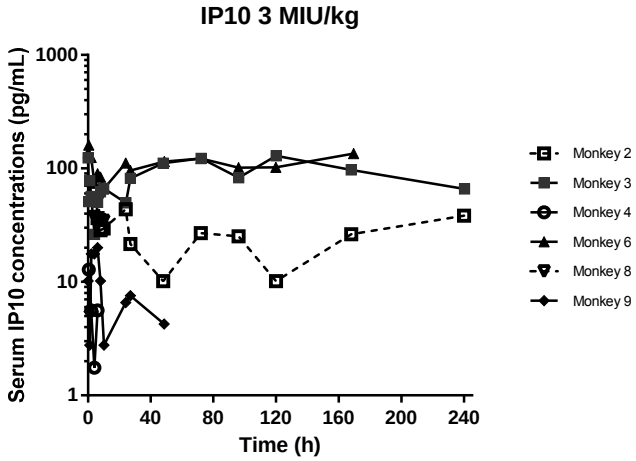

C

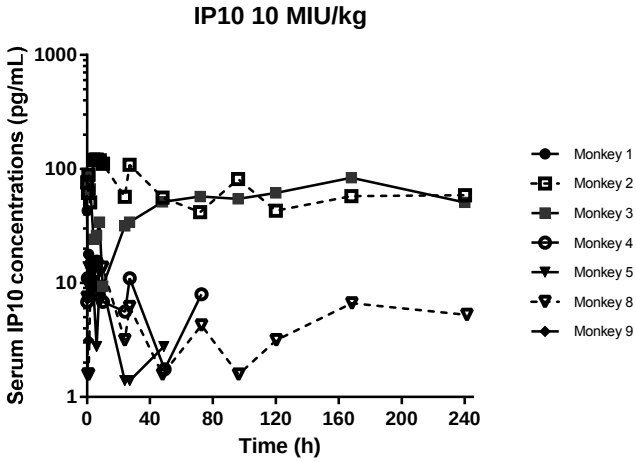

Appendix 2.4 **Individual serum concentration time profiles for GMCSF in male cynomolgus monkeys following subcutaneous administration of vehicle (A) and IFNα2b at target doses of (B) 3 and (C) 10 MIU/kg.**

A

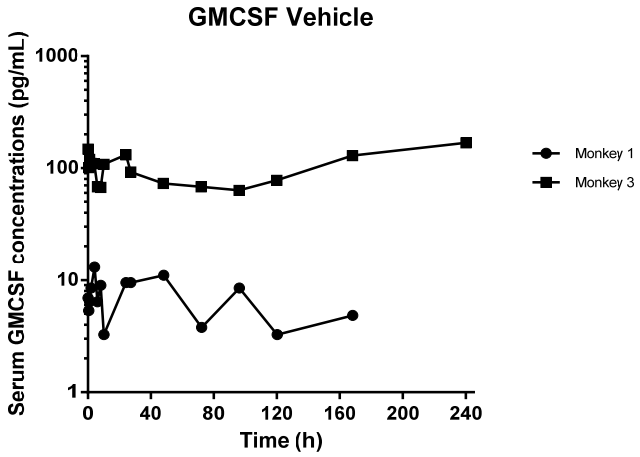

B

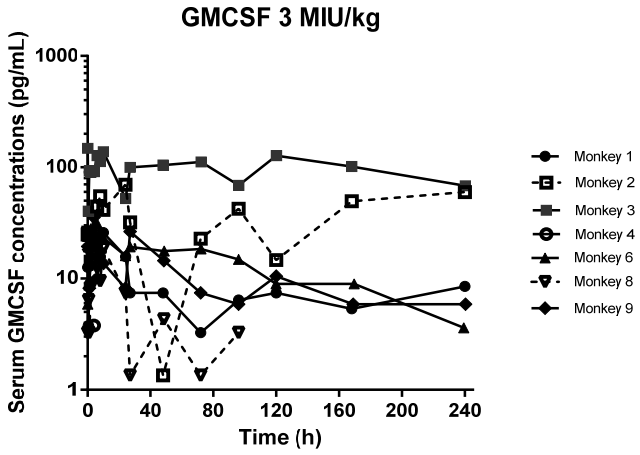

C

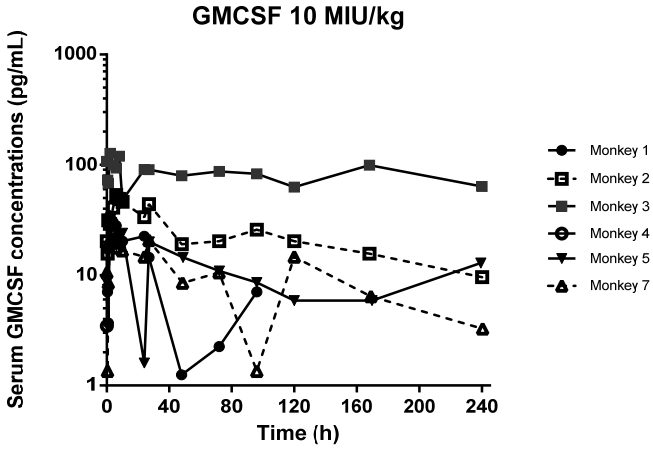

Appendix 2.5 **Individual serum concentration time profiles for IL7 in male cynomolgus monkeys following subcutaneous administration of vehicle (A) and IFNα2b at target doses of (B) 3 and (C) 10 MIU/kg.**

A

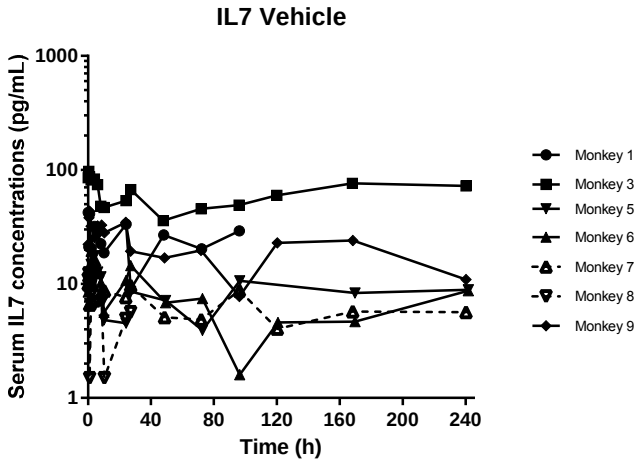

B

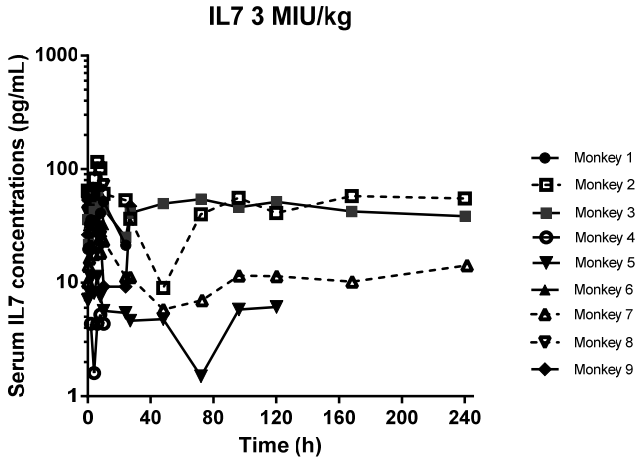

C

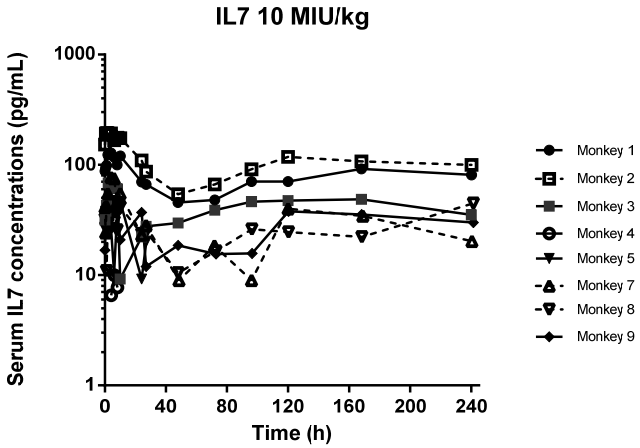

Appendix 2.6 **Individual serum concentration time profiles for IL12p70 in male cynomolgus monkeys following subcutaneous administration of vehicle (A) and IFNα2b at target doses of (B) 3 and (C) 10 MIU/kg.**

A

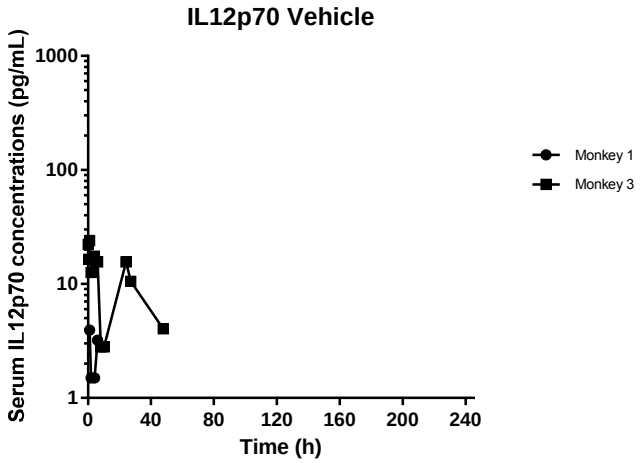

B

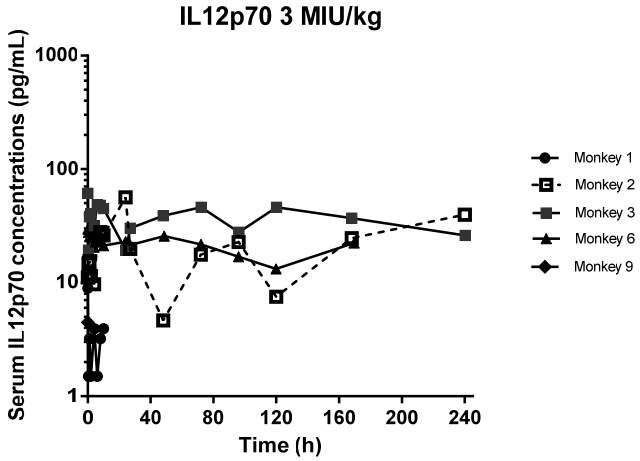

C

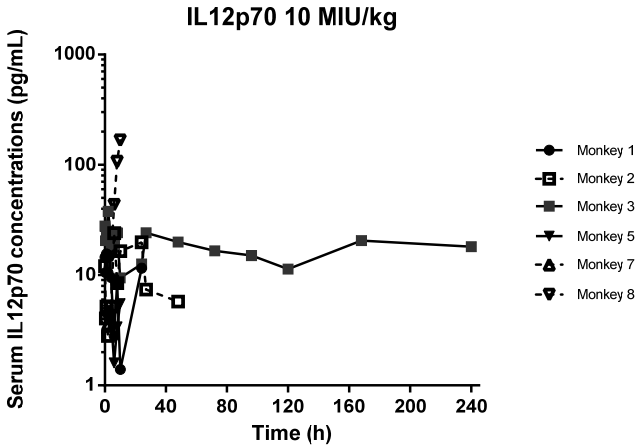

Appendix 2.7 **Individual serum concentration time profiles for IL17A in male cynomolgus monkeys following subcutaneous administration of vehicle (A) and IFNα2b at target doses of (B) 3 and (C) 10 MIU/kg.**

A

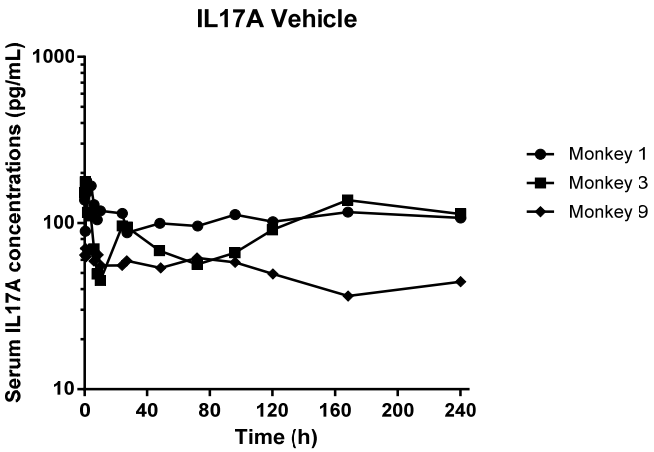

B

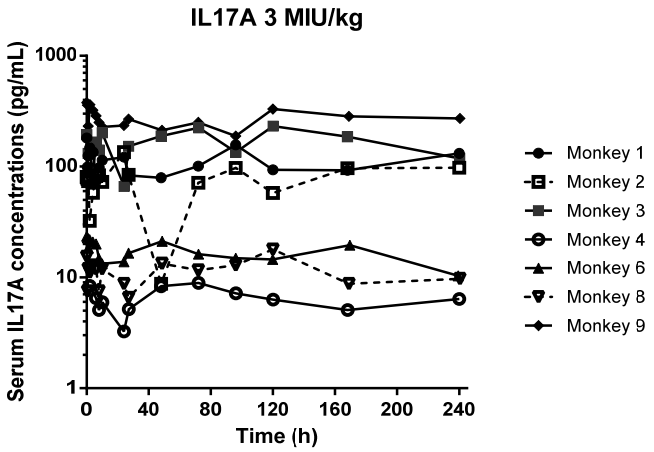

C

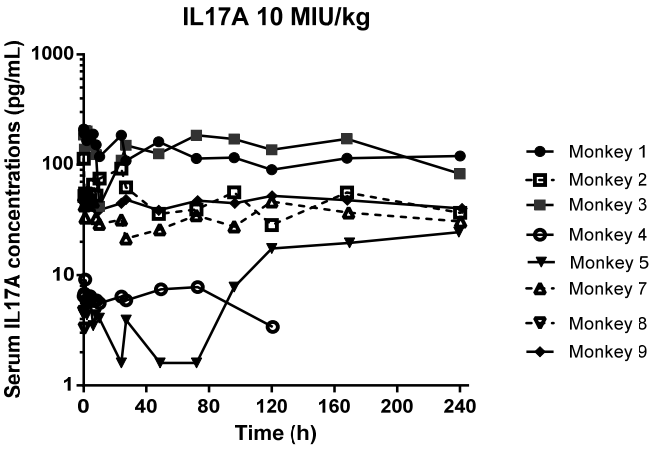

Appendix 2.8 **Individual serum concentration time profiles for IFNγ in male cynomolgus monkeys following subcutaneous administration of vehicle (A) and IFNα2b at target doses of (B) 3 and (C) 10 MIU/kg.**

A

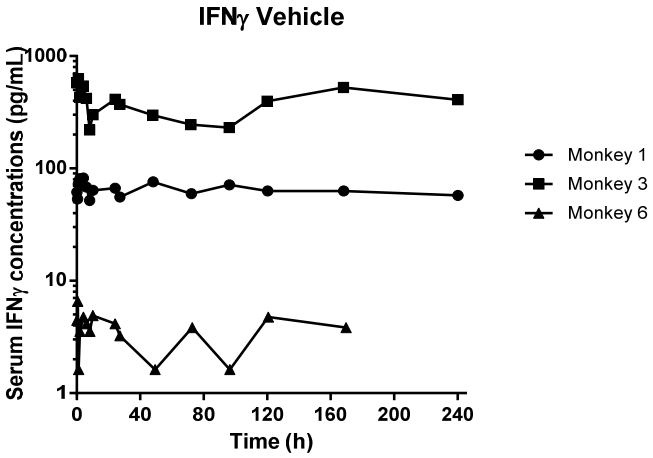

B

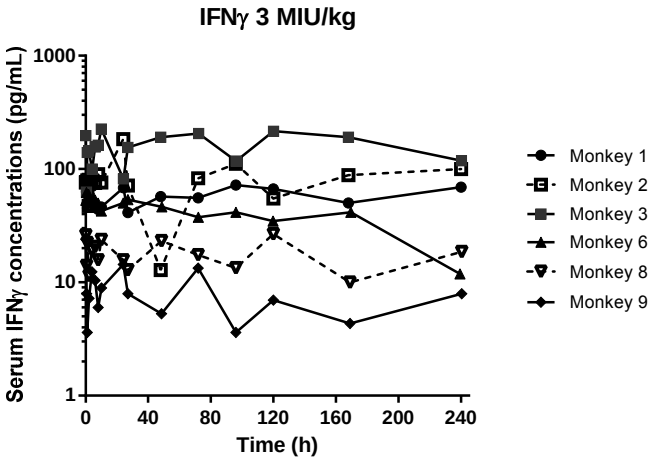

C

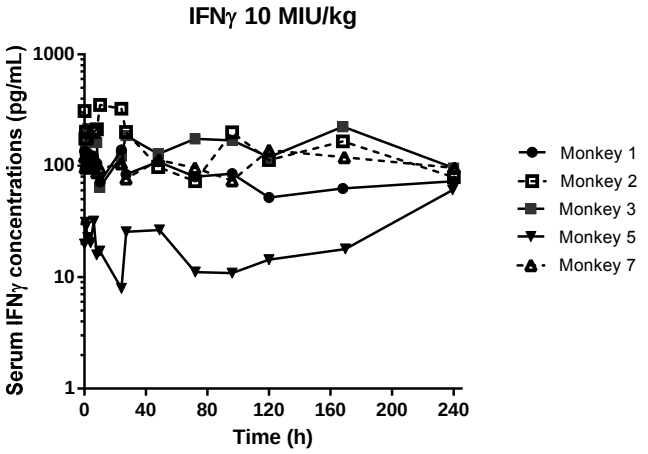

Appendix 2.9 Individual serum concentration time profiles various cytokines in male cynomolgus monkeys following subcutaneous administration of vehicle, and IFNα2b at target doses of 3 and 10 MIU/kg.

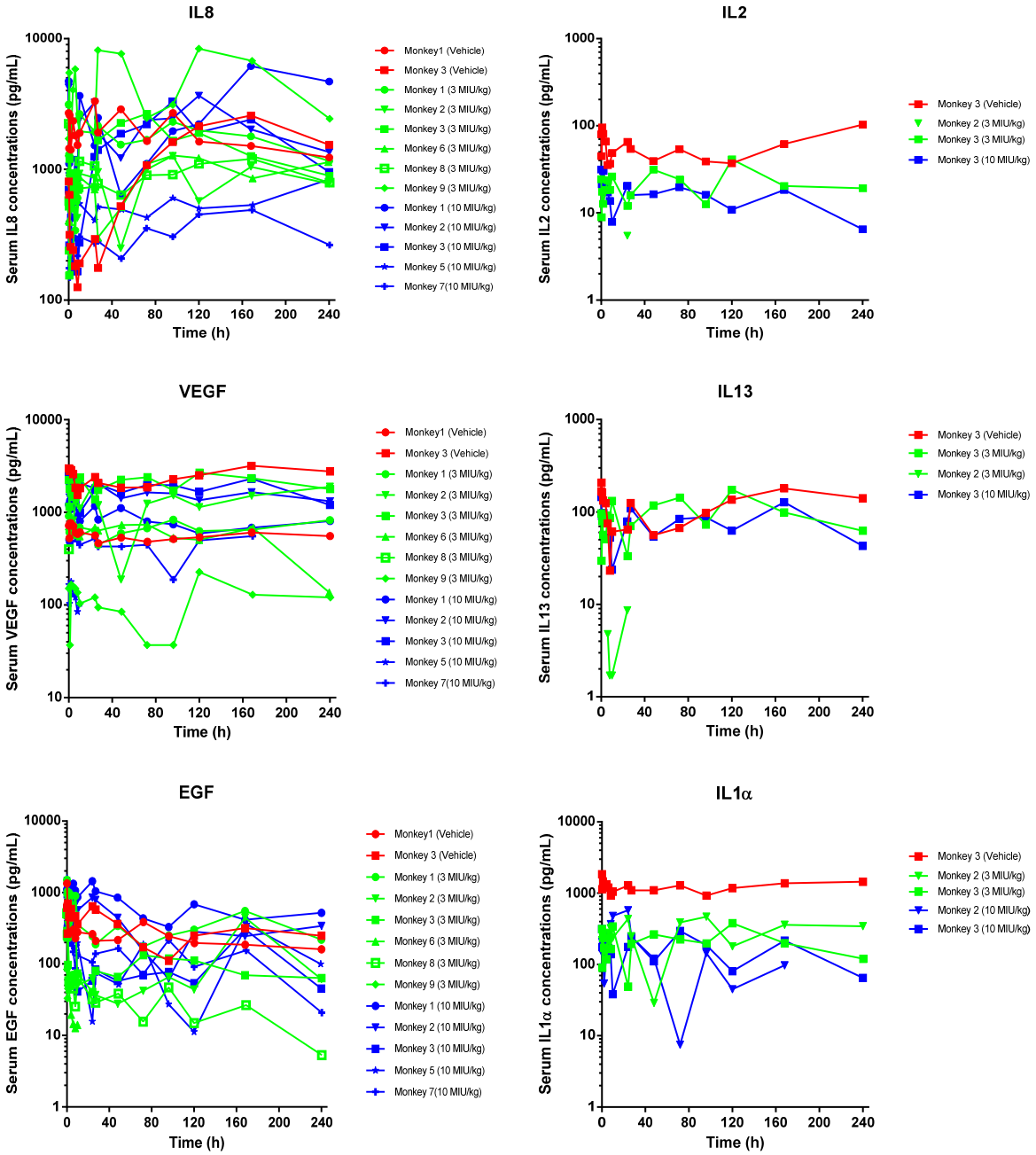

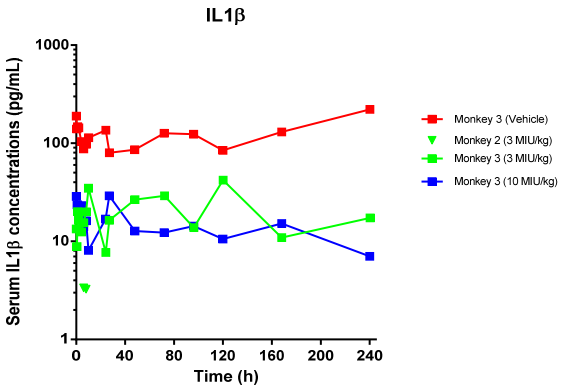
IL1β
Serum IL1β concentrations (pg/mL)
1000
100
10
1
0 40 80 120 160 200 240
Time (h)
Monkey 3 (Vehicle)
Monkey 2 (3 MIU/kg)
Monkey 3 (3 MIU/kg)
Monkey 3 (10 MIU/kg)

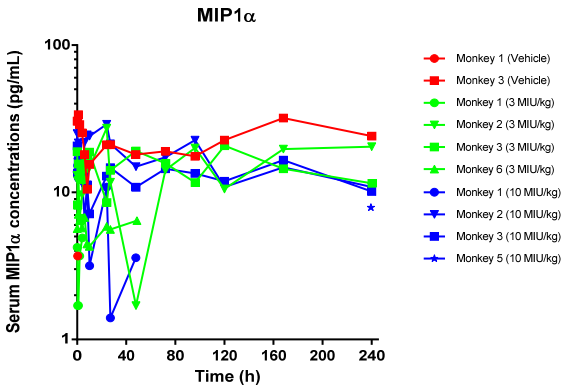
MIP1α
Serum MIP1α concentrations (pg/mL)
100
10
1
0 40 80 120 160 200 240
Time (h)
Monkey 1 (Vehicle)
Monkey 3 (Vehicle)
Monkey 1 (3 MIU/kg)
Monkey 2 (3 MIU/kg)
Monkey 3 (3 MIU/kg)
Monkey 6 (3 MIU/kg)
Monkey 1 (10 MIU/kg)
Monkey 2 (10 MIU/kg)
Monkey 3 (10 MIU/kg)
Monkey 5 (10 MIU/kg)

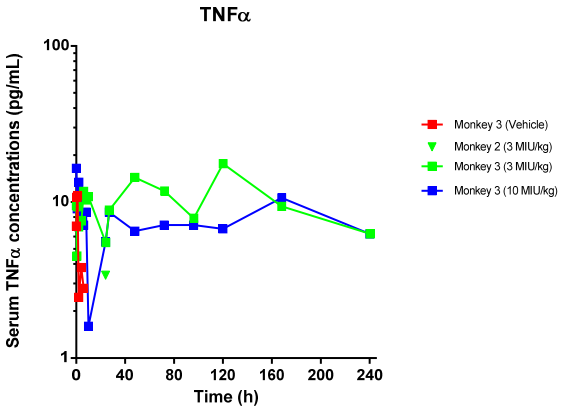
TNFα
Serum TNFα concentrations (pg/mL)
100
10
1
0 40 80 120 160 200 240
Time (h)
Monkey 3 (Vehicle)
Monkey 2 (3 MIU/kg)
Monkey 3 (3 MIU/kg)
Monkey 3 (10 MIU/kg)

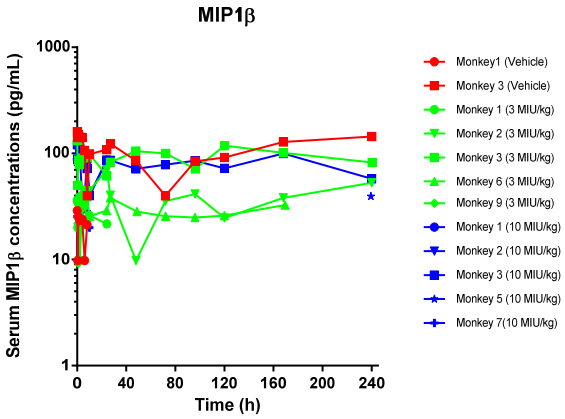
MIP1β
Serum MIP1β concentrations (pg/mL)
1000
100
10
1
0 40 80 120 160 200 240
Time (h)
Monkey1 (Vehicle)
Monkey 3 (Vehicle)
Monkey 1 (3 MIU/kg)
Monkey 2 (3 MIU/kg)
Monkey 3 (3 MIU/kg)
Monkey 6 (3 MIU/kg)
Monkey 9 (3 MIU/kg)
Monkey 1 (10 MIU/kg)
Monkey 2 (10 MIU/kg)
Monkey 3 (10 MIU/kg)
Monkey 5 (10 MIU/kg)
Monkey 7(10 MIU/kg)

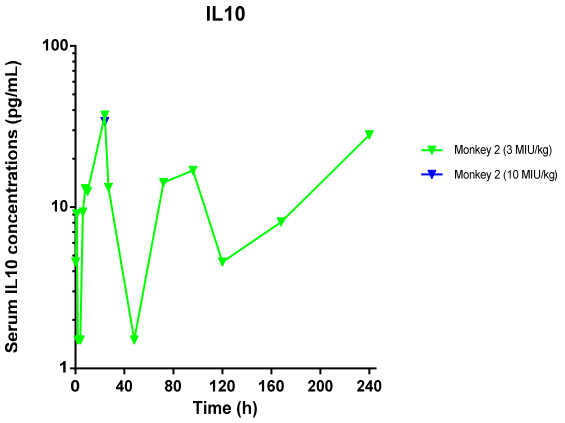
IL10
Serum IL10 concentrations (pg/mL)
100
10
1
0 40 80 120 160 200 240
Time (h)
Monkey 2 (3 MIU/kg)
Monkey 2 (10 MIU/kg)

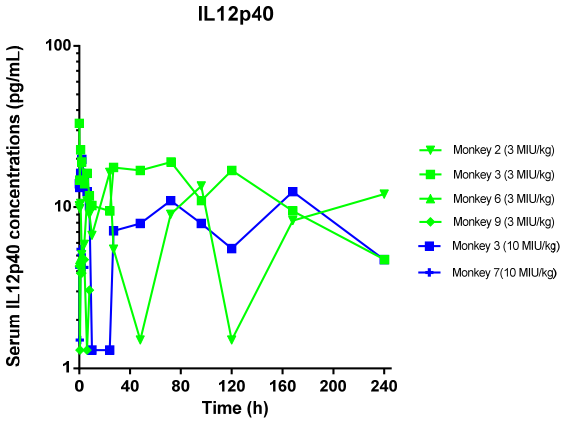
IL12p40
Serum IL12p40 concentrations (pg/mL)
100
10
1
0 40 80 120 160 200 240
Time (h)
Monkey 2 (3 MIU/kg)
Monkey 3 (3 MIU/kg)
Monkey 6 (3 MIU/kg)
Monkey 9 (3 MIU/kg)
Monkey 3 (10 MIU/kg)
Monkey 7(10 MIU/kg)

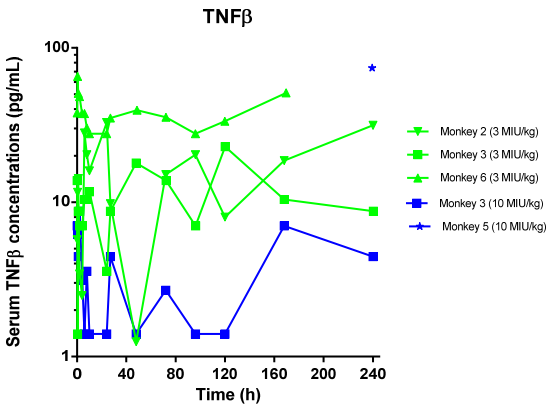

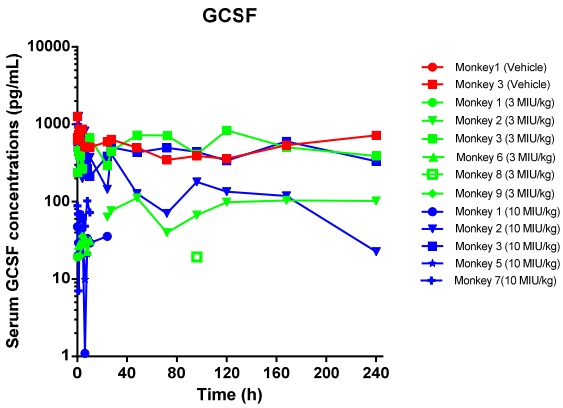

Appendix 3.1 **Neopterin observed vs population predicted concentrations (A), observed vs individual predicted concentrations (B), conditional weighted residuals vs population predicted concentrations (C) and conditional weighted residuals vs time (D)**

A

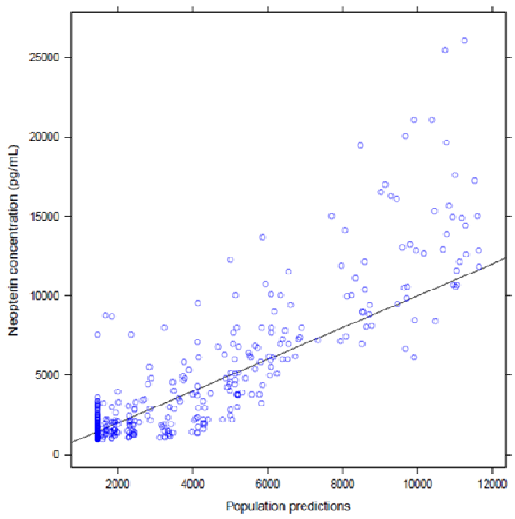

B

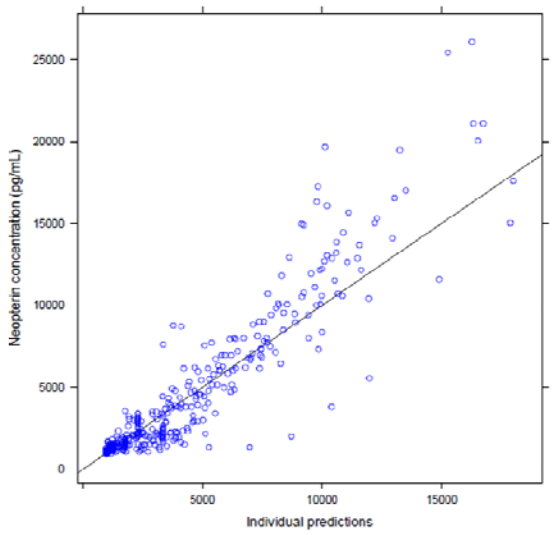

C

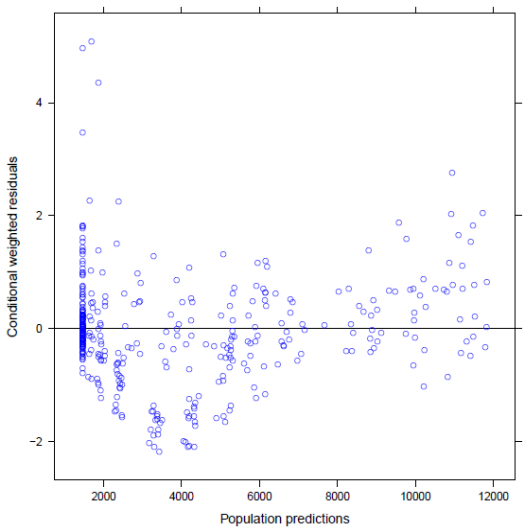

D

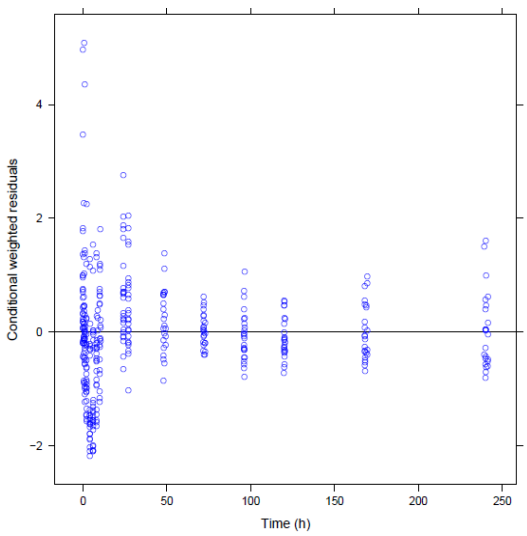

Appendix 3.2 IL15 observed vs population predicted concentrations (A), observed vs individual predicted concentrations (B), conditional weighted residuals vs population predicted concentrations (C) and conditional weighted residuals vs time (D)

A

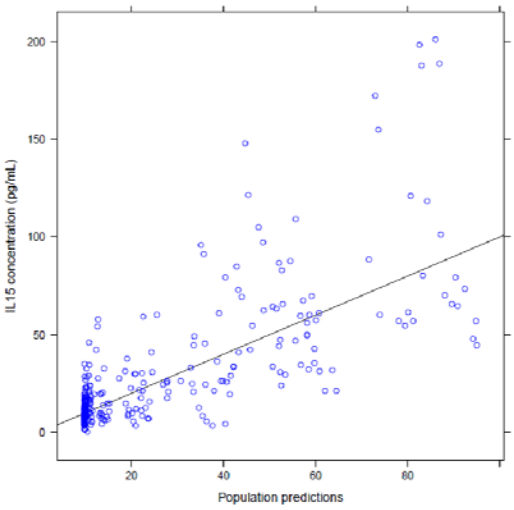

B

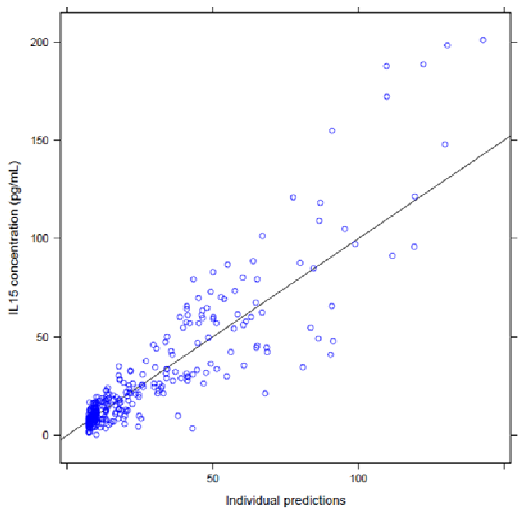

C

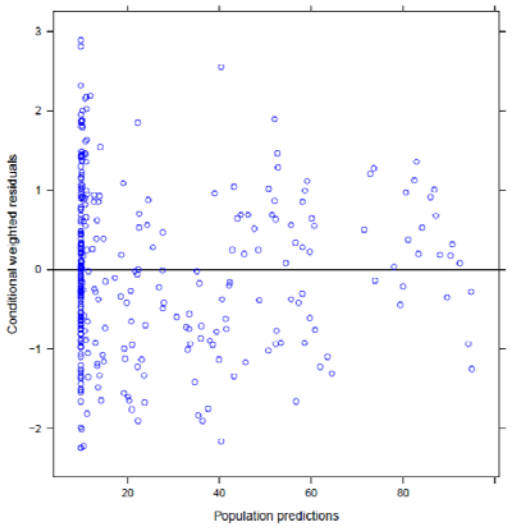

D

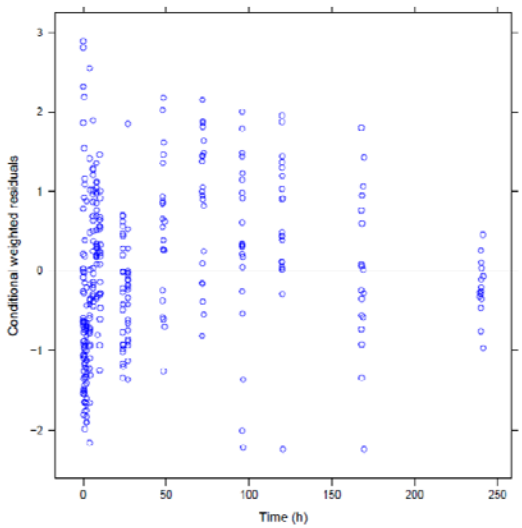

Appendix 3.3 **IL6 observed vs population predicted concentrations (A), observed vs individual predicted concentrations (B), conditional weighted residuals vs population predicted concentrations (C) and conditional weighted residuals vs time (D)**

A

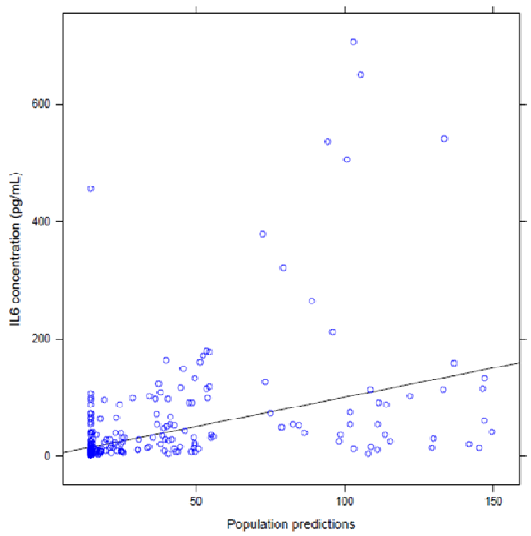

B

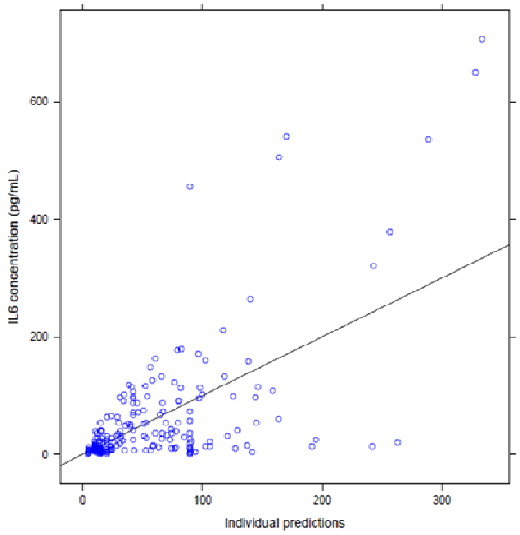

C

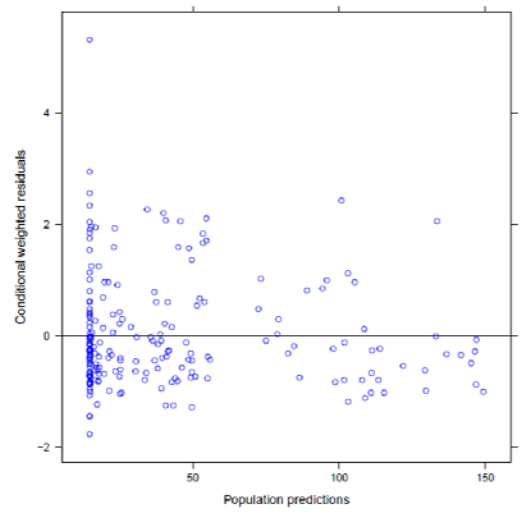

D

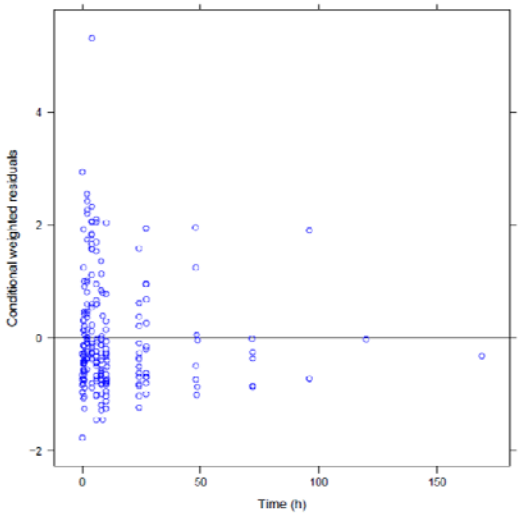

Appendix 3.4 MCP1 observed vs population predicted concentrations (A), observed vs individual predicted concentrations (B), conditional weighted residuals vs population predicted concentrations (C) and conditional weighted residuals vs time (D)

A

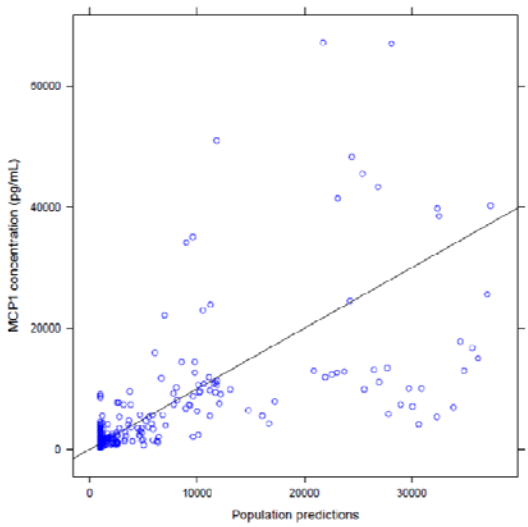

B

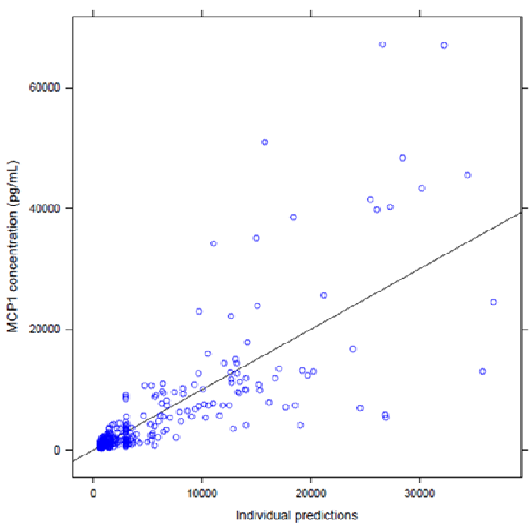

C

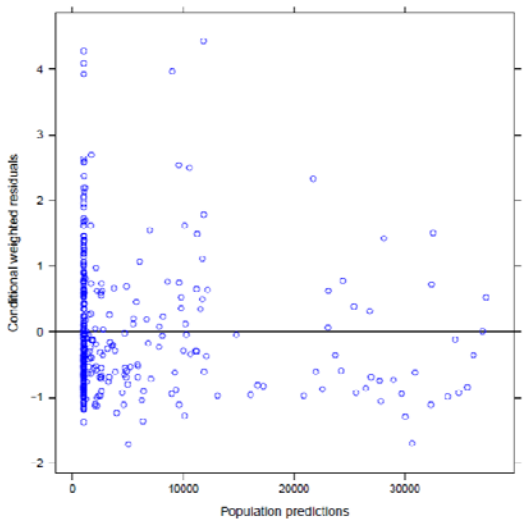

D

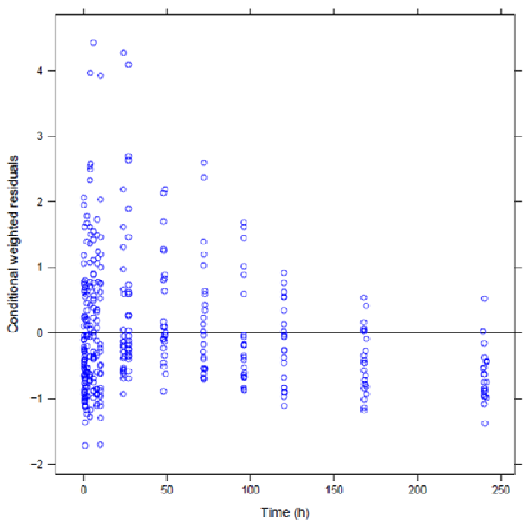

Appendix 3.5 IL1Ra observed vs population predicted concentrations (A), observed vs individual predicted concentrations (B), conditional weighted residuals vs population predicted concentrations (C) and conditional weighted residuals vs time (D)

A

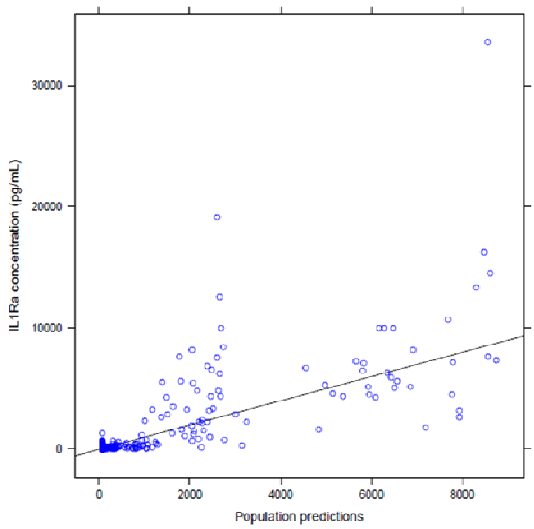

B

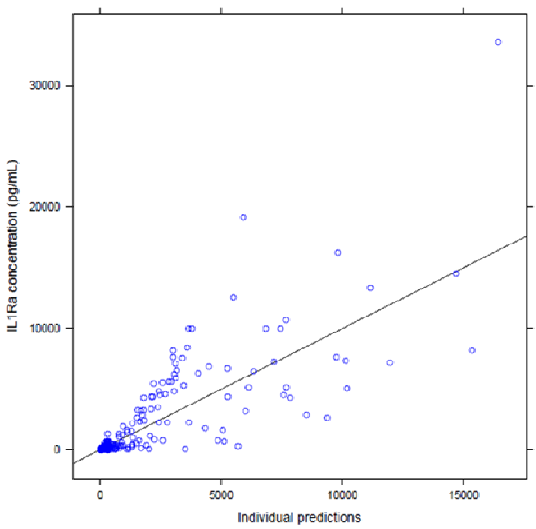

C

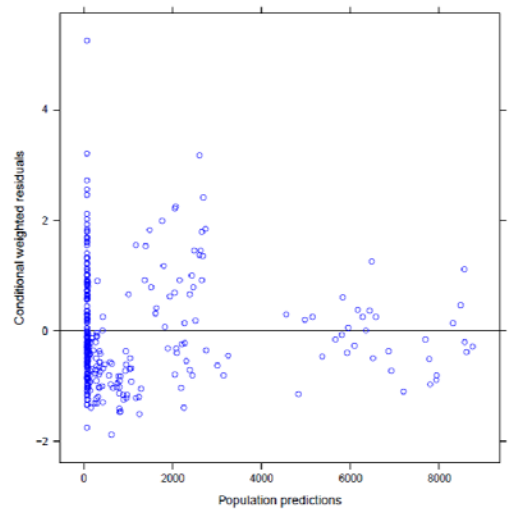

D

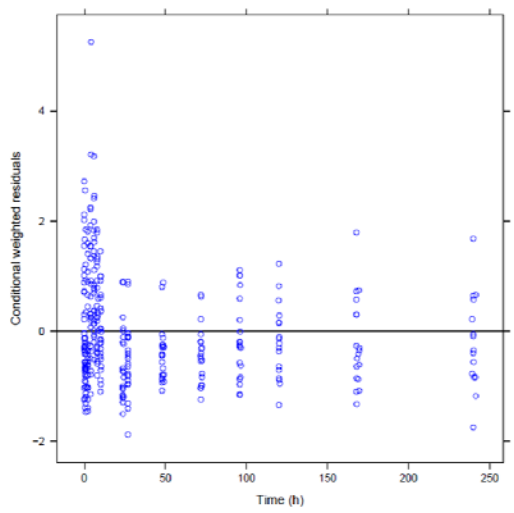

Appendix 3.6 Eotaxin observed vs population predicted concentrations (A), observed vs individual predicted concentrations (B), conditional weighted residuals vs population predicted concentrations (C) and conditional weighted residuals vs time (D)

A

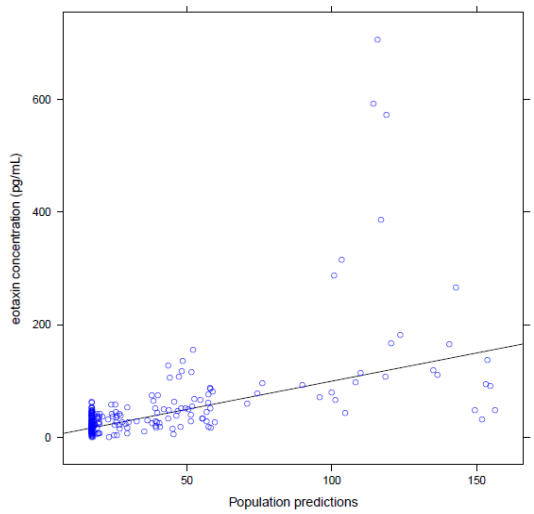

B

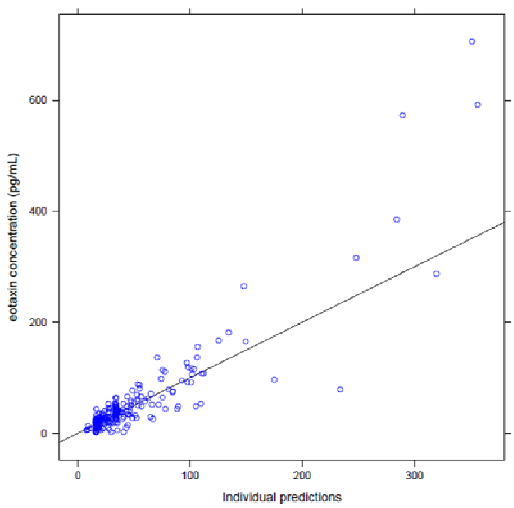

C

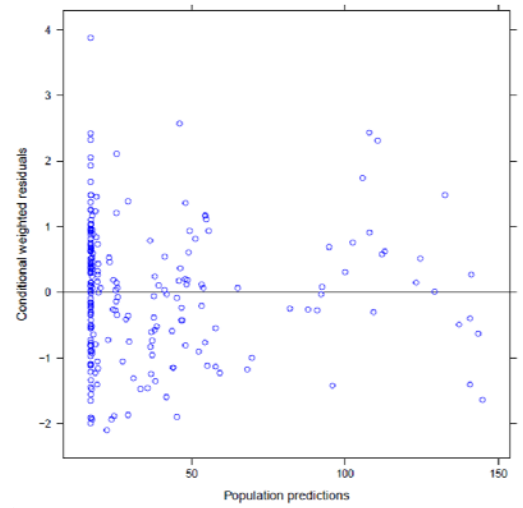

D